DTIC
ELECTE
SEP 15 1993
S E D

University of Hawaii at Manoa

College of Tropical Agriculture and Human Resources
Hawaii Institute of Tropical Agriculture and Human Resources
Gilmore Hall 202 • 3050 Maile Way
Honolulu, Hawaii 96822

Office of the Director

August 26, 1993

Defense Technical Information Center
Building 5, Cameron Station
Alexandria, Virginia 22314

Dear Sir:

Submitted herewith is the final report for Grant N00014-92-J-1523 for the Conference on Photosynthetic Responses to the Environment along with a copy of the proceedings. Also enclosed is a copy of the required "Patent Rights" clause.

Thank you very much for this support.

Sincerely yours,

Harry Y. Yamamoto
Director

hsi
Enclosures

cc: P. Kakugawa, ORA

CURRENT TOPICS IN PLANT PHYSIOLOGY:
AN AMERICAN SOCIETY OF PLANT PHYSIOLOGISTS SERIES

With this volume, the American Society of Plant Physiologists continues its series of publications on timely topics in plant physiology. Publication of proceedings devoted to focus areas, such as the present one on the photosynthetic responses to the environment, is designed to share information from plant science symposia with other scientists. This book is the eighth in the series "Current Topics in Plant Physiology: An American Society of Plant Physiologists Series." It is the wish of the Publications Committee and the Executive Committee of the Society to make these publications as useful as possible. To this end, copies of this publication and publications from previous years are available at an affordable price from the American Society of Plant Physiologists, 15501 Monona Drive, Rockville, Maryland 20855, telephone 301/251-0560.

The ASPP Publications Committee: Stanley Roux, Chair, Samuel I. Beale, Machi F. Dilworth, Richard Dixon, Natasha Raikhel
June 1993

Previous titles in the series are:

Volume 7, 1992: BIOSYNTHESIS AND MOLECULAR REGULATION OF AMINO ACIDS IN PLANTS,
Eds B. K. Singh, H. E. Flores, J. C. ShannonS

Volume 6, 1991: ACTIVE OXYGEN/OXIDATIVE STRESS AND PLANT METABOLISM,
Eds E. J. Pell, K. L. Steffen

Volume 5, 1990: POLYAMINES AND ETHYLENE: BIOCHEMISTRY, PHYSIOLOGY, AND
INTERACTIONS, Eds H. E. Flores, R. N. Arteca, J. C. Shannon

Volume 4, 1990: CALCIUM IN PLANT GROWTH AND DEVELOPMENT,
Eds R. T. Leonard, P. K. Hepler

Volume 3, 1990: THE PULVINUS: MOTOR ORGAN FOR LEAF MOVEMENT,
Eds R. L. Satter, H. L. Gorton, T. C. Vogelmann

Volume 2, 1989: PHYSIOLOGY, BIOCHEMISTRY, AND GENETICS OF NONGREEN PLASTIDS,
Eds C. D. Boyer, J. C. Shannon, R. C. Hardison

Volume 1, 1989: PLANT REPRODUCTION: FROM FLORAL INDUCTION TO POLLINATION,
Eds E. M. Lord, G. Bernier

Included among ASPP symposium publications within the past five years are:

1991:   MOLECULAR APPROACHES TO COMPARTMENTATION AND METABOLIC REGULATION,
Eds A. H. C. Huang, L. Taiz

1988:   LIGHT-ENERGY TRANSDUCTION IN PHOTOSYNTHESIS: HIGHER PLANT AND
BACTERIAL MODELS, Eds S. E. Stevens, Jr., D. A. Bryant

1988:   PHYSIOLOGY AND BIOCHEMISTRY OF PLANT MICROBIAL INTERACTIONS,
Eds N. T. Keen, T. Kosuge, L. L. Walling

1987:   PLANT SENESCENCE: ITS BIOCHEMISTRY AND PHYSIOLOGY,
Eds W. M. Thomson, E. A. Nothnagel, R. C. Huffaker

1987:   PHYSIOLOGY OF CELL EXPANSION DURING PLANT GROWTH,
Eds D. J. Cosgrove, D. P. Knievel

Current Topics in Plant Physiology:
An American Society of Plant Physiologists Series
Volume 8

Photosynthetic Responses to the Environment

Edited by
Harry Y. Yamamoto
Celia M. Smith

DTIC QUALITY INSPECTED 1

Proceedings
Photosynthetic Responses to the
Environment Symposium
August 24-27, 1992

93-21270

Department of Plant Molecular Physiology
Hawaii Institute of Tropical Agriculture and Human Resources
University of Hawaii

93 9 14 011

.

EDITORS' INTRODUCTION

Certain fundamental differences separate marine, aquatic and terrestrial plants as obviously as the differences in physical factors among their habitats. Yet at the core of their responses to environmental factors, photosynthesis ties these entities together in ways not typically seen in scientific meetings or collaboration among researchers. It was our optimistic intent in organizing this meeting "Photosynthetic Responses to the Environment" to try to bridge these diverse groups of plant life and scientists by bringing together leaders, researchers and young scientists for three days of in-depth discussions that could refresh us with new appreciation, new ideas and new colleagues.

What we saw over these days was that a remarkable degree of understanding exists for some model systems and for some environmental factors -- the principal events of stress responses are now isolated to specific sites of damage for some species. Other studies pushed the extents of our knowledge as to how intact cells and organisms respond to environmental factors. Finally, a third group presented a literal overview -- the challenges for plant scientists pushing satellite and remote sensing technologies to help us address growing concerns for changes in our global environment.

The invited contributions collected in this volume cover many aspects of our general session headings -- light, CO_2 and temperature effects on plants: for example, several aspects of photoinhibition and photosystem repair cycles, effects of UV radiation on production and photosynthesis, the roles of the xanthophyll cycle, lipids, ascorbate, carbon concentrating mechanisms in photosynthetic responses to the environment and the impact of nutrient limitations such as iron limitation to open ocean productivity are discussed in detail. Of all the posters, fifteen are published in this volume as minipapers. These minipapers follow the invited contributions and cover a broad sweep of photosynthesis research topics from molecule oriented studies of degradation of the D1 reaction-center protein following UV-B radiation to quantification of seasonal changes in photosynthetic capacity for a conifer in Norway. All poster sessions were well attended and supported by vigorous discussions. Abstracts of posters not published as minipapers follow as the the last section.

PARTICIPANTS

Randall S. Alberte, University of California at Los Angeles, California
Jan M. Anderson, CSIRO, Canberra, Australia
Joseph A. Berry, Carnegie Institution of Washington, Stanford, California
Danny J. Blubaugh, Utah State University, Logan, Utah
Harry Bolhir-Nordenkampf, University of Vienna, Vienna, Austria
Steven J. Britz, Climate Stress Laboratory, USDA, Beltsville, Maryland
Doug Carter, Central Connecticut State University, New Britain, Connecticut
Stephanie K. Clendennen, Hopkins Marine Station of Stanford University,
    Pacific Grove, California
Emmett W. Chappelle, NASA, Greenbelt, Maryland
Jim Collatz, Carnegie Institution of Washington, Stanford, California
John J. Cullen, Dalhousie University, Halifax, Nova Scotia, Canada
Barbara Demmig-Adams, University of Colorado at Boulder, Colorado
W. John S. Downton, CSIRO, Adelaide, South Australia
Marvin Edelman, Weizmann Institute of Science, Rehovot, Israel
Paul G. Falkowski, Brookhaven National Laboratory, Upton, New York
Graham D. Farquhar, Australian National University, Canberra, Australia
Christine Foyer, Laboratoire du Métabolisme, INRA, Versailles, France
David Galas, Department of Energy, Washington D. C.
Joseph Gale, Hebrew University of Jerusalem, Jerusalem, Israel
John Gamon, California State University, Los Angeles, California
Connie Geel, Wageningen Agricultural University, Wageningen, The
    Netherlands
Adam M. Gilmore, University of Hawaii at Manoa, Honolulu, Hawaii
Jeremy Harbinson, Agrotechnological Research Institute, Wageningen, The
    Netherlands
Gary Harris, Wellesley College, Wellesley ,Massachusetts
Tina Hazzard, University of Hawaii at Manoa, Honolulu, Hawaii
Stephen K. Herbert, University of Idaho, Moscow, Idaho
Nobuyasu Katayama, Tokyo Gakugei University, Tokyo, Japan
Zbigniew Kolber, Brookhaven National Laboratory, Upton, New York
Martina Koniger, Smithsonian Tropical Research Institute, Balboa, Republic
    of Panama
Bernd Kroon, University of California at Santa Barbara, California
Edward Laws, University of Hawaii at Manoa, Honolulu, Hawaii
Angela Lee, University of California at Los Angeles, California
Francesco Loreto, University of Wisconsin, Madison, Wisconsin
Jonathan B. Marder, The Hebrew University of Jerusalem, Rehovot, Israel
Donald Miles, University of Missouri, Columbia, Missouri
Patrick J. Neale, University of California at Berkeley, California
Christian Neubauer, Universtat Wurzburg, Wurzburg, Germany
John N. Nishio, University of Wyoming, Laramie, Wyoming

Teruo Ogawa, The Institute of Physical and Chemical Research, Saitama, Japan

Itzhak Ohad, Hebrew University, Jerusalem, Israel

C. Barry Osmond, Australian National University, Canberra, Australia

Polly Penhale, National Science Foundation, Washington D. C.

Arja Pennanen, University of Helsinki, Helsinki, Finland

Zvi Plaut, Hawaii Sugar Planters' Association, Aiea, Hawaii

Barbara B. Prézelin, University of California at Santa Barbara, California

John A. Raven, University of Dundee, Dundee, United Kingdom

Donald Redalje, University of Southern Mississippi, Stennis Space Center, Mississippi

David C. Rockholm, University of Hawaii at Manoa, Honolulu, Hawaii

John Rueter, Portland State University, Portland, Oregon

Piers Sellers, NASA, Greenbelt, Maryland

John J. Sheahan, University of Hawaii at Manoa, Honolulu, Hawaii

Celia M. Smith, University of Hawaii at Manoa, Honolulu, Hawaii

Jan F. H. Snel, Wageningen Agricultural University, Wageningen, The Netherlands

Alan Teramura, University of Maryland at College Park, Maryland

Ichiro Terashima, University of Tokyo, Tokyo, Japan

David H. Turpin, University of British Columbia, Vancouver, British Columbia, Canada

Olaf vanKooten, Agrotechnological Research Institute, Wageningen, The Netherlands

László Vigh, Hungarian Academy of Science, Szeged, Hungary

Hajime Wada, National Institute for Basic Biology, Saitama, Japan

John Whitmarsh, University of Illinois, Urbana, Illinois

Klaus Winter, Smithsonian Tropical Research Institute, Panama

Dan Yakir, Weizmann Institute of Science, Rehovot, Israel

Harry Y. Yamamoto, University of Hawaii at Manoa, Honolulu, Hawaii

Charles S. Yentsch Bigelow Laboratory for Ocean Sciences, West Boothbay Harbor, Maine

CONTENTS

CHAPTERS

MINI PAPERS

Acclimation and Senescence of Leaves: Their Roles in Canopy Photosynthesis[1]

Kouki Hikosaka, Katsuhiko Okada, Ichiro Terashima and Sakae Katoh

Department of Botany, Faculty of Science, University of Tokyo, Hongo, Bunkyo-ku, Tokyo 113, Japan

INTRODUCTION

Canopy photosynthesis has been studied intensively since the pioneering study by Monsi and Saeki (20). From an ecological viewpoint, Saeki (26) pointed out an importance of a vertical gradient of the rate of light-saturated photosynthesis (P_{max}[2]) of leaves within a leaf canopy of a herbaceous plant. However, this problem has not attracted much attention until recently. Based upon 'he cost-benefit analysis of leaf photosynthesis developed by Mooney and Gulmon (22), Field (9) hypothesized that carbon gain for a whole canopy is maximized when leaf nitrogen (N_L) is distributed in such a way that leaves in the microenvironments receiving the highest PPFD have the highest nitrogen content. In agreement with this hypothesis, gradients of P_{max} and of N_L across the leaf canopies have been found in stands of several species (14-17). Hirose and Werger (15) estimated that the daily photosynthetic production in a dense canopy of *Solidago altissima* L. would decrease by as much as 20% if N_L were uniform throughout the canopy. Therefore, the formation of the gradient of N_L or photosynthetic properties in a canopy is of a great adaptive significance.

Two mechanisms have been proposed for the formation of the gradient of N_L. Mooney *et al.* (21) showed that N_L in leaves of old-field plants declined with age even when plants were grown solitarily, whereas such a marked decrease in N_L was not observed in leaves of desert annuals. They proposed that, in old-field plants, the age-dependent decrease in N_L was genetically programmed. On the other hand, Hirose *et al.* (16) analyzed the artificial

[2]Abbreviations: CER, CO_2 exchange rate; LHC, light -harvesting chlorophyll-protein complexes; N_L, leaf nitrogen (content) on a leaf-area basis; NUE, nitrogen use efficiency; P_{max}, light-saturated rate of photosynthesis of the leaf on a leaf-area basis.

populations of *Lysimachia vulgars* L. grown at two different densities and found that the gradient of N_L across the leaf canopy was steeper in the denser canopy with the steeper gradient of PPFD. They concluded that the gradient of N_L is plastically formed depending on the gradient of PPFD (see also 17).

So far, in many ecophysiological studies on leaf or canopy photosynthesis, a relationship between P_{max} and N_L for a given species has been simply expressed by a single line (5). This may reflect a situation that more than half of N_L is invested to photosynthetic components (7). However, it should be noted that the partitioning of nitrogen among functional components of photosynthesis varies in response to different growth PPFD, and that this causes different photosynthetic performance of leaves (1,29). For example, P_{max} in a leaf grown at a high PPFD is greater than that of a leaf grown in the shade even though they have an identical N_L (29). Thus, the changes in partitioning of nitrogen among photosynthetic components in response to growth PPFD may also be of adaptive significance (6,7).

The amounts of photosynthetic components in leaves decrease during leaf senescence/ageing because proteins are degraded and their breakdown products (nitrogen) were translocated to other parts of plants (27). There are two factors to be considered. First, N_L will decrease with increasing age of a leaf. Second, N_L will be affected by increasing shading by upper young leaves. Previously, it was thought that the amounts of all the photosynthetic components decrease in parallel with the decrease in photosynthetic activity. However, recent studies showed that the decrease in chlorophyll or in chlorophyll-proteins is markedly slower compared with declines in photosynthetic capacity, rate of electron transport and contents of soluble proteins including Rubisco (12,18,19). Consequently, the composition of photosynthetic components in the aged leaves becomes similar to that of shade leaves. The significance of this apparent similarity between aged and shade leaves has not been addressed yet.

In this paper, we summarize our recent studies on adaptive changes in photosynthetic properties of leaves that occur in a leaf canopy. In Part I, variations of N_L and partitioning of nitrogen among photosynthetic components are examined with a new model of C_3 leaf photosynthesis. The results provide a useful and fundamental overview of effects of various environmental factors and of senescence/ageing on photosynthetic properties of leaves. Part II describes a study investigating effects of senescence/ageing and shading on leaf photosynthesis. In this study, vines of *Ipomoea tricolor* Cav. were grown horizontally over a net. Thus, the self-shading of leaves was negligible and PPFD levels of leaves were individually manipulated with small shade boxes. This enabled us to examine effects of PPFD and senescence/ageing separately. The results are compared with a vertical gradient of photosynthetic properties of leaves in a leaf canopy of *Helianthus tuberosus* L. In Part III, a study on the effects of PPFD levels and the light quality on senescence/ageing in leaves of *Oryza sativa* L. is described.

I. A MODEL OF C_3 LEAF PHOTOSYNTHESIS : NITROGEN PARTITIONING AND PHOTOSYNTHETIC PERFORMANCE

In general, a strong correlation exists between P_{max} and N_L. Because leaves grown at high PPFD (sun leaves) show higher P_{max} than do leaves grown at low PPFD (shade leaves), this implies that larger amounts of nitrogen are invested in the photosynthetic apparatus in sun leaves than in shade leaves. Allocation of nitrogen among photosynthetic components also varies depending upon PPFD during growth (1,29). For instance, shade leaves are enriched in light-harvesting chlorophyll-proteins relative to sun leaves. We constructed a model of C_3 leaf photosynthesis to examine effects of partitioning of nitrogen among photosynthetic components on leaf photosynthesis.

The Model

A light response curve of leaf photosynthesis is composed of three parts, the initial slope which is proportional to the quantum yield of photosynthesis, the light-saturated rate of photosynthesis (P_{max}), and the transitional region between these two parts.

In this model, photosynthetic components such as electron carriers and enzymes were categorized into five functional groups depending upon their contributions to P_{max} and/or the initial slope. These five groups are, (a), Rubisco; (b), electron carriers except for PSI and PSII core complexes, coupling factor, and Calvin cycle enzymes except for Rubisco; (c) PS II reaction center core complex; (d), PSI reaction center core complex associated with light harvesting chlorophyll-protein complexes of PSI (LHCI); (e), light harvesting chlorophyll-protein complexes of PSII (LHCII). Among these, (a) (b) (c) are related to P_{max}. Thus, in order to realize higher P_{max}, larger amounts of nitrogen should be invested in these photosynthetic components. We assume that amounts of these functional components are regulated so as to co-limit P_{max}. P_{max} is assumed to depend linearly on the amounts of components in (b) and (c), but curvilinearly on the amount of (a) because CO_2 concentration at the carboxylation sites decreases with increasing abundance of Rubisco due to the liquid phase resistance to diffusion of CO_2 from the cell wall surfaces to the carboxylation sites (4,8).

The initial slope of leaf photosynthesis is a product of quantum yield and leaf absorptance. The quantum yield, i.e. the amount of O_2 evolved or CO_2 absorbed per one absorbed quantum, is virtually identical in healthy C_3 plants (3), whereas leaf absorptance, a function of Chl content, varies among leaves (10). We express, therefore, the initial slope as a function of Chl content which can be calculated from the amounts of the components grouped in (c), (d) and (e). We assume that about a half of N_L is allocated to photosynthetic components in chloroplasts and that the rate of dark respiration is proportional to the amount of N_L. A light response curve for leaf photosynthesis expressed by a non-rectangular hyperbolic function is defined for given amounts of the

3

photosynthetic components in these 5 groups. From the ecological viewpoint, it is very important to evaluate relationship between the daily carbon dioxide exchange rate (CER) and N_L or the nitrogen partitioning. Assuming that the daily change in PPFD follows a square sine function, a daily CER was calculated by integrating the rate of net photosynthesis over a whole day (30).

Reuslts and Discussion

In Figure 1, daily CER realized by the optimum nitrogen partitioning among photosynthetic components is plotted against N_L. The data used for simulations are photosynthetic performances and the contents of various photosynthetic component in the leaves of *Spinacia oleracea* L. grown under various nutrient and PPFD conditions (29). Plotting of daily CER against N_L at each PPFD level gives a convex curve having a maximum. The N_L value that maximizes daily CER decreases with decreasing PPFD. The N_L value that gives the maximum daily nitrogen use efficiency (NUE, daily CER per N_L) also decreases as PPFD decreases. However, N_L that gives maximum daily NUE varies within a small range and are low, indicating that, under conditions of low nitrogen availability, N_L should be suppressed to low.

The partition pattern of nitrogen among photosynthetic components that gives the maximum CER is shown for three PPFD levels (Fig. 2). At low PPFD, the fraction of nitrogen partitioned into chlorophyll-protein complexes, especially into LHCII, is large. On the other hand, at high PPFD, a major fraction of nitrogen is allocated to the functional components related to P_{max}, in particular to Rubisco. This is due to the curvilinear relationship between P_{max} and the Rubisco content.

In shade leaves, large investment of nitrogen in the components related to P_{max} is wasteful and not paid back, as is clearly shown in Fig. 1. However, it is important for shade leaves to collect light as much as possible. Thus, a large fraction of nitrogen is allocated to chlorophyll-proteins, in particular to LHCII (Fig. 2). Since the dependency of leaf absorptance on Chl content show a

Leaf nitrogen content (mol N m^{-2})
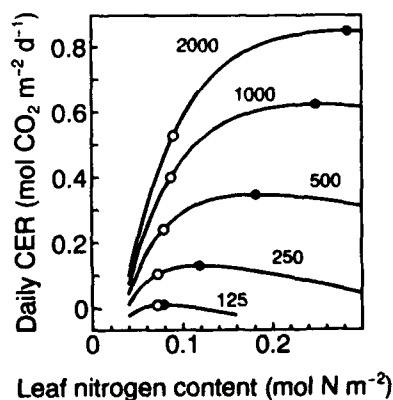
Figure 1. Relationship between daily CER and N_L at 5 PPFD levels. Daily CER realized by the optimum partitioning of nitrogen among photosynthetic components for given N_L and PPFD is plotted. Figures besides respective lines denote noon PPFD in µmol quanta m^{-2} s^{-1}, used for calculations of daily CER. Open and closed circles stand for the points giving maximal daily NUE and daily CER for each PPFD level. Simulations wer run based on the data obtained with leaves of *Spinacia oleracea* L. (29).

4
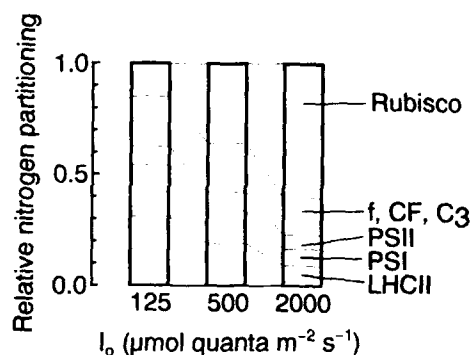
Figure 2. Optimal partitioning of nitrogen among five photosynthetic components an N_L giving the maximal daily CER. I_0 denotes noon PPFD.

saturating curve, and the Chl content of about 0.5 mmol Chl m^{-2} in ordinary leaves gives leaf absorptance of about 80 to 90%, the effect of preferential investment of nitrogen into light-harvesting chlorophyll-proteins on the initial slope of light response curves of photosynthesis is not so obvious. However, we stress that, at low PPFD levels, a slight difference in the initial slope results in a marked difference in daily CER. PSII reaction center core complex also carries a considerable amount of antenna chlorophyll a. However, the cost of nitrogen for Chl is as expensive as ca. 75 N/Chl in this complex, as compared with the nitrogen cost of Chl of ca. 24 N/Chl in LHCII. Thus, the light-harvesting capacity of shade leaves, in which P_{max} can be suppressed to low, is increased by preferential allocation of nitrogen to LHCII. It is noted that the nitrogen cost of Chl in PS I reaction center core complex with LHCI is also fairly cheap (ca. 28N/Chl).

II. EFFECTS OF PPFD, NITROGEN AVAILABILITY, AND AGE ON PHOTOSYNTHETIC PROPERTIES OF LEAVES OF *IPOMOEA TRICOLOR* CAV. GROWN WITHOUT SELF-SHADING EFFECT: COMPARISON WITH THE GRADIENT OF PHOTOSYNTHETIC PROPERTIES OF LEAVES ACROSS A NATURAL LEAF CANOPY OF *HELIANTHUS TUBEROSUS* L.

As mentioned in the introduction, there are two potential factors, i.e. leaf age and shading, that may be responsible for the formation of the vertical gradient of N_L in a leaf canopy. However, it is difficult to separate these factors, because aged leaves are generally located in lower positions and are shaded. In this study, we devised a system for separately studying the effects of leaf age and of growth PPFD.

Materials and Methods

I. tricolor plants were grown in a glasshouse. Seed were germinated in vermiculite, and seedlings were grown in Wagner pots that were filled with

5

continuously aerated hydroponic solutions of various nitrate concentrations according to Hewitt and Smith (11). Vines were laid over a wire net horizontally so that self-shading was negligible. PPFD levels of individual leaves were controlled with small screen-boxes of different transmittances. Chl was determined by the methods of Porra et al. (25). N_L was measured with a NC analyzer (NC-80, Sumitomo Chemical).

For comparison, a stand of *Helianthus tuberosus* L. was analyzed (20). Relative PPFD was measured at various heights with two matching quantum sensors (Li-Cor 1000). Chl and N_L in leaves sampled at various heights were measured. The plants had virtually no lateral shoots.

Results and Discussion

In Figure 3-A, relative PPFD is plotted against height within leaf canopy of *H. tuberosus*. PPFD decreased steeply from the surface of the canopy downward. Figure 3-B shows Chl and N_L of leaves sampled from various heights of the canopy. Both Chl and N_L of leaves decreased with increasing distance from the top. However, N_L decreased more markedly than Chl in the upper leaf canopy (above 60 cm). Thus, the Chl/N ratio increased with decreasing PPFD by shading and/or with leaf age. Chl a/b ratio also decreased with the decrease of height (data not shown).

The following experiments were carried out with *I. tricolor* grown horizontally. We first investigated the effect of age on distribution of nitrogen among leaves in respective plants. Figure 4-A shows nitrogen content of all the leaves in the plants grown for 43 days under full sunlight at various nitrate
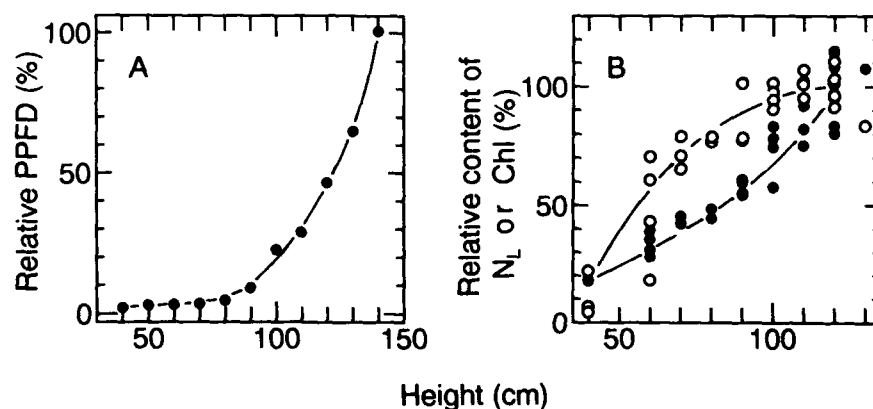
Figure 3. The relative PPFD (A) and N_L and Chl of leaves (B) in a leaf canopy of *Helianthus tuberosus* L., plotted against the height. In B, the data for the leaves that existed between heights from 110 and 120 cm are plotted at 120 cm. Open and closed circles denote Chl and N_L, respectively. The means of Chl values and N_L values at 120 cm, 0.3 mmol Chl m^{-2} and 0.071 mol N m^{-2}, are taken as 100%. Each circle stands for N_L or Chl of a single leaf

6

levels. When plants had been grown at 12 mM nitrate, all leaves showed high N_L and there was no apparent gradient of N_L along the gradient of leaf age. When grown at low nitrate concentrations, however, N_L markedly decreased with age. It is also noted that, as the nitrate level decreased, steepness of the gradient of N_L increased. These results show that leaf age is an important factor to regulate redistribution of nitrogen among leaves in plants grown under low nitrogen availability.

Next, we studied effects of shading on N_L. To simulate change in light environment in a developing leaf canopy, leaves were shaded in such a manner that PPFD of leaves decreased stepwise with time. The youngest leaves were exposed to full sunlight, whereas PPFD received by the oldest leaves decreased as the number of leaves increased. Figure 4-B shows that the gradient of N_L became steeper in plants shaded in the above-mentioned manner than in unshaded plants grown at the same nitrate level. This result indicates that the vertical gradient of PPFD in a leaf canopy contributes to the formation of the gradient of N_L. We also grew plants under the shading conditions, in which
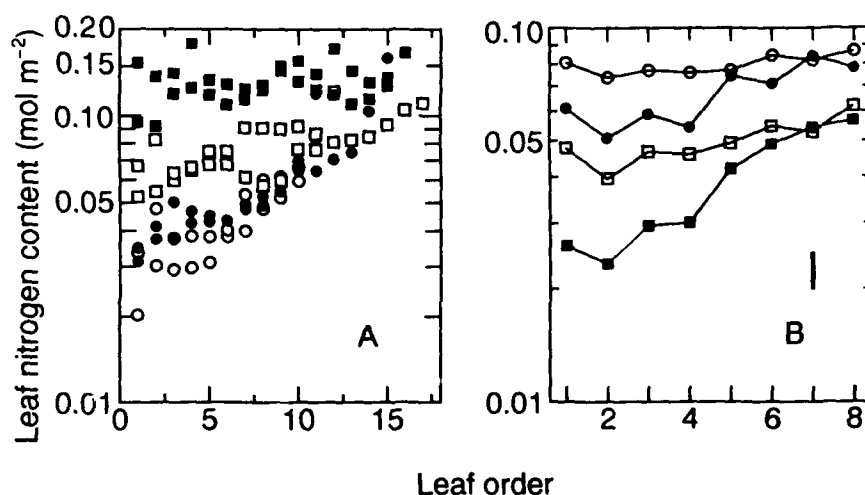
Leaf order

Figure 4. Relationships between N_L and leaf order in *Ipomoea tricolor* Cav. plants. (A) plants were grown under full sunlight for 43 d, at 0.04 (O), 0.24 (●), 1.2 (□) and 12 mM nitrate (■). Each symbol represents N_L of a single leaf. (B), effects of the shading simulating the gradient of PPFD in the leaf canopy were examined. Plants were grown for 37 d. Open and solid symbols indicate leaves exposed to full sunlight and leaves shaded, respectively. Circles and squares indicate the plants grown at 1.2 and 0.12 mM nitrate, respectively. The shading treatments were made in a manner that the PPFD decreased stepwise with time, and at harvest, 1st and 2nd, 3rd and 4th, 5th and 6th, and 7th and younger leaves had been receiving 3.7, 14, 35, and 100% of full sunlight, respectively, for 6 d. Each symbol represents mean of N_L in three leaves. A vertical bar indicates the mean of two standard deviations calculated for all the symbols.

7

PPFD of leaves increased with age. A notable gradient of N_L was generated but, in this case, N_L was higher in aged leaves at higher PPFD than in younger leaves at lower PPFD (13). It is concluded, therefore, that the gradient of PPFD plays a dominant role in the formation of the gradient of N_L in a leaf canopy.

The above conclusion was supported by analyses of photosynthetic performance of leaves and of nitrogen partitioning. Figure 5 compares changes in Chl content and in N_L of the 3rd leaves in *I. tricolor* plants grown at 0.24 mM nitrate under full sunlight. In contrast to the case in *H. tuberosus* shown in Fig. 3, Chl and N_L decreased in parallel. In Fig. 6, Chl contents are plotted against N_L: the data were obtained with leaves of various ages, from plants grown at various nitrate concentrations and at two PPFD levels. The Chl content is linearly related to N_L, virtually independent of nitrogen availability and of age in plants grown in full sunlight. However, growth of plants at lower PPFD (14% sunlight) resulted in enrichment of Chl relative to N_L. The regression line for the leaves grown under 14% sunlight lies above those for leaves grown at 100% sunlight. When the initial slope of leaf photosynthesis was compared in leaves with the same N_L, it was greater in leaves grown at 14% sunlight irrespective of the age, reflecting greater amounts of Chl (data not shown). Inversely, when P_{max} of leaves with the identical N_L were compared, it was lower in leaves grown at 14% sunlight than leaves grown under 100% sunlight (data not shown).

These results indicate that a major factor determining the partitioning of nitrogen among photosynthetic components seems to be PPFD rather than nitrogen nutrition or leaf age. In other words, the quality of chloroplasts is determined by PPFD. On the other hand, N_L, the quantity of nitrogen, is strongly affected by both growth irradiance and nitrogen availability. Decrease of N_L is further accelerated by leaf age in plants grown at low nitrate levels.

Both PPFD and leaf age could probably be responsible for the formation of the gradient of N_L in a plant canopy. However, as shown in this study, aged leaves at high PPFD had greater N_L than younger leaves at low PPFD, and the Chl/N_L ratio varied vertically within leaf canopies. We conclude, therefore, that
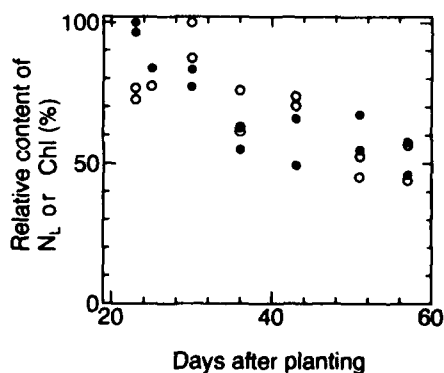
Figure 5. Declines of N_L and Chl with time in 3rd leaves of *Ipomoea tricolor* Cav. plants grown under full sunlight and at 0.24 mM nitrate. The third leaves unfolded 13 d after the planting. Closed and open circles denote N_L and Chl values, respectively. Maximal values for N_L and Chl, 0.076 mol N m^{-2} and 0.21 mmol Chl m^{-2}, are taken as 100%. Each symbol represents data of a single leaf.

8
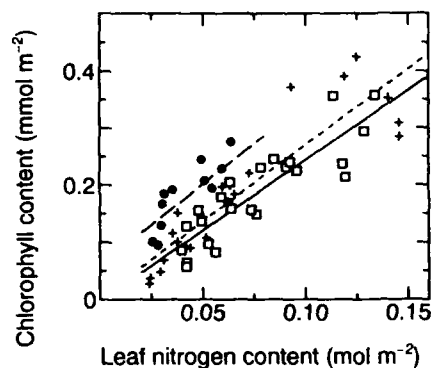
Figure 6. Relationships between Chl and N_L in 3rd leaves of various age in *Ipomoea tricolor* Cav. plants grown under various nitrate concentrations at 14% and 100% of sunlight. ●, leaves grown under 14% sunlight; +, aged leaves grown under 100% sunlight sampled from 43 to 57 d after planting; □, young leaves grown under 100% sunlight, sampled from 22 to 36 d after planting. Upper, middle and lower lines are regression lines fitted by the least squares method for ●, +, and □, respectively. Each symbol denotes data of a single leaf.

the gradient of PPFD is the major factor contributing to the formation of the gradient of photosynthetic properties of leaves.

III. EFFECTS OF PPFD LEVELS AND LIGHT QUALITY ON LEAF SENESCENCE/AGEING

A major fraction of nitrogen in leaf cells is protein nitrogen and more than half of proteins are located in chloroplasts. In this part, we describe effects of light on degradation of the two major photosynthetic components, Rubisco and Chl or Chl-carrying proteins. Underlying mechanisms of acclimational changes in composition of photosynthetic components in response to shading of leaves are proposed.

Materials and Methods

Oryza sativa L. cv. "Nipponbare" plants were grown in a greenhouse as described previously (18). When third leaves were fully expanded, plants were transferred into a growth cabinet. The air temperature in the cabinet was maintained at 30°C and the plants were continuously illuminated at various PPFD with incandescent lamps for 96 h. Where indicated, plants were illuminated with red or far-red light at 5 µmol m^{-2} s^{-1} for 15 min once every 8 h in a light-tight box (23b). Chl and proteins were extracted from leaves and determined as described previously (18).

Results and Discussion

Figure 7 shows effects of PPFD on degradations of Chl and of Rubisco. When plants were kept in the dark for 96 h, contents Chl and Rubisco decreased to about 25 and 10% of their original levels. Breakdown of these two

9

components was suppressed by continuous illumination with white light. However, the suppression of the degradation of these components occurred at very different PPFD levels. Breakdown of Chl was largely suppressed at the lowest PPFD tested, i.e. 3 μmol m^{-2} s^{-1}. This indicates that light functions as a signal rather than energy source (2). Involvement of phytochrome in regulation of Chl breakdown was indicated by experiments in which effects of red and far-red light were examined. Breakdown of Chl was strongly suppressed when plants were illuminated with red light for 15 min once every 8 h but otherwise kept in the dark. The effect of red light was largely nullified by the subsequent illumination with far-red light for 15 min. By contrast, degradation of Rubisco was suppressed only partially by continuous illumination at low PPFD, and high PPFD above 200 μmol m^{-2} s^{-1} was needed for complete suppression of the protein digestion.

These results show that there are at least two light-sensing systems which regulate degradation of chloroplast proteins. We checked that degradation of Chl in the dark was accompanied by loss of all chlorophyll-carrying proteins of the thylakoid membranes such as LHCII, and PSI and PSII reaction center complexes. Thus, breakdown of the intrinsic membrane proteins which bind Chl
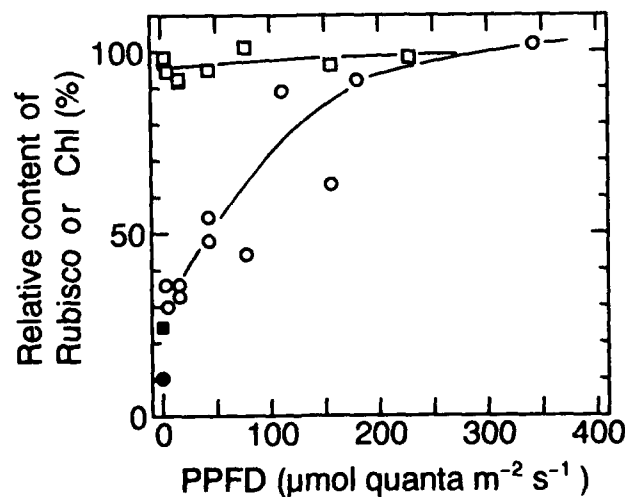
Figure 7. Effects of PPFD during the continuous illumination for 96 h on the degradations of Chl and Rubisco in attached 3rd leaves of Oryza sativa. At the onset of treatments, 3rd leaves were fully expanded. Original levels of Rubisco and Chl at the onset of the treatments are taken as 100%. Open and closed circles denote contents of Rubisco after the treatment for 96 h under continuous illumination, and in the dark respectively. Open and closed squares are for the data of Chl. Each symbol denotes a mean content of Chl or Rubisco measured in three leaves.

appears to be mainly regulated by an on-off type sensor involving phytochrome (23,28). However, it is also noted that the continuous illumination at low PPFD, but sufficient to mostly suppress the breakdown of Chl, resulted in an decrease in Chl a/b ratio (data not shown) indicating a change in composition of the chlorophyll-carrying proteins. Although it is unclear whether this change is caused by *de novo* synthesis of chlorophyll b-carrying LHCII or by slight degradation of reaction center complexes, this fine control is acclimational as already discussed in Part I (Fig. 2).

The amount of Rubisco changed in response to a wide range of PPFD, and relatively high PPFD was needed for complete suppression of the breakdown of Rubisco, suggesting involvement of a photosynthetic process. As shown in Fig. 3-B, N_L decreases more markedly than Chl with lowering position of leaves in the canopy of *H. tuberosus*. This probably reflects stability of Chl relative to soluble proteins such as Rubisco in shaded leaves. The decrease in the Rubisco/Chl ratio with a decrease in height in a leaf canopy of *Glycine max* (L.) Merrill was also reported (24). Since operation of the two systems, characterized in this study, results in a decrease in the Rubisco/Chl ratio with a decrease in PPFD, we propose that these two systems contribute to the acclimational adjustment of photosynthetic properties of leaves shaded by upper foliage by causing preferential degradation of photosynthetic components related to P_{max}.

CONCLUSION

The aim of this series of study is to clarify mechanisms responsible for the formation of adaptive gradients of photosynthetic properties of leaves in leaf canopies. Our results show that the vertical gradient of N_L could be generated responding to both of the gradients of PPFD and leaf age. However, the dominant factor to determine N_L is the gradient of PPFD. Leaves in the apical region of a canopy are sun leaves, but are gradually shaded by young leaves during development of the canopy. Responding to decline in PPFD, photosynthetic properties of the leaves change from sun-type to shade-type by means of preferential degradation of the photosynthetic components related to P_{max}. At least two systems that respond to PPFD differently are involved in this readjustment of photosynthetic properties. Further detailed studies in these lines introduced in this paper are now in progress.

LITERATURE CITED

1. **Anderson J** (1986) Photoregulation of the composition, function, and structure of thylakoid membranes. Annu Rev Plant Physiol **93**: 1184-1190
2. **Biswal UC, Biswal B** (1984) Photocontrol of leaf senescence. Photochem Photobiol **39**: 869-873

3. **Björkman O, Demmig B** (1987) Photon yield of O_2 evolution and chlorophyll fluorescence at 77 K among vascular plants of diverse origins. Planta **170**: 489-504

4. **Caemmerer S von, Evans JR** (1991) Determination of the average partial pressure of CO_2 in chloroplasts from leaves of several C_3 plants. Aust J Plant Physiol **18**: 287-305

5. **Evans JR** (1989) Photosynthesis and nitrogen relationships in leaves of C_3 plants. Oecologia **78**: 9-19

6. **Evans JR** (1989) Photosynthesis -- the dependence on nitrogen partitioning. *In* Lambers H, Cambridge ML, Kanings H, Pons TL eds, Causes and Consequences of Variation in Growth Rate and Productivity of Higher Plants, SPB Academic, The Hague, pp 159-160

7. **Evans JR, Seemann JR** (1989) The allocation of protein nitrogen in the photosynthetic apparatus: Costs, consequences and control. *In* Briggs WR ed, Photosynthesis, Alan R Liss, New York, pp 183-205

8. **Evans JR, Terashima I** (1988) Photosynthetic characteristics of spinach leaves grown with different nitrogen treatments. Plant Cell Physiol **29**: 157-165

9. **Field C** (1983) Allocating leaf nitrogen for the maximization of carbon gain: leaf age as a control on the allocating program. Oecologia **56**: 348-355

10. **Gabrielsen EK** (1948) Effects of different chlorophyll concentrations on photosynthesis in foliage leaves. Physiol Plant **1**: 6-37

11. **Hewitt EJ, Smith TA** (1975) Plant Mineral Nutrition. English University Press, London

12. **Hidema J, Makino A, Mae T, Ojima K** (1991) Photosynthetic characteristics of rice leaves aged under different irradiances from full expansion through senescence. Plant Physiol **97**: 1287-1293

13. **Hikosaka K, Terashima I, Katoh S** (1992) Effects of light, nutrient, and ageing on leaf nitrogen and photosynthesis. *In* Murata N ed, Proceedings of IX Photosynthesis Congress, Kluwer, Dordrecht, in press

14. **Hirose T, Werger MJA** (1987) Nitrogen use efficiency in instantaneous and daily photosynthesis of leaves in the canopy of a *Solidago altissima* stand. Physiol Plant **70**: 215-222

15. **Hirose T, Werger MJA** (1987) Maximizing daily canopy photosynthesis with respect to the leaf nitrogen allocation pattern in the canopy. Oecologia **72**: 520-526

16. **Hirose T, Werger MJA, Pons TL, van Rheenen JWA** (1988) Canopy structure and leaf nitrogen distribution in a stand of *Lysimachia vulgaris* L. as influenced by stand density. Oecologia **77**: 145-150

17. **Hirose T, Werger MJA, van Rheenen JWA** (1989) Canopy development and leaf nitrogen distribution in a stand of *Carex acutiformis*. Ecology **70**: 1610-1618

18. **Kura-Hotta M, Satoh K, Katoh S** (1987) Relationship between photosynthesis and chlorophyll content during leaf senescence of rice seedlings. Plant Cell Physiol **28**: 1321-1329

19. **Makino A, Mae T, Ohira K** (1983) Photosynthesis and ribulose 1,5-bisphosphate carboxylase in rice leaves. Plant Physiol **73**: 1002-1007

20. **Monsi M, Saeki T** (1953) Über die Lichtfaktor in den Pflanzengesellschaften und seine Bedeutung für die Stoffproduktion. Jpn J Bot **14**: 22-52

21. **Mooney HA, Field C, Gulmon SL, Bazzaz FA** (1981) Photosynthetic capacity in relation to leaf position in desert versus old-field annuals. Oecologia **50**: 109-112

22. **Mooney HA, Gulmon SL** (1979) Environmental and evolutionary constraints on the photosynthetic characteristics of higher plants. *In* Solbrig OT, Jain S, Johnson GB, Raven PH eds, Topics in Plant Population Biology, Columbia Univ Press, New York, pp 1-42

23. **Okada K, Katoh S** (1992) Effects of light on degradation of chlorophyll and chloroplast proteins during senescence of rice leaves. *In* Murata N ed. Proceedings of IX Photosynthesis Congress, Kluwer, Dordrecht, in press

23b **Okada K, Inoue Y, Satoh K, Katoh S** (in press) Effects of light on degradation of chlorophyll and proteins during senescence of detached rice leaves. Plant Cell Physiol

24. **Pearcy RW, Seemann JR** (1990) Photosynthetic induction state of leaves in a soybean canopy in relation to light regulation, ribulose-1,5-bisphosphate carboxylase and stomatal conductance. Plant Physiol **94**: 628-633

25. **Porra RJ, Thompson WA, Kriedemann PE** (1989) Determination of accurate extinction coefficients and simultaneous equations for assaying chlorophyll a and b extracted with four different solvents: Verification of the concentration of chlorophyll standards by atomic absorption spectroscopy. Biochim Biophys Acta **975**: 384-394

26. **Saeki T** (1959) Variation of photosynthetic activity with ageing of leaves and total photosynthesis in a plant community. Bot Mag Tokyo **72**: 404-408

27. **Stoddart JL, Thomas H** (1982) Leaf senescence. *In* Boulter D, Pathier B eds, Encyclopedia of Plant Physiology (New Series), Vol 14A, Springer, Berlin, pp 592-636

28. **Sugiura, M** (1963) Effects of red and far-red on protein and phosphate metabolism in tobacco leaf disks. Bot Mag Tokyo **76**: 174-180

29. **Terashima I, Evans JR** (1988) Effects of light and nitrogen on the organization of the photosynthetic apparatus in spinach. Plant Cell Physiol **29**:143-155.

30. **Terashima I, Takenaka A** (1986) Organization of photosynthetic system of dorsiventral leaves as adapted to the irradiation from the adaxial side. *In* Marcells R, Clijsters H, van Pouke M eds, Biological Control of Photosynthesis, Martinus Nijhoff, Dordrecht, pp 219-230

13

Dynamics of Photosystem II: Photoinhibition as a Protective Acclimation Strategy

Jan M. Anderson, Wah Soon Chow and Gunnar Öquist[1]

CSIRO, Division of Plant Industry, Canberra, ACT 2601, Australia; and Cooperative Centre for Plant Science Research, GPO Box 475, Canberra ACT 2601, Australia

DYNAMIC LIGHT ACCLIMATION OF PSII

Coordinated interactions between light-harvesting, energy conversion, electron transport and carbon assimilation are exquisitely orchestrated in photosynthesis. In nature there is a continuum of available light ranging from direct sunlight above the canopy, to light progressively filtered through upper leaves, and to light travelling through leaves, cells and even chloroplasts. Superimposed on these gradients are wide fluctuations in momentary, daily and seasonal irradiances. It is not surprising, therefore, that plants possess many acclimation strategies to cope with their extraordinarily variable light environment. The highly flexible organization of the photosynthetic apparatus is achieved by a cascade of dynamic adaptations at the molecular level. These regulatory mechanisms include both short-term and long-term adaptive changes. Short-term (millisec to min) adaptations, resulting from changes in the organization of existing components (e.g. state 1 - state 2 transitions), will not be discussed here. Long-term acclimation, discussed below, involves modulations in the actual content of chloroplast components due to both synthesis and degradation; this acclimation of chloroplast composition in turn influences structure and function (3, 4, 20).

Compared to sun plants, shade plants have larger chloroplasts with more thylakoid membranes in very large granal stacks, and greater appressed membrane domains. Lateral heterogeneity in the distribution of thylakoid complexes within the thylakoid membrane network, with PSII mainly in granal domains, and PSI complex and ATP synthase being located only in non-appressed membranes (stroma thylakoids, margins and end grana membranes), ensures that these striking morphological differences between sun and shade chloroplasts are accompanied by different amounts of thylakoid complexes (3, 4). Sun and high-light plants have very high rates of photosynthesis and growth

---

[1] Permanent address: Plant Physiology, University of Umeå, S-901 87, Umeå, Sweden

under high irradiance, while shade and low-light plants survive at very low irradiances with much lower maximum rates of photosynthesis. With acclimation to shade, the relative amounts of cytochrome b/f complex, mobile electron carriers and ATP synthase on a chlorophyll basis are much lower, consistent with the low irradiance received. Conversely, at high irradiance, maximal photosynthesis is greatly enhanced by increasing the amounts of thylakoid components on a chlorophyll basis. All these dynamic changes in the photosynthetic apparatus not only contribute to higher photosynthetic capacity but, by utilizing the higher irradiance more effectively, better avoid photoinhibition since less excitation energy has to be dissipated by means other than electron transport. Both cytochrome b/f content and ATP synthase activity are directly proportional to maximum electron transport capacity (3, 14). In contrast, neither P680 nor P700 is directly proportional to maximum photosynthetic capacity, since the photosystems are not limiting at light saturation (3, 14). Nevertheless, despite the photosystems not being linearly related to photosynthetic capacity, both photosystems undergo acclimation.

Many of the molecular mechanisms for optimizing and balancing light-harvesting in sun and shade habitats are targeted to PSII complex, which is the thylakoid complex most vulnerable to environmental stress, particularly high irradiance. Two main strategies are involved in acclimation of the light-harvesting apparatus of PSII and PSI. Firstly, the amount of PSII reaction centers relative to PSI reaction centers, i.e. the photosystem stoichiometry, can be altered by light quantity and quality (Table I; 11, 20). Secondly, the number of light-harvesting antenna pigment molecules serving each reaction center, become smaller with increasing irradiance (2). Sun and high-light plant chloroplasts have high Chl a/Chl b ratios and more PSII units with smaller light-harvesting antennae relative to PSI; conversely, shade and low-light chloroplasts have low Chl a/Chl b ratios and fewer PSII units with much larger light-harvesting units relative to PSI (Table I). It is now proven that adjustments in photosystem stoichiometry allow both sun and shade plants to achieve high and

Table I. *Photosystem stoichiometries in peas grown under varying irradiance and light qualities (3,11)*

Light regime	Chl a/Chl b	PSII/Chl	PSI/Chl	PSII/PSI
		(mmol mol⁻¹ Chl)		
High	3.00	2.42	· 4·	1.7
Low	2.55	1.75	¹ ¹··	1.3
PSII-light	2.24	1.97	1.73	1.1
PSI-light	1.97	2.67	1.05	2.5

constant quantum yields at limiting irradiance (11, 20), despite their pronounced differences in maximal photosynthetic capacity. Such adjustments and organization of the photosystem stoichiometry are extraordinarily important, since most chloroplasts function for most of the time in irradiances well below saturation, due to the pronounced attenuation of light within cells, leaves and canopies. Despite the time needed for both synthetic and degradative processes, the response of leaves to irradiance is dynamic: e.g. the half-time for changes in the photosystem stoichiometry in peas in response to changes in irradiance is about 2 days (3) and in light quality is 20 h (20).

NATURE OF PHOTOINHIBITION

Although light is the ultimate substrate for photosynthetic energy conversion, and despite the acclimation strategies described above, too much light leads to a marked decline in the efficiency of photosynthesis. Oxygen-evolving plants and algae are universally prone to photoinhibition, particularly under adverse environmental conditions. The primary target for photoinhibition is electron transfer through PSII. Photoinhibition of electron transfer through PSII and the rapid light-induced turnover of the central D1 protein of the D1/D2 heterodimer of PSII are currently the subject of intense research (5, 28). The prevailing use of *in vitro* rather than *in vivo* approaches has led to the notion that photoinhibition is a damaging process without any redeeming features. However, in these *in vitro* approaches, isolated PSII reaction centers, core PSII complexes and isolated membranes are often subjected to unrealistically strong light. Many highly reactive and potentially very damaging molecular species have been identified, including Tyr_Z^+, $P680^+$, $^3P680$, Ph^-, Q_A^{2-} and singlet O_2 all of which lead to damage on either the acceptor or donor side of PSII reaction centers (5, 28). The many scenarios for photodamage have been summed up as "there is more than one way to skin a cat" (7). It is important to remember that no matter how the cat is skinned, there is only one end result: the cat dies! The remarkable thing about PSII (thought by some to be "a delicate chemical machine with inherent weakness" (7)) is that it survives: *in vivo*, the cat lives! There are many photoprotective strategies (9, 12, 13, 19, 24, 28) which ensure that PSII, despite its inherent vulnerability, is extraordinarily robust. Perhaps the major protective mechanism against photoinhibition is the rapid, intrinsic light-induced turnover of D1 protein. Following photodamage D1 protein is degraded thereby minimizing the effects of harmful radical species, and newly synthesized precursor D1 protein is rapidly integrated into the damaged PSII centers (reviewed in 28). In this study we emphasize a major acclimation strategy for protection against high irradiance by the long-term "down-regulation" of PSII conferred by photoinhibition, ironically the very process deemed by many to be damaging.

To gain insights into photoinhibition *in vivo*, we compared photosynthesis and PSII function under both limiting and saturating light in relation to the level

of photoinhibition exhibited by three differently light-acclimated plants. A shade plant, *Tradescantia albiflora*, grown at 50 μmol photons m^{-2} s^{-1} ($Trad_{50}$) and peas acclimated to low (50 μmol photons m^{-2} s^{-1}; Pea_{50}) and moderate (300 μmol photons m^{-2} s^{-1}; Pea_{300}) irradiance were subjected to photoinhibition (1700 μmol photons m^{-2} s^{-1} for 4 h at 22°C). $Trad_{50}$ was the more sensitive to our photoinhibitory treatment, then Pea_{50}, while Pea_{300} was the most resistant, as judged by the quantum yield of photosynthetic oxygen evolution, and the ratio of variable to maximum chlorophyll fluorescence yields (Fv/Fm) in dark-adapted leaves (Fig. 1A) which is linearly related to quantum yield (24). This is consistent with shade plants being more prone to photoinhibition than sun plants (4).
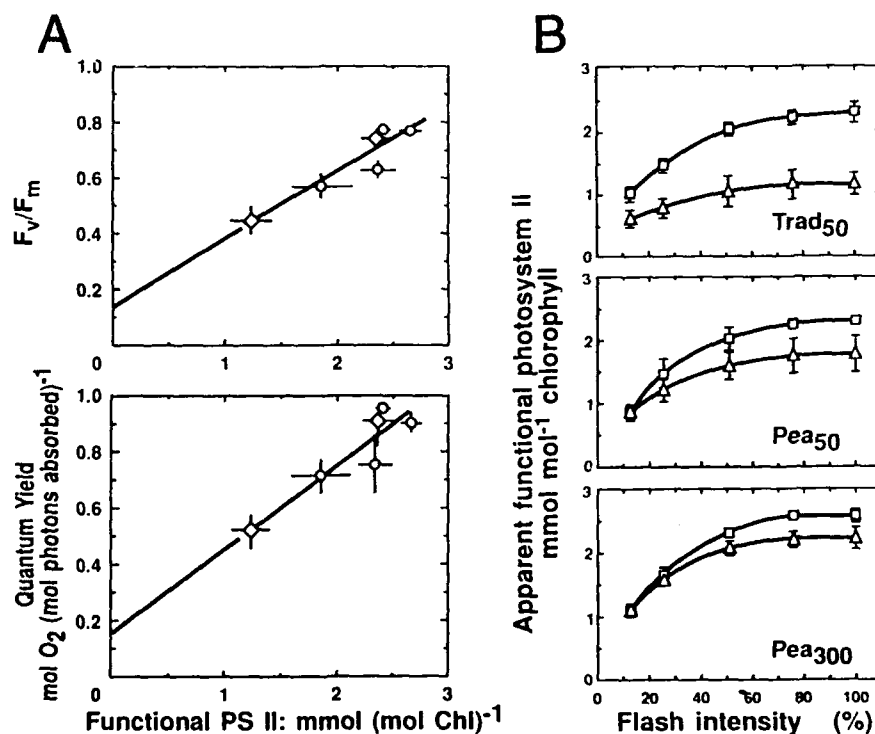
Figure 1. A. Correlation of the maximum efficiency of PSII photochemistry (Fv/Fm) with the quantum yield of O_2 evolution and numbers of functional PSII reaction centers in non-inhibited and photoinhibited leaves. **B.** The apparent number of functional PSII reaction centers (mmol mol^{-1} Chl) as a function of relative flash intensity in non-inhibited and photoinhibited leaf discs. *Tradescantia albiflora* ($Trad_{50}$) and peas (Pea_{50}) were grown at 50 μmol photon m^{-2} s^{-1} and peas (Pea_{300}) at 300 μmol photons m^{-2} s^{-1}. Standard photoinhibitory treatments were given to leaf discs floating on water at 22°C under 1,700 μmol photons m^{-2} s^{-1} for 4 h. Replotted from Öquist *et al.* (24).

17

We also determined the apparent number of functional PSII reaction centers on a chlorophyll basis as a function of increasing flash intensity. Two conclusions can be made. Firstly, the numbers of functional PSII reaction centers of each photoinhibited plant were always lower than in non-photoinhibited plants (Fig. 1B). This proves that photoinhibition occurs by direct inactivation of PSII reaction center itself, and not indirectly by antennae quenching. If the latter case pertained, the functional PSII reaction centers should be equal at saturating flash intensities, and this was not observed (Fig. 1B; 24). Secondly, at saturating flash intensity, the number of functional PSII reaction centers were linearly related to both the quantum yield of O_2 evolution and Fv/Fm (Fig. 1A). From this study, we conclude that photoinhibition results from a decrease in PSII efficiency in both sun and shade plants.

EQUIVALENCE OF PHOTOINHIBITION AND TRANSTHYLAKOID ΔpH IN THE DOWN-REGULATION OF PSII UNDER HIGH IRRADIANCE

The establishment of a transthylakoid ΔpH gradient is a well-known mechanism which rapidly regulates the efficiency of PSII photochemistry within seconds to minutes, in concert with the demand for ATP and NADPH to drive the carbon reduction cycle and other cellular functions (15). One consequence of this regulation is that PSII reaction center traps do not become 'closed' (i.e. Q_A reduced) in proportion to increasing irradiance: as the light saturation of photosynthesis is reached, some PSII reaction centers are still open due to an increased non-photochemical dissipation of excitation energy at the reaction center or at the antenna level (16, 31). Based on our results below, we suggest that under long-term conditions (hours, days or even weeks) photoinhibition provides an additional mechanism for the down-regulation of the yield of PSII photochemistry, which under high irradiance, is indistinguishable from the short-term down-regulation of PSII by the ΔpH gradient.

We determined the average quantum yield of PSII electron transport in vivo, according to Genty et al. (16), as the product of the fraction of open PSII reaction centers (estimated by q_p) and the fluorescence ratio (F'v/F'm) under different irradiances, where F'v and F'm are steady-state variable and maximum chlorophyll fluorescence yield, respectively, during illumination (Fig. 2A; 24). Measured under low light, the quantum yields of PSII electron transport were lower in photoinhibited than in non-inhibited plants. With increasing irradiance, however, the differences became less marked, until similar values were obtained under light-saturating conditions. Importantly, with irradiances high enough to saturate photosynthesis, the quantum yields of PSII electron transport of both photoinhibited and control plants were equal (Fig. 2A). Remarkably, photochemical quenching, q_p, which decreased with increasing irradiance as expected, was *identical* for each photoinhibited and non-inhibited plant at any given irradiance, irrespective of their degree of photoinhibition (Fig.
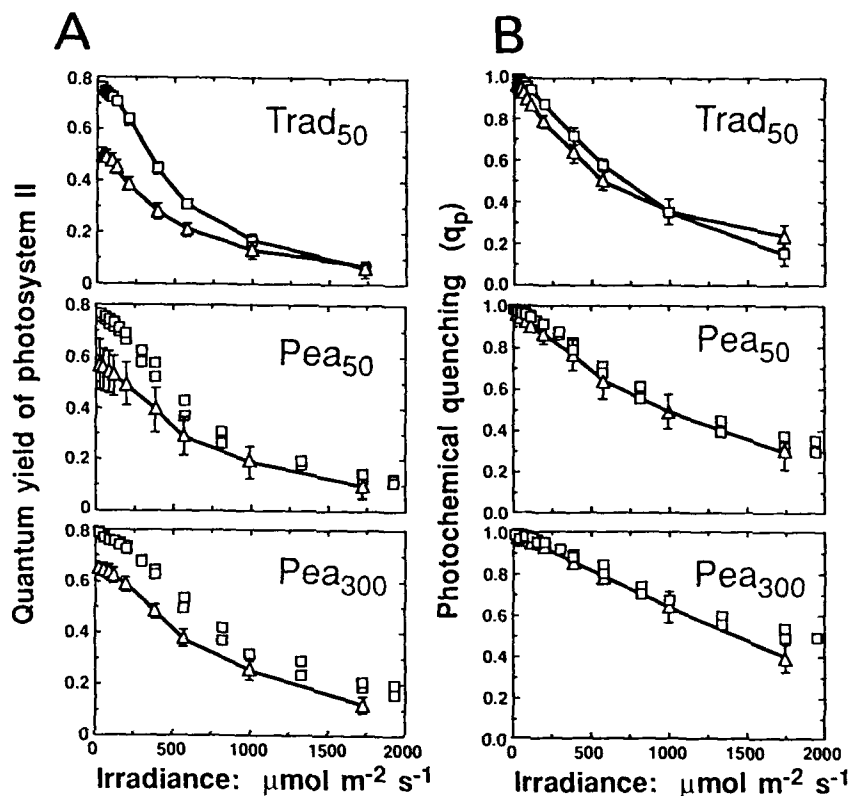
Figure 2. **A.** The quantum yield of PSII electron transport of non-inhibited (□) and photoinhibited (△) leaf discs, expressed as q_p x F'v/F'm according to Genty *et al.* (16) plotted as a function of incident irradiance **B.** Photochemical quenching, q_p, of non-inhibited (□) and photoinhibited (△) leaf discs as a function of incident irradiance Plants and photoinhibitory treatment as in Fig. 1. Redrawn from Öquist *et al.* (24).

2B). Hence the decline in the quantum yield of PSII electron transport in *photoinhibited plants* is fully explained by the steady-state fluorescence ratio, F'v/F'm. The lower F'v/F'm ratios of photoinhibited plants in turn imply an intrinsic lower efficiency of PSII electron transport in open PSII reaction centers as a consequence of photoinhibition.

Taken together, our results strongly suggest that in photoinhibited plants the redox state of functional PSII reaction centers under high irradiance is regulated by *both ΔpH and photoinhibition* acting in concert (24). Thus, photoinhibition of PSII reaction centers is not necessarily a destructive phenomenon, but

19

in plants experiencing sustained high irradiance, and replaces part of the regulation usually exerted by the rapid transthylakoid ΔpH gradient. Although we (24) and others (28) have shown that photoinhibition results from specific inactivation of PSII reaction centers, our studies do not address whether the energy quenching occurs in the light-harvesting antennae, PSII reaction centers, or both. Neither the mechanisms nor sites of fluorescence quenching via heat dissipation are yet resolved (9, 12, 13, 16, 31). We propose that down-regulated PSII reaction centers combine inhibited photochemistry with sustained, enhanced heat dissipation of excited chlorophylls (24). These long-term down-regulated PSII reaction centers may, as they accumulate, offer enhanced protection of the remaining, connected functional PSII centers (24). Photoinhibition, far from being a damaging phenomenon, represents a long-term acclimation strategy of PSII, by rendering protection from photodamage through thermal energy dissipation.

PHOTOINHIBITION IN RELATION TO CLOSURE
OF THE PSII TRAPS

It is generally assumed that photoinhibition, particularly in vitro photoinhibition, occurs as a result of excessive excitation of PSII centers whose Q_A's are mainly reduced due to sustained high light (5, 28). However, significant photoinhibition already occurs in plants which have less than 40% of steady-state closure of PSII reaction centers (23, 24) suggesting that total or over-reduction of Q_A is not a prerequisite for in vivo photoinhibition. To test this hypothesis further, the susceptibility to photoinhibition of 9 plants acclimated to different light environments was determined as a function of photochemical quenching (q_p) at the same high irradiance as used for photoinhibition (Fig. 3). Extrapolation of the Fv/Fm ratio vs q_p relationship back to a Fv/Fm ratio of 0.80, typical for non-inhibited plants (Fig. 1A), indicates that plants start to become photoinhibited when the steady-state value of q_p decreases below 0.57; that is, when most of the PSII reaction centers are still able to transfer electrons. We conclude that photoinhibition is a unique intrinsic PSII function in both sun and shade plants, which is inevitable as soon as 40% of the PSII traps become continually closed (24). Consequently, both sun and shade plants have identical intrinsic susceptibilities to photoinhibition, irrespective of light acclimation. Shade plants appear more photoinhibited relative to sun plants, because under sustained high light, shade plants receive greater excess irradiance than sun plants which are acclimated to much higher ambient irradiances. Dynamic responses resulting in varying resistances to photoinhibition are controlled primarily by factors that determine the redox state of Q_A, via the flow of electrons to and from Q_A (24).

20
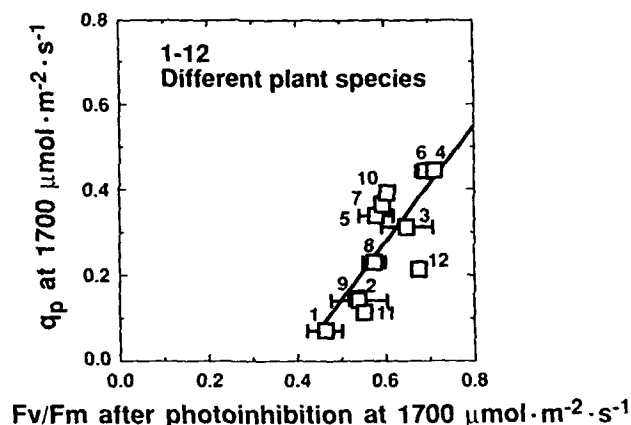
Figure 3. Photochemical quenching, q_p, measured at 1,700 μmol photons $m^{-2} s^{-1}$ as a function of maximum photochemical efficiency of PSII expressed as Fv/Fm after photoinhibitory treatment (1,700 μmol photons $m^{-2} s^{-1}$, 22°C, 4 h) of leaves acclimated to varying irradiances (μmol photons $m^{-2} s^{-1}$ denoted by subscripts; midday irradiance glasshouse): 1, $Trad_{50}$; 2, $Trad_{300}$; 3, Pea_{50}; 4, Pea_{300}; 5, Spinach$_{100}$, glasshouse; 6, Spinach$_{300}$, glasshouse; 7, Zea mays, glasshouse; 8, Sorghum sp., glasshouse; 9, Alocasia, glasshouse; 10, Atriplex, glasshouse; 11, Rhodendrum, shade; 12, Salix sp., outdoors (Data from ref. 24).

SUN PLANT AND SHADE PLANT STRATEGIES
TO COPE WITH PHOTOINHIBITION

While rapid light-induced turnover of D1 protein helps protect PSII against photodamage, net D1 protein degradation may occur during in vivo and in vitro photoinhibition (5, 7, 28). Surprisingly, there is no positive correlation between the amount of degraded D1 protein and the extent of photoinhibition. As seen in Table II, the amount of degraded D1 protein was greatest in Pea_{300} where photoinhibition was least, and least in the most photoinhibited leaves, $Trad_{50}$, suggesting slower D1 protein degradation in shade than sun plants. Since D1 protein synthesis is needed for an active PSII repair cycle (25, 28), we also tested the significance of this PSII repair cycle for protection against photoinhibition. In the presence of the chloroplast protein-synthesis inhibitor, chloramphenicol (CAP), the order of sensitivity to photoinhibition was reversed: $Trad_{50}$ was the least susceptible, then Pea_{50} and Pea_{300} (Table II). This also demonstrates that shade plants rely less than sun plants on an active PSII repair cycle as a protective mechanism against photoinhibition. Recovery from photoinhibition of CAP-treated leaves was much lower for Pea_{300} than $Trad_{50}$ (data not shown), again demonstrating that sun plants need greater D1 protein synthesis for recovery (25).

21

We suggest that different mechanisms appear to be involved in the strategies to cope with photoinhibition in sun and shade plants (25). Sun plants have an active repair cycle for PSII to replace photoinhibited PSII reaction centers with photochemically active centers, thereby conferring partial protection against photoinhibition. Acclimation of the photosynthetic apparatus to high irradiance, allows plants to effectively utilize high irradiance for electron transport thereby providing abundant energy sources for CO_2 assimilation/ O_2 fixation by Rubisco in C_3 plants, and other reductive reactions with O_2, N_2 and S. Despite an energy cost associated with *de novo* D1 protein synthesis (29), it is very small compared to the drastic photodamage that could occur if the potential damage demonstrated during *in vitro* photoinhibition were allowed to persist and "kill the cat". Sun plants have adequate energy resources to maintain both an active PSII repair cycle and high chloroplast activities. On the other hand, shade plants receive very much lower irradiance; there is insufficient capacity to counteract photoinhibition by a rapid turnover of the PSII repair cycle, which would be extremely costly relative to their limited photosynthetic capacity and hence energy resources. We suggest that in shade plants, the PSII repair cycle is much less significant for protection against photoinhibition. Instead, long-term, down-regulated PSII reaction centers confer, as they accumulate, increased protection of the remaining functional PSII centers by controlled, non-photochemical dissipation of excess excitation energy (25). Although our evidence does not unequivocally prove this hypothesis, the fact that D1 protein is not degraded in phase with photoinhibition (Table II) strengthens the feasibility of this concept. We suggest that these stable PSII centers still contain D1 protein; although they are unable to undergo charge stabilization, they may still be able to maintain their trapping ability and non-photochemical dissipation of absorbed light by charge separation and recombination.

Recently, Sundby *et al.* (30) determined D1 protein turnover in *Brassica napus* acclimated to a wide range of growth irradiances, as a function of both growth and incident irradiance. We demonstrated that D1 protein turnover is

Table II. *Comparisons of photoinhibition (1,700 µmol photons m-2 s-1 for 4 h at 22°C) in the absence and presence of D-chloramphenicol (CAP), and the amount of D1 protein degraded in differently acclimated plants.* Extents of photoinhibition and D1 protein degradation are expressed as the percentage of non-inhibited leaf discs (25)

| Plant | Photoinhibition (%) | | D1 protein |
	-CAP	+CAP	degraded (%)
$Trad_{50}$	45	27	11
Pea_{50}	24	19	17
Pea_{300}	15	17	35

maximal at growth irradiance. Below the growth irradiance, D1 protein turnover increases with increasing irradiance, as already known (cf. 28). Unexpectedly, above growth irradiance, D1 protein turnover *decreases with increasing irradiance*, consistent with long-term down-regulation of some PSII complexes (25, 30). Sundby *et al.* (30) also propose that all plants exhibit both the sun plant strategy (active PSII repair cycle) and the shade plant strategy (long-term, down-regulated PSIIs which still contain D1 protein). Below and up to growth irradiance for plants grown under constant irradiance, or for field plants to an acclimation irradiance set by prevailing ambient irradiance, the sun plant strategy prevails. Note this high D1 protein turnover is achieved without loss of PSII function. We postulate that above acclimation irradiance, those PSIIs which remain functional also maintain . r active PSII repair cycle, but those non-functional, long-term, dow   gulated PSIIs display the shade plant strategy.

ECOLOGICAL RELEVANCE OF PHOTOINHIBITION
AS A PHOTOPROTECTIVE STRATEGY UNDER
SUSTAINED HIGH IRRADIANCE

Our data support the view that photoinhibition of PSII centers of sun and shade plants, irrespective of light acclimation, brings about a stable, long-term down-regulation of some PSII centers which may be "locked-in" under sustained high irradiance; i.e. these PSII centers do not participate in the PSII repair cycle under prolonged high light. This long-term down-regulation of PSII replaces part of the regulation usually exerted by the transthylakoid ΔpH gradient under short-term conditions. By enhancing the non-photochemical dissipation of excitation energy, absorbed in excess to the capacity of photosynthesis, the long-term down-regulation of certain nonfunctional PSII reaction centers deep within the granal domains, serves to prevent other connected functional PSII centers from becoming non-functional (24). We conclude that photoinhibition does not necessarily damage PSII, but rather is an important acclimation strategy to ensure the superb dynamicity of PSII.

This stable long-term regulation of PSII by photoinhibition appears to be widespread in nature. Under high irradiance conditions, photoinhibition is observed in the mid-day depression of photosynthesis in both aquatic (21) and terrestrial (22) environments. Moreover, stable long-term down-regulation of PSII by photoinhibition is particularly prevalent when other environmental stresses (e.g. low temperature, high temperature, salinity, drought, nutrient deficiencies) predispose plants towards more Q_A being reduced. Stable down-regulation of PSII by photoinhibition is particularly evident under low temperatures, as exemplified by field studies of coniferous trees (26), Antarctic moss (27) and snowgum (6) where decreased photosynthetic efficiencies at limiting irradiance, were not accompanied by parallel decreases in photosynthetic capacities at higher irradiances. Öquist *et al.* (17, 26) suggest that cold-induced

23

photoinhibition also results in protective dissipation of excess excitation energy rather than damage to PSII *per se*.

The shade plant, *Tradescantia albiflora*, is interesting since its light-harvesting apparatus does not acclimate with light quantity: instead it is locked in the shade mode with low Chl a/Chl b ratios of 2.2 and PSII/PSI ratios of 1.3 at all growth irradiances (10). Nevertheless, it acclimates to full sunlight and flourishes as a weed, despite being chronically photoinhibited with 50% decreased quantum yields and lower light-saturated rates of photosynthesis compared to shade-acclimated plants (1). Hurry *et al*. (18) demonstrated that cold-hardened spring and winter wheat cultivars repeatedly exposed to high light of 1200 µmol photons m^{-2} s^{-1} exhibit daily reductions in Fv/Fm ratios of 41 and 24%, respectively. Both photoinhibited cultivars had similar yields of PSII electron transport under light-saturating conditions and similar rates of dry matter accumulation relative to control plants (18). Significantly, the markedly lower efficiency of PSII following sustained photoinhibition is largely overcome in high light (Figs. 1, 2). Although photosynthetic efficiency is suppressed by sustained photoinhibition, the light-saturated photosynthetic rates are sufficiently high under high light to offset any reduction in the photochemical efficiency of PSII (18). Moreover, since PSII is usually not limiting at high light, fewer than 40% functional PSII complexes in photoinhibited leaves can provide the same maximum photosynthetic capacity as 100% functional PSII complexes in non-inhibited plants. It should not be assumed that photoinhibition will necessarily result in dramatic reductions in crop yields.

LITERATURE CITED

1. **Adamson HY, Chow WS, Anderson JM, Vesk M, Sutherland MW** (1991) Photosynthetic acclimation of *Tradescantia albiflora* to growth irradiance: morphological, ultrastructural and growth responses. Physiol Plant **82**: 353-359
2. **Anderson JM, Andersson B** (1988) The dynamic photosynthetic membrane and regulation of solar energy. Trends Biochem Sci **13**: 351-355
3. **Anderson JM, Chow WS, Goodchild DJ** (1988) Thylakoid membrane organization in sun/shade acclimation. Aust J Plant Physiol **15**: 11-26
4. **Anderson JM, Osmond CB** (1987) Shade-sun responses: compromises between acclimation and photoinhibition. *In* DJ Kyle, CB Osmond, CJ Arntzen, eds, Photoinhibition. Elsevier Science Publishers BV, Amsterdam, pp 1-38
5. **Andersson B, Styring S** (1991) Photosystem II: Molecular organization, function and acclimation. *In* CP Lee ed, Current Topics in Bioenergetics Vol 16. Academic Press Inc, San Diego, pp 1-81
6. **Ball MC, Hodges VS, Laughlin GP** (1991) Cold-induced photoinhibition limits regeneration of snow gum at tree-line. Funct Ecol **5**: 663-668
7. **Barber J, Andersson B** (1992) Too much of a good thing: light can be bad for photosynthesis. Trends Biochem Sci **17**: 61-66

8. **Björkmen O, Demmig B** (1987) Photon yield of O_2 evolution and chlorophyll fluorescence characteristics at 77 K among vascular plants of diverse origins. Planta **170**: 489-504

9. **Chow WS** (1993) Photoprotection and photoinhibitory damage. In E Bittar, ed, Advances in Molecular and Cell Biology, Vol 7. Jai Press Inc, Greenwich (in press)

10. **Chow WS, Adamson HY, Anderson JM** (1991) Photosynthetic acclimation of Tradescantia albiflora to growth irradiance: Lack of adjustment of light-harvesting components and its consequences. Physiol Plant **81**: 175-182

11. **Chow WS, Melis A, Anderson JM** (1990) Adjustments of photosystem stoichiometry in chloroplasts improve the quantum efficiency of photosynthesis. Proc Natl Acad Sci USA **87**: 7502-7506

12. **Demmig-Adams B** (1990) Carotenoids and photoprotection in plants: A role for the xanthophyll zeaxanthin. Biochim Biophys Acta **1020**: 1-24

13. **Demmig-Adams B, Adams WW** (1992) Photoprotection and other responses of plants to high light stress. Annu Rev Plant Physiol **43**: 599-626

14. **Evans JR** (1987) The relationship between electron transport components and photosynthetic capacity in pea leaves grown at different irradiances. Aust J Plant Physiol **14**: 157-170

15. **Foyer C, Furbank R, Harbinson J, Horton P** (1990) The mechanisms contributing to photosynthetic control of electron transport by carbon assimilation in leaves. Photosynth Res **25**: 83-100

16. **Genty B, Briantais JM, Baker NR** (1989) The relationship between the quantum yield of photosynthetic electron transport and quenching of chlorophyll fluorescence. Biochim Biophys Acta **990**: 87-92

17. **Greer DH, Ottander C, Öquist G** (1991) Photoinhibition and recovery of photosynthesis in intact barley leaves at 5 and 20°C. Physiol Plant **81**: 203-210.

18. **Hurry V, Krol M, Öquist G, Huner NPA** (1992) Effect of long-term photoinhibition on growth and photosynthesis. Plant Physiol (in press)

19. **Krause GH** (1988) Photoinhibition of photosynthesis. An evaluation of damaging and protective mechanisms. Physiol Plant **74**: 566-574

20. **Melis A** (1991) Dynamics of photosynthetic membrane composition and function. Biochim Biophys Acta **105**: 87-106

21. **Neale PJ** (1987) Algal photoinhibition and photosynthesis in the aquatic environment. In DJ Kyle, CB Osmond, CJ Arntzen eds, Photoinhibition, Topics in Photosynthesis, Vol 9. Elsevier Science Publishers, Amsterdam, pp 39-65

22. **Ögren E** (1988) Photoinhibition of photosynthesis in willow leaves under field conditions. Planta **175**: 229-236

23. **Ögren E** (1991) Prediction of photoinhibition of photosynthesis from measurements of fluorescence quenching components. Planta **184**: 538-544

24. **Öquist G, Chow WS, Anderson JM** (1992) Photoinhibition of photosynthesis represents a mechanism for the long-term regulation of photosystem II. Planta **186**: 450-460

25. **Öquist G, Anderson JM, McCaffery S, Chow WS** (1992) Mechanistic differences in photoinhibition of sun and shade plants. *Planta* **188**: 422-431

26. **Öquist G, Huner NPA** (1991) Effects of cold acclimation on the susceptibility of photosynthesis to photoinhibition in Scots pine and in winter and spring cereals: a fluorescence analysis. *Funct Ecol* **5**: 91-100

27. **Post A, Adamson E, Adamson H** (1990) Photoinhibition and recovery of photosynthesis in Antarctic bryophytes under field conditions. *In* M Baltscheffsky ed, *Current Research in Photosynthesis*, Vol IV. Kluwer Academic Publishers, Dordrecht, pp 635-638

28. **Prásil O, Adir N, Ohad I** (1992) Dynamics of photosystem II: mechanism of photoinhibition and recovery process. *In* J Barber ed, *The Photosystems: Structure, Function and Molecular Biology*. Topics in Photosynthesis, Vol 11. Elsevier Science Publishers BV, Amsterdam, pp 231-250

29. **Raven JA** (1989) Fight or flight : the economics of repair and avoidance of photoinhibition of photosynthesis. *Funct Ecol* **3**: 5-19

30. **Sundby C, McCaffery S, Chow WS, Anderson JM** (1992) Photosystem II function, photoinhibition and turnover of D1 protein at different irradiances in normal and atrazine-resistant plants with an altered Q_B-binding site. *In* N. Murata ed, *Advances in Photosynthesis Research*. Kluwer Academic Press, Dordrecht, (In press)

31. **Weis E, Berry JA** (1987) Quantum efficiency of photosystem II in relation to "energy"-dependent quenching of chlorophyll fluorescence. *Biochim Biophys Acta* **894**: 198-208

Energy Dissipation and Photoprotection in Leaves of Higher Plants[1]

William W. Adams III and Barbara Demmig-Adams

Department of Environmental, Population, and Organismic Biology, University of Colorado, Boulder, CO 80309-0334

INTRODUCTION

When excess photons are absorbed by chlorophyll in a leaf, a photoprotective mechanism becomes engaged to prevent the photosynthetic apparatus from being damaged by the excess energy. The employment of this mechanism occurs routinely for a few hours each day during exposure to peak irradiance in exposed habitats. This mechanism, which is mediated by the carotenoids zeaxanthin and (possibly) antheraxanthin upon their formation from violaxanthin in the xanthophyll cycle, involves the dissipation of energy directly within the light-harvesting chlorophyll complexes where the light is absorbed (for a review see 5).

Some plants, of course, possess additional means of protecting the photosynthetic apparatus against damage from high light by diminishing the absorption of that light, including the movement of chloroplasts to decrease their absorptive area, the movement of entire leaves, either rapidly in response to the prevailing light (paraheliotropism) or as a growth response as the leaves develop, and increased leaf reflectance (due to pubescence or the secretion of waxes). Not all plants, however, employ such preemptive photoprotective mechanisms, and in those that do it is probably such that xanthophyll-associated energy dissipation occurs simultaneously with any mechanism used to decrease the absorption of light. Dissipation also occurs through the utilization of energy in photosynthetic electron transport, including the reduction of acceptors other than CO_2. The latter does not, however, by definition involve the dissipation of excess energy only. Thus dissipation of excess energy in the pigment bed, which

---

[2]Abbreviations: A, antheraxanthin; βC, β-carotene; CAP, chloramphenicol; F_m, maximal chlorophyll fluorescence from PSII when all reaction centers are fully reduced; F_m', maximal chlorophyll fluorescence during exposure to light; L, lutein; N, neoxanthin; NPQ, nonphotochemical quenching of chlorophyll fluorescence; PFD, photon flux density; V, violaxanthin; VDE, violaxanthin de-epoxidase; Z, zeaxanthin; ZE, zeaxanthin epoxidase.

is ubiquitous throughout the plant kingdom, is likely to be the major means of preventing damage to the photosynthetic apparatus.

The energy dissipation process associated with the de-epoxidation products of the xanthophyll cycle counteracts the accumulation of excess excitation energy in the photochemical system that might otherwise occur and result in harmful effects such as photooxidation. There have been numerous studies showing that leaves that are acclimated to low light, chloroplasts isolated from such leaves, or algae acclimated to low light experience some form of damage when exposed to high light. However, it has recently been reported that shade-acclimated leaves (4, 14) contain only very small pools of the xanthophyll cycle components and, in contrast, sun or high light-exposed leaves possess much larger xanthophyll cycle pools. In fact, the xanthophyll cycle pool responds to a change in growth PFD^2 more than any other carotenoid in the thylakoid membranes. For example, the sum of V+A+Z exhibited a 31% increase in spinach leaves grown in an open greenhouse (approximately 85% of full sunlight) relative to those grown in a growth cabinet under 130 µmol photons $m^{-2} s^{-1}$ (approximately 6.5% of full sunlight; Table I). The carotenoid to exhibit the second largest increase, β-carotene, is the immediate biochemical precursor for the xanthophylls of the xanthophyll cycle. Leaves with larger xanthophyll cycle pools presumably possess a greater capacity for energy dissipation in response to excessive light, and sun-exposed leaves and cactus cladodes did exhibit very high levels of energy dissipation during midday exposure (1, 3, 9). We have therefore postulated that sun-exposed leaves are protected by this photoprotective mechanism such that they do not commonly experience damage in the field.

THE XANTHOPHYLL CYCLE AND THE DISSIPATION OF EXCESS ABSORBED ENERGY

There are three xanthophylls (oxygenated carotenoids) in the photosynthetic membranes (thylakoids) of higher plants that undergo light-dependent interconversions (11, 13, 17). When the flux of light striking a leaf is excessive the activity of the enzyme violaxanthin de-epoxidase (VDE) is increased resulting in a conversion of violaxanthin into zeaxanthin via the intermediate antheraxanthin (Fig. 1). In low or limiting light the reverse sequence predominates, being catalyzed by the enzyme zeaxanthin epoxidase (ZE). The three xanthophylls of the cycle are loosely bound in the light-harvesting chlorophyll complexes of both photosystems (15). The main factor that induces de-epoxidation of violaxanthin under excessive light is a low pH at the inner side of the thylakoid membrane. VDE has an acidic pH optimum, and protons accumulate in the lumen under excess light when the rate of ATP utilization is insufficient to match that of ATP generation.

Assessing the role of the de-epoxidation products of the xanthophyll cycle in energy dissipation and photoprotection has been greatly facilitated by the use of an inhibitor of VDE. Dithiothreitol (DTT) inhibits the formation of

28

Table I. *Carotenoid and Chlorophyll Composition of Low Light and High Light Spinach (Spinacia oleracea L.) Leaves*

Low light spinach was grown in a growth chamber under 130 µmol m^{-2} s^{-1} PFD (10h day at 23°C and 14h night at 20°C, 90% relative humidity) and high light spinach in a naturally lit greenhouse in April 1992. All values are the mean of three replicates ±SD.

| Growth PFD | mmol mol^{-1} Chl a+b | | | | µmol m^{-2} | |
	V+A+Z	βC	L	N	Chl a+b	Chl a/b
Low light	83.6 ±0.9	106 ±3.1	144 ±1.1	39.2 ±0.4	442 ±9	3.02 ±0.04
High Light	109.4 ±4.0	118 ±4.8	143 ±0.4	42.2 ±1.2	415 ±16	3.27 ±0.02
% difference	+31	+11	-0.6	+7.7	-6.1	+8.3
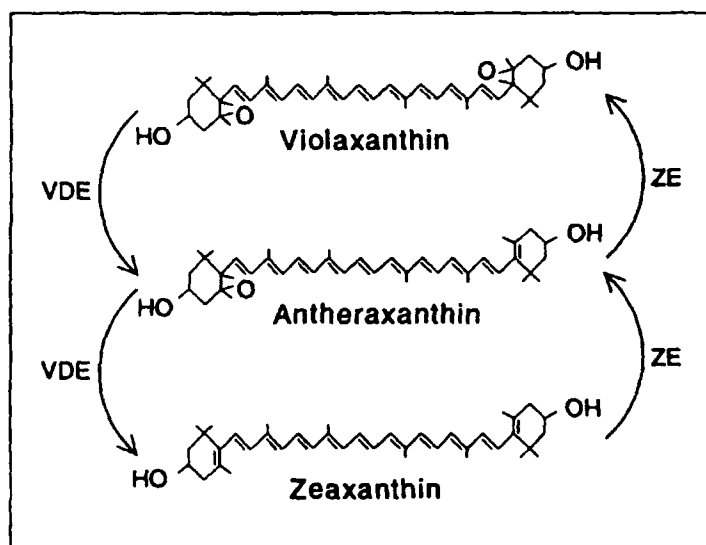
Figure 1. The reactions of the xanthophyll cycle include the de-epoxidation of violaxanthin to antheraxanthin and zeaxanthin by the enzyme violaxanthin de-epoxidase (VDE) when excess light energy is absorbed by chlorophyll and the epoxidation of zeaxanthin to antheraxanthin and violaxanthin by the enzyme zeaxanthin epoxidase (ZE) under conditions of limiting light.

zeaxanthin from violaxanthin, both *in vitro* and *in vivo* (2, 8, 18). Energy dissipation activity that develops in response to the absorption of excess light by chlorophyll can be quantified from the lowering of the yield of maximal

chlorophyll fluorescence from PSII (from F_m in the unquenched or fully relaxed state to F_m' during exposure to light). This decrease in chlorophyll fluorescence, or fluorescence "quenching" (NPQ), can be monitored from intact leaves as shown in Figure 2. The exposure of a control spinach (*Spinacia oleracea* L.) leaf to a PFD equivalent to almost half of full sunlight resulted in a marked lowering of F_m'. On the other hand, the inhibition of violaxanthin de-epoxidase by DTT prevented the majority of the decrease in F_m' from occurring.

The decrease in maximal fluorescence is referred to as nonphotochemical quenching, NPQ, since it does not result from photochemistry. It is due to thermal energy dissipation in the chlorophyll pigment bed that occurs when more energy is absorbed than can be utilized in photosynthesis. The parameter NPQ, calculated from the decrease in maximal chlorophyll fluorescence as $F_m/F_m' -1$, is directly proportional to the energy dissipation activity that is occurring in the pigment bed of a leaf. The calculated levels of NPQ are also shown below the actual traces of chlorophyll fluorescence in Fig. 2. In the control leaf NPQ reached a level of approximately 2.2 after 10 minutes exposure of the leaf to light, whereas in the leaf treated with DTT, NPQ was only 0.4 after 10 minutes exposure to light. Similar results have been obtained with several species of higher plants (2, 6, 8), lichens (7), green algae (12), and isolated chloroplasts (10). Such findings strongly support the involvement of the xanthophyll cycle in photoprotective energy dissipation within the chlorophyll pigment bed.

A determination of the capacity for NPQ in spinach grown under low light versus high light reveals that the high-light acclimated leaf possesses an increased capacity for energy dissipation in the pigment bed which parallels the larger capacity for the formation of zeaxanthin or zeaxanthin + antheraxanthin (Table II). Thus such sun leaves presumably have a greater capacity for photoprotection through this photoprotective mechanism.

PREVENTING AN ACCUMULATION OF EXCESS ENERGY IN HIGH LIGHT

Another parameter which can be calculated from measurements of chlorophyll fluorescence such as those shown in Fig. 2 is the reduction state of PSII. The reduction state of PSII indicates what percentage of the reaction centers are reduced or closed. A high reduction state is indicative of a large accumulation of excess energy and in such a state damage is more likely to occur to the system. The factors which can maintain the reduction state of PSII at a low and safe level include the utilization of electrons in photosynthesis and other reducing pathways as well as energy dissipation in the pigment bed.

Light response curves of the reduction state of PSII in a control leaf and one treated with DTT are shown in Figure 3. At low PFDs, when light is limiting photosynthesis (below 200 μmol m^{-2} s^{-1}), the reduction state of PSII was low in both leav... At subsequent, higher PFDs the measured reduction state of PSII was 22 to 29% higher in the leaf treated with DTT (-NPQ$_{meas}$), i.e. in the
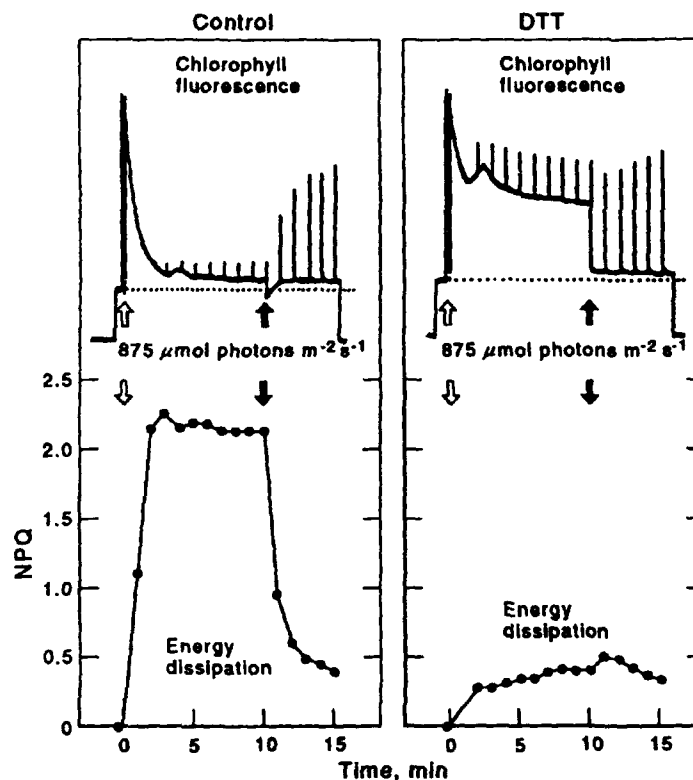
Figure 2. Time course of changes in chlorophyll fluorescence yield and in thermal energy dissipation calculated as NPQ in a control leaf of spinach (*Spinacia oleracea* L.) and one pretreated with DTT to inhibit the de-epoxidation of violaxanthin and the development of energy dissipation. The control level of maximal fluorescence (F_m), obtained with a saturating flash of light in darkness, is represented by the first spike in fluorescence at the left in each figure. Following these determinations, the actinic light (875 µmol m^{-2} s^{-1}) was switched on (at the open arrows) and maximal fluorescence determined at one minute intervals during illumination (F_m'). After 10 min of illumination the actinic light was switched off (at the black arrows). NPQ was calculated as F_m/F_m' -1. Recalculated from ref. 8.

absence of thermal energy dissipation, than in the control leaf. Thus the dissipation of excess excitation energy within the chlorophyll pigment bed acts to maintain the reduction state of PSII at a lower level than it might otherwise be when light is in excess. Furthermore, recalculation of the control leaf data such that the effect of NPQ on the reduction state was eliminated yielded results very similar to those of the DTT-treated leaf in which thermal energy dissipation as actually inhibited (Fig. 3). These data provide evidence for a photoprotective role of the xanthophyll-associated energy dissipation process in the pigment bed.

31

Table II. *Xanthophyll Cycle Composition and NPQ Determined from Low Light and High Light Spinach Leaves during Illumination with High Light*

Low and high light spinach were grown as described in Table I. NPQ was determined after equilibration to steady-state under 2050 µmol m^{-2} s^{-1} PFD in air at 25°C, and leaf discs removed rapidly for pigment analysis immediately thereafter. All pigment data are the mean of three replicates ±SD. The NPQ level was the maximal possible in each case and a further increase in PFD did not result in further quenching (not shown).

Growth PFD	mmol mol^{-1} Chl a+b				$Z/$ $(V+A+Z)$	$(Z+A)/$ $(V+A+Z)$	NPQ
	V	A	Z	Z+A			
Low light	21.5	9.0	53.1	62.7	0.635	0.743	2.56
	±1.0	±0.4	±1.1	±0.8	±0.014	±0.010	
High light	18.8	12.9	77.6	90.5	0.710	0.828	3.22
	±0.5	±0.5	±3.3	±3.6	±0.004	±0.004	
% change	-13	+43	+46	+44	+12	+11	+26

PREVENTING AN INHIBITION OF PHOTOSYNTHESIS IN HIGH LIGHT

As we stated in the introduction, a number of studies have been conducted that have shown that the photosynthetic apparatus of low-light acclimated organisms experiences some form of damage when exposed to excessive light. However, such organisms have not only a low capacity for the utilization of that light energy through photosynthesis, but also a lower capacity for the thermal dissipation of excess energy due to a relatively small xanthophyll cycle pool (e.g. Tables I and II). To examine the relative roles of photoprotective energy dissipation versus damage and repair in high light acclimated spinach leaves, such leaves were treated to inhibit each process individually and together during exposure to high light. During a subsequent 90 min period of recovery under low light the efficiency of photosynthetic energy conversion, which had been inhibited to 40% of the value determined prior to exposure to high light, exhibited almost no recovery in the leaf in which both thermal energy dissipation and chloroplast protein synthesis had been inhibited (Fig. 4). The control leaf exhibited the smallest reduction subsequent to the high light treatment (approximately a 25% inhibition), and also exhibited complete recovery to the pretreatment level after 90 min. The leaves in which only energy dissipation, or only chloroplast protein synthesis, were inhibited exhibited intermediate responses, with both showing substantial and continued recovery during the 90 min in low light subsequent to the exposure to high light.

These results indicate that during a high light treatment of sun leaves only those leaves (treated with CAP+DTT) that are incapable of dissipating energy

within the chlorophyll pigment bed as well as being unable to synthesis chloroplast proteins experience a sustained depression of the efficiency of photosynthetic energy conversion. On the other hand, high light acclimated CAP-treated leaves which can still dissipate energy, those which are DTT-treated and can still repair damage through the synthesis of chloroplast proteins, or those which can do both (untreated controls) do not experience irreversible damage to
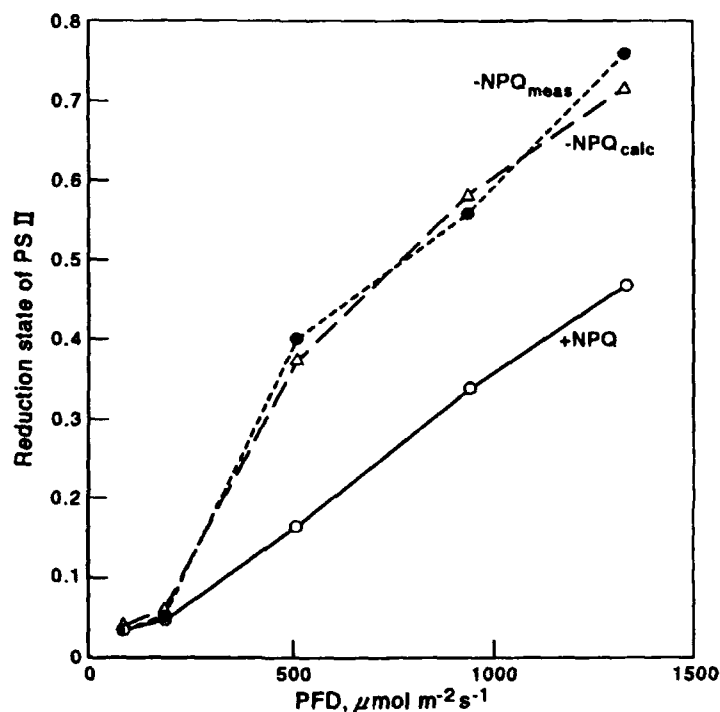
Figure 3. Reduction state of PSII at various PFD's in spinach leaves in the presence and absence of energy dissipation in the pigment bed (NPQ) in 5% CO_2 at 25°C. +NPQ = measured values of the reduction state of PSII in untreated control leaves. -NPQ_{meas} = measured values of the reduction state of PSII in DTT-treated leaves in which the de-epoxidation of violaxanthin, and thus NPQ, were inhibited. -NPQ_{calc} = calculated values of the reduction state in control leaves under the assumption that NPQ was absent. The latter was calculated from the actual photochemical efficiency of PSII F_m'-F/$F_m' = F_v'/F_m' \times (1$-$Q_r/Q_t)$, rearranged to $Q_r/Q_t = 1$-$(F_m'$-F/F_m' at each PFD)/(F_v'/F_m' at 50 μmol m^{-2} s^{-1} PFD). F_v'/F_m' at 50 μmol m^{-2} s^{-1} PFD is the intrinsic photon efficiency of PSII in the absence of energy dissipation in the pigment bed. See van Kooten and Snel (16) for an explanation of the chlorophyll fluorescence nomenclature. Q_r/Q_t is the ratio of reduced PSII centers to the total PSII centers, i.e. the reduction state of PSII or 1-q_p. Data calculated from ref. 8.
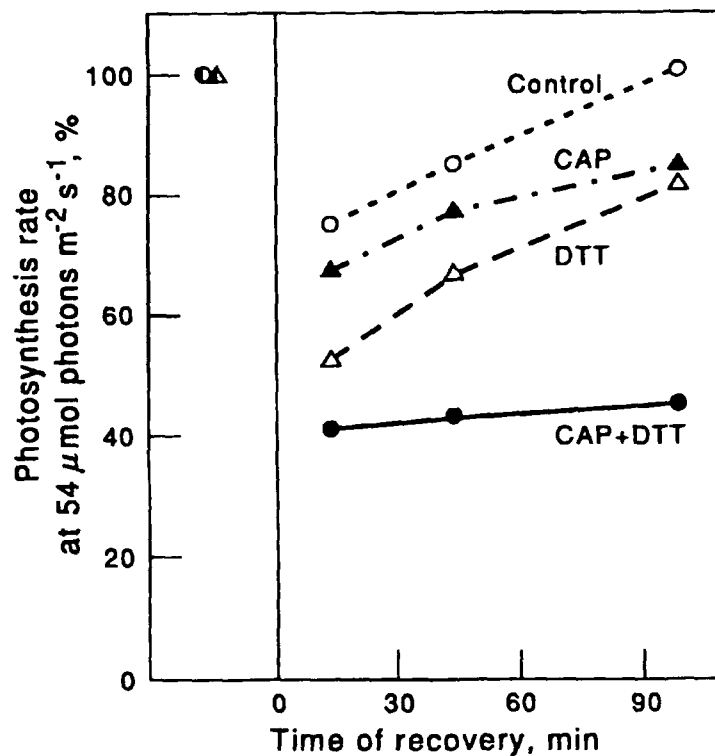
Figure 4. Effect of an inhibition of chloroplast protein synthesis (by CAP), or thermal energy dissipation (by DTT), or both (CAP+DTT) on the efficiency of photosynthetic energy conversion at low PFD subsequent to a high light treatment (1950 μmol m^{-2} s^{-1} for 60 min at 20°C in 5% CO_2) in spinach leaves. Leaves were pretreated by placing the cut petiole into either water (control), 300 μM CAP, 3 to 5 mM DTT, or both CAP and DTT and allowing the leaf to take up the solution for 90 min under an incident PFD of 40 μmol m^{-1} s^{-1}. The rate of photosynthesis was determined by measurements of O_2 evolution at saturating partial pressures of CO_2 and under a low PFD of 54 μmol m^{-2} s^{-1} at 20°C. Subsequent to the high light treatment the leaves were returned to low PFD and maintained at this PFD with the measurements of photosynthesis obtained at the indicated points in time. Photosynthesis is expressed as a percent of the value obtained prior to the exposure to high light for each leaf. This value was the same before and after the uptake of the various solutions under 40 μmol m^{-2} s^{-1} PFD for 90 min. Based on the amount of CAP solution taken up by the leaf the final CAP concentration in the bulk leaf water was estimated to be 150 μM CAP.

the photosynthetic apparatus during exposure to high light. These results are substantially different from those previously reported for shade-acclimated organisms.

34

We have verified that CAP is taken up by the sun leaves by exposing spinach leaves to a range of CAP concentrations. The CAP concentration used in the experiment shown in Figure 4 is 150 μM CAP in the bulk leaf water and is just below the concentrations that resulted in inhibitory side effects to photosynthesis in low light prior to exposure to high light. Thus our results suggest that sun leaves with large xanthophyll cycle pools depend strongly on repair processes only when energy dissipation in the pigment bed is inhibited during exposure to high light.

LITERATURE CITED

1. **Adams WW III, Díaz M, Winter K** (1989) Diurnal changes in photochemical efficiency, the reduction state of Q, radiationless energy dissipation, and non-photochemical fluorescence quenching in cacti exposed to natural sunlight in northern Venezuela. Oecologia 80: 553-561

2. **Bilger W, Björkman O** (1990) Role of the xanthophyll cycle in photoprotection elucidated by measurements of light-induced absorbance changes, fluorescence and photosynthesis in leaves of Hedera canariensis. Photosynth Res 25: 173-185

3. **Björkman O, Demmig-Adams B** (1993) Regulation of photosynthetic light energy capture, conversion and dissipation in leaves of higher plants. In E-D Schulze, MM Caldwell, eds, Ecology of Photosynthesis, Ecological Studies 100, Springer, Berlin, in press

4. **Demmig-Adams B, Adams WW III** (1992) Carotenoid composition in sun and shade leaves of plants with different life forms. Plant Cell Environ 15: 411-419

5. **Demmig-Adams B, Adams WW III** (1992) Photoprotection and other responses of plants to high light stress. Annu Rev Plant Physiol Plant Mol Biol 43: 599-626

6. **Demmig-Adams B, Adams WW III** (1993) The xanthophyll cycle. In A Young, G Britton, eds, Carotenoids in Photosynthesis. Springer, Berlin, in press

7. **Demmig-Adams B, Adams WW III, Czygan F-C, Schreiber U, Lange OL** (1990) Differences in the capacity for radiationless energy dissipation in green and blue-green algal lichens associated with differences in carotenoid composition. Planta 180: 582-589

8. **Demmig-Adams B, Adams WW III, Heber U, Neimanis S, Winter K, Krüger A, Czygan F-C, Bilger W, Björkman O** (1990) Inhibition of zeaxanthin formation and of rapid changes in radiationless energy dissipation by dithiothreitol in spinach leaves and chloroplasts. Plant Physiol 92: 293-301

9. **Demmig-Adams B, Adams WW III, Winter K, Meyer A, Schreiber U, Pereira JS, Krüger A, Czygan F-C, Lange OL** (1989) Photochemical efficiency of photosystem II, photon yield of O_2 evolution, photosynthetic capacity, and carotenoid composition during the "midday depression" of net CO_2 uptake in Arbutus unedo growing in Portugal. Planta 177: 377-387

10. **Gilmore AM, Yamamoto HY** (1991) Zeaxanthin formation and energy-dependent fluorescence quenching in pea chloroplasts under artificially-mediated linear and cyclic electron transport. Plant Physiol **96**: 635-643

11. **Hager A** (1980) The reversible, light-induced conversions of xanthophyils in the chloroplast. *In* F-C Czygan, ed, Pigments in Plants. Fischer, Stuttgart, pp 57-79

12. **Osmond CB, Ramus J, Levavasseur G, Franklin LA, Henley WJ** (1993) Fluorescence quenching during photosynthesis and photoinhibition of *Ulva rotundata* Blid. Planta, in press

13. **Siefermann-Harms D** (1977) The xanthophyll cycle in higher plants. *In* M Tevini, HK Lichtenthaler, eds, Lipids and Lipid Polymers in Higher Plants. Springer, Berlin, pp 218-230

14. **Thayer SS, Björkman O** (1990) Leaf xanthophyll content and composition in sun and shade determined by HPLC. Photosynth Res **23**: 331-343

15. **Thayer SS, Björkman O** (1992) Carotenoid distribution and deepoxidation in thylakoid pigment-protein complexes from cotton leaves and bundle sheath cells of maize. Photosynth Res 33:213-225

16. **van Kooten O, Snel JFH** (1990) The use of chlorophyll fluorescence nomenclature in plant stress physiology. Photosynth Res **25**: 147-150

17. **Yamamoto HY** (1979) Biochemistry of the violaxanthin cycle in higher plants. Pure Appl Chem **51**: 639-648

18. **Yamamoto HY, Kamite L** (1972) The effects of dithiothreitol on violaxanthin de-epoxidation and absorbance changes in the 500-nm region. Biochim Biophys Acta **267**: 538-543

Effects of UV-B Radiation on Plant Productivity

Alan H. Teramura and Joe H. Sullivan

Department of Botany, University of Maryland, College Park, MD 20742, USA

INTRODUCTION

Continued depletion of the earth's stratospheric ozone layer is of concern because this ozone column is the primary attenuator of solar ultraviolet-B radiation (UV-B region, between 290 and 320 nm). A decrease in this ozone column would lead to increases in UV-B radiation reaching the earth's surface. Though representing only a small fraction of the total solar electromagnetic spectrum, UV-B has a disproportionately large photobiological effect. One reason is that UV is readily absorbed by important macromolecules such as proteins and nucleic acids (8). Therefore, both plant and animal life would be greatly affected by increases in UV-B radiation penetrating to the earth's surface.

Previous studies have shown that tremendous variability exists among plant species in sensitivity to UV-B radiation (interspecific variation). Some species show sensitivity to current ambient levels of UV-B radiation (5), while others are apparently unaffected by large UV enhancements (22, 28). This interspecific variation is further exacerbated by reports of equally large response differences among cultivars of a single species (intraspecific variation) (29, 31).

A compilation of data from approximately two decades of study indicates that about one-half of all species studied are deleteriously affected by UV-B radiation levels above ambient. However, many species exhibit no such adverse effects and this suggests that some plants are well-adapted to UV-B radiation. The extent of these natural adaptations may be related to the geographic origin of the species. For example, species originating from areas which receive high levels of UV-B radiation may be highly resistant to UV-B radiation, *ceteris paribus*. Evidence for this was found in plants collected along a 3,000 m elevational gradient in Hawaii as UV-B radiation sensitivity was correlated with elevation of seed collection (28). Most plants native to low elevations were sensitive to UV-B radiation, but plants from the higher elevations, where natural UV-B radiation fluxes are greatest, were very tolerant to UV-B radiation.

Of ten major terrestrial ecosystems, representatives of only four have been studied for UV-B radiation sensitivity (Table 1). The vast majority of the

species tested have been annual agricultural species, which account for only approximately 9% of global net primary productivity, NPP[1]. This paucity of data coupled with the wide range in sensitivity already described, makes any assessment of potential consequences of ozone depletion at the ecosystem level quite speculative. This manuscript summarizes some of the physiological and morphometric responses commonly observed in plants grown in the presence of UV-B radiation and the integration of these responses into effects on productivity.

UV-B PENETRATION INTO THE LEAF

In order for UV-B radiation to be effective in altering plant biochemistry, physiology or productivity, it must penetrate the leaf to sensitive targets and be absorbed by chromophores present. Beggs *et al.* (3) summarized three general classes of protective responses to UV-B radiation as: 1) those that avoid damage by preventing UV-B from reaching sensitive targets (e.g. changes in leaf reflectance or epidermal absorbance), 2) those that minimize damage by growth delay, and 3) those that mitigate damage by repair mechanisms such as photoreactivation or post-transcriptional repair.

One commonly observed response to UV-B radiation, which might reduce UV-B penetration to sensitive targets, is an increase in leaf thickness. For

Table I. *Survey of UV studies by major terrestrial plant ecosystem (34).*

Ecosystem	Global NPP (10^9 ton yr^{-1})	Total Area (10^6 km^2)	Included in UV Study
Tropical Forest	49.9	24.5	no
Temperate Forest	14.9	12.0	yes
Savana	13.5	15.0	no
Boreal Forest	9.6	12.0	no
Agricultural	9.1	14.0	yes
Woodland or Shrubland	6.0	8.5	no
Temperate Grassland	5.4	9.0	yes
Swamp or Marsh	4.0	2.0	no
Desert and Semidesert	1.7	42.0	no
Tundra and Alpine	1.1	8.0	yes

example Murali *et al.* (17) reported that specific leaf weight (SLW), a surrogate for leaf thickness, increased in the soybean cultivar Williams but not in Essex and this response was correlated with sensitivity differences between those two cultivars, with Williams being classified as UV-B resistant. Likewise, Bornman and Vogelmann (6) reported increases in leaf thickness of 45% in *Brassica campestris* in response to UV-B radiation.

However, the mechanism of UV-B protection that has received the most attention by plant physiologists and ecologists has been that of the accumulation of UV-absorbing compounds in leaf tissue in response to UV-B radiation. Flavonoids are one group of compounds which may accumulate in the leaf epidermis in response to UV-B radiation. The role of flavonoids in UV-B radiation protection was hypothesized over two decades ago (10) and has since been considered frequently (e.g. 20, 25, 32). The accumulation of flavonoids in the epidermis has been shown to reduce epidermal transmittance of UV-B radiation (20).

Flavonoid accumulation is dependent upon a number of factors including both visible and UV fluence (14, 34) and almost any other environmental stress such as drought, temperature, nutrient stress or pathogen/insect infestation (12). The mechanistic basis of light or UV-induced accumulation appears to lie at the gene level as key enzymes in the flavonoid biosynthetic pathway are specifically induced by UV-B radiation. For example, it has been shown that UV-B radiation increases the levels of mRNA and enzymes, especially chalcone synthase and phenylalanine ammonia lyase (CHS and PAL), involved in flavonoid biosynthesis (7). This increase results in flavonoid accumulation (2).

However, several studies have indicated that the damaging effects of UV-B radiation may not be mitigated simply by an apparent increase in foliar flavonoid concentrations (13, 23, 25). Also, Barnes *et al.* (1) reported that the photosynthetic apparatus of some plants from high elevation tropical areas was inherently more resistant to UV-B radiation than that of other plants from lower elevation and that this difference was apparently not attributable to increases in flavonoid concentrations. Therefore a relationship between flavonoid accumulation and UV-protection often exists, but a number of inconsistencies suggest that a simple correlation between leaf flavonoid concentration and UV-B radiation tolerance may not always exist.

Clearly, anatomical and biochemical differences among species affect the penetration of UV-B radiation into the leaf. Using a fibre optic microprobe, a recent survey of some 22 plant species (T.A. Day, personal communication) has shown a wide range of differences in the penetration of UV-B radiation through the epidermis. However, additional protective and repair mechanisms, such as photoreactivation, where pyrimidine dimers may be repaired by a light-regulated DNA photolyase (11) are also associated with UV-B radiation sensitivity. In conclusion, plants have a number of natural adaptations which protect them from

39

the deleterious impacts of UV-B radiation, but we presently lack many mechanistic details in our efforts to fully understand UV-B radiation sensitivity.

UV-B RADIATION EFFECTS ON PHOTOSYNTHESIS

The penetration of UV-B radiation through the epidermis may result in reductions in net carbon assimilation (photosynthesis) by imposing a variety of direct and indirect limitations on photosynthesis (Table II). However, damage to photosynthetic processes has not been observed in all species upon exposure to UV-B radiation (e.g. 4), so it is apparent that some plants are well-protected from UV-B radiation damage as described above. Nonetheless, in sensitive species, UV-B radiation may indirectly limit photosynthesis by photodegradation of photosynthetic pigments, altering stomatal conductance or regulation, or by altering the visible light regime within the leaf due to anatomical (e.g. leaf thickness) or morphological (e.g. canopy architectural) changes (Table II).

Other studies have shown that UV-B radiation may limit photosynthesis by direct effects on the photosynthetic machinery (Table II). Direct damage to photosystem II, as indicated by changes in chlorophyll fluorescence, has been reported in isolated chloroplasts, cell suspensions and in intact tissue (6, 9, 24, 32). Also diagnostic assessments of the responses of CO_2 assimilation to light and internal CO_2 concentration under enhanced UV-B radiation have demonstrated reductions in apparent quantum efficiency and RuBP (substrate) regeneration capacity (25, 26).

Measurements of reductions in assimilation capacity are not necessarily correlated with reduced growth. Some studies have shown changes in growth without observed reductions in photosynthetic rate and other studies have observed reductions in some aspect of photosynthesis without concurrent growth reductions. One reason for this apparent inconsistency lies in the wide range UV-B radiation sensitivity present among plant species and cultivars. This is further confounded by contrasting growth conditions and irradiation protocols among previous studies and because UV-B effectiveness is strongly influenced by other environmental parameters. For example, sensitivity to UV-B radiation is reduced under conditions of drought stress (16, 26) and nutrient deficiency (15). However, under low background levels of visible irradiances, the effects of UV-B radiation on photosynthesis and growth may be exacerbated (13, 33). For these reasons, the results of growth chamber or greenhouse studies must be validated under realistic field conditions in order to adequately assess the potential consequences of increasing solar UV-B radiation on plant productivity.

GROWTH AND PRODUCTIVITY

A critical parameter assessed in most previous studies on the effects of UV-B radiation on plants is growth or productivity. Since growth and seed

40

Table II. *Summary of some effects of UV-B radiation on photosynthesis*

Apparent Effect	Methodology	Damage/Symptom
Direct Effects		
Quantum yield	O_2 evolution	Reduced slope/light curve[a]
	CO_2 assimilation	Reduced slope/light curve[26]
RuBP regeneration	CO_2 assimilation	Saturated A * Ci response[26]
Amax	O_2 evolution	Lower potential capacity[1,31]
Lower light saturation	CO_2 assimilation	Potential photoinhibition[26]
Electron transport	*In vivo* fluorescence	Photosystem II damage[6]
Altered thylakoid structure	Isolated chloroplasts	Reduced photochemical activity[18]
Indirect Effects		
Altered leaf optical Properties	Fiber-optic probe	Increased SLW/epidermal chemistry[6]
Altered canopy morphology	Canopy modeling	Reduced available light[21]
Chlorophyll reduction	Chlorophyll analysis	Reduced utilization of light[1,6]
Stomatal function	Porometry	Lower conductance/Ci[19]

[a]Sullivan and Teramura, unpublished

production may differ considerably between controlled environment and field studies, and due to the interaction of UV-B radiation sensitivity with microclimate, this discussion will examine field studies only. During the past decade, only 12 field studies have examined the effects of UV radiation enhancement on the yield of some 22 crop and three tree species. Over half of these studies were conducted over only a single growing season and only two were conducted over more than two years (27, 30). Thus, only scant information exists on the annual variation which occurs in field studies.

Two studies conducted over multiple field seasons have examined the effects of UV-B radiation on soybean yield. The first study was conducted over a two year period during 1981 and 1982 and UV-B radiation had little impact on biomass or yield of several soybean cultivars (22). These results contrast with

41

a six-year study on two soybean cultivars conducted at the University of Maryland (30) from 1981 to 1986. The results of that study demonstrated intraspecific differences in UV-B sensitivity in soybean yield and seed quality. Furthermore, the expression of these sensitivity differences to UV-B radiation was altered by other prevailin :, microclimatic factors. For the sensitive soybean cultivar, Essex, a simulated 25% ozone depletion reduced overall yield by 19-25% in 4 of the 6 years. However, no reductions in yield were detected in the 1983 and 1984 seasons. These years were characterized as hot and dry years with prolonged periods of drought, and such conditions may mask the effects of UV-B radiation (16, 26). That multiyear study demonstrated the necessity of field studies conducted over several growing seasons as crucial to the realistic assessment of the potential impact of increasing UV-B radiation on plant productivity.

The contrasts in results obtained between the two studies above may have bec. due to differences in cultivar sensitivity, microclimate or irradiation protocols. However, it is apparent that the potential for UV-induced reductions in yield exists under some conditions and in some plant cultivars. It is further apparent that studies of one or even two seasons may not be adequate to realistically assess the long-term consequences of ozone depletion on plant productivity.

In conclusion, it is apparent that plants possess a wide range of sensitivities to UV-B radiation and that concurrent environmental conditions (e.g. water or nutrient availabili, PAR, etc.) may alter this sensitivity. Therefore, until we further understand the mechanisms of UV-B radiation damage or protection, it will be difficult to predict the consequences of ozone depletion on untested species and within a changing global atmosphere and climate.

LITERATURE CITED

1. **Barnes PW, Flint SD, Caldwell MM** (1987) Photosynthesis damage and protective pigments in plants from a latitudinal arctic/alpine gradient exposed to supplemental UV-B radiation in the field. Arctic and Alpine Research **19**: 21-27
2. **Beerhues L, Robenek H, Wiermann R** (1988) Chalcone synthesis from spinach (*Spinacia oleracea* L.) II. Immunofluorescence and immunogold localization Planta **173**: 544-553
3. **Beggs CJ, Schneider-Ziebert U, Wellman E** (1985) UV-B radiation and adaptive mechanisms in plants. *In* RC Worrest, ed, Stratospheric Ozone Reduction, Solar Ultraviolet Radiation and Plant Life, Springer-Verlag, Berlin, pp 235-250
4. **Beyschlag W, Barnes PW, Flint SW, Caldwell MM** (1988) Enhanced UV-B radiation has no effect on photosynthetic characteristics of wheat (*Triticum aestivum* L.) and wild oat (*Avena fatua* L.) under greenhouse and field conditions. Photosynthetica **22**: 516-525

5. **Bogenrieder A, Klein R** (1978) Die abhangigkeit der UV-empfindlichkeit von der lichtqualitat bei der aufzucht (*Lactuca sativa* L.). Angew Botanik **52**: 283-293

6. **Bornman JF, Vogelmann TC** (1991) The effect of UV-B radiation on leaf optical properties measured with fiber optics. J Exp Bot **42**: 547-554

7. **Chappell J, Hahlbrock K** (1984) Transcription of plant defense genes in response to UV light or fungal elicitor. Nature (London) **311**:76-78

8. **Giese AC,** (1964) Studies on ultraviolet radiation action upon animal cells. *In* Editors A.C. Giese, ed., Photophysiology Vol. 2, , pp. 203-245. Academic Press, NY-London

9. **Iwanzik W, Tevini M, Dohnt G, Voss M, Weiss W, Graber P, Renger G** (1983) Action of UV-B radiation on photosynthetic primary reactions in spinach chloroplasts. Physiol Plant **58**: 401-407

10. **Jagger J** (1967) Introduction to research in ultraviolet photobiology. Prentice Hall, Englewood Cliffs, New Jersey.

11. **Langer B, Wellmann E** (1990) Phytochrome induction of photoreactivation in *Phaseolus vulgaris* L. seedlings. Photochem Photobiol **52**: 861-864

12. **McClure JW** (1986) Physiology of flavonoids in plants. pp. 77-85. *In* V. Cody, E. Middleton and J.B. Harborne, eds., Plant Flavonoids in Biology and Medicine: Biochemical, Pharmacological, and Structure-activity Relationships., Alan Riss, Inc.

13. **Mirecki RM, Teramura AH** (1984) Effects of ultraviolet-B irradiance on soybean. V. The dependence of plant sensitivity on the photosynthetic photon flux density during and after leaf expansion. Plant Physiol **74**: 475-480

14. **Mohr H, Drumm-Herrel H** (1983) Coaction between phytochrome and blue/UV light in anthocyanin synthesis in seedlings. Physiol Plant **58**: 408-414

15. **Murali NS, Teramura AH** (1985) Effects of ultraviolet-B irradiance on soybean. VI. Influence of phosphorus nutrition on growth and flavonoid content. Physiol Plant **63**: 413-416

16. **Murali NS, Teramura AH** (1986) Effectiveness of UV-B radiation on the growth and physiology of field-grown soybean modified by water stress. Photochem Photobiol **44**: 215-220

17. **Murali NS, Teramura AH, Randall SK** (1988) Response differences between two soybean cultivars with contrasting UV-B radiation sensitivities. Photochem Photobiol **47**: 1-5

18. **Nedunchezhian N, Kulandaivelu G** (1991) Evidence for the ultraviolet-B (280-320 nm) radiation induced structural reorganization and damage of photosystem II polypeptides in isolated chloroplasts. Physiol Plant **81**: 558-562

19. **Negash L, Bjorn LO** (1986) Stomatal closure by ultraviolet radiation. Physiol Plant **66**: 360-364

20. **Robberecht R, Caldwell MM** (1978) Leaf epidermal transmittance of ultraviolet radiation and its implications for plant sensitivity to ultraviolet-radiation induced injury. Oecologia (Berl.) **32**: 277-287

21. **Ryel RJ, Barnes PW, Beyschlag W, Caldwell MM, Flint SD** (1990) Plant competition for light analyzed with a multispecies canopy model. I. Model development and influences of enhanced UV-B conditions on photosynthesis in mixed wheat and wild oat canopies. Oecologia **82**: 304-310

22. **Sinclair TR, N'Diaye O, Biggs RH** (1990) Growth and yield of field-grown soybean in response to enhanced exposure to UV-B radiation. J Environ Qual **19**:478-481

23. **Sisson WB** (1981) Photosynthesis, growth, and ultraviolet irradiance absorbance of *Curcurbita pepo* L. leaves exposed to ultraviolet-B radiation (280-315 nm). Plant Physiol **67**: 120-124

24. **Smillie RM** (1982) Chlorophyll fluorescence *in vivo* as a probe for rapid measurement of tolerance to ultraviolet radiation. Plant Sci Letters **28**: 283-289

25. **Sullivan JH, Teramura AH** (1989) The effects of ultraviolet-B radiation on loblolly pine: 1. Growth, photosynthesis and pigment production in greenhouse-grown seedlings. Physiol Plant **77**: 202-207

26. **Sullivan JH, Teramura AH** (1990) Field study of the interaction between supplemental UV-B radiation and drought in soybean. Plant Physiol **92**: 141-146

27. **Sullivan JH, Teramura AH** (1992) The effects of ultraviolet-B radiation on loblolly pines. 2. Growth of field-grown seedlings. Trees. **6**:115-120

28. **Sullivan JH, Teramura AH, Ziska LH** (1992). Variation in UV-B sensitivity in plants from a 3000 m elevational gradient in Hawaii. Amer J Bot **79**: 737-743

29. **Teramura AH, Murali NS** (1986) Intraspecific differences in growth and yield of soybean exposed to ultraviolet-B radiation under greenhouse and field conditions. Environmental and Experimental Botany **26**: 89-95

30. **Teramura AH, Sullivan JH, Lydon J** (1990) The effectiveness of UV-B radiation in altering soybean yield: A six year field study. Physiol Plant **80**: 5-11

31. **Teramura AH, Ziska LH, Sztein AE** (1991) Changes in growth and photosynthetic capacity of rice with increased UV-B radiation. Physiol Plant **83**: 373-380

32. **Tevini M, Braun J, Fieser F** (1991) The protective function of the epidermal layer of rye seedlings against ultraviolet-B radiation. Photochem Photobiol **53**: 329-333

33. **Warner CW, Caldwell MM** (1983) Influence of photon flux density in the 400-700 nm waveband of inhibition of photosynthesis by UV-B (280-320 nm) irradiation in soybean leaves: separation of indirect and immediate effects. Photochem Photobiol **38**: 341-346

34. **Wellman E** (1983) UV radiation: Definitions, characteristics and general effects. *In* W. Shropshire & H. Mohr, ed., Encyclopedia of Plant Physiology, New Series. Vol. 16B. pp. 745-756. Springer Verlag, Berlin

35. **Whittaker RH** (1975) Communities and Ecosystems. MacMillan Co., New York

Quantifying the Effects of Ultraviolet Radiation on Aquatic Photosynthesis[1]

John J. Cullen and Patrick J. Neale

Department of Oceanography, Dalhousie University, Halifax, Nova Scotia, Canada B3H 4J1 (JJC), Department of Plant Biology, University of California, Berkeley, CA 94720 (PJN), and Bigelow Laboratory for Ocean Sciences, West Boothbay Harbor, Maine 04575 (JJC, PJN)

INTRODUCTION

Stratospheric ozone depletion is occurring world-wide, most severely in the Antarctic "ozone hole" (58). Accordingly, phytoplankton communities are receiving higher exposures to UVB[2] (280-320 nm) as a proportion of total irradiance (37, 55, 57). Because phytoplankton form the base of most aquatic food webs and because UVB is harmful to many biological processes (5, 14, 28, 61), a great deal of interest and concern has been expressed about the impact of increased UVB on phytoplankton in particular and marine ecosystems in general (19). Ecosystem function is complex, and it is likely that more than one direct effect of UVB will influence the species composition and productivity of aquatic systems (17, 19, 55, 64). Nonetheless, it is important to characterize the direct effect of UV on phytoplankton photosynthesis in order to estimate its importance to ecosystem response. With this in mind, we describe an approach to quantifying the acute effects of UV on aquatic photosynthesis.

[2]Abbreviations: UVB, middle ultraviolet radiation; BWF, biological weighting function; P-I, photosynthesis versus irradiance (PAR); UVA, near ultraviolet radiation; E_{PAR}, irradiance in energy units (PAR); P^B, rate of photosynthesis normalized to Chl; P_s^B, maximum attainable rate of photosynthesis as a function of E_{PAR}; E_s, I_k saturation parameters of P-I; E'_{inh}, biologically weighted dimensionless dose rate for photoinhibition of photosynthesis; ε, biological weighting coefficient; ε_{PAR}, biological weighting coefficient for damage to photosynthesis by E_{PAR}; BWF/P-I, photosynthesis versus PAR as influenced by biologically-weighted UV; PCA, principal component analysis; TOMS, Total Ozone Mapping System; DU, Dobson Units.

UVB AND THE MEASUREMENT OF PRIMARY PRODUCTION

Photosynthesis of phytoplankton is conventionally estimated by incubating water samples for several hours or more at the depths from which they were obtained, measuring the incorporation of ^{14}C bicarbonate into particulate matter or by determining changes of oxygen concentration in transparent and opaque bottles. A common expedient, the simulated *in situ* method, is to incubate samples under solar irradiance attenuated by neutral density screens, sometimes used in conjunction with colored filters (35). In either case, commonly used glass or plastic containers and the walls of incubators attenuate UVB radiation, potentially protecting the phytoplankton from photoinhibition. Numerous studies (52) have shown that the environmental UVB excluded by glass or plastics can reduce photosynthesis during incubations of phytoplankton (Fig. 1A), leading to the conclusion that UVB inhibits photosynthesis *in situ*. Quantitative extrapolation to nature has been problematic, however, because incubations do not fully mimic natural conditions. Thus, pioneering investigators (36, 56, 59) stated clearly that the effects they quantified were relevant to the *measurement* of primary productivity rather than to productivity *in situ*.

UV AND PRIMARY PRODUCTION *IN SITU*

Assessment of the acute effects of environmental UV on marine primary productivity *in situ* requires an integrated model with several components: 1) an atmospheric model for calculating spectral irradiance reaching the sea-surface (37); 2) a biological-optical model for specifying wavelength-dependent extinction of UV and visible radiation with depth in the water column, ideally as a function of Chl and dissolved organic matter in the water (1, 53, 54); 3) a BWF, or action spectrum (Fig. 1B), to account for the wavelength-dependence of photoinhibition of photosynthesis (5, 8, 11, 23, 41, 49, 56); 4) a description of the variable depth of phytoplankton during vertical mixing to account for the differences between static incubations and natural movements of phytoplankton (16, 25, 33, 54, 65); and 5) a biological model to predict photosynthesis in variable irradiance (13, 45) as influenced by UV (10, 32, 54). Components 1-3 are required to quantify the exposure of phytoplankton to UV and visible irradiance as a function of depth. The fourth component is needed to specify appropriately weighted exposure as a function of time; it is unnecessary if the water column is strongly stratified and therefore not mixing significantly. The final component is required to convert biologically-weighted exposure to a net effect. We focus here on the biological aspects of this integrated approach.

Chlorophyll a (mg m⁻³)

1° Productivity (mg C m⁻³ h⁻¹)
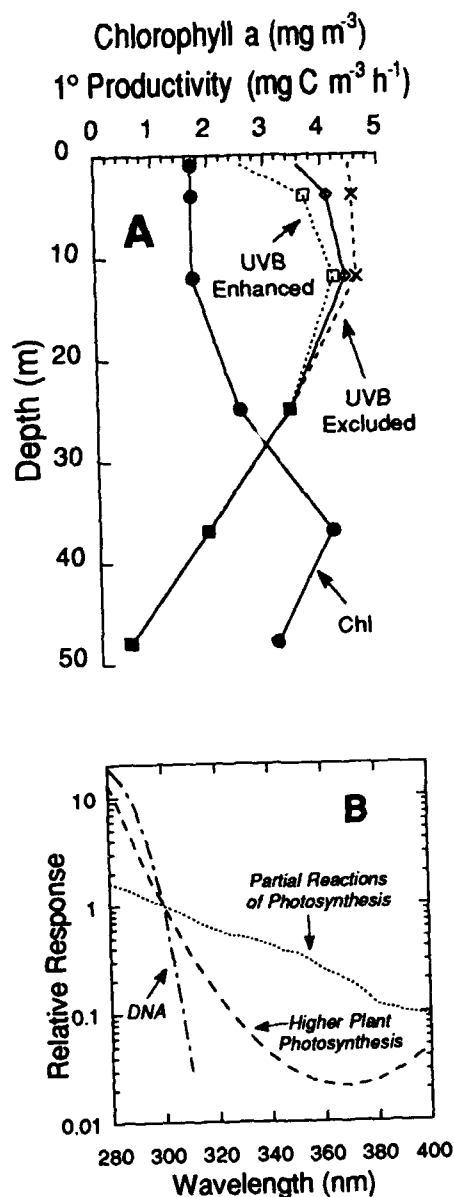
Figure 1. Effect of UV on the measurement of primary productivity (A) and biological weighting functions that describe the spectral dependence of UV effects on biological processes (B). The vertical profile in A idealizes the results of Smith *et al.* (56) using a typical profile of chlorophyll and productivity. The solid line represents photosynthesis in quartz containers that transmit environmental UV. Rates are enhanced by the exclusion of UVB with optical screen, whereas photosynthesis is reduced when UVB is enhanced with sunlamps during simulated *in situ* incubations. An appropriate BWF would describe the effects of different irradiance regimes on relative photosynthesis, as shown in A. Candidate weighting functions include that for damage to DNA (51), inhibition of higher plant photosynthesis (5, 49), and inhibition of partial reactions of photosynthesis (27), as presented in B. The analysis of Smith *et al.* (56) showed that their results were consistent with the Jones and Kok spectrum for photoinhibition of partial reactions (27), but not with either the DNA spectrum or a general spectrum of plant damage (4). More detailed measurements are required to derive a BWF from results of experimental exposures.

47

UV EXPOSURE AND PHOTOINHIBITION:
DOSE VERSUS DOSAGE RATE

In predictive models, biological responses to environmental radiation must be related to exposure, appropriately quantified. For example, photosynthesis is conventionally expressed as a function of irradiance (W m^{-2} or μmol m^{-2} s^{-1}) in the P-I function (2, 47). Historically, however, the effects of UV on biological processes have been expressed as functions of cumulative dose (biologically weighted J m^{-2}), rather than as functions of dosage rate (weighted W m^{-2}). Modeling the effects of environmental radiation as a function of dose requires the assumption of reciprocity, *i.e.*, that the response is a function solely of cumulative exposure, independent of rate (56). This is appropriate for irreversible reactions, effects which are reversed very slowly, or when counteracting processes can be considered separately. Although dose-dependence has been successfully assumed in the analysis of photoinhibition in a higher plant (5), it might not apply for photosynthesis of phytoplankton: when a marine diatom was exposed to different intensities and durations of supplementary UVB, reciprocity failed (8). In fact, for exposure times > 0.5 h, photoinhibition of photosynthesis was well described as a function of irradiance, consistent with a mechanistic model of photoinhibition as a balance between damage and recovery processes (42). Nonetheless, if a set of experiments uses approximately equal exposure times, relative dose and relative dosage rate are equivalent (10), so models relating photoinhibition to UV dose (56, 57) can be correct for the experimental time scale even though they might not be appropriate for extrapolation to other time scales.

BIOLOGICAL WEIGHTING FUNCTION FOR PHOTOINHIBITION

The BWF, or action spectrum (Fig. 1B), has been the centerpiece of seminal papers describing how to assess the effects of UVB and stratospheric ozone depletion on photosynthesis (5, 49, 56). A BWF describes biologically effective fluence rate (or dose) for the process under study. For example, the damaging effect of UV irradiance on photosynthesis can be described as a dimensionless fluence rate (11):

$$\text{Biologically Effective Fluence Rate} = \sum_{\lambda = 280}^{400} \varepsilon(\lambda)E(\lambda)\Delta\lambda \qquad (1)$$

where $E(\lambda)$ is spectral irradiance (W m^{-2} nm^{-1}) and $\varepsilon(\lambda)$ is the relative biological effectiveness of radiation at wavelength λ [(W m^{-2})$^{-1}$]. The challenge is to estimate $\varepsilon(\lambda)$. Ozone depletion influences spectral irradiance in a relatively narrow band of wavelengths (ca. 295 - 320 nm), and many BWF's

have steep slopes in the UVB, so it is important to obtain weighting functions with good spectral resolution (8).

For predicting the influence of environmental UV on photosynthesis, it is not enough to measure the harmful effects of individual wavebands during experimental exposures. Inhibition of photosynthesis by UV is countered by processes that are stimulated by longer wavelengths (24, 50, 62), so environmentally relevant action spectrum determinations should consist of progressively greater amounts of first UVA (320 - 400 nm), then UVB, added to a constant background of visible irradiance (9). Caldwell *et al.* (5, 49) used this approach in controlled experiments to measure the action spectrum for photosynthetic gas exchange in the terrestrial plant *Rumex patientia*. The same principles have been applied to estimate spectral weightings for phytoplankton photoinhibition during simulated *in situ* and *in situ* incubations using solar irradiance attenuated by different long-pass optical filters (23, 40, 41, 57). Spectral resolution of these functions for natural phytoplankton is limited (two to seven points), and weightings are in relative units.

INCORPORATING A BWF INTO A P-I MODEL

An appropriate weighting function for the inhibition of photosynthesis is essential, but to be useful for prediction, it must be incorporated into a model of photosynthesis versus PAR. In a recently developed model (11) photoinhibition is dependent on both absolute UV irradiance and UV relative to PAR:

$$P^B = P_s^B (1 - e^{(-E_{PAR}/E_s)}) \left(\frac{1}{1 + E_{inh}^*} \right) \qquad (2)$$

where E_{PAR} is PAR expressed in energy units (W m^{-2}), P^B (gC gChl^{-1} h^{-1})is the rate of photosynthesis normalized to chlorophyll, P_s^B is the maximum attainable rate in the absence of photoinhibition, and E_s is the saturation parameter for photosynthesis, comparable to the more familiar I_k (60). Similar to other models (42, 46), P^B is the product of potential photosynthesis, $P^B(1-\exp(-E_{PAR}/E_s))$, and inhibition, $1/(1+E_{inh}^*)$. The inhibition term is novel because it is a function of both UV irradiance (E_{UV}) and E_{PAR} as expressed using the form of Eq. 1:

$$E_{inh}^* = \mathcal{E}_{PAR}E_{PAR} + \sum_{\lambda = 280 \text{ nm}}^{400 \text{ nm}} \epsilon(\lambda)E(\lambda)\Delta\lambda \qquad (3)$$

where ϵ is in units of (W m^{-2})$^{-1}$ and $\mathcal{E}_{PAR}$ is the relative biological efficiency for damage to photosynthesis by E_{PAR}. The BWF/P-I model predicts P^B versus E_{PAR} as a function of biological dose rate per unit E_{PAR} (Fig. 2A) and thus can be used

to calculate photosynthesis versus depth in the water column, where both E_{PAR} and the ratio of E_{UV} to E_{PAR} change with depth. The predictions of the BWF/P-I model are different from those based on the assumption that percent photoinhibition is a function solely of weighted UV dose (Fig. 2).

EXPERIMENTAL DETERMINATION OF *BWF/P-I* PARAMETERS

In principle, the BWF/P-I model can be used to predict the effect of ozone-related changes in UV irradiance on aquatic photosynthesis by solving for water column photosynthesis in the presence and absence of ozone depletion. The model requires data from exposures of phytoplankton to a broad range of

E_{PAR} and E_{UV} to E_{PAR} ratios in order to specify P_s^B, E_s, $\tilde{\varepsilon}_{PAR}$, and $\varepsilon(\lambda)$ for UV wavelengths (Eqs. 2, 3). An experimental system (the Photoinhibitron) has been developed for this purpose (11). The apparatus can define up to 72 radiation treatments, including 8 different UVB/UVA/PAR ratios, determined by long-pass cut-off filters, with 9 different fluence rates in each, imposed by neutral density screens (Fig. 3). Results of an experiment on a marine diatom, when plotted as P^B versus E_{PAR} for different E_{UV} to E_{PAR} ratios (Fig. 4A) were consistent with the prediction of the BWF/P-I model: the depression of P at supersaturating intensities was stronger when the cultures were exposed to shorter wavelengths. An experiment on a marine dinoflagellate produced very similar results (11).
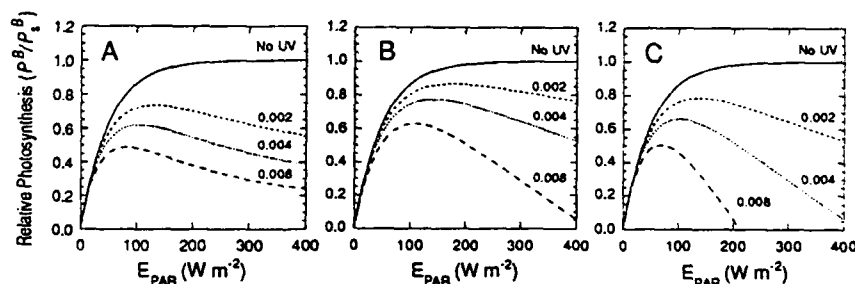
Figure 2. Predictions of the BWF/P-I model of photosynthesis (Eq. 2): relative photosynthesis versus E_{PAR} for different biological dose rates per unit E_{PAR} (A) compared to predictions of a model in which percent inhibition is modeled as a linear function of weighted UV dose (J m^{-2}) integrated over time (B, C). Expected curves after 1h exposure (B), and after 2h exposure (C). In this example, both models predict the same photosynthetic rate in the absence of UV; there is no inhibition by E_{PAR} alone ($\tilde{\varepsilon}_{PAR} = 0$). Percent photoinhibition due to UV is scaled to match the BWF/P-I prediction at 300 W m^{-2} for an exposure of 1 h with a biological dose rate per unit E_{PAR} of 0.008. The models predict very different photosynthesis versus E_{PAR} curves. Sufficiently long exposure to UV will lead to total loss of photosynthetic activity if photoinhibition is dose dependent, as in B and C, but to a stable steady-state in the case of dose-rate dependence, as in A.

Multivariate analysis and non-linear regression were applied to obtain quantitative estimates of the model parameters P_s^B, E_s, E_{PAR}, and $\varepsilon(\lambda)$ for UV wavelengths (11). Using PCA, we calculated a set of spectral components common to all UV treatments in each experiment (Fig. 3C). These sets of dimensionless spectral weightings were statistically defined so that any one UV treatment can be approximated by adding to or subtracting from the mean treatment spectrum a specific amount of each spectral component (the component

"score"). Instead of having to estimate directly the dependence of E_{inh}^* on the UV spectral irradiance (Eq. 3), which would have required estimating a total of 209 coefficients ($\varepsilon(\lambda)$, $\lambda = 286$-390 nm at 0.5 nm intervals), we estimated the

dependence of E_{inh}^* on the two spectral component scores; this procedure required a nonlinear regression estimate of only three coefficients (h_0, the mean treatment effect over the whole irradiance spectrum including both E_{PAR} and $E(\lambda)$, and the component effect, h_i, where i corresponds to components 1, 2). The coefficients h_i were then interpreted as the relative proportions of each spectral component required to generate a new spectral function describing the sensitivity of photosynthesis to UV, $i.e.$, the desired BWF. This application of PCA is an efficient method for estimating simple, smoothly-varying spectral responses without sacrificing spectral resolution and, unlike other methods (49) requires no a $priori$ assumptions about spectral shape.

Analysis of experiments on cultures of a marine diatom and a dinoflagellate (11) produced the first BWF's for the photoinhibition of phytoplankton photosynthesis with good spectral resolution in the UVB and expressed in
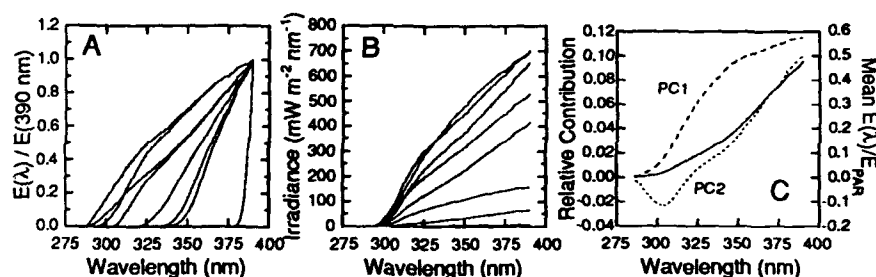
Figure 3. Characteristic spectra for the eight sections of the Photoinhibitron, corresponding to different E_{UV} to E_{PAR} ratios associated with each long-pass filter (A). Spectra for the 9 positions in one of the sections (305 nm long-pass filter), modified by insertion of screens, to produce a large range of E_{PAR} and E_{UV}, but similar E_{UV} to E_{PAR} ratio (B). One low-irradiance spectrum is obscured. Loadings for spectral components (PC1 and PC2, dashed lines) derived by PCA of spectra shown in A. Linear combinations of these two components with the mean treatment spectrum (solid line) explain 95% of the variation in treatment E_{UV} to E_{PAR} ratio. Details of methods are presented in ref. 11.
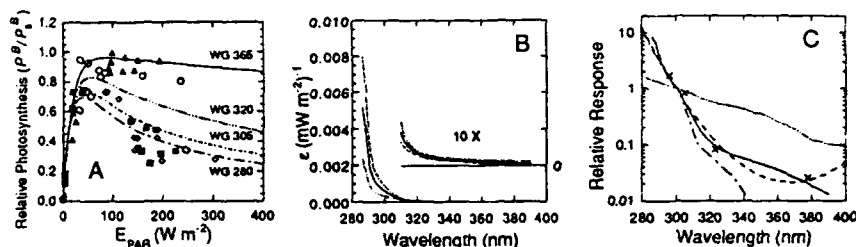
Figure 4. Relative photosynthesis versus E_{PAR} for *Phaeodactylum* sp. exposed to different E_{UV} to E_{PAR} ratios designated by the cut-off wavelength of long-pass filters (Schott WG-series) as in Fig. 3A. For clarity, only four of the eight spectral treatments are shown. The lines show a typical photosynthetic response for P^B versus E_{PAR} in each filter group when two spectral component scores for one of the cells are used to describe UV spectral irradiance. Spectral variation between cells in each treatment causes some of the scatter around these lines. In the analysis, each cell was scored and fitted individually, and the overall R^2 is > 93%. Symbols: WG365 (▲), WG320 (o), WG305 (■), WG280(◊). Results were used to determine biological weighting functions for the experimental inhibition of photosynthesis by UV (B). The solid line is estimated weight and the dotted lines show the estimated 95% confidence interval of the estimate. Values for 310 to 390 nm are shifted, multiplied by 10, and repeated, with the new origin on the right axis. The weighting function for *Phaeodactylum* (—) compared to previously published action spectra, normalized to 1.0 at 300 nm (C): (......) inhibition of photosynthetic electron transport *in vitro* (27) and (— · —) damage to DNA in alfalfa seedlings (48); (----) differential spectrum of inhibition of photosynthesis in the higher plant *Rumex patientia* (5, 49); and (X) broad-band action spectrum estimates from experiments on inhibition of photosynthesis in Antarctic phytoplankton (23). The estimated 95% confidence interval for *Phaeodactylum* after normalization is approximately ± 0.015 in the UVA spectral region. Data for *Phaeodactylum* are from (11), where methodological details can be found.

absolute units (Fig. 4C). As would be expected if a general biological weighting function existed, the weighting functions for two different laboratory cultures were very similar in shape. Furthermore, when normalized to 1.0 at 300 nm (Fig. 4C), the weighting functions are nearly the same as the spectrum for *Rumex patientia* (5, 49), and they are also consistent with broad-band weighting functions derived from experiments on natural assemblages in the Antarctic (23, 37, 41).

EVALUATION OF THE BIOLOGICAL WEIGHTING FUNCTION

Our spectrum is different from that for *in vitro* photoinhibition (27), which has been used to estimate biological dose in several previous studies of UV effects on phytoplankton photosynthesis (15, 54, 56). The *in vitro*

52

photoinhibition action spectrum does not have a steep slope in the UVB region. Our phytoplankton weighting function is steep below 300 nm, more like that for damage to DNA (48, 51). Steep slopes in the UVB range correspond to predictions of more severe effects of ozone depletion (5). However, unlike the DNA function, and more like the *in vitro* spectrum, our phytoplankton weighting function has significant influence well into the UVA, consistent with observations of photoinhibition in natural populations of phytoplankton (3, 23, 40, 41, 56, 57). A "tail" in the UVA range, where natural irradiance greatly exceeds that in the UVB, tends to reduce predictions of the relative depression of photosynthesis associated with ozone depletion (17, 48). The sensitivity of phytoplankton photosynthesis to UVA also limits the utility of DNA-based weightings for describing effects on photosynthesis (20), rather than on DNA *per se* (30).

Other BWF's for the inhibition of photosynthesis are expressed in relative units (5, 23, 37, 56). For practical application, a maximum photosynthetic rate must be specified for a given E_{PAR} and this rate is reduced according to a function relating inhibition to weighted UV exposure over the time scale of the experiment (Fig. 1B, C). Thus, percent inhibition is a function solely of weighted UV, regardless of E_{PAR}. By dealing explicitly with the combined effects of UV and PAR in one analytical equation, the BWF/P-I model permits more mathematical latitude in relationships between P and E_{PAR} as a function of E_{UV} to E_{PAR}. Predictions of other models can be consistent with BWF/P-I for particular sets of conditions (Fig. 1), but the newer model, which has parameters that are experimentally determined with short-term incubations, is potentially more general and powerful. Eventually, it should be possible to describe environmental variability of the BWF/P-I parameters as is now done for conventional P-I (22).

PREDICTING THE EFFECTS OF OZONE DEPLETION

The application of the BWF/P-I model can be illustrated with a trial calculation, based on measurements of spectral irradiance at McMurdo Station, Antarctica, as influenced by the ozone hole (Fig. 5). The analysis predicts that damage from UVA would dominate during hour-long near-surface exposures, producing about 40-50% inhibition of photosynthesis as compared to that under E_{PAR} alone. During high-ozone conditions, UVB has only a small incremental effect, whereas under low-ozone conditions, photosynthetic rates are further reduced. The difference between high-ozone and low-ozone predictions corresponds to an ozone-related decrease in photosynthesis of about 12-15% for E_{PAR} characteristic of the sea-surface in the Antarctic during the spring. The model predicts less total inhibition deeper in the water column, and a lower percent reduction due to ozone depletion. For an exemplary water column (57) at 4 m corresponding to 70% of PAR, total inhibition is approximately halved, as is the percent reduction due to ozone depletion.

53
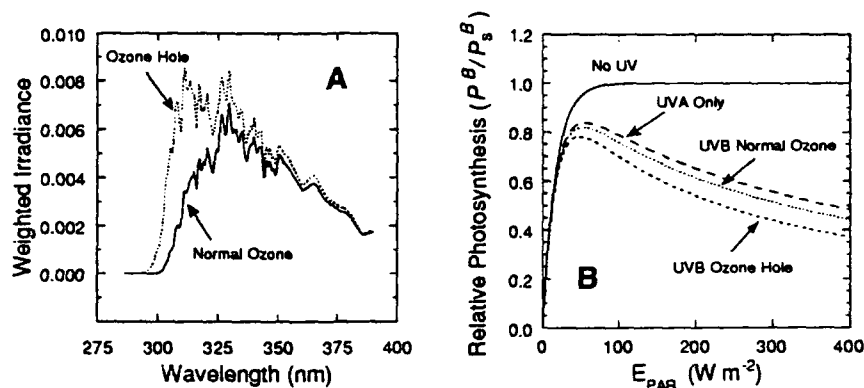
Figure 5. Biologically-weighted UV dose rate $(E(\lambda)E(\lambda)\Delta\lambda$ at 0.5 nm intervals, dimensionless) in incident irradiance at local noon (0100h GMT) for McMurdo station, Antarctica on days of low atmospheric ozone content (TOMS satellite estimate is ~ 175 DU) and high atmospheric ozone content (TOMS is ~ 350 DU): spectra corresponding to 200 W m^{-2} E_{PAR} were multiplied by the biological weighting coefficients estimated for *Phaeodactylum* sp. (A). A trial calculation, using results from laboratory experiments on *Phaeodactylum* sp. to predict photosynthesis versus E_{PAR} under irradiance regimes in the Antarctic (B). Biological dose rate was calculated from spectra in (A) using dose rate per unit E_{PAR} over 320 to 390 nm on 10 November, 1990 ("UVA only"), over 286 to 390 nm on 10 November, 1990 ("UVB , Normal Ozone") and over 286 to 390 nm on 28 October, 1990 ("UVB, Ozone Hole").

These relative estimates depend mainly on the shape of the biological weighting function, which so far appears to be similar between cultures grown in the laboratory at 20° C, samples of Antarctic phytoplankton (Neale *et al.*, unpublished data), and broad-band action spectra of natural assemblages in the Antarctic (23, 37, 41). Also, the trial calculations are broadly consistent with the *in situ* estimates of phytoplankton photosynthesis in the Bellingshausen sea under varying ozone thickness (57).

Further study is needed in order to understand how the BWF's vary between phytoplankton species [*i.e.*, temperate versus polar (23)] and how the BWF is affected by growth conditions. A number of Antarctic marine organisms have the capacity to synthesize compounds (mycosporine-like amino acids) which strongly absorb in the UV (31, 38). If, as hypothesized, these compounds are effective as UV-B protectants, we would expect a specific reduction in $E(\lambda)$ in the region of high absorbance. Measurement of BWF's for phytoplankton containing highly UV-absorbent compounds will enable a test of this hypothesis.

INCORPORATING DOSE VERSUS DOSAGE RATE INTO THE BWF MODEL

The BWF/P-I model is based on dose rates, just as conventional P-I models. The effects of UV on phytoplankton photosynthesis, however, can be a function of dose as well as dose rate (10), particularly for the time scales of < 30 min associated with wind-induced vertical mixing (12). Thus, when studying the effects of UV on phytoplankton photosynthesis, the time scales of experimental exposure should be considered jus. as when photoinhibition by visible light is studied (39, 42). For example, if the upper water column mixes weakly over the course of incubation experiments, then the variability of experimental irradiance in the bottles reasonably reflects that experienced by natural phytoplankton. The time scale of the measurement matches that of the process (21, 34), and measurements of photoinhibition can be considered as reasonable indications of photoinhibition *in situ*. But what if the water is mixing?

If vertical mixing significantly protects phytoplankton from photoinhibition, then the negative effects in near-surface incubation bottles will exceed those *in situ*. A series of measurements from the equatorial Pacific (Fig. 6) illustrate how the artifacts associated with static incubations of plankton from actively mixing surface layers can be identified. The premise, based on a series of studies of photoinhibition in Lake Titicaca (42, 44, 63), is that if photoinhibition is occurring *in situ*, it can be detected as a depression of short-term photosynthetic capacity near the surface. To evaluate the artifacts of incubation, one can compare samples held in bottles to fresh material from the water column. Results from the equatorial Pacific show clearly the artifact of static incubation: a sample incubated at surface irradiance through much of the day was severely affected whereas phytoplankton circulating in the water column showed little or no depression of photosynthetic potential near the surface at midday. The polycarbonate incubation vessels excluded UVB: if quartz vessels had been used, the artifact would have been even more severe. It can be concluded that a day-long experiment to study the spectral dependence of photoinhibition under these conditions would be describing the effects of UV on an artifact. Note, however, that photoinhibition has previously been detected *in situ* using similar methods (42) and that measurements at the equator (Cullen and Lewis, unpublished) showed a depression of photosynthetic potential near the surface during diurnal stratification of the water column.

OTHERS FACTORS TO BE CONSIDERED

Even if a BWF/P-I model is developed and validated for use in different aquatic environments, prediction of the acute effects of UV and ozone depletion on the photosynthesis of phytoplankton should not be assumed to describe the ultimate influence on primary productivity, fish production, or biogeochemical fluxes of carbon. Many other factors are involved. For example, physiological

Chlorophyll a (mg m⁻³)

$\text{Chlorophyll a (mg m}^{-3})$

0.0   0.1   0.2

0

10

20

30

40

50

Depth (m)

0630 h

1530 h
Incubated

1215 h

A

Potential Productivity (mgC m⁻³ h⁻¹)

$\text{Potential Productivity (mgC m}^{-3}\text{ h}^{-1})$

0.0 0.2 0.4 0.6 0.8

0

10

20

30

40

50

Depth (m)

1215 h

1530 h
Incubated

0630 h

B
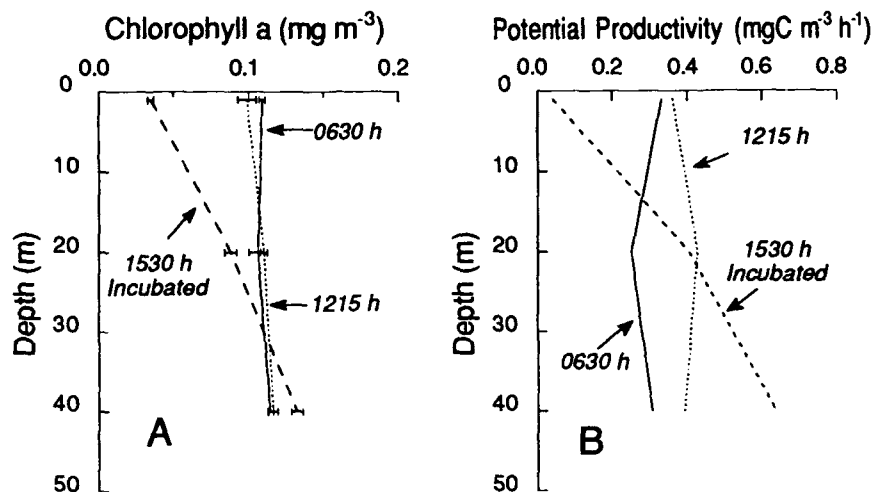
Figure 6. The artifacts associated with fixed-depth incubations during vertical mixing of the water column to about 50 m. These data are from a cruise in the equatorial Pacific Ocean (WEC88, 10°N, 150°W; Cullen and Lewis, unpublished). Solid lines are for samples from the morning bottle cast, dotted lines are for the midday cast, and the dashed lines are for samples from the morning cast, held in simulated *in situ* incubators until 1530 h in UVB-opaque polycarbonate bottles. Concentration of Chl (A); Potential productivity (B). Potential productivity was determined from short-term P-I measurements: it is maximal photosynthesis per unit Chl times the Chl concentration. When photoinhibition of photosynthesis occurs, potential productivity declines. *If incubations mimicked nature, the incubated samples would show the same vertical patterns as the fresh afternoon samples. They don't.* Instead, these data show severe photoinhibition during conventional incubations near the surface, resulting in massive net destruction of chlorophyll, even though UVB was excluded. Midday measurements on fresh samples suggest that vertical mixing moved the phytoplankton through the light gradient fast enough to protect them from such damage. This inference is supported by a calculation of photosynthesis in the mixed layer from P-I, Chl and PAR measurements: modeled productivity for incubated samples was 35% lower than for fresh samples. A conventional half-day experiment for assessing the effects of UV on photosynthesis under these conditions would be grossly compromised. It is possible that some inhibition of photosynthesis occurred near the surface and was averaged in by mixing. An upper bound to that process can be specified if the kinetics of damage and repair are known. Although the kinetics of photoinhibition and recovery have been incorporated into recent models of photosynthesis (13, 43, 45), neither the BWF/P-I model nor any other model of UV effects incorporates time-dependence in UV responses.

processes besides photosynthesis, such as nitrogen assimilation (14), motility (18), or reproduction (6, 26, 29) might be more sensitive than photosynthesis to UVB. Also, photoprotective responses (7, 31) and species succession (64) are very likely to complicate, but nonetheless to lessen any predictions of decreased primary productivity due to ozone depletion. A particularly important uncertainty is the influence of altered species composition on food web structure. As we learn to quantify the effects of UV on photosynthesis, it is important to remember these other processes that contribute to ecosystem response.

LITERATURE CITED

1. **Baker KS, Smith RC** (1982) Bio-optical classification and model of natural waters. 2. Limnol Oceanogr **27**: 500-509

2. **Bidigare RR, Prézelin BB, Smith RC** (1992) Bio-optical models and the problems of scaling. In PG Falkowski, A Woodhead, eds, Primary Productivity and Biogeochemical Cycling in the Sea. Plenum, New York, pp 175-212

3. **Bühlmann B, Bossard P, Uehlinger U** (1987) The influence of longwave ultraviolet radiation (u.v. A) on the photosynthetic activity (^{14}C-assimilation) of phytoplankton. J Plankton Res **9**: 935-943

4. **Caldwell MM** (1971) Solar ultraviolet radiation and the growth and development of higher plants. In AC Giese, ed, Photophysiology. Academic, New York, pp 131-177

5. **Caldwell MM, Camp LB, Warner CW, Flint SD** (1986) Action spectra and their key role in assessing biological consequences of solar UV-B radiation change. In RC Worrest, MM Caldwell, eds, Stratospheric Ozone Reduction, Solar Ultraviolet Radiation and Plant Life. Springer, pp 87-111

6. **Calkins J, Thordardottir T** (1980) The ecological significance of solar UV radiation on aquatic organisms. Nature **283**: 563-566

7. **Carreto JI, DeMarco SG, Lutz VA** (1989) UV-absorbing pigments in the dinoflagellates *Alexandrium excavatum* and *Prorocentrum micans*. Effects of light intensity. In T Okaichi, DM Anderson, T Nemoto, eds, Red Tides: Biology, Environmental Science, and Toxicology. Elsevier, pp 333-336

8. **Coohill TP** (1989) Ultraviolet action spectra (280 to 380 nm) and solar effectiveness spectra for higher plants. Photochem Photobiol **50**: 451-457

9. **Coohill TP** (1991) Action spectra again? Photochem Photobiol **54**: 859-870

10. **Cullen JJ, Lesser MP** (1991) Inhibition of photosynthesis by ultraviolet radiation as a function of dose and dosage rate: Results for a marine diatom. Mar Biol **111**: 183-190

11. **Cullen JJ, Neale PJ, Lesser MP** (1992) Biological weighting function for the inhibition of phytoplankton photosynthesis by ultraviolet radiation. Science **248**: 646-650

12. **Denman KL, Gargett AE** (1983) Time and space scales of vertical mixing and advection of phytoplankton in the upper ocean. Limnol Oceanogr **28**: 801-815

13. **Denman KL, Marra J** (1986) Modelling the time dependent photoadaption of phytoplankton in fluctuating light. *In* JCJ Nihoul, ed, Marine Interfaces Ecohydrodynamics. Elsevier, Amsterdam, pp 341-360

14. **Döhler G** (1988) Effect of UV-B (280-320 nm) radiation on the ^{15}N-nitrate assimilation of some algae. Plant Physiol (Life Sci Adv) **7**: 79-84

15. **El-Sayed SZ, Stephens FC, Bidigare RR, Ondrusek ME** (1990) Effect of ultraviolet radiation on Antarctic marine phytoplankton. *In* KR Kerry, G Hempel, eds, Antarctic Ecosystems. Ecological Change and Conservation. Springer Verlag, New York, pp 379-385

16. **Gallegos CL, Platt T** (1985) Vertical advection of phytoplankton and productivity estimates: a dimensional analysis. Mar Ecol Prog Ser **26**: 125-134

17. **Häder D-P, Brodhun B** (1991) Effects of ultraviolet radiation on the photoreceptor proteins and pigment in the paraflagellar body of the flagellate, *Euglena gracilis*. J Plant Physiol **137**: 641-646

18. **Häder D-P, Häder M** (1991) Effects of solar and artificial U.V. radiation on motility and pigmentation in the marine *Cryptomonas maculata*. Envir Exp Bot **31**: 33-41

19. **Häder D-P, Worrest RC** (1991) Effects of enhanced solar ultraviolet radiation on aquatic ecosystems. Photochem Photobiol **53**: 717-725

20. **Hardy J, Gucinski H** (1989) Stratospheric ozone depletion: Implications for marine ecosystems. Oceanogr Mag **2**: 18-21

21. **Harris GP** (1980) Spatial and temporal scales in phytoplankton ecology. Mechanisms, methods, models and management. Can J Fish Aquat Sci **37**: 877-900

22. **Harrison WG, Platt T** (1986) Photosynthesis–irradiance relationships in polar and temperate phytoplankton populations. Polar Biol **5**: 153–164

23. **Helbling EW, Villafañe V, Ferrario M, Holm-Hansen O** (1992) Impact of natural ultraviolet radiation on rates of photosynthesis and on specific marine phytoplankton species. Mar Ecol Prog Ser **80**: 89-100

24. **Hirosawa T, Miyachi S** (1983) Inactivation of Hill reaction by long-wavelength radiation (UV-A) and its photoreactivation by visible light in the cyanobacterium, *Anacystis nidulans*. Arch Microbiol **135**: 98-102

25. **Janowitz GS, Kamykowski D** (1991) An eulerian model of phytoplankton photosynthetic response in the upper mixed layer. J Plankton Res **13**: 983-1002

26. **Jokiel PL, York RH Jr** (1984) Importance of ultraviolet radiation in photoinhibition of microalgal growth. Limnol Oceanogr **29**: 192-199

27. **Jones LW, Kok B** (1966) Photoinhibition of chloroplast reactions. I. Kinetics and action spectra. Plant Physiol **41**: 1037-1043

28. **Karentz D** (1991) Ecological considerations of Antarctic ozone depletion. Ant Sci **3**: 3-11

29. **Karentz D, Cleaver JE, Mitchell DL** (1991) Cell survival characteristics and molecular responses of Antarctic phytoplankton to ultraviolet-B radiation. J Phycol **27**: 326-341

30. **Karentz D, Lutze LH** (1990) Evaluation of biologically harmful ultraviolet radiation in Antarctica with a biological dosimeter designed for aquatic environments. Limnol Oceanogr **35**: 549-561

31. **Karentz D, McKuen FS, Land MC, Dunlap WC** (1991) Survey of mycosporine-like amino acid compounds in Antarctic marine organisms: potential protection from ultraviolet exposure. Mar Biol **108**: 157-166

32. **Kullenberg G** (1982) Note on the role of vertical mixing in relation to effects of UV radiation on the marine environment. *In* J Calkins, ed, The Role of Solar UV Radiation on the Marine Ecosystems. Plenum Press, N.Y., pp 283-292

33. **Lande R, Lewis MR** (1989) Models of photoadaptation and photosynthesis by algal cells in a turbulent mixed layer. Deep-Sea Res **36**: 1161-1175

34. **Legendre L, Demers S** (1984) Towards dynamic biological oceanography and limnology. Can J Fish Aquat Sci **41**: 2-19

35. **Lohrenz SE, Wiesenberg DA, Rein CR, Arnone RA, Taylor CD, Knauer GA, Knap AH** (1992) A comparison of *in situ* and simulated *in situ* methods for estimating oceanic primary production. J Plankton Res **14**: 201-221

36. **Lorenzen CJ** (1979) Ultraviolet radiation and phytoplankton photosynthesis. Limnol Oceanogr **24**: 1117-1124

37. **Lubin D, Mitchell BG, Frederick JE, Alberts AD, Booth CR, Lucas T, Neuschuler D** (1992) A contribution toward understanding the biospherical significance of Antarctic ozone depletion. J Geophys Res **97**: 7817-7828

38. **Marchant HJ, Davidson AT, Kelly GJ** (1991) UV-B protecting compounds in the marine alga *Pheocystis pouchetii* from Antarctica. Mar Biol **109**: 391-395

39. **Marra J** (1978) Phytoplankton photosynthetic response to vertical movement in a mixed layer. Mar Biol **46**: 203-208

40. **Maske H** (1984) Daylight ultraviolet radiation and the photoinhibition of phytoplankton carbon uptake. J Plankton Res **6**: 351-357

41. **Mitchell BG** (1990) Action spectra of ultraviolet photoinhibition of Antarctic phytoplankton and a model of spectral diffuse attenuation coefficients. *In* BG Mitchell, O Holm-Hansen, I Sobolev, eds, Response of Marine Phytoplankton to Natural Variations in UV-B Flux. Chemical Manufacturers Association, Washington, D.C., Appendix H

42. **Neale PJ** (1987) Algal photoinhibition and photosynthesis in the aquatic environment. *In* DJ Kyle, CB Osmond, CJ Amtzen, eds, Photoinhibition. Elsevier, Amsterdam, pp 35-65

43. **Neale PJ, Marra J** (1985) Short-term variation of Pmax under natural irradiance conditions: a model and its implications. Mar Ecol Prog Ser **26**: 113-124

44. **Neale PJ, Richerson PJ** (1987) Photoinhibition and the diurnal variation of phytoplankton photosynthesis - I. Development of a photosynthesis-irradiance model from studies of in situ responses. J Plankton Res **9**: 167-193

45. **Pahl-Wostl C, Imboden DM** (1990) DYPHORA - A dynamic model for the rate of photosynthesis of algae. J Plankton Res **12**: 1207-1221

46. **Platt T, Gallegos CL, Harrison WG** (1980) Photoinhibition of photosynthesis in natural assemblages of marine phytoplankton. J Mar Res **38**: 687–701

59

47. **Platt T, Jassby AD** (1976) The relationship between photosynthesis and light for natural assemblages of coastal marine phytoplankton. J Phycol **12**: 421–430

48. **Quaite FE, Sutherland BM, Sutherland JC** (1992) Action spectrum for DNA damage in alfalfa lowers predicted impact of ozone depletion. Nature **358**: 576-578

49. **Rundel RD** (1983) Action spectra and estimation of biologically effective UV radiation. Physiol Plant **58**: 360-366

50. **Samuelsson G, Lönneborg A, Rosenqvist E, Gustafson P, Öquist G** (1985) Photoinhibition and reactivation of photosynthesis in the cyanobacterium *Anacystis nidulans.* Plant Physiol **79**: 992-995

51. **Setlow RB** (1974) The wavelengths in sunlight effective in producing skin cancer: a theoretical analysis. Proc Natl Acad Sci USA **71**: 3363-3366

52. **Smith RC** (1989) Ozone, middle ultraviolet radiation and the aquatic environment. Photochem Photobiol **50**: 459-468

53. **Smith RC, Baker KS** (1979) Penetration of UV-B and biologically effective dose-rates in natural waters. Photochem Photobiol **29**: 311-323

54. **Smith RC, Baker KS** (1982) Assessment of the influence of enhanced UV-B on marine primary productivity. *In* J Calkins, ed, The Role of Solar Ultraviolet Radiation in Marine Ecosystems. Plenum Press, pp 509-537

55. **Smith RC, Baker KS** (1989) Stratospheric ozone, middle ultraviolet radiation and phytoplankton productivity. Oceanogr Mag **2**: 4-10

56. **Smith RC, Baker KS, Holm-Hansen O, Olson RS** (1980) Photoinhibition of photosynthesis in natural waters. Photochem Photobiol **31**: 585-592

57. **Smith RC, Prezelin BB, Baker KS, Bidigare RR, Boucher NP, Coley T, Karentz D, MacIntyre S, Matlick HA, Menzies D, Ondrusek M, Wan Z, Waters KJ** (1992) Ozone depletion: Ultraviolet radiation and phytoplankton biology in Antarctic waters. Science **255**: 952-959

58. **Solomon S** (1988) The mystery of the Antarctic ozone "hole". Rev Geophys **26**: 131-148

59. **Steemann Nielsen E** (1964) On a complication in marine productivity work due to the influence of ultraviolet light. J Cons Perm Int Explor Mer **22**: 130-135

60. **Talling JF** (1957) The phytoplankton population as a compound photosynthetic system. New Phytol **56**: 133–149

61. **United Nations Environmental Programme** (1991) Environmental Effects of Ozone Depletion: 1991 Update. United Nations Environmental Programme, Nairobi

62. **Van Baalen C** (1968) The effects of ultraviolet irradiation on a coccoid blue-green alga: Survival, photosynthesis, and photoreactivation. Plant Physiol **43**: 1689-1695

63. **Vincent WF, Neale PJ, Richerson PJ** (1984) Photoinhibition : algal responses to bright light during diel stratification and mixing in a tropical alpine lake. J Phycol **20**: 201-211

64. **Worrest RC, Thomson BE, Dyke HV** (1981) Impact of UV-B radiation upon estuarine microcosms. Photochem Photobiol **33**: 861-867

65. **Yamazaki H, Kamykowski D** (1991) The vertical trajectories of motile phytoplankton in a wind-mixed water column. Deep-Sea Res **38**: 219-241

Physiological Bases for Detecting and Predicting Photoinhibition of Aquatic Photosynthesis by PAR and UV Radiation[1]

Patrick J. Neale, John J. Cullen, Michael P. Lesser and Anastasios Melis

Department of Plant Biology, University of California Berkeley, CA 94720 (PJN, AM), Bigelow Laboratory for Ocean Sciences, West Boothbay Harbor ME 04575 (PJN, JJC, MPL) and Department of Oceanography, Dalhousie University, Halifax NS Canada B0R 1A0 (JJC)

INTRODUCTION

Phytoplankton photosynthesis is the basis of almost all aquatic primary production in the world's oceans, estuaries and lakes. Oceanic primary production is a major portion of the global carbon budget (see other contributions this volume). Currently, we are unable to account for all the CO_2 that is leaving the atmosphere and debate continues whether the "missing carbon" is going into either terrestrial and oceanic sinks (7). In this context, it is important to improve our knowledge of how phytoplankton photosynthesis responds to the aquatic environment. The aquatic light environment is primary among several factors governing aquatic photosynthesis. To understand phytoplankton response to aquatic irradiance, we must consider how light propagates underwater, variations in light spectral quality as well as intensity. Also important is how these optical characteristics relate to processes of light absorption and utilization by phytoplankton cells. Considerable progress has been made on answering many of these questions (e.g. 27).

---

[2]Abbreviations: α, initial slope of the photosynthesis-irradiance curve; F, F_s, steady state fluorescence; F_{DCMU}, steady state fluorescence measured in the presence of DCMU; F_o, nonvariable fluorescence yield; F_m, maximum fluorescence; F_v, variable fluorescence = F_m - F_o; P680, reaction center of PSII; PAR, photosynthetically available radiation; Pheo, pheophytin; P_m, light-saturated rate of photosynthesis; Q_A, primary quinone electron acceptor of PSII; Q_B secondary quinone electron acceptor of PSII; PSII-Q_B-nonreducing, PSII center with impaired Q_A-Q_B interaction; Z, secondary PSII donor.

One topic, phytoplankton responses to irradiance stress induced by photosynthetically available radiation (PAR[2]) and UV, has become increasingly important. The primary consequence in both cases is a time-dependent loss of photosynthetic activity (photoinhibition). Concern over the effects of solar UV irradiance has recently intensified with the advent of stratospheric ozone depletion, which allows for an increase of the mid-ultraviolet (UVB 280-320 nm) irradiance, especially in the Antarctic. The sensitivity of phytoplankton photosynthesis to irradiance stress can be readily demonstrated (36), however, showing whether this stress actually occurs in the aquatic environment remains difficult. The essential problem is that phytoplankton are in suspension. Their irradiance exposure will be determined by mixing processes that transport cells over a vertical gradient in light availability. The response to irradiance stress is usually time dependent (12, 36); the light history of the cells must be known to specify the overall effect. The established method for measuring phytoplankton production, photosynthetic incorporation of ^{14}C into organic carbon during a 12-24 h bottle incubation, may seriously misrepresent irradiance regimes actually experienced by phytoplankton *in situ*. Further discussion of the interaction of photoinhibition and mixing can be found in (36).

We propose that an integrated modeling-sampling approach is needed to define the effects of irradiance stress on productivity *in situ*. The model should incorporate an optical specification of the underwater irradiance environment, a biological weighting function to account for the wavelength-dependence of photoinhibition of photosynthesis, and a response function of biological action during vertical mixing to account for the differences between static incubations and natural movements of phytoplankton. Recently, excellent progress has been made toward defining the individual components of this model (See also Cullen and Neale, this volume). To verify the model, we need to detect reliably the occurrence of irradiance stress *in situ*. This is the sampling side of the integrated approach. In particular, we would like to differentiate between the effects of PAR and UV. We propose that such detection can be accomplished by indicator assays (or "diagnostic markers"). Such assays would involve little or no incubation of samples, so that the measurement corresponds as closely as possible to the physiological state of the phytoplankton at time of sampling.

Our objective here is to review selected aspects of irradiance stress at biophysical and molecular levels, and then proceed to examine how that information can be used to design indicator assays of irradiance stress for phytoplankton photosynthesis *in situ*. The effects of PAR and UV at the cellular level and the use of *in vivo* fluorescence and molecular probes as detection systems will be discussed.

MECHANISMS OF LIGHT STRESS IN
THE AQUATIC ENVIRONMENT

The first step in oxygenic photosynthesis is the oxidation of water and reduction of plastoquinone by the membrane complex photosystem II (PSII). PSII has emerged as a target for many types of plant stresses, not only irradiance stress but also high- and low- temperature stress (see other contributions in this same volume). This has important implications for detecting phytoplankton responses to changes in environmental conditions, since PSII function can be monitored through changes in the *in vivo* emission of Chl *a* fluorescence (30). Exposure to both PAR and UV irradiance can have damaging effects on PSII functioning, but different mechanisms have been identified, therefore the effects of these two types of irradiance will be discussed separately.

MECHANISMS OF PAR-INDUCED INHIBITION

The vast majority of PAR photons absorbed by the PSII complex are dissipated without affecting the functional integrity of the complex, and the absorbed excitation energy is ultimately used either for photochemistry, production of heat (nonphotochemical dissipation), or fluorescence. However, there is a certain low probability that the absorbed energy will lead to alteration of the complex and the loss of its function. There is no complete agreement on the exact event that occurs, however there is consensus that it involves the core of the PSII reaction center, composed of the heterodimer of D1 and D2 polypeptides. While damage can occur at any intensity, the problem becomes critical at saturating irradiances for photosynthesis, when the number of absorbed photons far exceeds the number that can be used for photochemistry, i.e. the quantum yield of photochemistry is low. Damage can be avoided by decreasing the amount of absorbed energy that reaches the reaction center core or can be rapidly counteracted by replacing damaged complexes. Plants appear to use both approaches to maintain PSII activity: At high irradiance an increasing portion of energy absorbed by PSII is deflected away from the reaction center core and dissipated by nonphotochemical quenching (heat) (see Adams and Demmig-Adams this volume), also there is a very active PSII "repair cycle" that serves to rapidly replace damaged PSII reaction centers (see below).

These defense mechanisms have only limited capacity to counteract the damaging potential of PAR, and, at sufficiently high PAR, a net loss of PSII function occurs. This is manifested as a time dependent decrease in photosynthesis at high PAR (photoinhibition, reviews 29,45). The mechanism of damage to PSII is under intensive investigation using *in vitro* experimental systems. These investigations seek to establish the single or several sites of light- dependent damage to the PSII reaction center core. One group of studies has focused on the primary electron-transport events:

$$P680^* \ Pheo \ Q_A \rightarrow P680+ \ Pheo^- \ Q_A \rightarrow P680+ \ Pheo \ Q_A^-$$

When isolated spinach thylakoids are illuminated with strong PAR irradiance (PPFD=2500 μmole m^{-2} s^{-1}) at 0°C, quantitations of both Q_A (320 nm absorbance change) and Pheo (685 nm absorbance change) are lowered in parallel, indicating inhibition of primary photochemistry (10,14). This suggests that PAR stress induces damage on the donor side of PSII between the secondary donor (Z) and Pheo, and prevents a stable charge separation. However, different results can be obtained when thylakoids are illuminated at 20°C or under anaerobic conditions. This has lead to support for a donor side mechanism (8,55) or suggestions of alternate mechanisms involving loss of Q_A (57) or degradation of D1 (1). Few studies have tried to confirm the operation of these mechanisms in intact microalgae. The PSII primary charge separation was inhibited in low light grown *Chlamydomonas reinhardtii* when cells were exposed to PAR comparable to midday surface intensities at mid latitudes (PPFD = ca. 2000 μmole m^{-2} s^{-1}) (Fig. 1) (40,41). Both *in vitro* and *in vivo* losses of PSII primary charge separation show quasi first-order kinetics with half times on the order to 10-30 min. This suggests that loss of the function of the PSII primary charge separation is the primary mechanism responsible for PAR photoinhibition in the aquatic environment.

It has also been suggested that more than one mechanism may be operating during the time course of PAR damage. An initial modification may occur at the Q_B site followed by loss of primary charge separation and formation of completely heat dissipating centers (6,49). A thermoluminescent study of photoinhibition of intact *C. reinhardtii* is also consistent with a two step mechanism (43).
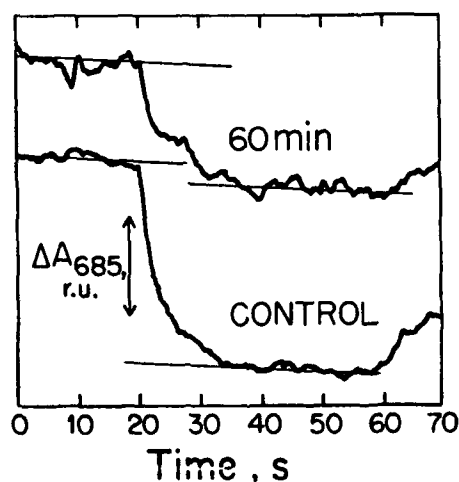
Figure 1. Light-induced absorbance change at 685 nm in isolated *C. reinhardtii* thylakoids attributed to the photoreduction of the primary PSII acceptor, Pheo. For details on methods see (14,40). Actinic illumination was turned 'on' at time = 20 s and turned 'off' at time = 60s. The upper trace is from cells of *C. reinhardtii* after 60 min exposure to strong irradiance (2000 μmol m^{-2} s^{-1}). The lower trace is from thylakoids isolated from control cells of *C. reinhardtii*. Less than 50% of the PSII reaction centers are able to form a stable charge separation after photoinhibition, which is comparable to the change in P_m (40).

Independent of the exact damage mechanism, interruption of photosystem electron transport results in a clear change in *in vivo* fluorescence. Under normal conditions, *in vivo* fluorescence varies between a minimum yield, F_o, and an enhanced yield, F_m. These limits correspond to whether the stable PSII electron acceptor of the complex, Q_A, is oxidized (low light, F_o) or is reduced (high light, F_m), and the light modulated variation between these two limiting yields is the fluorescence induction (review 30). The difference between the F_o and F_m fluorescence yields is the variable fluorescence, F_v, a relative measure of the ability of the reaction center to accumulate reduced Q_A. Damaged PSII complexes are unable to carry out photochemistry and do not display variable fluorescence. Thus a progressive loss of variable fluorescence with high irradiance exposure (time scale min - h) occurs during photoinhibition by PAR irradiance. This decrease is conveniently measured by the ratio F_v/F_m, a measure of PSII quantum yield (3). Note, however, that PSII damage will affect both the maximum quantum yield (photosynthetic efficiency) and light saturated rate of photosynthesis (P_m). The decrease in P_m depends on the extent to which photosynthesis is limited by the electron turnover rate of PSII. In phytoplankton, the decrease in P_m and quantum yield is usually comparable (37,42), though "activation" of a PSII reserve pool can counteract loss of P_m (see below, 40). As will be shown below, the *in vivo* fluorescence can be used to detect the occurrence of photoinhibition of phytoplankton photosynthesis in the aquatic environment.

Kinetic analyses of the fluorescence induction curve also reveal that PSII is heterogeneous. Among vascular plants and chlorophyte algae, two forms have been identified. A large antenna form, $PSII_\alpha$, is localized exclusively in appressed membrane regions, while the non-appressed membranes contain a smaller antenna form, $PSII_\beta$. Under physiological conditions, it has been shown that $PSII_\alpha$ displays the full photochemical activity associated with water oxidation and plastoquinone reduction (34). On the other hand, $PSII_\beta$ has a functional reaction center and forms a stable charge separation upon illumination but cannot reduce plastoquinone. Thus, $PSII_\beta$ has been termed Q_B-nonreducing in comparison with the Q_B-reducing $PSII_\alpha$ centers (21).

The physiological significance of PSII heterogeneity has been explained in terms of a "PSII repair cycle" operating between appressed and non-appressed membrane regions (Fig. 2, 22,34). It was postulated that once damaged, $PSII_\alpha$ units dissociate into the peripheral LHCII and a $PSII_\beta$-like complex. These photochemically silent $PSII_\beta$ centers are translocated into the stroma-exposed region. Damaged PSII centers in the stroma exposed region are then repaired, a process that includes replacement of the apoprotein(s) of the PSII reaction center. Repaired centers accumulate in the non-appressed region as a reserve pool of PSII in the form of $PSII_\beta$-Q_B-nonreducing. In a subsequent step, these centers are "activated" to a $PSII_\beta$-Q_B-reducing form and become incorporated into the appressed membrane region as fully functional PSII units. Such a cycle is consistent with the localization and movement of the PSII reaction center "D1"
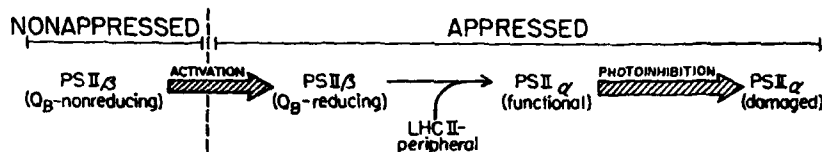
Figure 2. A schematic of part of a proposed PSII repair cycle (21,40). The wide hatched arrows indicate those steps emphasized during irradiance stress induced damage to PSII.

polypeptide which first appears as a precursor in the stroma-exposed region (33). The mature protein is then obtained after post-translational modification and intra-membrane transfer to the appressed membranes (33).

During PAR irradiance stress, the operation of the repair cycle is critical to the maintenance of photosynthesis. A large demand for reaction center repair is created when PSIIα centers are damaged due to photoinhibition (40). In *C. reinhardtii*, PAR irradiance stress is associated with a conversion of Q_B-nonreducing centers to the Q_B-reducing form (40). These "activated" PSII$_\beta$ centers counteract the loss of PSII by photoinhibition. PSII$_\beta$ also is selectively depleted from the non-appressed membrane regions of *C. reinhardtii* following exposure to strong irradiance (41). These results are consistent with the operation of a repair cycle that translocates PSII complexes between non-appressed and appressed membrane regions during photoinhibition (Fig. 2). The dynamics of the PSII repair cycle in other classes of planktonic microalgae are unknown.

So far, we have described mechanisms for decreased PSII activity in high PAR which result from damage to the photosynthetic apparatus. This is photoinhibition in the classical sense (45). There are other ways, however, that short-term exposure to high irradiance might lead to a reduction in photosynthesis. For example, the strong nonphotochemical quenching that is induced as a photoprotective process will continue affecting light utilization by the PSII complex even after high intensity exposure has stopped. The result is an apparent decrease in the maximum quantum yield of PSII in low irradiance and thus of photosynthetic efficiency. This has been called photoinhibition of quantum yield, since the saturated photosynthetic rate is unaffected (3). A more descriptive term might be "quenching hysteresis", which avoids the implication of irradiance damage. The rate of recovery from quenching hysteresis will depend on the rate at which the photoprotective mechanisms are disengaged. The relative importance of light-dependent damage and quenching hysteresis in reducing photosynthetic efficiency can be inferred from changes in F_o: increased F_o is linked to PSII damage while decreased F_o is connected with photoprotective quenching mechanisms (17,18). A similar scheme could possibly be used to interpret phytoplankton fluorescence, though caution must be exercised since dissolved compounds and pheopigments also contribute to natural "F_o".

MECHANISMS OF UV-INDUCED INHIBITION

Increased incident UVB irradiance is a present and future consequence of stratospheric ozone depletion and the possible effects on marine primary production are largely unknown. Cullen and Neale (this volume) present additional background on the response of phytoplankton photosynthesis to increases in environmental UVB irradiance. We consider here mechanisms that maybe involved during *UV-induced inhibition, with emphasis on effects* of UVB irradiance, and how the operation of those mechanisms in the aquatic environment might be detected.

While the primary site of PAR photoinhibition has been intensively studied over the last decade, much less is known about the target sites of UVB irradiance among plants (4). In either case, PSII appears to be an important target. One suggestion is that UVB irradiance damages the primary charge separation of the PSII reaction center, similar to what occurs in PAR (23). Other work has suggested that UVB irradiance does not affect the reaction center, but instead targets donor or acceptor molecules which subsequently carry out electron transport (35, 48, 60). A third possible site of damage in the PSII complex is within the light-harvesting complex (11).

There are several observations which point to the unique effect of UV exposure on the photosynthetic apparatus. Photoinhibition action spectra of isolated chloroplasts (24,48) show a more or less constant quantum yield of damage in the PAR region but a substantially higher quantum yield in the ultraviolet (290-400 nm) range. This suggests that the light-harvesting pigments (mainly chlorophyll) sensitize PAR photoinhibition but other sensitizers are implicated in the UV region. Several PSII donor and acceptor molecules have significant absorbance in the UV region and almost no visible absorbance. One possible target is the tyrosine donor to the PSII (Z). The radical Z^+ absorbs strongly in the 300 to 320 nm range (2). In this case, inhibition of isolated PSII activity by UVB damage to Z can be relieved by the addition of a PSII donor (48). Similarly, formation of donor radicals can no longer be detected after UVB illumination (60), even though the donors appear to be intact after visible light exposure (31).

Photosystem II also contains quinone acceptors, Q_A and Q_B, which absorb in the UV region and can form damaging radicals. The irradiation of thylakoid membranes by a UVB source induced damage to Q_A and impairment of the function of plastoquinone (35). The relative amount of damage to the donor or acceptor side of PSII may depend on experimental conditions. For example, in some cases a screened mercury lamp is used as a UVB source (35), while in other cases filtered output from a xenon arc lamp is used (48). These sources have different spectral profiles which may favor damage at different sites. In any case, it appears that there may be one or several sites of UV action away from the PSII reaction center. This may offer a molecular and biophysical basis

for distinguishing between when phytoplankton photosynthesis has been lowered by exposure to PAR alone, UVB alone, or a combination of both spectral types. PAR damages the reaction center, but donors and acceptors may not be affected (see previous discussion of PAR-induced inhibition). UVB irradiance may primarily damage donors/acceptors, but the reaction center remains functional. A combination of PAR and UVB irradiance may damage all components. In fact, reports of UVB irradiance damage to the PSII reaction center usually stem from experiments where varying UVB irradiance exposures were combined with a fixed background of PAR (23,54). This suggests that UV irradiance and PAR can act synergistically, an interaction already demonstrated to occur when chemical damage to donor/acceptors is combined with PAR exposure (8,55).

The above conceptual model for UV damage and UV-PAR interactions can aid the construction of fluorescence measurement protocols. Studies of PAR and UVB irradiance induced photoinhibition report a loss of F_v. However, few attempts have been made to systematically test the effects of artificial donors on F_v. This is important if the donor side (oxidizing side) of PSII is a primary site of UVB damage. In the case of PAR inhibition, loss of the reaction center means that no electron transport can occur (10,14). Loss of the donor site with an intact reaction center means that charge separation can occur but the electrons cannot accumulate on Q_A. However, if an artificial donor is added, then reduced Q_A can accumulate, and F_v should be restored. Such a possibility is supported by the results of Bornmann et al. (5) who reported that the artificial donor hydroxylamine (NH_2OH) could restore variable fluorescence after exposure of spinach chloroplasts to UVB. Renger et al. (48) found that the donor diphenylcarbazide (DPC) could restore electron transport after UVB exposure. However, Melis et al. (35) found DPC couldn't restore PSII activity after UVB inhibition of spinach thylakoids, consistent with their interpretation of UVB irradiance affecting the acceptor side of PSII. Damage to PSII acceptors cannot be distinguished from damage to the primary charge separation based on variation in F_v alone. However, supplementary measurements such as quantitation of Pheo reduction can differentiate between PAR damage to primary charge separation and UV damage of PSII acceptors (35). Variations in other fluorescence characteristics may also be particular to UV exposure (51). Bornmann et al. (5) found a characteristic change in the rise time of fluorescence, which was interpreted as another manifestation of lost activity of the PSII donor side.

Most of the investigations of UV effects cited so far have dealt with the responses measured after treatment of isolated chloroplast membranes. There may be important differences between the primary response target in an isolated system and in the intact plant. In the latter case recovery/repair processes may play a role. These are inactive in the isolated system. Because the loss of photosynthetic potential in phytoplankton exposed to UVB irradiance appears to plateau after a short transitional exposure time (12), the rate of damage must be opposed by a significant, albeit lesser, rate of recovery. An indicator of the rate

68

of recovery processes which repair PSII is the rate of turnover of the PSII D1 polypeptide. Greenberg *et al.* report that D1 turnover can occur in UVB alone, and the combination of UV and PAR increases turnover rates that are already saturated with respect to PAR (19). This may mean that there is a separate sensitizer for repair of UV damage to PSII.

Other studies of intact plant responses to UV irradiance suggest that soluble components necessary for photosynthesis may be affected as much, or to a greater extent, than the membrane components. Anderson and co-workers reported that a UVB irradiance supplementation of a PAR growth regime induced a decrease in both the number of functional PSII reaction centers and the activity and protein abundance of ribulose-1,5-carboxylase/oxygenase (Rubisco) enzyme in a UV sensitive variety of pea (52). Also, UVB exposure lead to a rapid decline in mRNA for both the small and large subunit (SSU and LSU) of the Rubisco complex (26), and for PSII polypeptides (25). The decline in Rubisco activity confirmed the earlier report of the inhibitory effect of UVB on Rubisco activity in pea and soybean (58). Tevini *et al.* found only negligible decrease in F_v/F_m in sunflower seedlings growing in chambers exposed to ambient solar UVB compared to UVB protected controls, even though there was a significant difference in photosynthesis and growth (53).

In summary, PSII is target for UVB stress, but other photosynthetic components, such as a Rubisco, may show greater net sensitivity in plants under natural irradiance conditions. It may be that moderate amounts of UV damage to the PSII complex can be adequately counteracted by the removal and replacement of the D1/D2 polypeptides as part of the PSII repair cycle. The PSII damage does not contribute directly to a loss of photosynthetic activity, but the long-term consequence of this increase in the photosynthetic "operating cost" (*sensu* 47) could be significant.

This selective review of current research on the mechanisms of irradiance stress in plants suggests that PAR and UV irradiance have common targets for causing decreases in photosynthesis, in addition, UV irradiance appears to damage complexes that are unaffected by PAR exposure. If such mechanisms are identified as operating in phytoplankton populations, inferences can be drawn about whether photosynthesis by phytoplankton exposed to full spectrum solar radiation is damaged by the PAR component, the UV component or by both components. This will be qualitative information, and will not tell us what portion of the inhibition is due to UV irradiance and what portion (if any) is due to PAR. However, the results should be consistent with any proposed quantitative model of irradiance stress effects in the aquatic environment.

DETECTION OF IRRADIANCE STRESS IN NATURAL PHYTOPLANKTON POPULATIONS

As already stated, photoinhibition in phytoplankton is a time-dependent phenomenon, so any attempt to determine whether photoinhibition is occurring *in situ*, as opposed to during incubations, has to take into account the effect of vertical mixing on the residence time of phytoplankton within the depth range of inhibiting irradiance (36). What is needed are incubation-free or "fresh sample" methods that can be used to infer *in situ* photosynthetic characteristics. These methods are constructed and interpreted using physio'ogical information on the process of interest. We briefly review some examples of these methods as applied in studies of natural phytoplankton populations.

One diagnostic indicator of *in situ* photosynthetic response is the light response curve of phytoplankton photosynthesis (*P-I* curve, Fig. 3). If measured rapidly (e.g. 32), the curve will reflect the physiological status of phytoplankton at the time of sampling. Photoinhibitory loss of PSII function, previous to sampling, results in a decrease in both α (initial slope) and P_m (37). Therefore, *in situ* photoinhibition can be inferred from a time course of the variation of *P-I* parameters for surface layer phytoplankton. For example, in high altitude, tropical Lake Titicaca, both P_m and α of midday and afternoon near-surface samples averaged 55% lower than control samples taken from depths where irradiance was only 5% of the surface intensity (42).

The diagnostic decrease in F_v/F_m for PAR-induced photoinhibition can be measured in natural phytoplankton using several approaches (13,37).
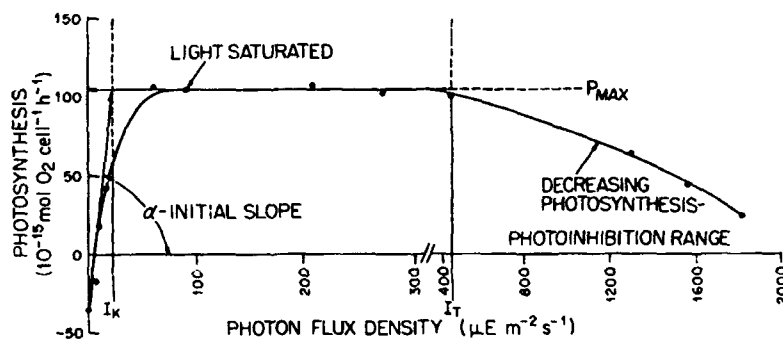
Figure 3. Schematic diagram of the algal photosynthesis-irradiance (*P-I*) curve showing the initial phase of light limitation, which is followed by a range of saturating light intensities and then by a decrease in photosynthesis due to high-light photoinhibition. The parameters P_m (=P_{max}) and a correspond to the light-saturated rate and initial slope of the *P-I* curve, respectively. Two characteristic light intensities are the onset of light saturation, I_k (=Pmax/α), and threshold of photoinhibition, I_T (From 36).

70

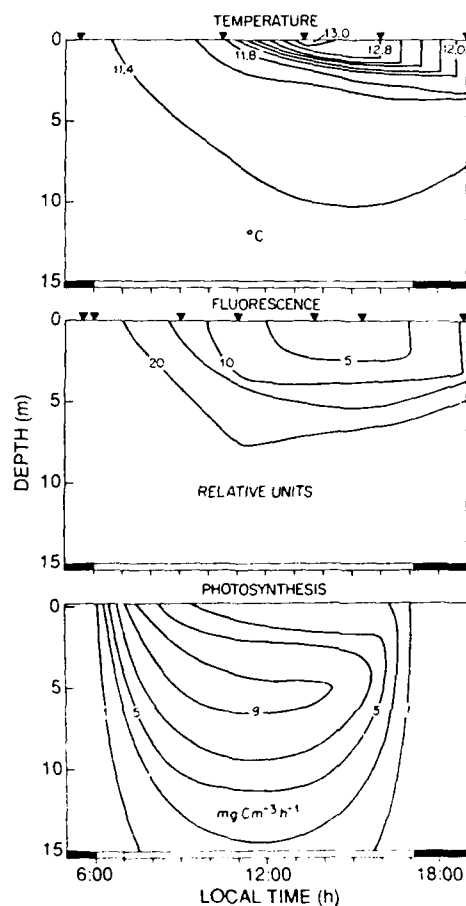**Figure 4.** Diurnal variation of temperature, fluorescence (dark adapted F_{DCMU}-F), and photosynthesis in Lake Titicaca (Peru/Bolivia) (From 36). Solid triangles indicate the times when profiles of temperature and fluorescence were measured; photosynthesis was calculated from phytoplankton *P-I* curves measured for samples taken at the surface and below the diurnal thermocline during morning, midday and afternoon.

Measurements of steady-state fluorescence at low excitation intensity can be made on discrete samples before (F) and after (F_{DCMU}) addition of DCMU. The difference approximates F_v (38). Time series of vertical profiles of dark adapted F and F_{DCMU} in Lake Titicaca showed the *in situ* occurrence of photoinhibition in a layer extending from the surface to about 7 m (10% light depth) (42,56). At the surface, F_{DCMU} - F decreased by 50-100% from morning to midday and remained depressed for most of the afternoon. Time-series experiments showed that the fluorescence decline is correlated with the decline in P_m (56). Photoinhibition of primary production in Lake Titicaca was closely coupled to the development of diurnal stratification (Fig. 4). Thus, vertical mixing regime is a primary factor controlling photoinhibition *in situ* (additional discussion in 36). The occurrence of high surface irradiance year-round at low latitude suggests that *in situ* photoinhibition may occur in many tropical systems.
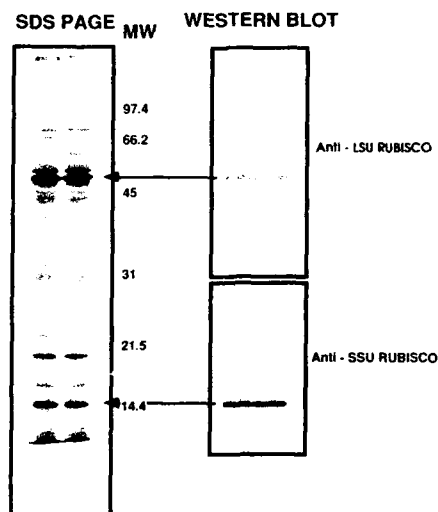
71

SDS PAGE MW   **WESTERN BLOT**

97.4
66.2   Anti - LSU RUBISCO
45
31
21.5   Anti - SSU RUBISCO
14.4

Figure 5. Isolation and identification of LSU and SSU of Rubisco using SDS/PAGE and electrotransfer of proteins to nitrocellulose followed by immunostaining (Western blotting). Replicate samples from a UV exposed culture are shown, each lane contains proteins extracted from an algal sample with total biomass of 1.6 µg Chl *a*. *Left Panel*: SDS-PAGE gel with Coomassie stain to visualize isolated proteins. *Right Panels*: Western blots showing identification of LSU and SSU polypeptides. Arrows indicate inferred position of LSU and SSU on stained gel (From 39).

MW   - +

97.4
66.2
45   ← LSU RUBISCO →
31
21.5
14.4   ← SSU RUBISCO

Relative Abs.

UV
+ UV

Relative Distance
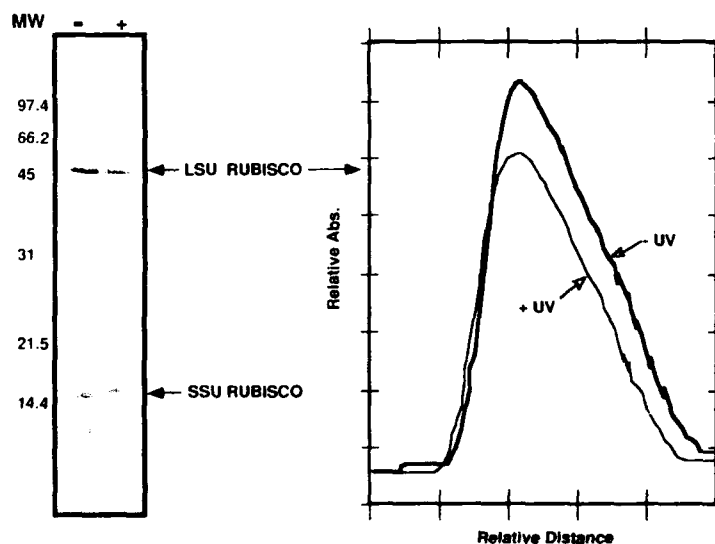
Figure 6. Comparisons of proteins isolated from microalgal samples from the UV exposed ('+') and UV protected ('-') tanks. Each lane was loaded with proteins from 0.5 µg Chl *a* of algal sample. *Left Panel* SDS-PAGE gel stained with Coomassie. Bands at 53 and 15 kD were identified as the LSU and SSU of Rubisco. *Right Panel* Densitometric scan of the gel LSU bands for samples from UV exposed ('+UV') and UV protected ('-UV') tanks. The integrated area under the curve is a relative measure of LSU protein per unit Chl, it is 20% less for sample from the UV exposed tank (From 39).

72

Photoinhibition in conjunction with diurnal stratification has been observed in the Equatorial Pacific (Cullen and Lewis unpublished data). Other investigations have used DCMU induced fluorescence to show that photoinhibition also occurs in temperate systems during the late spring and summer (15,46). Photoinhibition also contributes to decline of the spring diatom abundance maximum in the Windermere (English Lake District) (38).

Recently, technological developments in fluorescence instrumentation have enabled measurements of phytoplankton F_v/F_m without application of DCMU (28, 50, see also other chapters in this volume) and the measurement of solar stimulated or "natural" fluorescence (e.g. 9), in essence the steady-state fluorescence, F_s. These technologies promise to improve the accuracy of measuring fluorescence, particularly F_v/F_m, in aquatic environments. Routine measurement of fluorescence parameters throughout the day will help clarify the frequency of occurrence of photoinhibition in phytoplankton populations.

Fluorescence measurements may not detect photoinhibition by UV irradiance (as previously discussed), so other diagnostic methods may be necessary. An alternative approach may be found in "molecular probe" methods of identifying phytoplankton proteins (59) or nucleic acids (44,61). A preliminary investigation has been made of the application of Rubisco LSU antibody probes to detecting UV inhibition in Antarctic diatoms (39). Exposure of diatoms in tanks to UV irradiance (290 - 375 nm) under "ozone hole" conditions was linked to a 25% decrease in P_m but no change in α (39). The estimated Rubisco content (per unit Chl) declined about 20% in samples taken under similar conditions of UV irradiance exposure (Figs. 5 and 6). There was no difference in the $(F_{DCMU} - F)/F_{DCMU}$ ratio between UV exposed and UV protected tanks (Neale *et al.* unpubl. data). These results motivate the test of Rubisco assays as a probe of UV inhibition under a wider variety of conditions, as well as development of other molecular-probe-based indicator assays (16).

CONCLUSION

While there are presently only a few examples of the application of indicator assays to the detection of irradiance stress of phytoplankton photosynthesis, the approach is promising. The strategy is to seek useful connections between physiological studies and the design of field methods. Establishing such connections is an important purpose of having a conference on "Photosynthetic Responses to the Environment". Hopefully, the next conference on this theme will record how this interaction has lead to significant improvements in our understanding of the effects environmental change on the photosynthetic activities of plant communities, both aquatic and terrestrial.

LITERATURE CITED

1. **Aro EM, Hundell T, Carlsberg I, Andersson B** (1990) *In vitro* studies on light induced inhibition of Photosystem II and D1-protein degradation at low temperatures. Biochim Biophys Acta **1019**: 269-275
2. **Bent DV, Hayon E** (1975) Excited-state chemistry of aromatic amino-acids and related peptides. 1. Tyrosine. J Am Chem Soc **97**: 2599-2606
3. **Björkman O** (1987) Low-temperature chlorophyll fluorescence in leaves and its relationship to photon yield of photosynthesis in photoinhibition. *In* DJ Kyle, CB Osmond, CJ Arntzen, eds, Photoinhibition. Elsevier, pp 123-144
4. **Bornmann JF** (1989) Target sites of UV-B radiation in photosynthesis of higher plants. J Photochem Photobiol **4**: 145-158
5. **Bornmann JF, Bjorn LO, Akerlund H-E** (1984) Action spectrum for inhibition by ultraviolet radiation of photosystem II activity in spinach thylakoids. Photobiochem Photobiophys **8**: 305-313
6. **Briantais JM, Ducruet JM, Hodges M, Krause GH** (1992) The effects of low temperature acclimation and photoinhibitory treatments on photosystem-II studied by thermoluminescence and fluorescence decay kinetics. Photosyn Res **31**: 1-10
7. **Broecker WS** (1991) Global change and oceanography programs. Science **254**: 1566
8. **Callahan FE, Becker DW, Cheniae GM** (1986) Studies on the photoactivation of the water-oxidizing enzyme II. Characterization of weak light photoinhibition of PSII and its light-induced recovery. Plant Physiol **82**: 261-269
9. **Chamberlin WS, Booth CR, Kiefer DA, Morrow JH, Murphy RC** (1990) Evidence for a simple relationship between natural fluorescence, photosynthesis and chlorophyll in the sea. Deep-Sea Res Pt. A **37**: 951-973
10. **Cleland RE, Melis A, Neale PJ** (1986) Mechanism of photoinhibition: photochemical reaction center inactivation of system II of chloroplasts. Photosyn Res **9**: 79-88
11. **Clendennen SK, Alberte RS, Powers DA** (1992) A mechanism of UV-B damage in chromophytic marine macrophytes. Abs. ASLO Aquatic Sciences Meeting, Santa Fe N.M.
12. **Cullen JJ, Lesser MP** (1991) Inhibition of photosynthesis by ultraviolet radiation as a function of dose and dosage rate: Results for a marine diatom. Mar Biol **111**: 183-190
13. **Cullen JJ, Yentsch CM, Cucci TL, MacIntyre HL** (1988) Autofluorescence and other optical properties as tools in biological oceanography. *In* Ocean Optics 9, Proc. SPIE **925**: 149-156
14. **Demeter S, Neale PJ, Melis A** (1987) Photoinhibition: impairment of the primary charge separation between P-680 and pheophytin in photosystem II of chloroplasts. FEBS Letters **214**: 370-374
15. **Elser JJ, Kimmel BL** (1985) Photoinhibition of temperate lake phytoplankton by near-surface irradiance: Evidence from vertical profiles and field experiments. J Physcol **21**: 419-427

16. **Falkowski PG** (1992) Molecular ecology of phytoplankton photosynthesis. *In* PG Falkowski, AD Woodhead, eds, Primary Productivity and Biogeochemical Cycles in the Sea, Plenum, pp 47-67

17. **Franklin LA, Levasseur G, Osmond CB, Henley WJ, Ramus J** (1992) Two components of onset and recovery during photoinhibition of *Ulva rotundata*. Planta **186**: 399-408

18. **Giersch C, Krause GH** (1991) A simple model relating photoinhibitory fluorescence quenching in chloroplast to a population of altered photosystem-II reaction centers. Photosyn Res **30**: 115-121

19. **Greenberg BM, Gaba V, Canaani O, Malkin S, Mattoo AK, Edelman M** (1989) Separate photosensitizers mediate degradation of the 32-kDa photosystem II reaction center protein in the visible and UV spectral regions. Proc Natl Acad Sci USA **86**: 6617-6620

20. **Greer DH, Berry JA, Björkman O** (1986) Photoinhibition of photosynthesis in intact bean leaves: role of light, temperature and requirement for chloroplast-protein synthesis during recovery. Planta **168**: 253-260

21. **Guenther JE, Melis A** (1990) The physiological significance of photosystem II heterogeneity in chloroplasts. Photosyn Res **23**: 105-109

22. **Guenther JE, Nemson JA, Melis A** (1988) Photosystem stoichiometry and chlorophyll antenna size in *Dunaliella salina* (green algae). Biochim Biophys Acta **934**: 108-117

23. **Iwanzik W, Tevini M, Dohnt G, Voss M, Weiss W, Graber P, Renger G** (1983) Action of UV-B radiation on photosynthetic primary reactions in spinach chloroplasts. Physiol Plant **58**: 401-407

24. **Jones LW, Kok B** (1966) Photoinhibition of chloroplast reactions II: Multiple effects. Plant Physiol **41**: 1044-1049

25. **Jordan BR, Chow WS, Strid A, Anderson JM** (1991) Reduction in *cab* and *psbA* RNA transcripts in response to supplementary ultraviolet-B radiation. FEBS Lett **284**: 5-8

26. **Jordan BR, He J, Chow WS, Anderson JM** (1992) Changes in mRNA levels and polypeptide subunits of ribulose-1,5-carboxylase in response to supplementary ultraviolet-B radiation. Plant Cell Env **15**: 91-98

27. **Kirk JTO** (1983) Light and photosynthesis in aquatic ecosystems. Cambridge University Press

28. **Kolber Z, Zehr JR, Falkowski PG** (1988) Effects of growth irradiance and nitrogen limitation on photosynthetic energy conversion in photosystem II. Plant Physiol **88**: 923-929

29. **Krause GH** (1988) Photoinhibition of photosynthesis. An evaluation of damaging and protective mechanisms. Physiol Plant **74**: 566-574

30. **Krause GH, Weis E** (1991) Chlorophyll fluorescence and photosynthesis - The basics. Annu Rev Plant Physiol Plant Mol Bol **42**: 313-349

31. **Kyle DJ, Ohad I, Arntzen CJ** (1984) Membrane protein damage and repair: Selective loss of a quinone-protein function in chloroplast membranes. Proc Natl Acad Sci USA **81**: 4070-4074

32. **Lewis MR, Smith JC** (1983) A small volume, short-incubation-time method for measurement of photosynthesis as a function of incident irradiance. Mar Ecol Prog Ser **13**: 99-102

33. **Mattoo AK, Edelman M** (1987) Intramembrane translocation and post-translational palmitylation of the chloroplast 32-kDa herbicide-binding protein. Proc Natl Acd Sci USA **84**: 1497-1501

34. **Melis A** (1985) Functional properties of photosystem II-β in spinach chloroplasts. Biochim Biophys Acta **808**: 334-342

35. **Melis A, Nemson JA, Harrison MA** (1992) Damage to functional components and partial degradation of photosystem II reaction center proteins upon chloroplast exposure to ultraviolet-B radiation. Biochim Biophys Acta **1100**: 312-320

36. **Neale PJ** (1987) Algal photoinhibition and photosynthesis in the aquatic environment. In Kyle DJ, Osmond CB, Arntzen CJ., eds, Photoinhibition, pp 39-65

37. **Neale PJ, Cullen JJ, Yentsch CM** (1989) Bio-optical inferences from chlorophyll a fluorescence: What kind of fluorescence is measured in flow cytometery? Limnol Oceanogr **34**: 1739-1748

38. **Neale PJ, Heaney SI, Jaworski GH** (1991) Responses to high-irradiance contribute to the decline of the spring diatom maximum. Limnol Oceanogr **36**: 761-768

39. **Neale PJ, Lesser MP, Cullen JJ, Goldstone J** (1992) Detecting UV-induced inhibition of photosynthesis in Antarctic phytoplankton. Ant J U S (in press)

40. **Neale PJ, Melis A** (1990) Activation of a reserve pool of Photosystem II in Chlamydomonas reinhardtii counteracts photoinhibition Plant Physiol **92**: 1196-1204

41. **Neale PJ, Melis A** (1991) Dynamics of Photosystem II heterogeneity during photoinhibition: Depletion of PSIIβ from non-appressed thylakoids during strong-irradiance exposure of Chlamydomonas reinhardtii. Biochim Biophys Acta **1056**: 195-203

42. **Neale PJ, Richerson PJ** (1987) Photoinhibition and the diurnal variation of phytoplankton photosynthesis-I Development of a photosynthesis-irradiance model from studies of in situ responses. J Plankton Res **9**: 167-193

43. **Ohad I, Koike H, Shochat S, Inoue Y** (1988) Changes in the properties of reaction center II during the initial stages of photoinhibition as revealed by thermoluminescence measurements. Biochim Biophys Acta **933**: 288-298

44. **Pichard SL, Paul JH** (1991) Detection of gene expression in genetically engineered microorganisms and natural phytoplankton populations in the marine environment by mRNA analysis. Appl Env Microbiol **57**: 1721-1727

45. **Powles SB** (1984) Photoinhibition of photosynthesis induced by visible light. Annu Rev Plant Physiol **35**: 15-44

46. **Putt M, Harris GP, Cuhel RL** (1987) Photoinhibition of DCMU-fluorescence in Lake Ontario phytoplankton. Can J Fish Aquat Sci **44**: 2144-2154

47. **Raven JA, Samuelsson G** (1986) Repair of photoinhibitory damage in anacystis nidulans 625 (Synechococcus 6301): Relation to catalytic capacity for, and energy supply to, protein synthesis, and implications for μmax and efficiency of light limited growth. New Phytol **103**: 625-643

48. **Renger G, Volker M, Eckert HJ, Fromme R, Hohm-Veit S, Graber P** (1989) On the mechanism of Photosystem II deterioration by UV-B irradiation. Photochem Photobiol **49**: 97-105

49. **Richter M, Rühle W, Wild A** (1990) Studies on the mechanism of photosystem II photoinhibition I. A two-step degradation of D1-protein. Photosyn Res **24**: 229-235

50. **Schreiber U, Schliwa U, Bilger W** (1986) Continuous recording of photochemical and nonphotochemical quenching with a new type of modulation fluorometer. Photosyn Res **10**: 51-62

51. **Smillie RM** (1983) Chlorophyll fluorescence *in vivo* as a probe for rapid measurement of tolerance to ultraviolet radiation. Plant Science Lett **28**: 283-289

52. **Strid Å, Chow WS, Anderson JM** (1990) Effects of supplementary ultraviolet-B radiation on photosynthesis in *Pisum sativum*. Biochim Biophys Acta **1020**: 260-268

53. **Tevini M, Mark U, Fieser G, Saile M** (1991) Effects of enhanced solar UV-B radiation on growth and function of selected crop plant seedlings. *In* E Riklis, ed, Photobiology, Plenum, pp 635-649

54. **Tevini M, Pfister K** (1985) Inhibition of photosystem II by UV-B radiation. Z Naturforsch **20**: 885-889

55. **Theg SM, Filar LJ, Dilley RA** (1986) Photoinactivation of chloroplasts already inhibited on the oxidizing side of Photosystem II. Biochim Biophys Acta **849**: 104-111

56. **Vincent WF, Neale PJ, Richerson PJ** (1984) Photoinhibition: algal responses to bright light during diel stratification and mixing in a tropical alpine lake. J Phycology **20**: 201-211

57. **Virgin I, Salter H, Hagman Ä, Vass I, Styring S, Andersson B** (1992) Molecular mechanisms behind light-induced inhibition of Photosystem II electron transport and degradation of reaction centre polypeptides. Biochim Biophys Acta **1101**: 139-142

58. **Vu CV, Allen LH, Garrard LA** (1984) Effects of enhanced UV-B radiation (280-320 nm) on ribulose-1,5-phosphate carboxylase in pea and soybean. Env Exp Bot **24**: 131-143

59. **Yentsch CM, Mague FC, Horan PK** (1988) Immunochemical approaches to coastal, estuarine, and oceanographic questions. Springer-Verlag, New York

60. **Yerkes CT, Kramer DM, Fenton JM, Crofts AR** (1990) UV-photoinhibition. Studies *in vitro* and in intact plants. *In* M Baltscheffsky, ed, Current Research in Photosynthesis, Vol II, Kluwer, pp 381-384

61. **Zehr JP, Limberger RJ, Ohki K, Fujita Y** (1990) Antiserum to nitrogenase generated from an amplified fragment from natural populations of *Trichodesmium* spp. Appl Env Microbiol **56**: 3527-3531

Role of Lipids in Low-Temperature Adaptation[1]

**Hajime Wada, Zoltan Gombos, Toshio Sakamoto and
Norio Murata**

*Department of Regulation Biology, National Institute for Basic Biology
(HW, ZG, NM); and Department of Molecular Biomechanics, Graduate
University of Advanced Studies, Myodaiji, Okazaki 444, Japan (TS, NM)*

INTRODUCTION

A number of organisms can regulate the fatty-acid composition of their
membrane lipids in response to a change in ambient temperature (14, 19). Such
temperature-induced changes in fatty-acid composition are explained in terms of
the regulation of membrane fluidity that is necessary to maintain proper
functioning of biological membranes (4).

Prokaryotic algae, the cyanobacteria, resemble chloroplasts of eukaryotic
plants with respect to lipid and fatty-acid composition (10) and membrane
structure (18). Thus, the cyanobacteria can be regarded as a model system for
elucidation of the effects of temperature on membrane lipids in chloroplasts.

Sato and Murata (15, 16) demonstrated that a cyanobacterium, *Anabaena
variabilis*, responds to low temperature by desaturating the fatty acids of
membrane lipids. This low temperature-induced desaturation can be regarded as
emergency acclimation to compensate the decrease in membrane fluidity due to
a decrease in temperature. However, the role of increased unsaturation of fatty
acid in tolerance of low temperatures is not clear, because the acclimation to
low temperature induces not only unsaturation of fatty acids but also a number
of metabolic alterations. Therefore, it is possible to speculate that such metabolic
alterations, but not the unsaturation of membrane fatty acids, alter cyanobacteria
tolerance to low temperatures. In order to verify whether the unsaturation of
fatty acids contributes to low-temperature tolerance, we employed tools of

[2]Abbreviations: BQ, 1,4-benzoquinone; Chl, chlorophyll; DCIP, 2,6-dichlorophenol
indophenol; DGDG, digalactosyl diacylglycerol; DPC, 2,2'-diphenylcarbazide; MGDG,
monogalactosyl diacylglycerol; Km^r, kanamycin-resistance gene; PG, phosphatidylglycerol;
PS, photosystem; SQDG, sulfoquinovosyl diacylglycerol; X:Y(Z), fatty acid containing X
carbon atoms with Y double bonds in the *cis* configuration at position Z counted from the
carboxy terminus

molecular biology to introduce genes for fatty acid desaturation to modify the unsaturation of fatty acid without affecting any other metabolic processes for select cyanobacteria.

To clone the genes required for unsaturation of fatty acids we isolated two mutants of *Synechocystis* PCC6803, Fad6 and Fad12, which are defective in the ability to desaturate C_{18} fatty acids at the $\Delta6$ and $\Delta12$ positions, respectively (20). This cyanobacterium can be transformed *in situ* by exogenously added DNA (22). Using the mutant Fad12, we isolated a gene, designated *desA*, which is responsible for desaturation at the $\Delta12$ position of fatty acids esterified to glycerolipids (21).

In this study, we manipulated the unsaturation of fatty acids of membrane lipids in two ways. First, in *Synechocystis* PCC6803 we transformed wild-type and Fad6 strains with a disrupted *desA* gene. Second, in *Anacystis nidulans* R2-SPc, we transformed wild-type cells with the *desA* gene. With use of genetically manipulated strains, the effect of unsaturation of fatty acids in membrane lipids on the growth and the photosynthesis at low temperature was studied.

MATERIALS AND METHODS

Organisms and Culture Conditions

Wild-type and mutant Fad6 cells of *Synechocystis* PCC6803 were grown at 34°C or 22°C in the light in BG-11 medium, as described previously (20). The transformants of wild type and mutant Fad6 of *Synechocystis* PCC6803 with a disrupted *desA* gene, that are termed WT/*desA*::Km^{r2} and Fad6/*desA*::Km^r, respectively, were grown in BG-11 medium supplemented with 5 µg ml^{-1} kanamycin. Wild type and transformants of *A. nidulans* R2-SPc with pUC303 and pUC303/*desA* (termed T-pUC303 and T-pUC303/*desA*, respectively) were grown at 34°C in BG-11 medium, the transformants were grown in the presence of chloramphenicol at 7.5 µg ml^{-1}. The growth of cells was measured in terms of turbidity at 730 nm, and doubling times during the exponential phase of growth were calculated.

Extraction of Lipids and Analysis of Fatty Acids

Lipids were extracted from the collected cells by the method of Bligh and Dyer (2). Analysis of lipids was carried out according to the method of Sato and Murata (17).

Transformation of *Synechocystis* PCC6803 and *A. nidulans* R2-SPc

The disrupted *desA* gene, *desA*::Km^r, was constructed by interrupting the coding region of *desA* gene with Km^r. A plasmid containing the disrupted *desA* was used to transform the wild type and Fad6 of *Synechocystis* PCC6803 by the method of Golden *et al.* (5). For transformation of *A. nidulans* R2-SPc, *desA* gene was subcloned into pUC303, a shuttle vector between *A. nidulans* and

Escherichia coli. This plasmid, termed pUC303/*desA*, was used to transform *A. nidulans* R2-SPc by the method of Kuhlemeier and van Arkel (8).

Photoinhibition

Cells corresponding to 60 µg Chl were suspended in 30 ml of BG-11 medium. The cell suspension was illuminated at various temperatures in a thermostated reaction vessel with white light of various intensities supplied by two incandescent lamps (150 W, Toshiba, Japan) in aerated with sterile air that contained 1% CO_2. The light intensity was regulated in the range of 0-2500 µE m^{-2} s^{-1}.

Measurement of Photosynthetic Activities

Photosynthetic oxygen evolution of intact cells suspended in BG-11 medium was monitored by means of oxygen exchange with a Clark-type oxygen electrode. The oxygen-evolving activity of intact cells due to PS II activity was measured with 1 mM BQ and 1 mM $K_3Fe(CN)_6$ as electron acceptors (13). Light at 3500 µE m^{-2} s^{-1} was provided from an incandescent lamp combined with a red optical filter (R-62, Hoya Glass Co., Tokyo). Chl concentration was determined according to Arnon *et al.* (1).

RESULTS AND DISCUSSION

Genetic Manipulation of Unsaturation of Fatty Acid

The disrupted *desA* gene was used to transform both wild type and Fad6 mutant of *Synechocystis* PCC6803. Kanamycin-resistant transformants, WT/*desA*::Km^r and Fad6/*desA*::Km^r, were selected on agar plates that contained BG-11 and kanamycin. Southern blot analysis of genomic DNAs, using the *desA* gene as a probe, indicated that both transformants contained disrupted *desA* gene but no native *desA* gene in their chromosomes. Major unsaturated fatty acids of total glycerolipids isolated from wild type, mutant Fad6 and transformants, WT/*desA*::Km^r and Fad6/*desA*::Km^r, all grown at 34°C, are shown in Fig. 1. The most abundant unsaturated fatty acids of the wild type were 18:1(9), 18:2(9,12) and 18:3(6,9,12). The major unsaturated fatty acids of Fad6 were 18:1(9) and 18:2(9,12), indicative of the defect in desaturation of fatty acid at the Δ6 position (20). In the transformant WT/*desA*::Km^r, as compared with that of the wild type, level of 18:1(9) was significantly elevated and a new fatty acid, 18:2(6,9) emerged in the cells whereas the relative contents of 18:3(6,9,12) and 18:2(9,12) fell to zero. The major unsaturated fatty acids of this strain were the same as those of Fad12, as described previously (20). The transformant, Fad6/*desA*::Km^r contained only monounsaturated fatty acid, 18:1(9), as a major unsaturated fatty acid. These findings indicate that the extent of unsaturation of fatty acids in membrane lipids can be modified by genetically introducing the *desA* gene into *Synechocystis* PCC6803. Because about 90% of the total glycerolipids of cyanobacteria originate from the thylakoid membranes (9), the fatty-acid
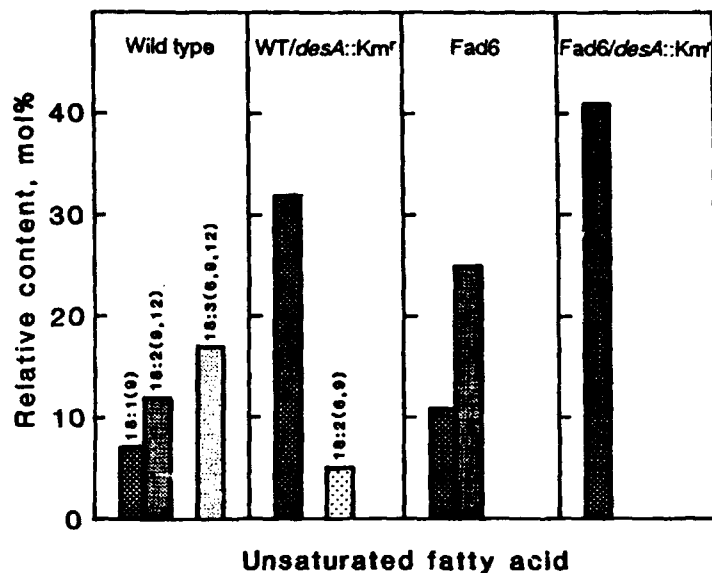
80

Figure 1. Major unsaturated fatty acids in wild type, WT/*desA*::Km^r, Fad6 and Fad6/*desA*::Km^r of *Synechocystis* PCC6803. Cells were grown at 34°C. Values are the relative contents of unsaturated fatty acids in the total fatty acids.

composition of the total lipids would be close to that of the thylakoid membrane lipids. By comparing the low-temperature sensitivity of these strains, it is possible to study the relationship between the unsaturation of fatty acid of thylakoid membrane lipids and the low-temperature sensitivity of photosynthesis.

Effect of Unsaturation of Fatty Acid on Growth and Photosynthesis

With use of genetically manipulated strains described above, the effect of unsaturation of fatty acid on growth and photoinhibition of photosynthesis at low temperatures were studied with the minimum interference of the other factors.

The doubling times during the exponential phase of growth of the wild-type cells, the mutant Fad6 cells, and the transformed cells of WT/*desA*::Km^r and Fad6/*desA*::Km^r are shown in Table I. At 34°C, there was no significant difference between the various types of cell. At 22°C, Fad6 cells grew at the same rate as wild-type cells. By contrast, the growth rates of WT/*desA*::Km^r and Fad6/*desA*::Km^r cells were much lower than those of wild-type cells. The growth rates at 34°C and 22°C of the transformant, WT/*desA*::Km^r, were the same as those of Fad12, as described previously (20). These observations suggest that elimination of polyunsaturated fatty acids by transformation of Fad6 cells with a disrupted *desA* gene has a deleterious effect on the growth of *Synechocystis* PCC6803 at 22°C but not at 34°C.

Table I. *Doubling time at the exponential growth phase of the wild type*
Synechocystis *PCC6803, Fad6 and the transformants of wild type and Fad6*
with a disrupted desA *gene*

Strain	Growth Temperature	
	34°C	22°C
	(h)	
Wild type	14	20
WT/desA::Km^r	15	48
Fad6	13	21
Fad6/desA::Km^r	14	>96

The photosynthetic activities of wild type, Fad6, and Fad6/desA::Km^r cells, grown at 34°C, were compared at 18°C, 25°C and 34°C. Under saturating-light conditions, the activity of electron transport from H_2O to BQ and the oxygen-evolving activity of photosynthesis without any electron acceptor were highly dependent on temperature. In all strains the activity of photosynthesis at 34°C was 5 times as high as that at 18°C, while the activity of electron transport from H_2O to BQ at 34°C was about 4 times as high as that at 18°C. However, despite the considerable differences in unsaturation of fatty acid among the three strains, no significant alterations in the activities of photosynthesis and electron transport were observed at the three temperatures of measurements.

Figure 2 presents the temperature dependence of photoinhibition in intact cells of wild type, Fad6 and Fad6/desA::Km^r. When the cells were exposed to light of 1500 μE m^{-2}sec^{-1}, the photoinhibition of photosynthesis occurred and the extent of photoinhibition increased at low temperature in all strains. However, the extent of photoinhibition in Fad6/desA::Km^r cells was much greater, especially at low temperature, than those in wild type and Fad6 cells. At 30°C, wild type and Fad6 cells were resistant to photoinhibition. Fad6/desA::Km^r cells still suffered photoinhibition, but the extent was much lower than at low temperatures such as 10°C or 20°C. Figure 3 shows the effect of light intensity on photoinhibition at 20°C. The extent of photoinhibition was pronounced at high light intensity. At 1500 μE m^{-2} s^{-1}, Fad6/desA::Km^r cells lost 80% of the photosynthetic activity. In contrast, wild-type and Fad6 cells still preserved 90 to 100% of original activity. These observations suggest that Fad6/desA::Km^r cells are much more susceptible to the photoinhibition than wild type and Fad6 cells.

Photoinhibition in intact kiwifruit leaves is accelerated at low temperatures (7). Here, we demonstrated that photoinhibition of all strains of *Synechocystis* PCC6803 was more pronounced at low temperatures than at their growth
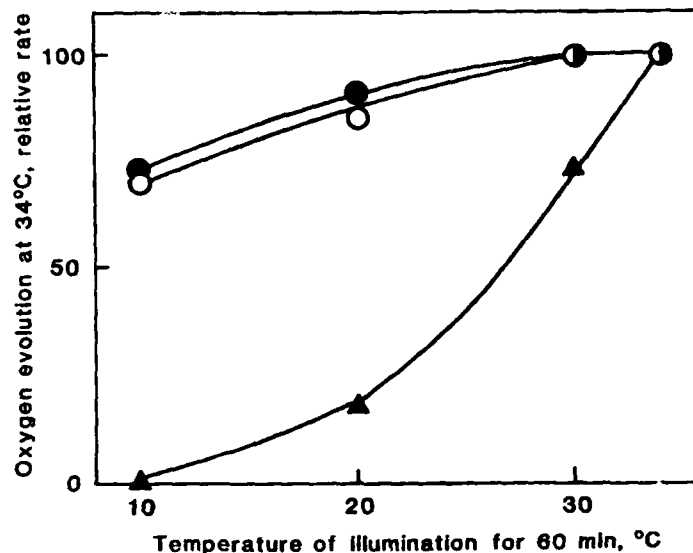
Figure 2. The effect of temperature on photoinhibition of photosynthesis in wild type, Fad6 and Fad6/*desA*::Km^r of *Synechocystis* PCC6803 grown at 34°C. Cells, grown at 34°C, were suspended in BG-11 medium at a concentration that corresponded to 2 µg Chl ml^{-1}, and were exposed to the light intensity of 1500 µE m^{-2} s^{-1} for 60 min at designated temperatures. After the treatment the activity of photosynthesis was measured at growth temperature, 34°C. The symbols indicate wild type (O), Fad6 (●) and Fad6/*desA*::Km^r (Δ). The activity of 100% corresponded to 320, 330 and 310 µmol O$_2$ (mg Chl)$^{-1}$ h^{-1} in wild type, Fad6 and Fad6/*desA*::Km^r, respectively.

temperature. Photoinhibition at low temperatures is accelerated further by elimination of polyunsaturated fatty acids from membrane lipids. However, it was also observed that the photoinhibition at 30°C was faster in Fad6/*desA*::Km^r than in wild type and Fad6. Therefore, it is very likely that at low and normal temperatures the unsaturation of fatty acid is related to the tolerance to photoinhibition, although this effect appears more pronounced at low temperatures.

Transformation of *A. nidulans* R2-SPc with *desA* Gene

Anacystis nidulans R2-SPc was transformed with pUC303 and pUC303/*desA*. Transformants, T-pUC303 and T-pUC303/*desA*, were selected on agar plates that contained BG-11 and chloramphenicol. The wild type and the transformant of *A. nidulans* R2-SPc with pUC303 alone (control) contained 16:0, 16:1(9), 18:0 and 18:1(9) as major fatty acids, indicating that this cyanobacterium can introduce only one double bond into the C$_{16}$ and C$_{18}$ fatty acids. In the transformant with pUC303/*desA*, fatty acids having two double bonds, 16:2(9,12)
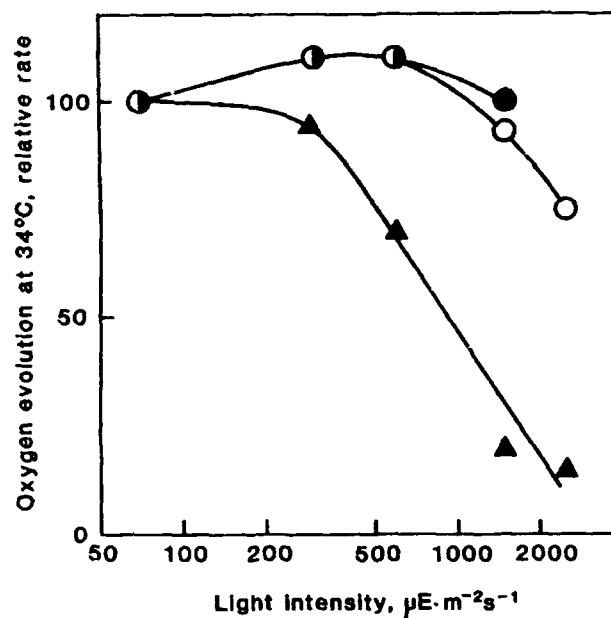
83

Figure 3. The effect of light intensity on photoinhibition of photosynthesis in wild type, Fad6 and Fad6/desA::Km^r of *Synechocystis* PCC6803. Cells were grown at 34°C. The symbols indicate wild type (O), Fad6 (●) and Fad6/desA::Km^r (Δ). The activity of photosynthesis was measured at 34°C and the activity of 100% corresponded to 320, 330 and 310 μmol O$_2$ mg Chl^{-1} h^{-1} in wild type, Fad6 and Fad6/desA::Km^r, respectively.

and 18:2(9,12), emerged to significant levels at the expense of 16:1(9) and 18:1(9). These observations demonstrate that the transformant with *desA* gene has acquired the desaturase activity in introducing the second double bond at the Δ12 position of fatty acids.

Anacystis nidulans is sensitive to chilling temperature (10, 11, 13). At growth temperature, both plasma and thylakoid membranes are in the liquid-crystalline state. With decrease in temperature, first the thylakoid membrane goes into the phase-separated state only with reversible deterioration of photosynthesis. Upon further decrease in temperature, the plasma membrane enters the phase-separated state, in which leakage of the cytosolic solutes of low-molecular weight into the medium irreversibly damages physiological activities (10, 11). Because the phase transition temperature depends on the degree of unsaturation of fatty acids of membrane lipids (3), it could be predicted that the chilling tolerance of *A. nidulans* can be altered by transformation with *desA* gene by introducing double bonds into fatty acids of membrane lipids.

When the wild type and transformant with pUC303 of *A. nidulans* R2-SPc grown at 34°C were exposed to 5°C for 120 min, 70% of photosynthetic activity
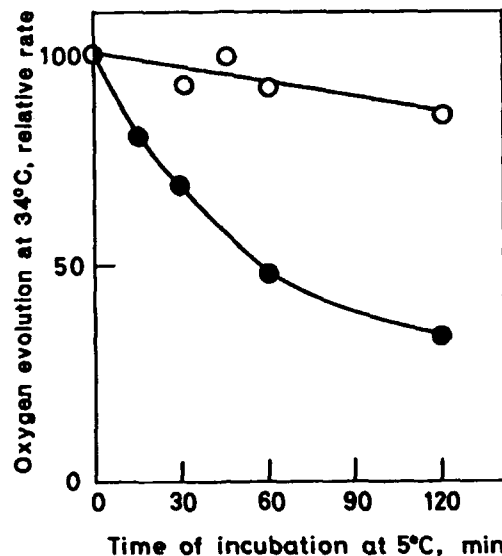
Figure 4. The effect of transformation with *desA* gene on the low-temperature tolerance measured by the activity of photosynthesis in *Anacystis nidulans* R2-SPc. Cells, grown at 34°C, were exposed to 5°C in darkness for designated periods and then the activity of photosynthesis was measured at growth temperature, 34°C. The symbols indicate transformant with pUC303 (●) and transformant with pUC303/*desA* (○). The activity before exposure to 5°C corresponded to about 190 μmol O_2 mg^{-1} Chl h^{-1} for both transformants.

was lost (Figure 4). In contrast, the transformant with pUC303/*desA* lost only 15% of photosynthetic activity during the exposure to 5°C for 120 min. This observation demonstrates that chilling tolerance of *A. nidulans* R2-SPc was enhanced by transformation with *desA* gene.

The phase transition from the liquid-crystalline to the phase-separated state of the plasma membrane in intact cells of *A. nidulans* can be studied by changes in the absorption spectrum of carotenoids (6, 10, 12, 13). The phase transition of the plasma membranes of the transformants containing pUC303 or pUC303/*desA*, both grown at 34°C, appeared in temperature ranges from 8°C to 4°C with a mid point at 6°C, and from 6°C to 2°C with a mid point at 4°C, respectively. The lowering in the phase transition temperature of the plasma membrane by *desA* gene can be regarded as a result of the introduced desaturase activity.

85

LITERATURE CITED

1. **Arnon DI, McSwain BD, Tsujimoto HY, Wada K** (1974) Photochemical activity and components of membrane preparations from blue-green algae. I. Coexistence of two photosystems in relation to chlorophyll *a* and removal of phycocyanin. Biochim Biophys Acta **357**: 231-245

2. **Bligh EG, Dyer WJ** (1959) A rapid method of total lipid extraction and purification. Can J Biochem Physiol **37**: 911-917

3. **Chapman D** (1975) Phase transitions and fluidity characteristics of lipids and cell membranes. Quart Rev Biophys **8**: 185-235

4. **Cossins AR, Sinensky M** (1984) Adaptation of membranes to temperature, pressure, and exogenous lipids. *In* M Shinitzky ed, Physiology of Membrane Fluidity, Vol II. CRC Press, Boca Raton, Florida, pp 1-20

5. **Golden SS, Brusslan J, Haselkorn R** (1987) Genetic engineering of the cyanobacterial chromosome. Methods Enzymol **153**: 215-231

6. **Gombos Z, Vigh L** (1986) Primary role of the cytoplasmic membrane in thermal acclimation evidenced in nitrate-starved cells of the blue-green alga, *Anacystis nidulans*. Plant Physiol **80**: 415-419

7. **Greer DH, Laing WA** (1989) Photoinhibition of photosynthesis in intact kiwifruit (*Actinidia deliciosa*) leaves: effect of growth temperature on photoinhibition and recovery. Planta **180**: 32-39

8. **Kuhlemeier CJ, van Arkel GA** (1987) Host-vector systems for gene cloning in cyanobacteria. Methods Enzymol **153**: 199-215

9. **Murata N, Sato N, Omata T, Kuwabara T** (1981) Separation and characterization of thylakoid and cell envelope of the blue-green alga (cyanobacterium) *Anacystis nidulans*. Plant Cell Physiol **22**: 855-866.

10. **Murata N, Nishida I** (1987) Lipids of blue-green algae (cyanobacteria). *In* PK Stumpf, ed, The Biochemistry of Plants, Vol 9. Academic Press, Orlando, Florida, pp 315-347

11. **Murata N** (1989) Low-temperature effects on cyanobacterial membranes. J Bioenergetics Biomembranes **21**: 61-75

12. **Omata T, Murata N** (1983) Isolation and characterization of the cytoplasmic membranes from the blue-green alga (cyanobacterium) *Anacystis nidulans*. Plant Cell Physiol **24**: 1101-1112

13. **Ono T, Murata N** (1981) Chilling susceptibility of the blue-green alga *Anacystis nidulans*. I. Effect of growth temperature. Plant Physiol **67**: 176-181

14. **Russell NJ** (1984) Mechanisms of thermal adaptation in bacteria: blueprints for survival. Trends Biochem Sci **9**: 108-112

15. **Sato N, Murata N** (1980) Temperature shift-induced responses in lipids in the blue-green alga, *Anabaena variabilis*. Biochim Biophys Acta **619**: 353-366

16. **Sato N, Murata N** (1981) Studies on the temperature shift-induced desaturation of fatty acids in monogalactosyl diacylglycerol in the blue-green alga (cyanobacterium), *Anabaena variabilis*. Plant Cell Physiol **22**: 1043-1050

17. **Sato N, Murata N** (1988) Membrane lipids. Methods Enzymol **167**: 251-259

18. **Stanier RY, Cohen-Bazire G** (1977) Phototrophic prokaryotes: the cyanobacteria. Ann Rev Microbiol **31**: 225-274
19. **Thompson Jr GA** (1980) The effects of environmental factors on lipid metabolism. *In* The Regulation of Membrane Lipid Metabolism. CRC Press, Boca Raton, Florida, pp 171-196
20. **Wada H, Murata N** (1989) *Synechocystis* PCC6803 mutants defective in desaturation of fatty acids. Plant Cell Physiol **30**: 971-978
21. **Wada H, Gombos Z, Murata N.** (1990) Enhancement of chilling tolerance of a cyanobacterium by genetic manipulation of fatty acid desaturation. Nature **347**: 200-203
22. **Williams JGK** (1988) Construction of specific mutations in photosystem II photosynthetic reaction center by genetic engineering methods in *Synechocystis* 6803. Methods Enzymol **167**: 766-778

The Roles of Ascorbate in the Regulation of Photosynthesis

Christine H. Foyer and Maud Lelandais

Laboratoire du Metabolisme, I.N.R.A., Route de St-Cyr, 78026 Versailles cedex, France

INTRODUCTION

Precise co-regulation of the electron transport processes and carbon metabolism appears to be essential for the efficient functioning of photosynthesis (14, 16, 20). The molecular mechanisms involved in this regulation are poorly understood but it is clear that some of the processes that modify the relative fluxes through the photosynthetic electron transport system and the carbon reduction cycle also initiate, or are associated with, the defense systems that serve to protect against the damaging effects of excess irradiance and/or over-reduction of the electron transport system (10, 16, 20). L-Ascorbic acid which is synthesized from D-glucose in leaves, has been shown to play a pivotal role in the defense systems of the chloroplast (13, 15, 26, 27). Ascorbate is a powerful antioxidant that ensures the uninterrupted functioning of photosynthetic carbon assimilation in an oxidizing environment, by scavenging H_2O_2 and other toxic oxidants produced during photosynthesis (2, 3, 18, 26, 27). Ascorbate is also essential for the cycling of α-tocopherol, a lipid soluble antioxidant that protects membrane proteins against oxidative damage (12, 23). Ascorbate is thus central to the defense systems in both the hydrophilic and hydrophobic environments of the chloroplasts (13).

THE ASCORBATE CYCLE

It is important to note that catalase is not present in the chloroplasts of plant cells. In these organelles H_2O_2 is scavenged by the enzyme ascorbate peroxidase (E.C. 1.11.1.7) (4) and the oxidized forms of ascorbate are recycled by the enzymes of the ascorbate-glutathione cycle (Fig. 1). It is clear that the ascorbate-dependent H_2O_2-scavenging system is closely associated with both pseudocyclic electron flow (that produces superoxide and thence H_2O_2 via dismutation) and also non-cyclic electron flow which produces NADPH for the regeneration of ascorbate. Chloroplasts contain a copper-zinc superoxide dismutase (SOD). Both this enzyme and ascorbate peroxidase (4, 17, 18) *exist in soluble and*
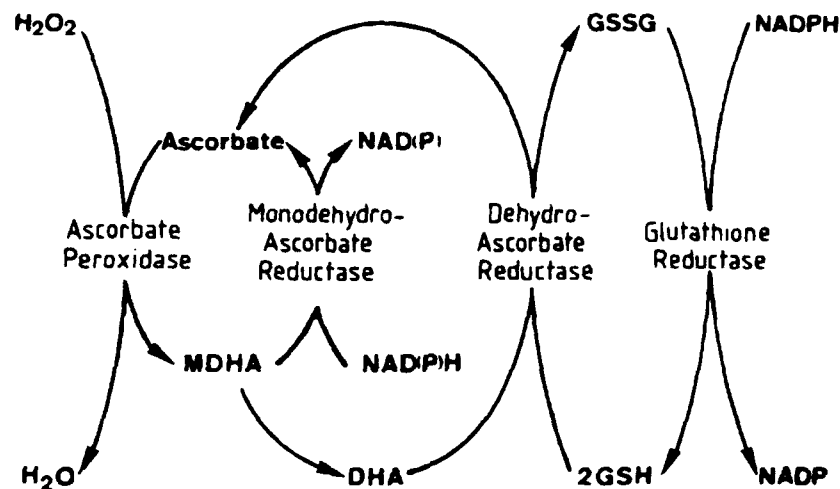
88

Figure 1. Diagrammatic representation of the cycle of ascorbate-dependent H_2O_2 scavenging in the chloroplasts and the mechanisms of regeneration of ascorbate. In addition, it may be noted that ascorbate also plays a role in scavenging the superoxide radical (O_2^-) in chloroplasts. The rate constant of the reaction of ascorbate with O_2^- is much smaller $(2.7 \times 10^{-5} \, M^{-1} \, s^{-1})$ than that for the reaction with superoxide dismutase $(2 \times 10^9 \, M^{-1} \, s^{-1})$ but the concentration of ascorbate in the stroma (10-25 mM) is much greater than that of superoxide dismutase and thus the reaction rates are comparable.

thylakoid-bound forms. Although SOD is vitally important in protecting against oxidative damage, it can only convert one toxic derivative of oxygen (O_2^-) to another (H_2O_2). Effective defense requires the subsequent detoxification of H_2O_2 by ascorbate peroxidase. Ascorbate is regenerated through reactions which consume reducing equivalents while participating in the generation of a transthylakoid pH gradient. Hence the regeneration of ascorbate involves the production of ATP. The role of the ascorbate system in the turnover and regulation of the photosynthetic electron transport chain is a point of particular interest and will be discussed in detail later. First of all, it is necessary to consider the mechanisms employed to maintain the ascorbate pool of the chloroplast largely in its reduced form.

Ascorbic acid has two oxidized forms, monodehydroascorbate and dehydroascorbate. Oxidation of ascorbate occurs in two sequential steps producing first monodehydroascorbate and subsequently dehydroascorbate. The monodehydroascorbate radical is the primary product of destruction of H_2O_2 in the ascorbate peroxidase reaction in the chloroplasts and cytosol of higher plants (reaction 1).

$$H_2O_2 + 2 \text{ ascorbate} \rightarrow 2H_2O + 2 \text{ monodehydroascorbate} \qquad (1)$$

89
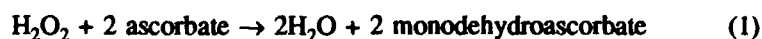
Monodehydroascorbate is also produced by the univalent oxidation of ascorbate, for example in the reduction of superoxide and hydroxyl radicals and also in the regeneration of α-tocopherol. If it is not rapidly re-reduced to ascorbate the monodehydroascorbate radical spontaneously disproportionates to ascorbate and dehydroascorbate. Dehydroascorbate is also highly unstable at pH values greater than 6.0 and, therefore, must be rapidly recycled to ascorbate. It is thus not surprising that two enzymes are involved in the regeneration of L-ascorbic acid *in situ*. These are monodehydroascorbate reductase (E.C. 1.6.5.4) which uses NAD(P)H directly to recycle ascorbate and dehydroascorbate reductase (E.C. 1.8.5.1) which uses reduced glutathione (GSH) for the regeneration process.

The H_2O_2 scavenging system is highly efficient (2, 3, 28, 30). It provides a mechanism for eliminating excess reducing power in the chloroplast. The work of Schreiber and his colleagues (28, 30, 31) has demonstrated that metabolism of H_2O_2 leads to membrane energization, the reduction rate of monodehydroascorbate being equivalent to that of methyl viologen. It has also been suggested that the H_2O_2 scavenging systems form the metabolic basis for the "Kautsky effect", observed in chlorophyll fluorescence induction (30). Thus it is pertinent to consider the interactions between the ascorbate-dependent oxidant-scavenging systems and the processes of photosynthetic electron transport and carbon assimilation.

PROTECTION OF THE ENZYMES OF THE CALVIN CYCLE

Thiol-disulphide exchange reactions provide one of the basic mechanisms of regulation of the carbon reduction or Calvin cycle, operating to convert several of the component enzymes from inactive forms in the dark to active forms in the light. Two major classes of low molecular weight thiol compounds are involved in thiol-disulfide exchange reactions in the chloroplasts. These are the thioredoxin system and the GSH-GSSG system (1, 19). The latter appears to be involved in the protection of thiol groups associated with proteins against oxidation while the former constitutes a major regulation mechanism that serves to activate synthetic pathways in the light and catabolic pathways in the dark (8, 9, 11). The ferredoxin-thioredoxin system in chloroplasts regulates several of the enzymes of the carbon reduction cycle. Reduced thioredoxin activates fructose-1,6 bisphosphatase, phosphoribulokinase, sedeheptulose- 1,7-bisphosphatase and NADP-glyceraldehyde 3-phosphate dehydrogenase (8, 9, 11) through the reduction of specific disulphide bridges. The reduction state of these biosynthetic enzymes reflects the balance between the flux of reducing equivalents through the electron transport system and the oxidizing environment of the stroma which continuously favors oxidation and, hence, inactivation. Molecular O_2 is the natural oxidant involved in the inactivation processes (24). H_2O_2 is a powerful oxidant that interferes with the delicate balance of this system since it oxidizes enzyme thiol groups and prevents thioredoxin-dependent reductive activation (6,

22, 33). H_2O_2 is an extremely potent inhibitor of photosynthetic carbon assimilation even at very low concentrations (22). In addition, H_2O_2 will tend to oxidize all exposed thiol groups and many other enzymes and proteins will be modified if H_2O_2 is not removed. Thus the ascorbate-dependent H_2O_2-scavenging system is vital in protecting photosynthetic carbon assimilation and chloroplast metabolism in general.

ELECTRON TRANSPORT PROCESSES ASSOCIATED WITH H_2O_2 SCAVENGING AND TURNOVER OF THE ASCORBATE POOL

The redox pairs dehydroascorbate-ascorbate and oxidized glutathione reduced glutathione (GSSG-GSH) have previously been shown to be intermediate electron carriers in the reduction of H_2O_2 by NADPH in chloroplasts (2, 3). H_2O_2-dependent O_2 evolution in isolated intact chloroplasts, washed free from contaminating catalase, is associated with the turnover of both the ascorbate and glutathione pools (3). As a result of the turnover of NADPH during the metabolism of H_2O_2, quenching of chlorophyll a fluorescence is observed (Fig. 2a). The addition of H_2O_2 results in increases in both the non-photochemical (qNP) and photochemical components (qQ) of chlorophyll a fluorescence quenching (Fig. 2b). When H_2O_2 is added to isolated intact chloroplasts the fluorescence yield decreases sharply. Photochemical quenching (qQ) increases immediately because H_2O_2 oxidizes the electron acceptors of PSII. Electron transport associated with H_2O_2 metabolism generates an increase in the transthylakoid ΔpH which is evidenced by an increase in non-photochemical quenching, qNP. Furthermore, the effect of the ascorbate-dependent H_2O_2-scavenging system on chlorophyll a fluorescence quenching has also been observed in cyanobacteria that contain ascorbate peroxidase. Ascorbate peroxidase containing cyanobacteria such as *Synechocystis 6803* show a transient quenching of chlorophyll a fluorescence that is proportional to the amount of H_2O_2 added whereas *Anacystis nidulans*, that lacks ascorbate peroxidase and uses catalase to destroy H_2O_2, did not show any change in chlorophyll fluorescence quenching upon the addition of H_2O_2 (25). This suggests that the destruction of H_2O_2 in cyanobacterial cells that use catalase alone is not linked to the electron transport system, whereas, cyanobacteria that scavenge H_2O_2 using ascorbate peroxidase require photoreductants produced from the electron transport processes.

As discussed by Neubauer and Schreiber (28) the changes in chlorophyll a fluorescence quenching characteristics induced by the addition of H_2O_2 are typical of the action of Hill reagents (that is reagents that are good acceptors of electrons from the photosynthetic electron transport chain). Clearly, the ascorbate-dependent H_2O_2-scavenging system is capable of supporting high rates of electron transport (3), equivalent to the electron acceptor methyl viologen (28), and should be far in excess of the capacity of H_2O_2 formation (5) when the system is functioning optimally. However, it must be noted that the ascorbate-
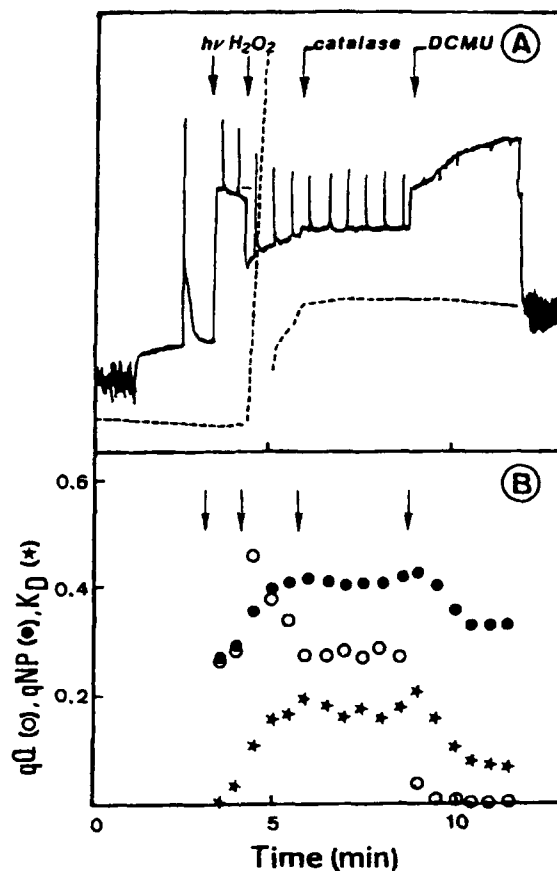
91

Figure 2. Changes in chlorophyll a fluorescence quenching and oxygen evolution in intact pea chloroplasts induced by the addition of H_2O_2 (500 µM). The reaction medium consisted of 0.33 M sorbitol, 2 mM EDTA, 2 mM $MgCl_2$, 50 mM HEPES-KOH buffer (pH 7.6) and chloroplasts at a chlorophyll concentration of 25 mg ml^{-1}. Actinic irradiance (35 µmol m^{-2} s^{-1}) commenced as indicated (hv). Catalase (220 U) and DCMU (10 µM were added at the times indicated by arrows. Fluorescence and oxygen traces (A) and fluorescence quenching components (B) are given.

dependent peroxidase is not a robust enzyme since activity is lost rapidly when challenged with H_2O_2 in the absence of ascorbate (21). In addition, the regeneration of the ascorbate pool can be impeded in certain stress conditions, such as low temperature (13, 34). The oxidation and loss of the ascorbate pool may be considered as physiological indicators of severe stress and of the failure of the defense systems against oxidative stress (32).

We have examined the effect of several inhibitors of ascorbate peroxidase activity. Cyanide is a particularly effective inhibitor of the fluorescence

quenching associated with H_2O_2 scavenging (28). However, cyanide is not specific in its action, the Cu-Zn superoxide dismutase of the chloroplast is also inhibited; indeed, we use KCN to distinguish between the different forms of superoxide dismutase. Sodium azide and hydroxyurea are known to be inhibitors of ascorbate peroxidase (7), although azide is a much better inhibitor of catalase (2). We found that we could still measure substantial H_2O_2-induced fluorescence quenching in pea chloroplasts in the presence of 1 mM sodium azide. 50 mM hydroxyurea had no effect on H_2O_2-induced fluorescence quenching in isolated pea chloroplasts (Fig. 3) presumably because the ascorbate peroxidase is protected by the endogenous stromal ascorbate pool (7).

We have tried to investigate the role of the ascorbate-dependent scavenging system in more complex systems than isolated chloroplasts. Feeding intact leaves with substantial quantities of H_2O_2 failed to induce changes in chlorophyll a fluorescence, possibly because the H_2O_2 is destroyed long before it reaches the chloroplasts, for example, by the peroxidases in the cell walls. However, we have observed changes in chlorophyll fluorescence quenching associated with the metabolism of H_2O_2 in intact protoplasts where catalase was present and active (Fig. 4). In intact protoplasts the addition of H_2O_2 leads to a decrease in photochemical quenching (Fig. 4). This occurred in the presence or absence of CO_2 (Fig. 4). The addition of H_2O_2 also led to an increase in non-photochemical quenching. The decrease in photochemical quenching presumably resulted from photosynthetic control of electron flow (16). These effects of H_2O_2 were also evident in the presence of sodium azide which inhibits the endogenous catalase and partially inhibits the chloroplast ascorbate peroxidase (Fig. 5). Sodium azide had no effect on CO_2 dependent O_2 evolution but photochemical quenching and non-photochemical quenching were increased (Fig. 5). The subsequent addition of H_2O_2 increased both photochemical and non-photochemical quenching (Fig. 5b).

Neubauer and Schreiber (28) have suggested that an oxidation product of ascorbate, for example, monodehydroascorbate is the natural electron acceptor with an efficiency equivalent to a Hill reagent. Although we have previously shown that both the ascorbate and glutathione pools turn over during light dependent H_2O_2 scavenging in the chloroplasts (2) it is clear from studies with isolated thylakoid membranes that monodehydroascorbate is also a good electron acceptor (Fig. 6). When H_2O_2 is added to isolated thylakoids in the absence of ascorbate very little effect on chlorophyll a fluorescence quenching is observed (Fig. 6a). If, however, ascorbate is added significant H_2O_2-induced fluorescence quenching is observed (Fig. 6b). This is because some of the chloroplast ascorbate peroxidase is associated with the thylakoid membranes (17). However, addition of ascorbate oxidase, that produces mono- dehydroascorbate from ascorbate, induces a rapid quenching of chlorophyll a fluorescence (Fig. 6c). This is reversed quickly, presumably because ascorbate oxidase cannot function well in the assay conditions used here (having a pH optimum of about pH 5.6). These experiments were carried out in the absence of NADPH or NADH so we
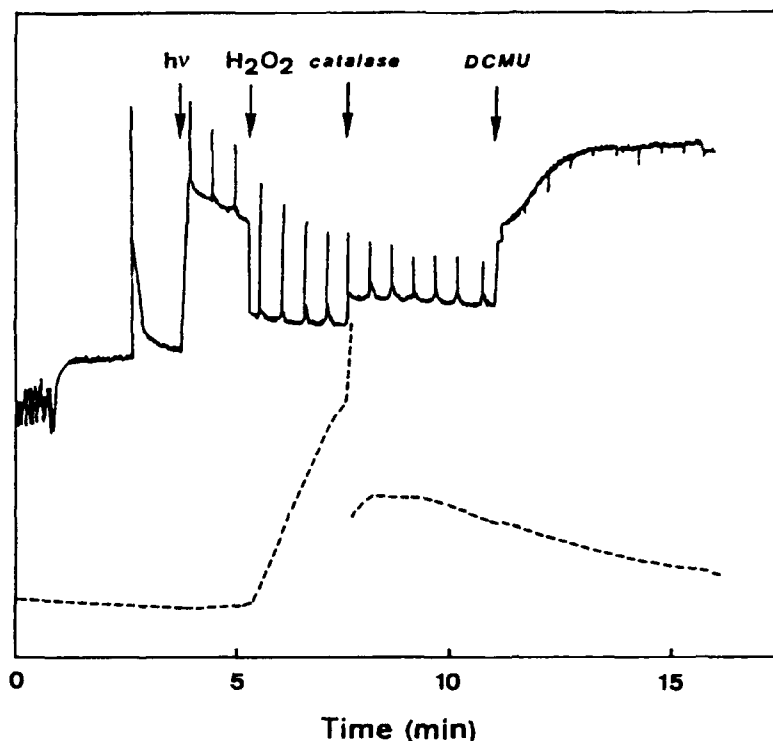
Figure 3. Chlorophyll *a* fluorescence and oxygen evolution in intact pea chloroplasts, isolated from pea leaf protoplasts, in the presence of hydroxyurea (50 mM) upon the addition of H_2O_2 (500 μM) catalase (220 U) and DCMU (10 μM). The reaction medium consisted of 0.33 M sorbitol, 2 mM EDTA, 2 mM $MgCl_2$, 50 mM HEPES-KOH buffer (pH 7.6) and chloroplasts at a chlorophyll concentration of 25 μg ml^{-1}. Hydroxyurea (50 mM) was added in darkness prior to the onset of actinic irradiance (35 μmol m^{-2} s^{-1}) which commenced as indicated (*hv*). H_2O_2, catalase and DCMU were added to the points indicated by arrows.

may eliminate the possibility that ascorbate is regenerated *via* the NAD(P)H-monodehydroascorbate reductase. A more simple explanation is that monodehydroascorbate itself is a good electron acceptor. Indeed, the addition of NADPH or NADH did not change the monodehydroascorbate-induced chlorophyll *a* fluorescence characteristics. This supports the view that neither of these electron donors is actually needed in this system for the regeneration of ascorbate from monodehydroascorbate.
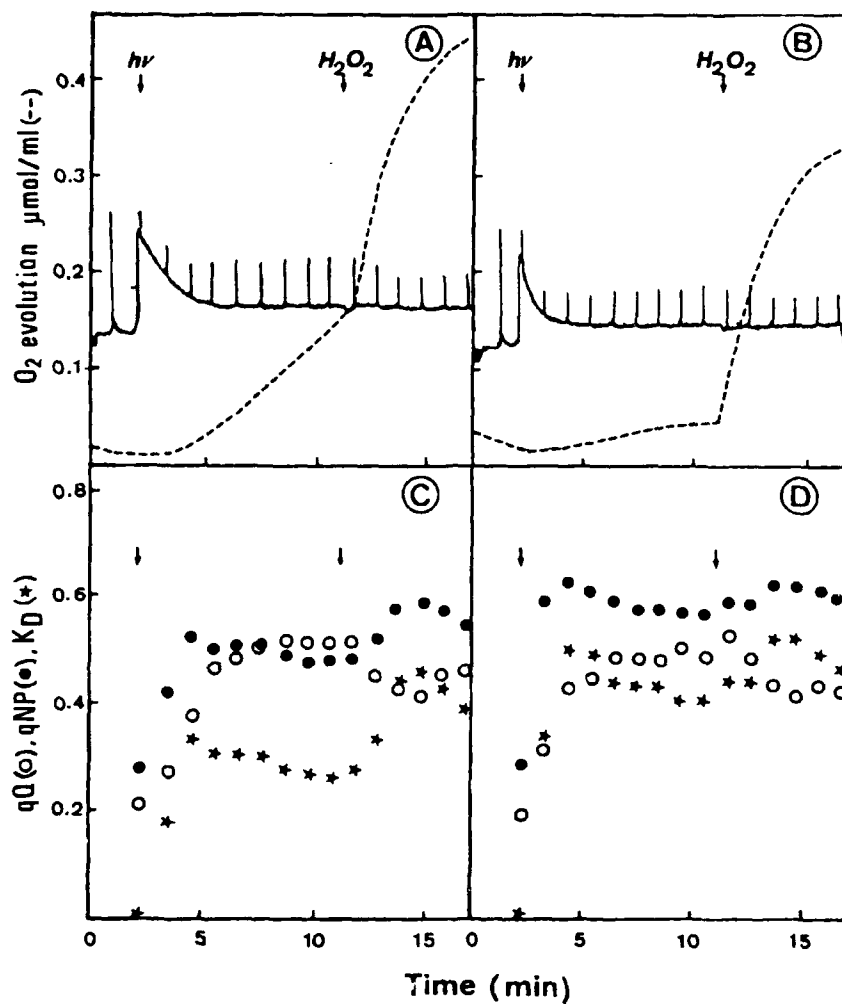
94

Figure 4. The effect of the addition of 500 μM H_2O_2 to intact pea leaf protoplasts in the presence (A, C) or absence (B, D) of 5 mM $NaHCO_3$. The reaction mixture consisted of 0.5 M sorbitol, 1 mM $CaCl_2$, 30 mM tricine KOH buffer (pH 7.6). Actinic irradiance (155 μmol m^{-2} s^{-1}) commenced at the point indicated ($h\nu$) and H_2O_2 (500 μM) was added as indicated by the arrows. The fluorescence traces (solid lines) and oxygen evolution (broken lines) are given in (A) and (B) while the fluorescence quenching components qQ (O), qNP (●), and KD (★) arising are given in (C) and (D).
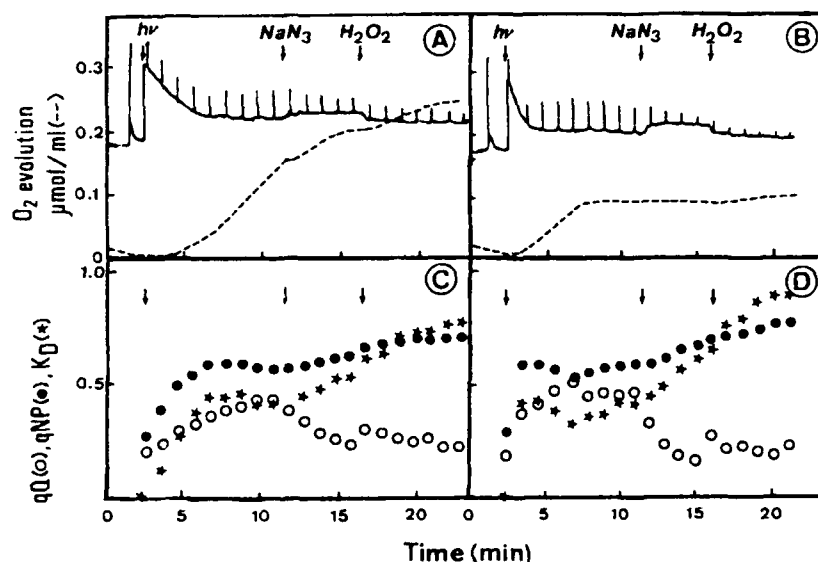
95

Figure 5. The effect of the addition of NaN_3 (I mM) and H_2O_2 (500 μM) to intact pea leaf protoplasts in the presence (A, C) and absence of 5 mM $NaHCO_3$ (B, D). All other details are as in Fig. 4. qQ (O), qNP (●), KD (★).

ASCORBATE AN ELECTRON DONOR

The significance of ascorbate in plant metabolism resides largely in its reducing ability. This is exploited to minimize the damage caused by oxidative process. Ascorbate is also used as a reductant in several enzyme reactions. Energetic and kinetic considerations of the redox reactions of ascorbate suggest that cycling between reduced and oxidized forms occurs via the transfer of single hydrogen atoms rather than separate electron transfer and protonation reactions (29). At physiological pH values a process of hydrogen atom transfer minimizes deleterious events, such as direct reduction of molecular oxygen, and yet allows the vitamin to react efficiently with free radicals. Hence at physiological pH values ascorbate is a poor electron donor but a good donor of single hydrogen atoms. For this reason ascorbate is not a particularly good electron donor to the electron transport chain. Ascorbate is known to reduce several of the electron transport components but is relatively slow and rates of ascorbate-dependent reduction cannot compete with reduction by photosystem II. However, the binding of ascorbate to electron transport components and membrane bound enzymes and proteins may have significance for their function. Ascorbate-dependent reduction of several components of the electron transport chain, e.g. plastoquinone, plastocyanin, cytochrome b_{559} and cytochrome f will affect the poising of the redox state of these electron carriers under some conditions. In
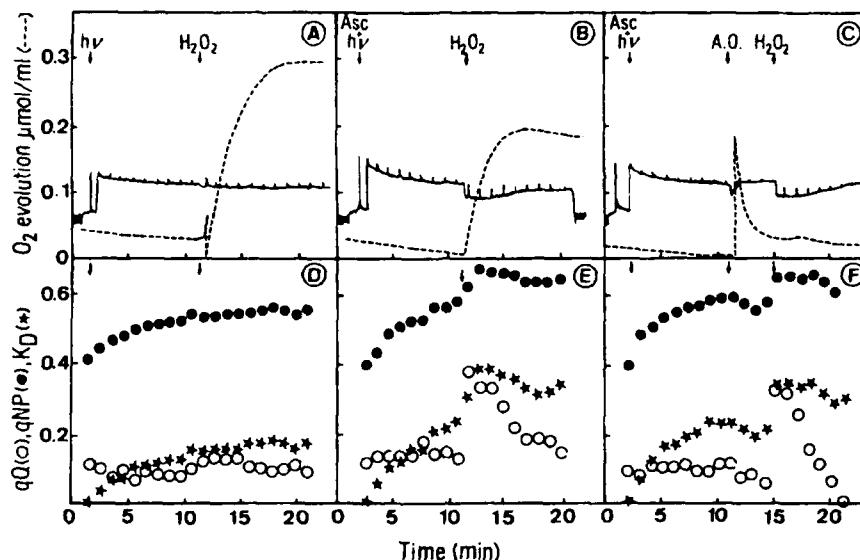
Figure 6. The effect of the generation of the monodehydroascorbate radical on the quenching of chlorophyll *a* fluorescence and oxygen evolution in pea thylakoids. The reaction medium contained 0.33 M sorbitol, 10 mM KCl, 1 mM EDTA, 2 mM $MgCl_2$, 150 mM HEPES/KOH buffer (pH 7.9) and thylakoids at a chlorophyll concentration of 25 µg ml^{-1}. Irradiance, 20 µmol m^{-2} s^{-1}, was applied at the point indicated (*hv*). H_2O_2 (500 µM) was added to this system at the point indicated. In (B), (C), (D) and (E) the reaction medium was supplemented with 5 mM L-ascorbate. In (C) and (E) ascorbate oxidase (A.O.; 5 U) was added at the points indicated. (A), (B) and (C) show the oxygen evolution and fluorescence traces while (D) and (E) show their respective fluorescence quenching components qQ (O), qNP (●), and KD (★).

addition, the binding of ascorbate will bring about localized changes in proteins such as alterations in redox potential and electrical charge that accelerate charge transfer reactions.

CONCLUSIONS

(i) In intact chloroplasts the scavenging of H_2O_2 catalyzed by ascorbate peroxidase is highly efficient. The ascorbate peroxidase of the chloroplasts is localized partly on the thylakoid membranes and partly in the stroma. The monodehydroascorbate radical produced as a result of this process is recycled to ascorbate by several mechanisms. In the stroma monodehydroascorbate may decompose to ascorbate and dehydroascorbate and the dehydroascorbate thus produced can be recycled to ascorbate using reduced glutathione (Fig. 1). Alternatively, monodehydroascorbate may be recycled using either NADPH or

97

NADH, *via* the monodehydroascorbate reductase. Finally, it appears that monodehydroascorbate is reduced *via* the electron transport chain by a more direct route and is itself an electron acceptor.

ii) The metabolism of H_2O_2 in the chloroplast has repercussions for regulation of the electron transport system since it can modify both the photochemical and nonphotochemical components of chlorophyll *a* fluorescence quenching. These events can be observed in intact protoplasts where catalase is present and active as well as in isolated chloroplasts. The fact that H_2O_2 causes substantial nonphotochemical quenching has led Schreiber *et al.* (31) to suggest that the ascorbate-dependent scavenging system plays a decisive role in the regulation of electron transport *in vivo* particularly in (1) the decrease of the intrinsic quantum yield of PSII activity in excess light; (2) the "Kautsky effect" of chlorophyll fluorescence induction and (3) diminishing electron pressure on the PSII acceptor side and thus helping to prevent photoinhibitory damage. The degree to which the ascorbate-dependent scavenging system fulfills these functions *in vivo* remains to be fully elucidated. It must be remembered that ascorbate also has other roles in the modulation of thylakoid reactions such as the formation of zeaxanthin and α-tocopherol (10, 12, 13). Ascorbate is an essential co-factor for the synthesis of zeaxanthin which also makes an important additional contribution to the lowering of the efficiency of photochemistry in photosystem II under stress conditions.

iii) Univalent reduction of O_2 to form superoxide *via* the process of pseudocyclic electron flow is inevitable, but the rate of superoxide generation *in vivo* is always considered to be rather low (5, 35). Efficient scavenging of H_2O_2 is clearly essential if photosynthetic carbon assimilation is to proceed without oxidative inhibition. Whether H_2O_2 generation coupled to H_2O_2 scavenging within the leaf ever occur to such an extent as to have appreciable effects on the photosynthetic electron transport system is a question that must be resolved if we are to understand the regulation of the photosynthetic electron transport system *in vivo*. One way in which this may be achieved is *via* the study of transgenic plants in which one or more of the enzymes involved in H_2O_2 production and scavenging are modified. Such plants are now available. Until corroborative evidence is obtained and the question of the flux through the pathways of H_2O_2 production resolved, the *in vivo* relevance of the system in terms of the regulation of electron transport and the rate of associated ATP synthesis remains open to debate.

LITERATURE CITED

1. **Alscher RG** (1989) Biosynthesis and antioxidant function of glutathione in plants. Physiol Plant **77**: 457-464
2. **Anderson JW, Foyer CH and Walker DA** (1983a) Light-dependent reduction of dehydroascorbate and uptake of exogenous ascorbate by spinach chloroplasts. Planta **158**: 442-450

98

3. **Anderson JW, Foyer CH and Walker, DA** (1983b) Light-dependent reduction of hydrogen peroxide by intact spinach chloroplasts. Biochim Biophys Acta **724**: 69-74

4. **Asada K** (1991) Molecular properties of ascorbate peroxidase in chloroplasts. *In* J Lobarzewski, H Greppin, C Penel and TH Gaspar, eds, Biochemical molecular and physiological aspects of plant peroxidases, University of Geneva, pp 147158

5. **Asada K and Takahashi M** (1987) Production and scavenging of active oxygen in photosynthesis. *In* DJ Kyle, CB Osmond and CJ Arntzen, eds, Photoinhibition, Elsevier Science Publishers BV, pp 227-287

6. **Charles SA and Halliwell B** (1980) Effect of hydrogen peroxide on spinach *(Spinacia oleracia)* chloroplast fructose bisphosphatase. Biochem J **189**: 373-376

7. **Chen GX and Asada K** (1990) Hydroxyurea and p-aminophenol are the suicide inhibitors of ascorbate peroxidase. J Biol Chem **265**: 2775-2781

8. **Crawford NA, Droux M, Kosower NS and Buchanan BB** (1989) Evidence for function of the feredoxin/thioredoxin system in the reductive activation of target enzymes of isolated intact chlorop٢٠ts. Arch Biochem Biophys **271**: 223-239

9. **Cséke C and Buchanan BB** (1986) Regulation of the formation and utilization of photosynthate in leaves. Biochim Biophys Acta **853**: 43-63

10. **Demmig-Adams B and Adams WW** (1991) Light photosynthesis and the xanthophyll cycle. *In* EJ Steffen and KL Steffen, eds, Active oxygen/oxidative stress and plant metabolism, Current topics in plant physiology: An American Society of Plant Physiologists series, vol. 6, pp 171179

11. **Droux M, Jacquot JP, Miginlac-Maslow M, Gadal P, Huet JC, Crawford NA, Yee BC and Buchanan BB** (1987) Ferredoxin-thioredoxin reductase: an iron-sulfur enzyme linking light to enzyme regulation in oxygenic photosynthesis. Purification and properties of the enzyme from C3, C4 and cyanobacteria species. Arch Biochem Biophys **252**: 426-439

12. **Finckh BF and Kunert KJ** (1985) Vitamin C and E: an antioxidative system against herbicide-induced lipid peroxidation in higher plants. J Agric Food Chem **33**: 574-577

13. **Foyer CH** (1992a) Ascorbic acid. *In* RG Alscher, JL Hess, eds, Antioxidants in higher plants, CRC Press Inc, in press

14. **Foyer CH** (1992b) Interactions between electron transport and carbon assimilation in leaves. Coordination of activities and control. *In* Govindjee, Abrol, Mohanty eds, Photosynthesis and Plant Productivity, Oxford and IBH Publishing Co, PVT Ltd, in press

15. **Foyer CH and Halliwell B** (1976) Presence of glutathione and glutathione reductase in chloroplasts: a proposed role in ascorbic acid metabolism. Planta **133**: 21-25

16. **Foyer CH, Furbank RT, Harbinson J, Horton P** (1990) The mechanisms contributing to photosynthetic control of electron transport by carbon assimilation in leaves. Photosynth Res **25**: 83-100

17. **Groden D and Beck E** (1979) H_2O_2 destruction by ascorbate-dependent systems from chloroplasts. Biochim Biophys Acta **546**: 426-435

18. **Halliwell B** (1987) Oxidative damage, lipid peroxidation and antioxidant protection in chloroplasts. Chem and Physics of Lipids **44**: 327-340

19. **Holmgren A** (1985) Thioredoxin. Annu Rev Biochem **54**: 237-271

20. **Horton P** (1989) *Interactions between electron transport and carbon assimilation: regulation of light-harvesting and photochemistry. In* WR Briggs, ed, Photosynthesis, Plant Biology series, Vol. 8, Alan R Liss Inc, New York, pp 393-406

21. **Hossain MA and Asada K** (1984) Inactivation of ascorbate peroxidase in spinach chloroplasts on dark addition of hydrogen peroxide: its protection by ascorbate. Plant Cell Physiol **25**: 1285-1295

22. **Kaiser WM** (1979) Reversible inhibition of the Calvin cycle and activation of oxidative pentose phosphate cycle in isolated chloroplasts by hydrogen peroxide. Planta **145**: 377-382

23. **Kunert KJ, Homrighausen C, Böhme H and Böger P** (1985) Oxyfluorfen and lipid peroxidation: protein damage as a phytotoxic consequence. Weed Sci **33**: 766-770

24. **Leegood RC** (1990) Enzymes of the Calvin cycle. *In* PJ Lea,, ed, Methods in Plant Biochem, Vol 3, Chapter 2, Academic Press, London, pp 15-37

25. **Miyake C, Michihata F and Asada K** (1991). Scavenging of hydrogen peroxide in prokaryotic and eukaryotic algae: acquisition of ascorbate peroxidase during the evolution of cyanobacteria. Plant Cell Physiol **32**: 33-43

26. **Nakano Y and Asada K** (1980) Spinach chloroplasts scavenge hydrogen peroxide on illumination. Plant Cell Physiol **21**: 1295-1307

27. **Nakano Y and Asada K** (1981) Hydrogen peroxide is scavenged by ascorbatespecific peroxidase in spinach chloroplasts. Plant Cell Physiol **22**: 867-880

28. **Neubauer C and Schreiber U** (1989) Photochemical and non-photochemical quenching of chlorophyll fluorescence induced by hydrogen peroxide. Z Naturforsch **44C**: 262-270

29. **Njus D and Kelly PM** (1991) Vitamins C and E donate single hydrogen atoms in *vivo*. FEBS Lett **284**: 147-151

30. **Schreiber U and Neubauer C** (1990) O_2 dependent electron flow, membrane energisation and the mechanism of non-photochemical quenching of chlorophyll fluorescence. Photosynth Res **25**: 279-293

31. **Schreiber U, Reising H and Neubauer C** (1991) Contrasting pH optima of light-driven O_2 and H_2O_2 reduction in spinach chloroplasts as measured via chlorophyll fluorescence quenching. Z Naturforsch **46C**: 635-643

32. **Stegmann HB, Schuler P, Ruff HJ, Knollmüller M and Loreth W** (1991) Ascorbic acid as an indicator of damage to forest. A correlation with air quality. Z Naturforsch **46C**: 67-70

33. **Tanaka K, Otsubo T and Kondo N** (1982) Participation of hydrogen peroxide in the inactivation of Calvin cycle SH enzymes in SO_2-fumigated spinach leaves. Plant and Cell Physiol **23**: 1009-1018

34. **Wise RR and Naylor AW** (1987) Chilling-enhanced photooxidation. Evidence for the role of singlet oxygen and superoxide in the breakdown of pigments and endogenous antioxidants. Plant Physiol **83**: 278-282

35. **Wu J, Neimanis S and Heber U** (1991) Photorespiration is more effective than the Mehler reaction in protecting the photosynthetic apparatus against photoinhibition. Bot Acta **104**: 283-291

Response of Aquatic Macrophytes to Changes in Temperature and CO_2 Concentration[1]

John A. Raven and Andrew M. Johnston

Department of Biological Sciences, University of Dundee, Dundee DD1 4HN, United Kingdom

INTRODUCTION

Aquatic macrophytes are a very heterogenous group of organisms. Of the primarily aquatic macroalgae, the Rhodophyta have been separate from the Phaeophyta and Chlorophyta for at least 750 million years (32). Secondarily aquatic higher plants are derived from terrestrial forebearers which were derived from charophycean aquatic green algae at least 400 million years ago. This heterogeneity of ancestry of aquatic macrophytes could mean that the details of the means by which the organisms deal with changes in CO_2 availability or temperature could differ even if the responses are generally similar. Bearing in mind this diversity of aquatic macrophytes, we consider responses to increases in atmospheric CO_2 partial pressure (47) and to temperature separately before considering their interaction, and finally some wider implications for plant distribution. We consider (1) short-term effects of changes in CO_2 partial pressure or temperature on plants grown at present-day natural conditions; (2) the extent of (phenotypic) acclimation to prolonged (in the context of the organisms life cycle) exposure to changed CO_2 or temperature and (3) (genetic) adaptation to even more prolonged changes in CO_2 partial pressure or temperature.

EFFECT OF INCREASING ATMOSPHERIC CO_2 PARTIAL PRESSURE

CO_2 distribution between air and pure water for the atmospheric CO_2 partial pressures in the range 18 Pa (last glacial maximum) to 100 Pa (2100 A.D. ? ref.13) shows a linear proportionality increase of dissolved CO_2 (44). An

---

[2]Abbreviations: CAM, Crassulacean acid metabolism; CCM, carbon concentrating mechanism; C_i, inorganic carbon; PFD, photon flux density; RUBP, ribulose-1,5-bis-phosphate; Rubisco, ribulose-1,-5-bisphosphate carboxylase-oxygenase.

atmospheric CO_2 increase from 33 to 100 Pa for sea water at 15°C and a total alkalinity of 2.47 eq m^{-3} causes an increase in total C_i^2 from 2.237 to 2.412 mol m^{-3} and in CO_2 from 12.69 to 38.46 mmol m^{-3}; the ratio of total C_i to CO_2 falls from 176 to 62.7 and pH decreases from 8.168 to 7.735 (44). Similar effects would be seen in fresh waters of relatively high alkalinity, allowing for ionic concentration effect on CO_2 solubility and the dissociation constants for the C_i system.

Before considering the implications of such changes for the photosynthesis of aquatic macrophytes, it is important to consider the extent to which CO_2 in the water bathing aquatic macrophytes is at air-equilibrium. It is clear that the CO_2 concentration in this water can range from an order of magnitude less to an order of magnitude more than air-equilibrium, with the larger upward deviations confined to freshwaters (31, 32). The basis for these variations relates to the balance between the rates of photolithotrophic consumption of CO_2, of its chemoorganotrophic regeneration, of bulk water movements, and of CO_2 exchange between water and atmosphere.

Dealing first with CO_2 in the euphotic zone at concentrations lower than the air-equilibrium concentration, the obvious way in which this comes about is by net excess of photolithotrophy over chemoorganotrophy. This requires not only high photon availability but also the availability of nutrients such as (combined) N, P and Fe *other* than from regeneration in chemoorganotrophic processes which, in this case, are *less* rapid than their photolithotrophic consumption. In the terminology of phytoplankton ecologists this is 'new production'(11). An example of CO_2 drawdown involving aquatic macrophytes can be seen in the marine environment in intertidal rock pools, and especially those in the high intertidal where flushing with fresh seawater is only found at spring tides, leaving periods of several days at neap tides in which successive photoperiods/scotoperiods alternations give cumulative CO_2 drawdown. The nutrients for this 'new' production could be provided *via* terrestrial run-off and other anthropogenic inputs, as well as seabird excreta (36). A freshwater example is a relatively nutrient (N, P, Fe)-rich shallow pool with submerged macrophytes, where phytoplankton or macrophyte photosynthesis can draw down CO_2 concentrations.

The opposite effect is CO_2 enrichment caused by an excess of chemoorganotrophic CO_2 production over photolithotrophic CO_2 uptake plus CO_2 evasion to the atmosphere. The fate of the organic C produced in 'new production' in aquatic systems is frequently sedimentation followed by chemoorganotrophy producing CO_2 at depth with negligible evasion to the atmosphere in the *absence* of mass water flux in upwellings. Such static systems yields high CO_2 concentrations in sediments, whence CO_2 can, in shallow freshwaters, be directly used by plants of the isoetid life form by diffusion into root gas spaces and thence to shoot gas spaces and photosynthesizing cells (40). There is also a CO_2 concentration gradient between organic-rich sediments and immediately overlying water, and macrophytes growing close to these sediment-

water interface can benefit from such increases in CO_2 availability, especially with large diffusion boundary layers resulting from absence of significant water movement over the plants (21, 22). When mass flow of water *does* occur, this CO_2-enriched water can be upwelled to the surface, so that it is made available to attached macrophytes at higher levels.

A related mechanism, but involving atmospheric CO_2 as the C source for photolithotrophy followed by chemoorganotrophy, accounts for high CO_2 concentrations in many rivers and streams. Here CO_2 fixation by terrestrial plants produces organic matter which is in part reconverted to CO_2 in the soil by respiration of below-ground plant parts and by microbial respiration of dead plant material. Restricted diffusive exchange of this CO_2 with the atmosphere means that a significant fraction is lost in solution in ground waters supplying streams which are thus CO_2-enriched. Cycling of N, P and Fe in natural soils is 'tighter' than is that of C, so that the inorganic C supply in the streams fed by ground-water is oversupplied relative to N, P and Fe, so that photolithotrophs are unable to draw down CO_2 to below atmospheric-equilibrium values; this situation is exacerbated if allochthonous inputs of *organic* C, are oxidized to CO_2 in the streams so that chemoorganotrophic reactions exceed photolithotrophic reactions. Accordingly, there is net CO_2 evasion from streams to the atmosphere (16).

This discussion of the processes leading to under- or oversaturation of the habitats of aquatic macrophytes with CO_2 relative to the atmospheric-equilibrium values at the prevailing temperature shows that the interpretation of the impact of increased atmospheric CO_2 on inorganic C availability to submerged aquatic plants is not simple. All that we can say is that increased atmospheric CO_2 levels will tend to increase the dissolved free CO_2 in all of the varied regimes considered.

In considering the influence of any increase in free CO_2, and total C_i, concentrations on photosynthesis by aquatic macrophytes we first examine the effects of short-term exposure to C_i concentrations different from the concentration (the natural one) used for growth. Experiments of this type show that some aquatic macrophytes are saturated with C_i under natural light, temperature and water flow conditions. The perennial freshwater red macroalga *Lemanea mamillosa* grows in small streams with CO_2 at 5 times (100 mmol m^{-3} rather than 20 mmol m^{-3}) or more the air-equilibrium values which, despite exposure of the annual gametophyte phase to essentially full sunlight in the winter and spring, saturates photosynthesis and growth; this does not occur with experimentally imposed air-equilibrium CO_2 levels (25-27). The sublittoral marine red macroalga *Delesseria sanguinea* grows in temperate coastal air-equilibrated seawater; the most rapid growth of this perennial alga is in the spring. Under near-natural (low light) conditions this alga is C_i-saturated but, in the laboratory, seawater levels of C_i do not saturate photosynthesis at higher photon flux densities (15, 24). Both *Lemanea* and *Delesseria* rely on CO_2 diffusion to supply CO_2 to Rubisco under natural conditions and thus show both C_3 biochemistry and C_3 physiology. The intertidal marine macroalgae

104

investigated (1, 4, 45, 46), i.e. species of *Ulva, Enteromorpha* (Ulvophyceae) and *Fucus, Pelvetia* and *Ascophyllum* (Phaeophyceae), by contrast, all have characteristics consistent with C_3 biochemistry supplied with CO_2 *via* a CCM and are all saturated with the C_i concentrations found in air-equilibrated seawater (but see ref. 17). Furthermore, the photosynthesis by these seaweeds when emersed in high light and at a hydration level sufficient for photosynthesis is almost saturated by present atmospheric partial pressures of CO_2 (1, 45). Such photosynthesis is a significant contribution to overall C gain by high intertidal macroalgae in temperate regions (23, 29).

A substantial number of aquatic macrophytes are not C_i-saturated for photosynthesis in their ambient C_i concentrations when tested at natural temperatures, photon flux density and water movement conditions. This is true of some intertidal marine macrophytes (e.g. the rock pool populations of such brown seaweeds as *Halidrys* and *Laminaria*); however, restricted light availability for subtidal populations of these algae might well make them C_i saturated at the normal values of air-equilibrated seawater (15, 45). For freshwater macrophytes, it is likely that many are at least seasonally subject to limitation of photosynthetic rate by availability of inorganic C (21, 22, 28, 30, 42). Many of these organisms rely on diffusive entry of CO_2; others employ a CCM with a relatively low affinity for external C_i.

This discussion shows that photosynthesis *in situ* by a number of macrophytes is limited by C_i supply, while in others it is not. Turning now to acclimation experiments of aquatic macrophytes at higher C_i levels than they normally encounter in nature, these have been carried out less frequently than experiments based on growth at natural C_i levels. The CO_2 levels with which growth media were equilibrated usually greatly exceeded the partial pressures likely within the next century. The limited data available show that growth at higher free CO_2 levels lowers the affinity for external C_i in photosynthesis of marine (1, 14) and freshwater (10, 19, 43) macrophytes with a CCM, but not in one which relies on CO_2 diffusion (28). While many more investigations are needed, using a more realistic CO_2 enrichment in the context of likely increases over the next century, and a wider range of macrophytes, we may tentatively conclude that increased CO_2 may not necessarily alleviate inorganic C limitation of photosynthesis *in situ*, since the organisms may reduce their effective affinity for C_i. For those organisms which rely on CO_2 diffusion (cf. ref. 28) this could reflect a decrease in the excess of Rubisco capacity (at CO_2 and RUBP saturation) over the capacity to regenerate RUBP; for those with a CCM it could reflect partial repression of the pump.

A final point concerning CO_2 acclimation is the extent to which C_i limitation of photosynthesis, as measured in short-term experiments, is reflected in C_i limitation of growth which involves *inter alia* photosynthate allocation. Growth can be C_i-limited in natural waters for aquatic macrophytes: an example is the red marine macroalga *Gracilaria*, when light and other nutrients are not limiting (35). Here the investigation necessarily involves acclimation of the macrophytes

105

to changed C_i regimes in view of the time required (days or weeks) for the growth measurements.

Having considered acclimation to changed C_i availability we now consider adaptation to C_i availability, i.e. genetic change related to the selective pressure of the mean value; and range of values, of C_i availability which individuals encounter. The diversity of CCMs which aquatic macrophytes possess, and the diversity of 'add-ons' to C_3 metabolism such as CAM and C_4-like mechanisms and CO_2 uptake through roots which occur in them, betoken polyphyletic origins of means of CO_2 acquisition other than totally diffusive entry of CO_2 (32).

As far as the time taken for this diversification is concerned, a datum which might help to indicate how rapidly adaptation to increased CO_2 in the future could occur, we note that the general trend (with many fluctuations) has been for atmospheric CO_2 partial pressure to *decrease* through geological time (5). Accordingly, CCMs in aquatics have probably been evolving over hundreds of millions of years. In the absence of molecular characterization of these membrane-based CCMs the molecular clock cannot tell us when they evolved (32). Equally, fossil evidence from morphology or $^{13}C/^{12}C$ does not give definitive evidence of the occurrence of CO_2 concentrating mechanisms (39). These considerations mean that we do not know if adaptation has occurred in aquatic macrophytes to recent (< 200,000 years) changes in atmospheric CO_2 partial pressure from ~ 18-20 Pa in the last glaciation to 28-30 Pa in the last interglacial and the pre-industrial part of the present interglacial (3). Accordingly, historical data do not give us any real indication of the rate and extent of adaptation of aquatic macrophytes to known changes in atmospheric CO_2 concentrations.

While not directly addressing responses to atmospheric CO_2 changes, data (38) on *Fucus vesiculosus* from the Gulf of Bothnia at the northern salinity-determined limit of its distribution there are of interest. Salinity changes in the Baltic Sea mean that this population has only been exposed to the low salinity and, from our point of view, low total C_i environment of the Baltic for about 3000 years. The HCO_3^- concentration in the Gulf of Bothnia is about 1 mol m^3 as compared to the 2 mol m^{-3} in the seawater in which the ancestors of the Baltic *F. vesiculosus* grew; the free CO_2 concentration is slightly higher than in seawater at the same temperature due to the lower ion concentration in the Gulf of Bothnia (37). The C_i affinity of light-saturated photosynthesis of the Baltic population (38) was closely similar to that of *F. vesiculosus* from normal seawater salinity populations both from the Eastern Atlantic (44) and at its southern limit in the Western Atlantic (37). These data show that acclimation and adaptation to a two-fold change in C_i concentration has not occurred within 3000 years although a marked adaptation in salinity requirement/tolerance for growth has occurred (2).

EFFECT OF INCREASED TEMPERATURE

As a link to the preceding and the succeeding topics, we reiterate that increased temperature decreases CO_2 solubility. Temperature effects on growth and metabolism of aquatic macrophytes have recently been reviewed (7, 20, 34) while important new data and perceptive interpretations may be found refs. 21, 22, 48-50. In a number of experiments macrophytes were acclimated to a range of temperatures (similar to, or greater than, those in which they are normally found) with subsequent measurements of photosynthesis and/or growth at the temperature to which the organisms were acclimated and, in several cases, other temperatures as well. Such experiments show that a high photosynthetic rate can usually be maintained at temperatures in excess of those normally encountered by the organism, that the optimal acclimation temperature in terms of maximal light-saturated photosynthesis is not invariably at or above the maximum temperature usually experienced by the macrophyte, and that a broad 'temperature optimum' is often found. Such experiments show that the organisms have some temperature acclimation capacity in reserve as far as dealing with temperature *increases* are concerned for photosynthesis and for vegetative growth. However, reproduction in some groups (e.g. Laminariales) may well, with extant genotypes, be a significant problem for long-term survival of such seaweeds whose sporophytes live for 1-10 years and whose gametophytes are generally shorter-lived (20).

As for temperature adaptation, we note that the world has generally been warmer over the last few hundreds of millions of years, and that the most recent trends over the last few million years is one of cooling (12). This has important repercussions for the length of time which aquatic macrophytes have had to adapt to their thermal environment. This is particularly important for cold habitats for marine plants which have no high altitude cold habitats to retreat to in a warm world. There have always been warm marine environments for aquatic macrophytes; today's tropical marine flora will not tolerate temperature below 5-14°C, depending on species (6). By contrast, the Antarctic ice-sheet and the corresponding cold marine habitats have only existed for about 25 million years, while for the Arctic the time available is only 3 million years (9, 20). Temperature responses of photosynthesis and growth in temperature-acclimated seaweeds suggest closer adaptation of temperature responses to environmental temperatures in the long-standing austral flora than in the more recently recruited boreal flora (8, 20, 48-50). While the austral polar seaweed flora contains many endemic species, genera, families and orders, this is not true of the younger boreal polar seaweed flora, whose members have similar temperature responses to that of the conspecific organisms in the boreal cool-temperate. It would be expected that any genotypic differentiation with respect to photoperiodism within arctic/temperate seaweed species could survive *in situ* since they would not have to migrate for temperature-change reasons. The situation may be different in the Antarctic, with endemics possessing specific temperature adaptations and,

presumably, photoperiodic adaptations (33). With warming of the Antarctic ocean there is likely to be a mismatch of temperature (inappropriate) and photoperiod (appropriate) for seaweeds growing at a particular latitude; survival of the species require adaptation of temperature requirement *in situ*, since the option of migration with photoperiodic adaptation but constant temperature adaptation is not available; it does not correspond to an available habitat in the warmer world. Alternatively, if the Antarctic seaweeds cannot adapt to higher temperatures as rapidly as lower latitude seaweeds can adapt their photoperiodic response *and* migrate to the Antarctic, then they could be replaced by the lower-latitude plants. Currently the oceanic circulation in the Antarctic greatly limits seaweed migration latitudinally (20). Clearly this could change with global warming. Although the comparison of the Antarctic and the Arctic seaweed flora above is consistent with a very slow adaptation to *lower* temperatures, it is possible that adaptation to higher temperatures is more rapid and could occur over the time-scales and rate of change projected for global warming. Similarly, it is possible that photoperiodic behavior can adapt within the time scale of warming (33). We note that adaptation to changed environmental salinity can occur over times less than 3,000 years (2, 20).

For freshwater plants colder environments will have been available at high latitudes even in the earlier (more than a few million years ago) warmer global climates, although not all kinds of freshwater habitats (e.g. large rivers) will have been present at very high altitudes. Accordingly, we would anticipate better temperature adaptation in freshwater plants with no effects analogous to those mentioned for arctic seaweeds.

INTERACTIONS OF INCREASED ATMOSPHERIC CO_2 WITH INCREASED TEMPERATURE

The interactions of increased CO_2 partial pressure with increased temperature have recently been analyzed very thoroughly and elegantly (18) for C_3 photosynthesis by land plants. Again based on short-term studies, Maberly (21, 22) investigated interactions of photon flux density, CO_2 concentration and temperature for a *Fontinalis antipyretica* (C_3 physiology; Bryophyta) population in a lake in the English Lake District harvested at 4 different times of year with substantial differences in ambient temperatures, CO_2 concentration and photon flux density. The changes in short-term photosynthesis at the respective environmental temperatures and imposed C_i and light regimes showed that the CO_2 affinity at a given photon flux density was highest in August, when the environmental CO_2 concentration was lowest. However, there was no variation with season in light- and CO_2-saturated photosynthesis other than that related to temperature, and no acclimation of this parameter to temperature could be discerned (22). Furthermore, acclimation with season of both the half-saturation PFD at a given CO_2 concentration and the half-saturation CO_2 concentration at a given PFD did not prevent variations in the environmental factor which limited

photosynthesis at different times of year: major restrictions by photon flux (November), temperature (March, May) and CO_2 concentration (August) were noted (22). More work of this exemplary type, with extensions to higher temperatures, is needed if predictions of the effects of increased CO_2 and temperature on a range of aquatic macrophytes in terms of acclimation are to be made. No studies of adaptation to increased CO_2 and temperature seem to be available.

A rather different perspective on CO_2-temperature interactions comes from work mimicking summer and winter conditions for photosynthesis by freshwater macrophytes in Florida by holding plants in lower-temperature, shorter-daylength (12°C, 10 h photoperiod: 'winter') and higher-temperature, longer-daylength (30°C, 14 h photoperiod: 'summer') conditions (41). All of the plants tested (including a characean, a moss and several flowering plants) showed acclimation to 'summer' conditions by decreasing their CO_2 compensation concentrations, presumptive evidence for acclimation by derepression of a mechanism for accumulating CO_2. Whether this is a direct response to temperature and/or photoperiod, or relates to the lower CO_2 solubility in warmer waters, cannot be decided on the basis of current evidence.

The two cases discussed above suggest that much further work is needed on the effect of increased CO_2 *and* temperature on photosynthesis by aquatic macrophytes; this conclusion is in no way meant to denigrate the work (21, 22, 41) marking an excellent start in studying interactions of factors related to climate change in the context of photosynthetic acclimation. Alas, essentially nothing is known of adaptation of aquatic macrophytes to changes in both CO_2 and temperature.

CONCLUSIONS

Increased atmospheric CO_2 partial pressures will have less influence on inorganic C availability to aquatic macrophytes than to terrestrial plants. Acclimatory responses may further mitigate the effects of atmospheric CO_2 increase on both CO_2-diffusion and CO_2-pumping aquatic macrophytes. The rate at which genetic adaptation responses could occur is not known. For temperature increases, acclimatory responses are known; adaptation, at least to a temperature *decrease*, seems to be slow. Little is known of the interaction of increased CO_2 with increased temperature for either acclimation or adaptation.

LITERATURE CITED

1. **Axelsson L, Uusitalo J, Ryberg, H** (1991) Mechanisms for concentrating and storage of inorganic carbon in marine macroalgae. *In*: G Garcia Reina, M Pedersén, eds, Seaweed Cellular Biotechnology Physiology and Intensive Cultivation, Universidad de Las Palmas de Gran Canaria. pp 185-198

109

2. **Bäck S, Collins JC, Russell G** (1992) Effects of salinity on growth of Baltic and Atlantic *Fucus vesiculosus*. Br Phycol J. **27**: 39-47

3. **Barnola JM, Raynaud D, Korotkevich YS, Lorius YS** (1987) Vostok ice core provides 16000-year record of atmospheric CO_2. Nature **329**: 351-358

4. **Beer S, Israel A, Drechsler Z, Cohen Y** (1990) Photosynthesis in *Ulva fasciata*. V. Evidence for an inorganic carbon concentrating system, and ribulose-1,5-bisphosphate carboxylase/oxygenase CO_2 kinetics. Plant Physiology **94**: 1542-1546

5. **Berner RA** (1990) Atmospheric carbon dioxide levels over Phanerozoic time. Science **249**: 1382-1386

6. **Biebl R** (1962) Temperaturrenresistenz tropischen meeresalgen (Veglichen mit jeren von Algen in temperienten meeresgebeiten). Bot Mar **4**: 241-254

7. **Davison IR** (1991) Environmental effects on algal photosynthesis:temperature. J Phycol **27**: 2-8

8. **Dieck I tom** (1989) Vergleicherde Untersuchungen zur Ökophysiologie und Kreuzbarkeit innerhalb der digitaten Sektion der Gattung *Laminaria* Lamoureux. Ph.D. thesis, University of Hamburg.

9. **Dunton K** (1992) Arctic biogeography: the paradox of the marine benthic fauna and flora. Trends Ecol Evol **7**: 183-198

10. **Elzenga JTM, Prins MBA** (1988) Adaptation of *Elodea* and *Potamogeton* to different inorganic carbon levels and the mechanism for photosynthetic bicarbonate utilization. Austr J Plant Physiol **15**: 727-735

11. **Eppley RW** (1990) New production: history, methods, problems. *In*: W H Berger, V S Smetack, G Weber eds, Productivity of the Oceans: Past and Present, John Wiley & Sons, Chichester. pp 85-97

12. **Frakes LA** (1979) Climates throughout Geologic Time. Elsevier, Amsterdam.

13. **Houghton JT, Jenkins GJ, Ephraums JJ** (1990) Climate Change. The IPCC Scientific Assessment. Cambridge University Press, Cambridge.

14. **Johnston AM, Raven JA** (1991) Effects of culture in high CO_2 on the photosynthetic physiology of *Fucus serratus*. Brit Phycol J **25**: 75-82

15. **Johnston AM, Maberly SC, Raven JA** (1992) The acquisition of inorganic carbon by four red macroalgae from different habitats. Oecologia: in press.

16. **Kling GW, Kipphub GW, Miller MC** (1991) Arctic lakes and streams as gas conduits to the atmosphere: Implications for Tundra carbon budgets. Science **251**: 298-301

17. **Levavasseur G, Edwards GE, Osmond CB, Ramus J** (1992) Inorganic carbon limitation of photosynthesis in *Ulva rotundata* (Chlorophyta). J Phycol **27**: 667-672

18. **Long SP** (1991) Modification of the response of photosynthetic productivity to rising temperature by atmospheric CO_2 concentrations: has its importance been underestimated? Plant Cell Environm **14**: 729-739

19. **Lucas WJ, Brechignac F** (1987) Photosynthetic responses to oxygen and inorganic carbon of low- and high-CO_2-grown cells of *Chara corallina*. *In*: J Biggins, ed, Progress in Photosynthesis Research Volume 4, Martinus Nijhoff Publishers, Dordrecht. pp 341-344

20. Lüning K (1990) Seaweeds. Their Environment, Biogeography and Ecophysiology. Wiley-Interscience, New York
21. Maberly SC (1985a) Photosynthesis by *Fontinalis antipyretica*. I. Interaction between photon irradiance, concentration of carbon dioxide and temperature. New Phytol 100: 127-140
22. Maberly SC (1985b) Photosynthesis by *Fontinalis antipyretica*. II. Assessment of environmental factors limiting photosynthesis and production. New Phytol 100: 141-155
23. Maberly SC, Madsen TV (1990) Contribution of air and water to the carbon balance of *Fucus spiralis*. Mar Ecol Progr Ser 62: 175-183
24. Maberly SC, Raven JA, Johnston JA (1992) Discrimination between ^{12}C and ^{13}C by marine plants. Oecologia: in press
25. MacFarlane JJ, Raven JA (1985) External and internal CO_2 transport in *Lemanea*: interaction with the kinetics of ribulose bisphosphate carboxylase. J Exp Bot 36: 610-622
26. MacFarlane JJ, Raven JA (1989) Quantitative determination of the unstirred layer permeability and kinetic parameters of Rubisco in *Lemanea mamillosa*. J Exp Bot 40: 321-327
27. MacFarlane JJ, Raven JA (1990) C, N and P nutrition of *Lemanea mamillosa* Kutz. (Batrachospermales, Rhodophyta) in the Dighty Burn, Angus, Scotland. Plant Cell Environ 13: 1-13
28. Madsen TV (1991) Inorganic carbon uptake kinetics of the stream macrophyte *Callitriche cophocarpa* Sendt. Aq Bot 40: 321-332
29. Madsen TV, Maberly SC (1990) A comparison of air and water as environments for photosynthesis by the intertidal alga *Fucus spiralis* (Phaeophyta). J Phycol 26: 24-30
30. Madsen TV, Maberly SC (1991) Diurnal variation in light and carbon limitation of photosynthesis by two species of submerged freshwater macrophyte with a differential ability to use bicarbonate. Freshwater Biol 26: 175-187
31. Raven JA (1991) Physiology of inorganic carbon acquisition and implications for resource use efficiency by marine phytoplankton: relation to increased CO_2 and temperature. Plant Cell Environm 14: 779-794
32. Raven JA (1991b) Implications of inorganic carbon utilization: ecology, evolution, and geochemistry. Can J Bot 69: 908-924
33. Raven JA (1992) The coastal fringe: habitats threatened through global warming. Trans Bot Soc Edin 45: 437-462
34. Raven JA, Geider RJ (1988) Temperature and algal growth. New Phytol 110: 441-461
35. Raven JA, Johnston AM (1991a) Carbon assimilation mechanisms: implications for intensive culture of seaweeds. In: G Garcia Reina, M Pedersén, eds, Seaweed Cellular Biotechnology Physiology and Intensive cultivation, Universidad de Las Palmas de Gran Canaria, pp 151-166
36. Raven JA, Johnston AM (1991b) Photosynthetic carbon assimilation by *Prasiola stipitata* (Prasiolales, Chlorophyta) under emersed and submersed conditions: relationship to the taxonomy of *Prasiola*. Br Phycol J 26: 247-257

111

37. **Raven JA, Osmond CB** (1992) Inorganic C assimilation processes and their ecological significance in inter- and sub-tidal macroalgae of North Carolina. Funct Ecol **6**: 41-47

38. **Raven JA, Samuelsson G** (1988) Ecophysiology of *Fucus vesicularus* L. close to its Northern limit in the Gulf of Bothnia. Bot Mar **31**: 399-410

39. **Raven JA, Sprent JA** (1989) Phototrophy, diazotrophy and palaeoatmospheres: biological catalysis and the H, C, N and O cycles. J Geol Soc **146**: 161-170

40. **Raven JA, Handley LL, McInroy S, McKenzie L, Richards JH, Samuelsson G** (1988) The role of root CO_2 uptake and CAM in inorganic C acquisition by plants of the isoetid life form. A review, with new data on *Eriocaulon decangulare*. New Phytol **108**: 1-20

41. **Salvucci ME, Bowes G** (1991) Induction of reduced photorespiratory activity in submersed and amphibious aquatic macrophytes. Plant Physiol **67**: 335-340

42. **Sand-Jensen K** (1903) Photosynthetic carbon sources of stream macrophytes. J Exp Bot **34**: 198-210

43. **Sand-Jensen K, Gordon DM** (1986) Variable HCO_3^- affinity of *Elodea canadensis* Michaux in response to different HCO_3^- and CO_2 concentrations during growth. Oecologia **70**: 426-432

44. **Stumm W, Morgan JJ** (1981) Aquatic Chemistry. An Introduction Emphasizing Chemical Equilibria in Natural Waters. Wiley-Interscience, New York

45. **Surif MB, Raven JA** (1989) Exogenous inorganic carbon for photosynthesis in seawater by members of the Fucales and Laminamales (Phaeophyta): ecological and taxonomic implications. Oecologia **78**: 97-105

46. **Surif MB, Raven JA** (1990) Photosynthetic gas exchange under emersed conditions in intertidal and normally submersed members of the Fucales and Laminamales: interpretation in relation to C isotope ratio and N and water use efficiency. Oecologia **82**: 68-80

47. **Wetzel RG, Grace JB** (1983) Aquatic plant communities. *In* ER Lemon, ed. The Response of Plants to Rising Levels of Atmospheric Carbon Dioxide. Westview Press, Boulder, Colorado. pp 223-280

48. **Wiencke C, tom Dieck I** (1989) Temperature requirements for growth and temperature tolerance of macroalgae endemic to the Antarctic region. Mar Ecol Progr Ser **54**: 189-197

49. **Wiencke C, tom Dieck I** (1990) Temperature requirements for growth and survival of macroalgae from Antarctica and Southern Chile. Mar Ecol Progr Ser **59**: 157-170

50. **Wiencke C, Fischer G** (1990) Growth and stable carbon isotope composition of cold-water macroalgae in relation to light and temperature. Mar Ecol Progr Ser **65**: 283-292

Molecular Analysis of the CO_2-Concentrating Mechanism in Cyanobacteria[1]

Teruo Ogawa

Solar Energy Research Group, The Institute of Physical and Chemical Research (RIKEN), Wako, Saitama 351-01, Japan

INTRODUCTION

The occurrence of CO_2-concentrating mechanism (CCM[2]) in cyanobacteria and algae is now well established (2-4, 10, 11, 15). The CCM involves active C_i transport and enables cyanobacterial and algal cells to cope with the low affinity of their Rubisco for CO_2, thus to grow at air levels of CO_2. The cyanobacterial CCM consists of two basic components, a C_i transport system and the Rubisco-containing carboxysome. The C_i-transport system is activated and energized by light. The activation requires PSI and PSII (12), whereas the energization requires only PSI (22, 23). Both CO_2 and HCO_3^- are transported into the cells by this mechanism, and HCO_3^- is the species delivered to the cytosol regardless of the species supplied (6, 14, 33). The intracellular HCO_3^- is dehydrated to CO_2 by CA in the carboxysome and then fixed by Rubisco.

Recently, there has been much progress in understanding the molecular and physiological basis of the CCM in cyanobacteria (4, 11). The use of the transformable strains, *Synechocystis* PCC6803 and *Synechococcus* PCC7942, enabled the molecular analysis of the CCM through selection and analysis of mutants defective in parts of this mechanism. Several types of mutants defective in the CCM have been isolated from these cyanobacterial strains and, their mutant genes have been cloned and sequenced. Some of these results have been already described in the Proceedings of Second International Symposium on Inorganic Carbon Utilization by Aquatic Photosynthetic Organisms held in 1990 (4). New mutants have been isolated since this symposium and the sites of their lesions have been identified. The present paper focuses on molecular and physiological analyses of the cyanobacterial CCM done by using these mutants.

[2]Abbreviations: C_i, inorganic carbon; CCM, CO_2-concentrating mechanism; CA, carbonic anhydrase; PS, photosystem; HCR, high CO_2-requiring; kbp, kilobase pair; WT, wild type; Rubisco, ribulose,1,5-bisphosphate carboxylase/oxygenase.

MUTANT LIBRARY AND ISOLATION OF MUTANTS

Two kinds of techniques are available for the isolation of mutants. The classical technique is to mutagenize the WT cells of *Synechocystis* PCC6803 or *Synechococcus* PCC7942 with a mutagen. The most widely used mutagen is N-methyl-N'-nitro-N-nitrosoguanidine. After mutagenesis, cells are washed and then grown under non-selective conditions (at 3% CO_2). At this stage, cells are suspended in BG11 medium (32) containing 5% dimethylsulfoxide, frozen in liquid nitrogen and stored at -80°C. This "mutant library" contains various types of mutants and a specific mutant can be recovered from this library by applying the method designed to select for a particular type of phenotype. For isolation of HCR mutants, cells from the mutant library were grown under selective conditions (at low CO_2 concentrations) in the presence of ampicillin for a few days. Cells were then washed and plated on agar plates containing BG11 medium. Plates were incubated under 3% CO_2 conditions in the light until colonies appeared. Colonies were screened on duplicate plates under non-selective and selective conditions. Mutants defective in the CCM were recovered as colonies grown only under non-selective conditions (13, 16, 28).

The other technique is targeted mutagenesis through insertional inactivation or deletion of defined regions of DNA. There is also a technique to express foreign genes on host specific plasmids (27). Details of these techniques are described elsewhere (34). These techniques have been used to create various specific mutants of the CCM.

COMPLEMENTATION TEST

Complementation test was performed by the method of transformation reported by Dzelzkalns and Bogorad (5). Genomic libraries of WT *Synechocystis* constructed in pUC18 or pUC19 were kind gifts of Dr. J.G. Williams at E.I. du Pont de Nemours & Co. (Wilmington, DE). Mutant cells at logarithmic phase of growth were plated in 0.8% top agar onto 1.5% agar plates. After solidification of the agar, each library (50-500 ng DNA/1 µl of water) was applied directly onto the surface of the plate. Transformants capable of growing under low CO_2 were detected in 7 d. The complementation test was done with fractionated library and then with clones obtained from a complementing fraction.

CLASSIFICATION OF HCR MUTANTS DEFECTIVE IN THE CCM

Since Marcus *et al.* (13) isolated the E1 mutant from *Synechococcus* PCC7942, many HCR mutants defective in CCM have been isolated from this strain (1, 20, 28) and *Synechocystis* PCC6803 (16). These mutants are classified into three groups according to their lesions (Fig. 1); 1) Mutants defective in C_i transport systems, 2) mutants defective in energization of C_i transport systems and 3) mutants which have normal C_i transport activity but are unable to utilize

114

intracellular C_i pool for photosynthesis. Most frequently recovered mutants are those of the third group and the E1 mutant is classified into this group. Figure 2 shows CO_2 exchange profiles of WT and mutant cells (one from each group) measured using an open gas-analysis system (22). The CO_2 uptake activity of the mutants in the first (SC) and second (RKb) groups is much lower than that of the WT whereas the activity of the mutant (G3) in the third group is as high as that of the WT.

MUTANTS DEFECTIVE IN ENERGIZATION OF C_i TRANSPORT

Mutants Defective in NAD(P)H Dehydrogenase

RKa and RKb are the HCR mutants of *Synechocystis* PCC6803 that do not have the ability to transport extracellular C_i into the cells (16). A clone that
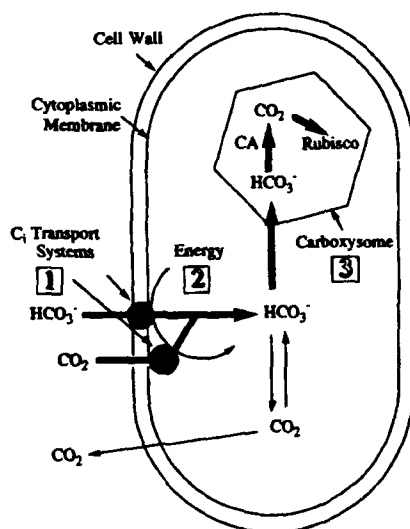
Figure 1. Possible sites for lesions in three groups of HCR mutants. 1) The protein components of the CO_2 and HCO_3^- transport systems. 2) The energization of the transport systems, i.e. NAD(P)H dehydrogenase. 3) Alternation in the properties of the carboxysome.

complements RKa was isolated from a genomic library. Sequencing of DNA in the region of mutation revealed that the gene mutated in RKa encoded a 521 amino acid protein which had extensive sequence homology to the products of *ndhB* (*ndh2*) genes in the chloroplast and mitochondrial genomes (17). The gene mutated in RKb encodes a hydrophobic protein consisting of 80 amino acids and was designated *ictA* (renamed *ndhL*) (18). No homologous gene has been found in the database. M55, M9, M-ndhC and M-ndhK mutants were constructed by inactivating *ndhB*, *ictA/ndhL*, *ndhC* and *ndhK* genes of the WT *Synechocystis*, respectively, as described previously (17-19). The activity of CO_2 uptake in the light was completely abolished in RKa, RKb, M9, M55 and M-ndhK and was decreased to 40% the activity of WT in M-ndhC (19). The significant effect on CO_2 uptake by inactivating genes encoding the subunits of NAD(P)H
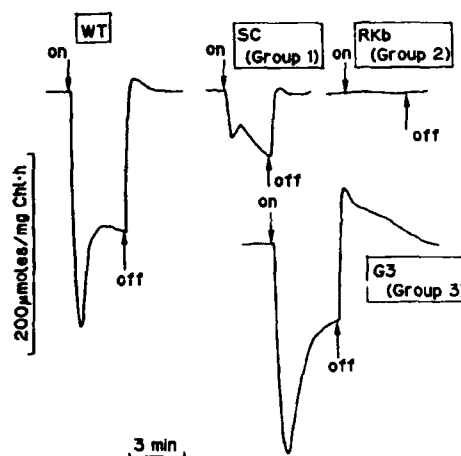
115

Figure 2. The. CO_2 exchange profiles of low CO_2-adapted cells of WT and HCR mutants (SC, RKb and G3 from the 1st, 2nd and 3rd groups, respectively) of *Synechocystis* PCC6803. Cells were grown with 3% CO_2 in air and then bubbled with air for 15 h in the light. For details of the gas-exchange system, see ref. 22.

dehydrogenase clearly demonstrated that this enzyme is involved in C_i transport in *Synechocystis*.

Identification and Characterization of the *ictA/ndhL* Gene Product

The *ictA/ndhL* gene was cloned into the expression vector pGEX-2T and expressed in *E. coli* (*DH5α*) as the protein (the *ic'A* gene product, IctA, fused to glutathione s-transferase). An antibody was raised against this protein and was used to detect the reacting polypeptide using goat antirabbit IgG/alkaline phosphatase conjugate as the second antibody.

Western analysis of the thylakoid membrane of WT *Synechocystis* PCC6803 revealed that a protein with an apparent molecular mass of 6.7 kDa crossreacted with the antibody raised against the fusion protein (lane a in Fig. 3). Thylakoid membranes prepared from the RKb and M9 mutants did not contain reacting protein at 6.7 kDa (lanes b and c). Thus, the reacting protein is IctA. No reacting protein was found at 6.7 kDa in the thylakoid membrane of M55 (lane d) and the crossreactivity of the membranes of M-ndhC and M-ndhK with the antibody was very weak (data not shown, see ref. 19). Thus, the synthesis of the subunits of NAD(P)H dehydrogenase is essential to IctA to be assembled to the membrane. The result indicated that IctA is one of the subunits of this enzyme. Presumably in these mutants, the *ictA/ndhL* gene is transcribed and translated, but not properly assembled into the complex of NAD(P)H dehydrogenase.

116

The immunoblot of the cytoplasmic membrane of WT *Synechocystis* showed a band at 6.7 kDa (lane e, Fig. 3). The immunostaining was, however, much weaker than that with the band in the thylakoid membrane. It was concluded that the reacting band in the cytoplasmic membrane preparation originated from contaminated thylakoid membrane (for details, see ref . 19).

NAD(P)H Dehydrogenase as a Component of PSI Cyclic Electron Flow Energizing the C_i Transport

Since NAD(P)H dehydrogenase is confined in the thylakoid membrane, the role of this enzyme is either in activation or energization of the C_i transport. The M55 mutant did not show CO_2 uptake activity even in the presence of dithiothreitol which activates the C_i-transport system in the WT cells in the presence of DCMU (17). It is evident that NAD(P)H dehydrogenase is involved in the energization of the C_i transport. C_i transport in cyanobacteria is energized by PSI cyclic electron flow (22, 23) and, therefore, NAD(P)H dehydrogenase is one of the components involved in this cyclic electron flow. ATP produced by coupling to the cyclic electron flow may be the direct energy source of the C_i
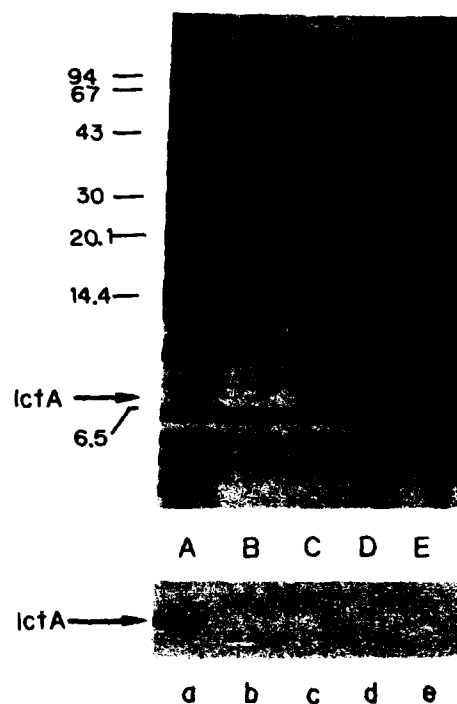
Figure 3. Electrophoretic profiles showing CBB-staining patterns (lanes A-E) of polypeptides and immunoblots (lanes a-e) of IctA in the thylakoid membranes (A-D, a-d) and cytoplasmic membranes (E, e) of WT (A, E, a, e), RKb (B, b), M9 (C, c) and M55 (D, d) mutants.

117

transport. Since all the NAD(P)H dehydrogensase mutants grew well under high CO_2 conditions, transport of other ions (NO_3^-, SO_4^-, etc.) energized by ATP should be functioning normally. It is conceivable that C_i transport requires higher levels of ATP than the transport of other ions.

MUTANTS DEFECTIVE IN C_i TRANSPORT SYSTEMS

CO_2 Transport and HCO_3^- Transport

Both CO_2 and HCO_3^- are transported by the CCM (6, 14, 33). The transport of HCO_3^- requires high concentrations (about 20 mM) of Na^+ while the transport of CO_2 proceeds at micromolar levels of Na^+ (7, 14, 33). In addition, the affinity of the transport system to CO_2 is much higher than that to HCO_3^- (14, 33). These differences between the CO_2 and HCO_3^- transport led Canadian groups to claim the presence of separate transport systems for CO_2 and HCO_3^- (4, 6, 14). On the other hand, models of a common system for the two C_i species have been proposed by other groups (24, 26, 33). One such model is that extracellular CO_2 is hydrated by a membrane-bound CA-like moiety and then transferred to a HCO_3^- transporter (21, 33). However, no evidence has been obtained to conclude which is the right model.

SC Mutant Defective in CO_2 Transport

To date, mutants defective in C_i transport system(s) have not been recovered. Recently, I have isolated a mutant of *Synechocystis* PCC6803, SC, which grew as fast as the WT at 3% CO_2 or at air levels of CO_2 but is unable to grow at CO_2 concentrations lower than 80 ppm (Fig. 4). Measurement of CO_2 and HCO_3^- uptake by the silicone-oil filtering centrifugation method revealed that the uptake of CO_2 into the intracellular C_i pool of the SC mutant was only one third of the WT cells while the WT and mutant cells showed the same HCO_3^- transport activity (Fig. 5). Thus, SC is the mutant defective in the CO_2 transport system. The result demonstrates the presence of separate transport systems for CO_2 and HCO_3^-. A clone that complements the SC mutant was isolated from a genomic library of WT *Synechocystis* PCC6803. The clone contained 9.5 kbp DNA insert (restriction map shown in Fig. 6A). Complementation test with subclones revealed that the site of mutation in the SC mutant is within 1.1 kbp from the *Eco*RI site. Sequencing of nucleotides in this region revealed an ORF which expands beyond the *Eco*RI site. Cloning of DNA in the region beyond the *Eco*RI site is in progress. Hydropathy profile of a part (379 amino acids) of the protein encoded by the ORF (data not shown) indicates that the protein is hydrophilic in this region and does not contain membrane spanning sequence. It appears possible that CO_2 transport is not mediated by a membrane-bound transporter but is a metabolic process which occurs in the cytosol. If there is a membrane bound CO_2 transporter, the permeability of CO_2 through the cytoplasmic membrane must be very low in the absence of such transporter. However, when CA gene was expressed in the cytosol of *Synechococcus*, the

118

cells could not maintain the high level of intracellular C_i because of the leakage of CO_2 produced from the C_i pool (27). This indicates that CO_2 can pass through the cytoplasmic membrane easily. If there is a metabolic process which actively converts CO_2 in the cytosol into HCO_3^- or other C_i forms such as carbamate, it will keep the intracellular CO_2 concentration low enough for the diffusion of extracellular CO_2 into the cells. Identification of the product of the gene mutated in SC and elucidation of its function are crucial for the understanding of CO_2 transport system.

Mutants Defective in HCO_3^- Transport

The presence of separate transport systems for CO_2 and HCO_3^- indicates that mutation of one transport system does not produce HCR mu ts. It is presumed that a HCO_3^- transporter is located in the cytoplasmic n brane and has a homology with transporters for other anions such as NO_3^- and $_3O_4^-$. The 42-kD protein in the cytoplasmic membrane was a candidate for such a transporter (24). However, inactivation of the gene (cmpA) encoding this protein did not produce a mutant defective in HCO_3^- transport (25). A new strategy is needed to isolate a mutant defective in HCO_3^- transport.
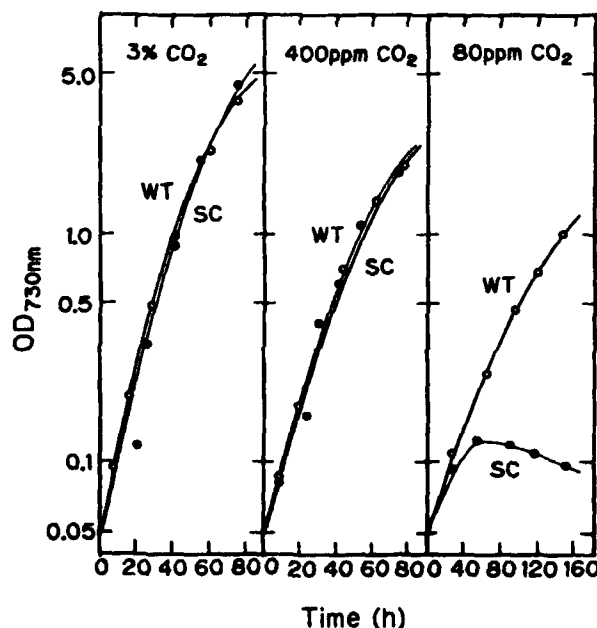
Figure 4. Growth curves of WT and SC mutant with 3% CO_2 in air (left column), air (400 ppm CO_2; middle column) and 20% air in N_2 gas (80 ppm CO_2; right column). WT, open circles; SC, closed circles.

119
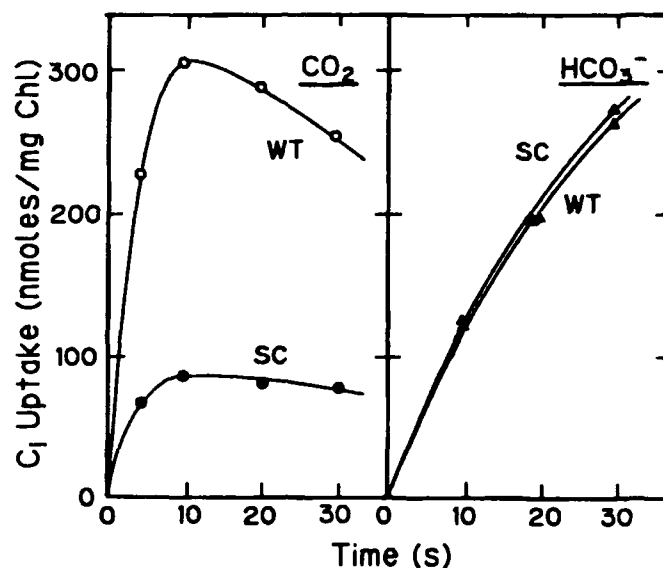
Figure 5. The time courses of uptake of CO_2 (left column) and HCO_3^- (right column) into the intracellular C_i pool of low CO_2-adapted cells of WT and SC mutant. Open symbols, WT; closed symbols, SC mutant. The concentrations of CO_2 and HCO_3^- was 8.8 and 161 μM, respectively.

MUTANTS DEFECTIVE IN THE ABILITY TO UTILIZE INTRACELLULAR C_i POOL FOR PHOTOSYNTHESIS

E1 (13), 0221 (30), RK1 (20), C3P-O (1), types I and II (28) of *Synechococcus* PCC7942 and G3 and G7 (this report) of *Synechocystis* PCC6803 are classified into this group. The DNA fragments that transformed E1 and 0221 mutants to the WT phenotype were mapped to the 5'-flanking region of *rbc* (8). The mutations in these mutants occur in ORFs (ORF1 and ORF2) that encode proteins consisting of 191 and 275 amino acids, respectively. These mutants are classified as type I mutants characterized by having a C_i pool size similar to the WT but displaying a CO_2 efflux after a light to dark transition that is more rapid in WT cells (28). Type I mutants exhibit abnormal carboxysomes that appear as long, rod-shaped structures (8, 28). Two ORFs (named *ccmL* and *ccmn*) located on the upstream of the ORF1 (renamed *ccmM*), were found to be mutated in several type I mutants (29). Type II mutant is characterized by having a C_i pool that is considerably in excess of WT cells, a CO_2 efflux that is slower than WT. This type of mutant possesses more carboxysomes when grown at high CO_2 conditions (28). The C3P-O mutant is one of the type II mutants. The mutation in this mutant occurs in the gene encoding CA that was mapped about 20 kbp
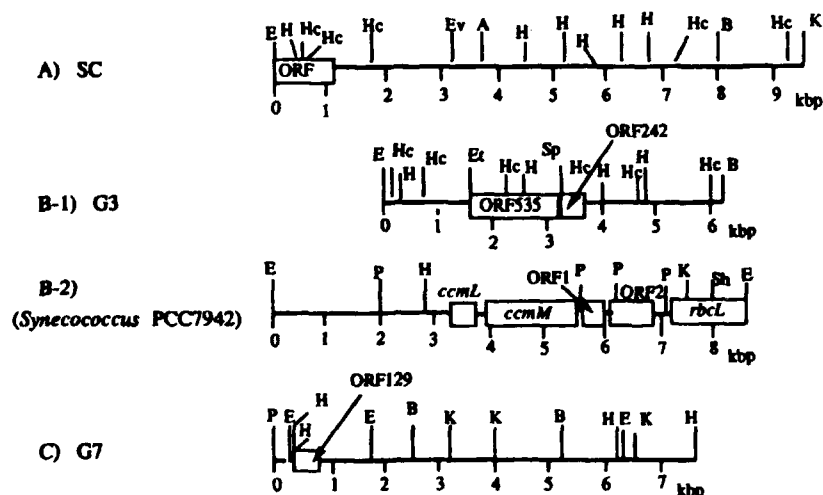
Figure 6. Restriction maps of the clones isolated from *Synechocystis* PCC6803 showing the locations of the ORFs mutated in SC (A), G3 (B-1) and G7 (C) mutants, respectively. Restriction map and the locations of the ORFs on the upstream of *rbcL* of *Synechococcus* PCC7942 are shown in B-2 for comparison with the map in B-1. E, *Eco*R I; H, *Hind* III; Hc, *Hinc* II; Ev, *Eco*R V; B, *Bam*H I; A, *Apa* I; K, *Kpn* I; P, *Pst* I; Sh, *Sph* I; Sp, *Spe* I.

downstream of *rbc* (9). Thus, in *Synechococcus* PCC7942, the DNA regions in the upstream and downstream of *rbc* are essential for the cells to grow under air levels of CO_2 and in the organization of the carboxysomes (Fig. 6B-2).

G3 and G7 of *Synechocystis* PCC6803 are classified into the first group of the HCR mutants. A clone that complements the G3 mutant was isolated from a genomic library of WT *Synechocystis*. The clone contained a 6.4 kbp DNA insert (the restriction map shown in Fig. 6B-1). By complementation test with subclones, the site of mutation in G3 was mapped between the *Eco*RV and *Spe*I sites in the middle of the clone. Sequencing of nucleotides in this region revealed two ORFs, ORF535 and ORF242, with the ORF535 being mutated in G3. There was a significant homology between ORF535 and *ccmM* (40.6% /367 amino acids, homology score 767) and between ORF242 and *ccmN* (42.4%/132 amino acids, homology score 283). Thus, ORF535 and ORF242 in *Synechocystis* PCC6803 correspond to *ccmM* and ORF1/*ccmN*) in *Synechococcus* PCC7942, respectively. Although nucleotides in the upstream region of ORF535 and the down stream region of ORF242 have not been sequenced, it is possible that there are ORFs which correspond to *ccmL* and ORF2. The most significant difference between *Synechocystis* and *Synechococcus* is that no *rbc* operon is present in the vicinity of ORF535 and ORF242 (judging from the restriction map of the *rbc*

121

operon of *Synechocystis* PCC6803 kindly provided by Dr. Gurevitz at Tel Aviv Univ.). Thus, there is no generality of the presence of the *ccm* genes near the *rbc* operon. ORF535 encodes a protein which showed a homology to the small subunit of Rubisco. The homology was present in two regions of the protein (Fig. 7). The significance of such homology is not known.

G7 is another mutant which is classified into the first group. The mutation occurs in ORF encoding a protein consists of 129 amino acids (Fig. 8). No homologous gene was found in the database. There was no *rbc* operon in the vicinity of ORF131 (Fig. 6C). Further characterization of the mutant will reveal the role of ORF129 in the CCM.

```
ORF535 (S.6803)  1'  MHSLVQDVEIPPNKSVPSGAMITQQHQADSLPDVQAGDRHFVQQIAAMHGQSASPTQGTD
               61'  PTVCVLPESLPAVTPVTETPYINSIDNMSINSDITNQIRSLLAQGYGIGAEHANERRFKT
                         .**    . ... .*. ..... *...*.  *   . .  .. .**.*   *
rbcS (S. 6301)   1"  MSMKTLPKERRFETFSYLPPLSDRQIAAQIEYMIEQGFHPLIKF-NEHSNPEEFYW

              121'  KSWQSCGTADGFRPDQVIATVEGWLQKFAGEYVRLIGIDQGAKRQVVEVIIQRPGDVPGS
                     . *.    *  .*.**...*.   *... *.*. *.*.  . *.*. *..***
               56"  THWKL-PLFDCKSPQQVLDKVRECRSEYGDCYIRVAGFDNIKQCQTVSFIVHRPGRY

              181'  PSRGTTTAKALSSGGSGRSAVARQTGNLAGDSANQLRALLHQGYKIGLEYASARRFKTGS
                                          . *.*.  ...**..  .*... .. ..
rbcS (S.6301)    1"  MSMKTLPKERRFETFSYLPPLSDRQIAAQIEYMIEQGFHPLIEFNEHSNPEEFY

              241'  W--LTGGTIGSHREGEALQELNRFLADHTNEYVRIIGIDPAGKRRVAEIVVHRPNGNGNG
                     *  .  .....  ..*.*..    ..... *.*. *.*  . .......****
               65"  VTMWKLPLFDCKSPQQVLDKVRECRSEYGDCYIRVAGFDNIKQCQTVSFIVHRPGRY

              299'  KPSSSSSSVGYKSAPVSSAGGSSAGGLTPEVIATVRGLLANGHSIGTEHTDKRRFKAKSW
              359'  DTCPTIDGGREAEVLAKLEACLVDHAGEYVRIIGIDRVGKRRVLEQIIQRPGDNVVAGRS
              419'  PSSSSASTSSSASSNGFGSGHGGGYSNSAVRLDNSVVTQVRSLLAQGYKIGTEHTDKRRF
              479'  KAKSWQSCAPITSTHESEVLRALEGCLADHNGEYVRLLGIDPTAKRRVLETIIQRP
```

Figure 7. Comparison of the deduced amino acid sequences (single-letter code) for the product of the ORF535 of *Synechocystis* PCC6803 and the product of rbcS of *Synechococcus* PCC6301 (underlined) (31). *, Identical residues; ., conserved residues.

CONCLUDING REMARKS

HCR mutants are powerful tools for studying CCM. The findings of the involvement of NAD(P)H dehydrogenase in C_i transport demonstrates the significance of this enzyme in photosynthetic organisms, like in mitochondrial respiratory chain. Other roles of this enzyme in photosynthesis, if any, remains to be determined. *Synechocystis* mutants defective in NAD(P)H dehydrogenase will serve as a powerful tool for such study. The mechanism of CO_2 transport will be solved in few years after molecular and physiological analyses of the SC mutants and relevant mutants that are isolated or constructed. Once complete

```
  1   AGCTGCTGCCAACAGACCTAGAGCACTTTCCCCATGACCTTGGAAAGCGTAGGGAGAGGT
 61   ACGGGGTTTGAAGGCGCCGCCCCGTAAAAACTGGGCCCCGGCCGCCTTAACTCGACGGGC
121   CGTTTCCACAATCATGGTTTCATTTTCCACCGAACAGGGGCCTGCTACCACAGCCACCGG
                M  V  S  F  S  T  E  Q  G  P  A  T  T  A  T  G

181   ATGGTTTTTGCCGATCGCCACGGGGCCAGCGGGGGTAGAAACGATTACTTCACTGTATTC
                W  F  L  P  I  A  T  G  P  A  G  V  E  T  I  T  S  L  Y  S

241   CCCATGGCGGAAAGTCAAACTAGCCCGTTTAAAAGGTTGTTCCACCCGTAATACATCTTC
                P  W  R  E  V  K  L  A  R  L  K  G  C  S  T  R  N  T  S  S

301   AATCCAGGGGCTAACCTCTTGGATTTGCAAAGGATCAAGTCCGGCTGTTTCCCCCACCAA
                I  Q  G  L  T  S  V  I  C  K  G  S  S  P  A  V  S  P  T  N

361   CCCCATCACAACTTTGTGCTTACCAACAATCTTTTCGGGGGTGAGGCCCCGTTCGGCAAA
                P  I  T  T  L  C  L  P  T  I  F  S  G  V  R  P  R  S  A  N

421   CTCCTTACCAATGCGCTCAATTTCTATTTCTGGGGTGCCGACTTTCATGACGACGATCAT
                S  L  P  M  R  S  I  S  I  S  G  V  P  T  F  M  T  T  I  M

481   GACAAACTTCCTCTATTCGATAGGTTGGGACAGGGAGGGTTAAAAGCTTGGTTTTCAGCA
                T  N  F  L  Y  S  I  G  W  D  R  E  G  *

541   TATTGATGACTGAAATAATCAGGGTGTAAATCTGCAACAATTTCCTGGGGAGAGAAATCG
601   TATAGCTGGCT
```

Figure 8. Nucleotide sequence of the ORF129 mutated in the G7 mutant and deduced amino acid sequence (standard one-letter symbols).

inactivation of CO_2 transport is achieved, it will not be difficult to isolate mutants defective in HCO_3^- transport. There appear to be several genes not yet cloned which are involved in the efficient utilization of C_i for photosynthesis. Cloning and identification of these genes are essential to the understanding of the CCM.

LITERATURE CITED

1. **Abe T, Tsuzuki M, Kodakami Y, Miyachi S** (1988) Isolation and characterization of temperature-sensitive, high-CO_2requiring mutant of *Anacystis nidulans* R₂. Plant Cell Physiol **29**: 1353-1360

2. **Badger MR, Kaplan A, Berry JA** (1980) The internal inorganic carbon pool of *Chlamydomonas reinhardtii*: Evidence for a CO_2 concentrating mechanism. Plant Physiol **66**: 407-413

3. **Berry JA, Boynton J, Kaplan A, Badger MR** (1976) Growth and photosynthesis of *Chlamydomonas reinhardtii* as a function of CO_2 concentration. Carnegie Inst YB **75**: 423-432

4. **Colman B ed.** (1991) Second International Symposium on Inorganic Carbon Utilization by Aquatic Photosynthetic Organisms. Can J Bot **69**: 907-1024

5. **Dzelzkalns VA, Bogorad L** (1988) Molecular analysis of a mutant defective in photosynthetic oxygen evolution and isolation of a complementing clone by a novel screening procedure. EMBO J **7**: 333-338

6. **Espie GS, Miller AG, Birch DG, Canvin DT** (1988) Simultaneous transport of CO_2 and H_3CO^- by the cyanobacterium *Synechococcus* UTEX 625. Plant Physiol **87**: 551-554

7. **Espie GS, Miller AG, Canvin DT** (1988) Characterization of the Na^+ requirement in the cyanobacterial photosynthesis. Plant Physiol **88**: 757-763

8. **Friedberg D, Kaplan A, Ariel R, Kessel M, Seijffers J** (1989) The 5'flanking region of the gene encoding the large subunit of ribulose-1,5-bisphosphate carboxylase/oxygenase is crucial for growth of the cyanobacterium Synechococcus sp. strain PCC 7942 at air levels of CO_2. J Bacteriol **171**: 6069-6076

9. **Fukuzawa H, Suzuki E, Komurai Y, Miyachi S** (1992) A gene homologous to chloroplast carbonic anhydrase (icfA) is essential to photosynthetic carbon dioxide fixation by Synechococcus PCC7942. Proc Natl Acad Sci USA **89**: 4437-4440

10. **Kaplan A, Badger MR, Berry JA** (1980) Photosynthesis and the intracellular inorganic carbon pool in the blue green alga Anabaena variabilis; response to external CO_2 concentration. Planta **149**: 219-226

11. **Kaplan A, Schwarz R, Lieman-Hurwitz J, Reinhold L** (1991) Physiological and molecular aspects of the inorganic carbon concentrating mechanism in cyanobacteria. Plant Physiol **97**: 851-855

12. **Kaplan A, Zenvirth D, Marcus Y, Omata T, Ogawa T** (1987) Energization and activation of inorganic carbon uptake by light in cyanobacteria. Plant Physiol **84**: 210-213

13. **Marcus Y, Schwarz R, Friedberg D, Kaplan A** (1986) High CO_2 requiring mutant of Anacystis nidulans R_2. Plant Physiol **82**: 610-612

14. **Miller AG, Canvin DT** (1985) Distinction between HCO_3^- and CO_2 dependent photosynthesis in the cyanobacterium Synechococcus leopoliensis based on the selective response of HCO_3^- transport to Na^+. FEBS Lett **187**: 29-32

15. **Miller AG, Colemen B** (1980) Active transport and accumulation of bicarbonate by a unicellular cyanobacterium. J Bacteriol **143**: 1253-1259

16. **Ogawa T** (1990) Mutants of Synechocystis PCC6803 defective in inorganic carbon transport. Plant Physiol **94**: 760-765

17. **Ogawa T** (1991) A gene homologous to the subunit-2 gene of NADH dehydrogenase is essential to inorganic carbon of Synechocystis PCC6803. Proc Natl Acad Sci USA **88**: 4275-4279

18. **Ogawa T** (1991) Cloning and Inactivation of a gene essential to inorganic carbon transport of Synechocystis PCC6803. Plant Physiol **96**: 280-284

19. **Ogawa T** (1992) Identification and characterization of the ictA/ndhL gene product essential to inorganic carbon transport of Synechocystis PCC6803. Plant Physiol **99**: 1604-1608

20. **Ogawa, T, Kaneda T, Omata T** (1987) A mutant of Synechococccus PCC7942 incapable of adapting to low CO_2 concentration. Plant Physiol **84**: 711-715

21. **Ogawa T, Kaplan A** (1987) The stoichiometry between CO_2 and H^+ fluxes involved in the transport of inorganic carbon in cyanobacteria. Plant Physiol **83**: 888-891

22. **Ogawa T, Miyano A, Inoue Y** (1985) Photosystem-I-driven inorganic carbon transport in the cyanobacterium, Anacystis nidulans. Biochim Biophys Acta **808**: 77-84

23. **Ogawa T, Ogren WL** (1985) Action spectra for accumulation of inorganic carbon in the cyanobacterium, *Anabaena variabilis*. Photochem Photobiol 41: 583-587

24. **Omata T, Ogawa T** (1986) Biosynthesis of a 42-kD polypeptide in the cytoplasmic membrane of the cyanobacterium *Anacystis nidulans* strain R_2 during adaptation to low CO_2 concentration. Plant Physiol 80: 525-530

25. **Omata T, Carlson TJ, Ogawa T, Pierce J** (1990) Sequencing and modification of the gene encoding the 42-kilodalton protein in the cytoplasmic membrane of *Synechocystis* PCC7942. Plant Physiol 93: 305-311

26. **Price GD, Badger MR** (1989a) Ethoxyzolamide inhibition of CO_2-uptake in the cyanobacterium *Synechococcus* PCC7942 without apparent inhibition of internal carbonic anhydrase activity. Plant Physiol 89: 37-43

27. **Price GD, Badger MR** (1989b) Expression of human carbonic anhydrase in the cyanobacterium *Synechococcus* PCC7942 create a high CO_2-requiring phenotype. Evidence for a central role for the carboxysome in the CO_2 concentrating mechanism. Plant Physiol 91: 505-513

28. **Price GD, Badger MR** (1989c) Isolation and characterization of high CO_2-requiring-mutants of the cyanobacterium *Synechococcus* PCC7942. Two phenotypes that accumulate inorganic carbon but are apparently unable to generate CO_2 within the carboxysome. Plant Physiol 91: 514-525

29. **Price GD, Howitt SM, Harrison K, Badger MR** (1992) Analysis of a genomic DNA region for the cyanobacterium, *Synechococcus* PCC7942, involved in carboxysome assembly and function. Plant Physiol in press.

30. **Schwarz R, Friedberg D, Kaplan A** (1988) Is there a role for the 42kDa polypeptide in inorganic carbon uptake by cyanobacteria? Plant Physiol 88: 284-288

31. **Shinozaki K, Sugiura M** (1983) The gene for the small subunit of ribulose-1,5-bisphosphate carboxylase/oxygenase is located close to the gene for the large subunit in the cyanobacterium *Anacystis nidulans* 6301. Nucleic Acid Res 11: 6957-6964

32. **Stanier RY, Kunisawa R, Mandel M, Cohen-Bazire G** (1971) Purification and properties of unicellular blue-green algae (order Chroococcales) Bacterial Rev 35: 171-205

33. **Volokita M, Zenvirth D, Kaplan A, Reinhold L** (1984) Nature of the inorganic carbon species actively taken up by the cyanobacterium *Anabaena variabilis*. Plant Physiol 76: 599-602

34. **Williams JGK, Szalay AA** (1983) Stable integration of foreign DNA into the chromosome of the cyanobacterium *Synechococcus* R_2. Gene 24: 37-51

Limitation of Primary Productivity in the Oceans by Light, Nitrogen and Iron[1]

John G. Rueter

Department of Biology and Environmental Sciences and Resources Program, Portland State University, Portland, OR 97207-0751

INTRODUCTION

Primary production in the ocean is directly related to photosynthesis and other reductive biosynthetic processes that lead to the net growth of phytoplankton. The rate at which light energy is converted into reduced carbon, nitrogen and sulfur forms is determined by the amount and efficiency of phytoplankton. Phytoplankton biochemistry, physiology, and ecology have all been integrated into a common discipline by the study of the factors that control growth. The biochemical composition of cells has been used to describe the physiological growth response, for example by Shuter (11). The efficiency of particular physiological responses has been used to describe competition for resources between species by Tilman (12). Competition, at steady state for relative long periods of time, may even lead to exclusion of the inefficient species and this has been linked to the process of natural selection. These biochemical, physiological, population, and evolutionary models for optimization have been integrated so completely in biological oceanography that it is not uncommon to describe the net productivity in terms of the carbon fixation rate per chlorophyll (even though the community is made up of many algal species and various numbers of individuals of each of those species) or to describe the naturally occurring community of phytoplankton as being selected to using the limiting resources most efficiently. Although these statements may be valid in steady state systems, it is important to examine their validity in systems with variability. In this paper we will critique steady-state optimization models and descriptions of light, nitrogen and iron limited cells. Then we will address two challenges to optimization models: variability in environmental parameters and that cells should logically have survival as their main goal. We will present a new model that blends optimal physiology with cell survival.

OPTIMIZATION MODELS FOR PHYTOPLANKTON GROWTH

Algal cell physiology has been studied using models that are based on the assumption that cell components are used in an optimal manner that leads to maximum growth rate (6, 11). Biochemical components of the cell are assumed to perform the functions of: light harvesting, carbon reduction, assimilatory nitrate reduction, respiration, biosynthesis and storage. The solution to the optimization model requires that the efficiency (defined as growth per resource used) of each cellular component be identified and then the relative amounts of these components are determined by the minimum cost function. The growth rate, as calculated by this function, is limited by the process that contributes the least to the overall growth. Optimization of growth will occur by cellular investment in whichever process is limiting until the marginal cost for any added investment in that limiting process is the same as the marginal cost for the investment in any other cellular component. This "economic algorithm" is the essence of linear optimization models. The responses of these model simulations are very close to the behavior of steady state algal cultures, and these theoretical models have been very useful in understanding several important aspects of autotrophic metabolism and physiology. For example, these models illustrate that the growth rate is directly related to the amount of biosynthetic and respiratory machinery of the cell, in particular that the amount of RNA is highly correlated to the growth rate. The decrease in growth rate by light and nitrogen limitation is because investment in cell components specifically needed to use these resources causes a reduction in the biosynthesis of other components.

Steady state cultures have been used to examine the physiological effects of light, nitrogen and iron limitation. Limitation by light, in circumstances with abundant nutrition, leads to the classical physiological changes that favor light harvesting processes at the expense of growth rate and nutrient uptake. Classically, low light adapted cells have more chlorophyll and thylakoid membranes and less Rubisco and ribosomes. The actual mechanism of increased pigment content may be an increase in the amount of pigment per photosynthetic reaction center or an increase in the numbers of photosynthetic units and amount of thylakoid or a mixture of both strategies. These adaptation responses require heavy investments of N and Fe into biochemical compartments that trap and convert the maximum amount of light (7). Consequently, the nitrogen and iron efficiencies of low light adapted cells is severely decreased. The net effect of nitrogen limitation on photosynthesis and growth is predicted by Shuter's model (11) to be a combination of limited investment in the nitrogen constituents of photosynthesis and the distortion of the cell's physiology and morphology to favor membrane uptake processes at the expense of light harvesting processes. Iron limitation effects have been less extensively studied than nitrogen limitation. Many of the effects of nitrogen limitation are also seen in iron limited cells (3,8) (Table I).

Table I. *Some observed effects of N- and Fe- limitation on photosynthesis (Abstracted from 2,3,8,13).*

Effects common to N and Fe limitation:

    decrease in chlorophylls and phycobiliproteins pigments

    change in the ratio of chlorophylls

    changes in thylakoid membrane structure and stacking

    change in the specific absorption of Chl a

    lower efficiency of energy transfer from PSII

    less efficient harvesting and conversion of light

    decreased relative fluorescence with DCMU addition

Effects specific to N-limitation:

    decrease in Rubisco

Effects specific to Fe-limitation:

    cytochrome b6/f decreases per cell

    less ferredoxin (may be replaced partially by flavodoxin)

    decrease in the nitrite reductase rate

    pattern of photosynthate distribution is greater into the protein
        fraction (similar to light limited cells)

Light, nitrogen and iron are inter-related physiologically in ways that makes it impossible to discuss one process without addressing the roles of the other two. These three resources represent crucial aspects of metabolism: light represents the energy flux available to : ipport biological activity; nitrogen represents the synthesis of macromolecules and general increase in biomass; and iron represents the efficiency of energy transfer and the efficiency of proteins in energy transduction. The response to one resource is related to the response to all resources, as illustrated by the overlap in responses to nitrogen or iron limitation listed in Table I. For example, the ability of cells to grow on nitrate depends on the light energy available and the amount of cellular iron invested in nitrate assimilation enzymes. In systems such as these, the components and the organization of the components that lead to overall efficiency must be considered favorable. It would not be beneficial for a cell, limited by nitrogen and iron availability, to respond to light limitation with heavy investments of new photosynthetic units which require iron and nitrogen. There are several biochemical effects that seem to be specific to iron limitation (as opposed to light or nitrogen limitation) and it has been proposed that measurement of these parameters could provide a diagnostic approach to studying natural populations

128

(3). This approach has been an extremely valuable tool in other complex, inseparable systems. Thus, the solution to multiple resource limitation of metabolism is more complex than simply understanding the ratio and biochemical efficiencies of the individual components, rather the solution depends on cellular organization and regulation.

THE IMPORTANCE OF VARIABILITY

In any water mass that would be of interest for the study of primary productivity in the open ocean the resources of N, Fe and light are highly variable with overlapping time scales (Figure 1) such that it is impossible to describe all of them as being in "steady-state" for even a single generation. The input of light at the surface varies over the day and is zero at night. Chemical and biological properties of the water column determine light attenuation with depth. The mixing regime in the water column determines the time scale of variation in the light field for individual cells. There are two major sources of nitrogen that must be considered. New growth (net annual productivity) is strongly dependent on the advection of nitrate from deeper water into the

Physical Governing Processes

Time scale of Variation

Eolian transport of dust with iron

Diel Light Cycle

Org-N → NH4

Supply of NH4 from recycling

Advective supply of NO3 to the base of the euphotic zone
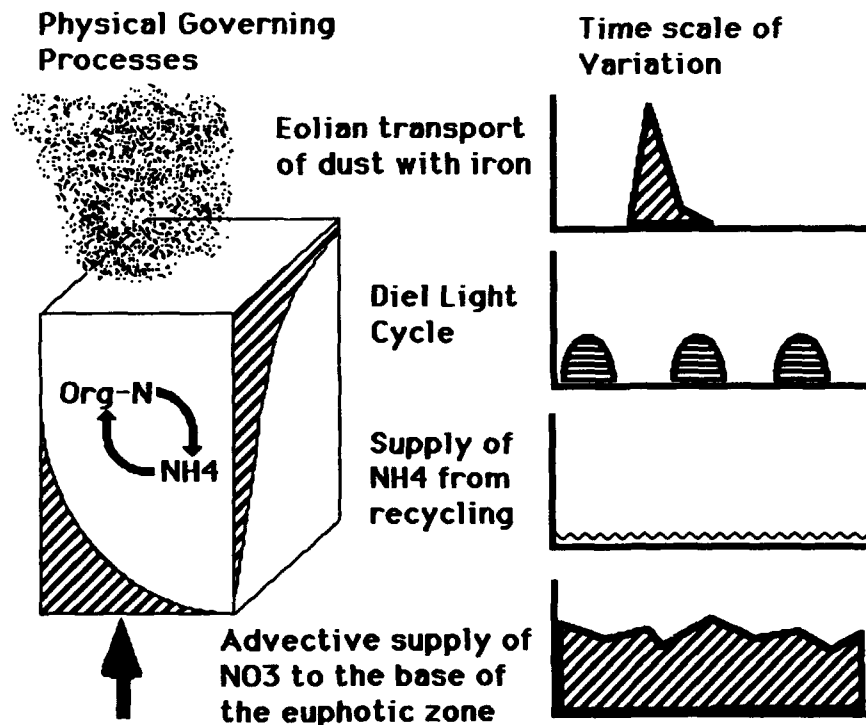
Figure 1. Variation of light, nitrogen sources and iron input to an open ocean water column.

129

euphotic zone. The amount of nitrate depends on the water column mixing characteristics and the nitrate concentration "field" depends on the uptake by plankton. Characteristically, the nitrate concentration profile is high at the base of the euphotic zone and decreases toward the surface. Mixing into and within the euphotic zone determines a critical time scale for both light and nitrate availability to individual cells. The nitrogen contained in biomass in the water column is regenerated into ammonium or urea. Ammonium concentration is extremely variable on even the smallest time and space scales (seconds and 10^{-6} m), because the source (predation) is tightly linked to the sink (phytoplankton and heterotrophic bacterioplankton uptake). The net availability of iron is a function of continental weather and eolian transport processes. For a particular water mass the input of iron as continental dust to the surface may be episodic with time scales of weeks (such as in the North Tropical Atlantic) to months (such as in the central Pacific gyre). Within the water column, iron availability is probably highly controlled by biological mechanisms that favor retention and recycling (10). These mechanisms operate at the same community structure level as N-cycling and thus would also have extremely small time and spatial scales. Thus, the availability of light, nitrogen and iron depends on input functions which are unlinked, characteristic of larger systems, and vary over time scales from seconds to weeks.

We have attempted to examine the potential optimization of oceanic cyanobacteria to "small" changes in their environment, i.e. changes that might be expected in less than a division time for light, nitrogen or iron. We grew steady state continuous cultures of the marine *Synechococcus* strain WH7803 under different combinations of light, nitrogen source and iron. The results from these experiments demonstrate that cells do reach a different optimal physiological make up and response when grown in slightly different conditions (Table II). The magnitude of some of these changes is large. For example, cells that are exposed to ammonium have 30% more chlorophyll *a* per cell than if they were grown on nitrate. Similarly, decreasing the light by 1/2 results in an 88% increase in the chlorophyll *a* per cell. The rate of adaptation is an important consideration in evaluating these results. In the above case, even if cells could put all of their biosynthetic output into the exact components needed to shift from one condition to another it is unlikely that they could adapt at anywhere near the time scale for which nitrogen source or light may vary. Rapid genetic and physiological responses to environmental parameters may not even be desirable; cells might end up adapting to the "previous" state of the environment.

CELL SURVIVAL MODEL

Any sample of water that we may study contains an assembledge of cells that have somehow survived and reproduced. Any cell that we collect, even rare clones of a single species isolated from a water mass, contains genetic strategies

Table II. *Comparison of cell composition and physiological responses with minor shifts in culture conditions.*

The "base conditions" for growth of *Synechococcus* strain WH7803 (9) was a dilution rate of 0.2 d^{-1} at 25 °C with continuous illumination at 50 $\mu E\ m^{-2}\ s^{-1}$. AQUIL medium (5) with 300 $\mu M\ NO_3$ and $5 \times 10^{-8}\ M$ Fe was used. Four comparisons were run. Column A is for an increase in dilution rate to 0.4 d^{-1}; column B is for an increase in iron to $5 \times 10^{-7}\ M$, column C is the decrease in irradiance to 27 $\mu E\ m^{-2}\ s^{-1}$; and D is the comparison of cultures grown on 150 $\mu M\ NO_3$ to 150 $\mu M\ NH_4$. The values in the columns are the ratio of new conditions divided by the "base conditions".

	dilution to 0.4 d^{-1}	Fe to 5×10^{-7}	light to 27 $\mu E\ m^{-2} s^{-1}$	N source to NH_4
	A	B	C	D
Chl *a* cell^{-1}	1.40	1.42	1.88	1.30
PBP cell^{-1}	1.60	1.45	0.81	1.10
Pmax Chla^{-1}	0.68	0.75	0.96	1.59
Pmax cell^{-1}	0.94	1.06	1.81	2.07
α Chla^{-1}	0.83	0.76	N.D.	1.93
α cell^{-1}	1.16	1.08	N.D.	2.51

that have responded to environmental parameters in a way that insures their survival over supra-annual time scales. These cells may or may not be under any pressure to grow rapidly. In fact, there are certainly some examples of species that do very well without rapid growth, such as *Trichodesmium*. We feel that the consideration of survival is a more general case than the optimization of physiological content. As explained above, the assumption that cellular metabolism is optimized is based on an "economic algorithm" for the linear optimization by a minimum cost function. This economic algorithm is not valid in the general condition but only under conditions in which the long term survival has been assured, i.e. that business or cell can avoid extinction through variable markets or environments (1). Thus the primary algorithm that should be evident in cell genetic regulation and physiology is for survival. Optimization for vegetative growth should only be important as it makes a contribution to survival.

As an example of how survival can be used as a goal in population models, we have constructed a model in Hypercard. Each card represents a cell and contains the code for physiological processes for growth and optimization, i.e. each card has a program that is a stand alone physiological model very similar to that of Shuter (11). A number of these cards are assembled to make a population which can have a diverse assembledge of cell types depending on the

programs of each card. The population grows as a result of the individual cells responding to nitrate concentration and light. For each hour of the simulation the metabolism of each card is run, new cards are made from those cells that have accumulated enough cellular material to divide, the nitrate concentration is recomputed and a set proportion of random cards are removed from the
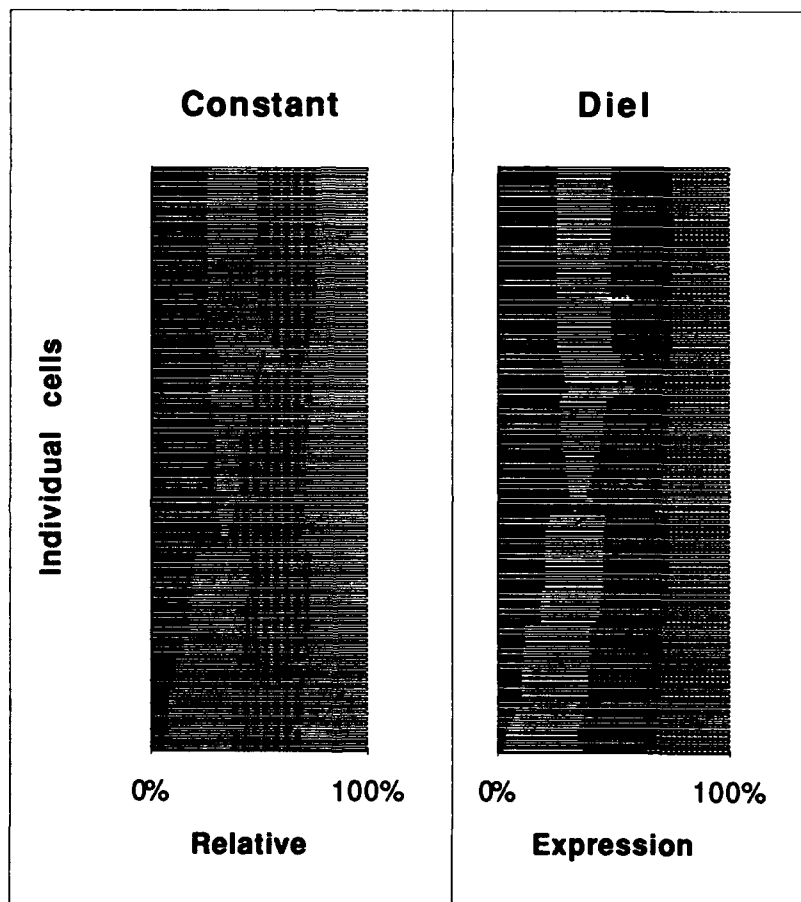
Figure 2. Profiles of populations of cells from a genetic algorithm model for cell response to constant light and diel light regimes. The simulation conditions provided the same daily integrated light, nitrate and dilution rate. The four columns in each bar diagram represent the relative expression rate of the proteins for (from left to right): reductive nitrate assimilation, photosynthetic membranes, reductive pentose phosphate pathway, biosynthesis and ribosomes. This simulation has nested time scales. The physiological sub-model runs for six minutes; the cell regulation and division sub-models run for one hour; and the total simulation was run for 29 days. Mutations were randomly introduced at the rate of 2 per day.

population. The population of cells will grow up to a steady state number of cards determined by nitrate depletion from the media and the nitrate uptake kinetics necessary to match the growth rate, just as in a continuous culture. The population of cards at any time is composed of the survivors and the new cells that derived from survivors of previous time periods. In this model the characteristics of the population, growth rate and density, emerge from the collective (but not necessarily average) behavior of individual cells.

This model can also be used to look for cell characteristics that may lead to survival in variable environments. For example we used this model to explore the relative expression rates for the major components of phytoplankton physiology because we felt that this could provide a picture of how cells would potentially deal with variability in light, nitrogen and iron. We started with a homogeneous population of cells for which the relative rates of expression for the major components of the physiology (reductive nitrate assimilatory enzymes, photosynthetic membrane, carbon fixation enzymes and biosynthesis enzymes and ribosomes) were initially set to be equal. As the population grew, mutations in the relative rates were introduced to individual cards. The results from this simulation demonstrate the importance of examining population heterogeneity. Several viable sub-populations emerged even under constant light. The population grown under a diel light regime had more individuals that had a decreased response to nitrate assimilation. These sub-populations probably did well because they had a more rapid synthesis of the other components involved in *photosynthesis* that would be important in a variable light regime. This example also illustrates the utility of the "genetic algorithm" approach to individual cell optimization (4) that could be extended to include other organisms into community ecosystem models.

CONCLUSIONS

There are fundamental differences in our approach to the relationship between primary productivity and phytoplankton physiology, depending whether we address the question as one of optimization or survival. If we assume that the ocean can be treated as a steady-state system, then it is valid to include competitive exclusion and natural selection as processes that have narrowed the species composition to only those that use the resources of light, nitrogen and iron efficiently. If we assume steady-state and optimization processes, it may be possible to describe community output functions and responses based on biochemical and biophysical efficiencies. If environmental parameters are variable, as we suspect is important for the net availability of light, nitrate and iron in the ocean, we may need to use a more general model that does not assume optimization and exclusion. Instead we may assume that the primary goal of individual cells is to survive. Optimization of physiology helps cells reach this goal but there are possibly other strategies that help cells survive through the variation of parameters. In a complex population model, competitive

133

exclusion and natural selection are emergent properties and are not inherent properties of the cells or their genetic regulation strategies. The important point is that there is a theoretical discontinuity between biochemical efficiency and net community efficiency. We can not always expect that "efficient" and rapidly growing species will dominate; it may be that the variability of resources leads to diversity in the species and physiologies that can survive. Diverse, dynamic and highly variable populations of oceanic phytoplankton may respond rapidly and robustly to global climatic changes and may not suffer major disruptions in the net productivity functions that are predicted for many terrestrial biomes. In order to understand these responses, however, we will have to shift our approach to studying the oceans from the current mechanistic paradigm to a more general and relational view of complex systems.

ACKNOWLEDGEMENTS

LITERATURE CITED

1. **Browning, EK and JM Browning** (1989) Micreconomic theory and applications. Glenview, Scott, Foresman and Company.
2. **Cullen, JJ, Yang X, MacIntyre HL** (1992) Nutrient limitation of marine photosynthesis. *In* Falkowski PJ, Woodhead AD, eds. Primary productivity and biogeochemical cycles in the sea. Plenum Press, NY pp 69-88.
3. **Greene, RM, RJ Geider, Falkowski, PJ** (1991) Effect of iron limitation on photosynthesis in a marine diatom. Limnol. Oceanogr. **36**: 1772-1782.
4. **Levy, S** (1992) Artificial Life: The quest for a new creation. Pantheon Books. New York.
5. **Morel, FMM, JG Rueter, Anderson DM, Guillard RRL** (1979) AQUIL: A chemically defined culture medium for trace metal studies. J Phycol **15**: 135-141.
6. **Myers, JE** (1980) On the algae: Thoughts about physiology and measurements of efficiency. *In* Falkowski, PG, ed, Primary Productivity in the Sea. Plenum Press, New York pp 1-16.
7. **Raven, JA** (1988) The iron and molybdenum use efficiencies of plant growth with different energy, carbon and nitrogen sources. New Phytologist **109**: 279-287.
8. **Rueter, JG and DR Ades** (1987) The role of iron nutrition in photosynthesis and nitrogen assimilation in *Scenedesmus quadricauda* (Chlorophyceae) J Phycol **23**: 452-7.
9. **Rueter, JG and NL. Unsworth** (1991) Response of marine Synechococcus (Cyanophyceae) cultures to iron nutrition. J. Phycol. **27**: 173-178.
10. **Rueter, JG, Hutchins, DA, Smith, RW, Unsworth NL** (1991) Iron nutrition of Trichodesmium. *In* EJ Carpenter, DG Capone, JG Rueter, eds, Marine

Pelagic Cyanobacteria: Trichodesmium and other Diazotrophs. Kluwer, Dordrecht. pp 289-306.

11. **Shuter, B** (1979) A model of physiological adaptation in unicellular algae. J. Theor. Biol. **78**: 519-552.

12. **Tillman, D** (1982) Resource Competition and Community Structure. Princeton, N. J. Princeton University Press.

13. **Turpin, DH** (1991) Effects of inorganic N availability on algal photosynthesis and carbon metabolism. J. Phycol. **27**: 14-20.

Ultraviolet-B Radiation Effects on Leaf Fluorescence Characteristics in Cultivars of Soybean[1]

Donald Miles

Div. of Biological Sciences, University of Missouri, Columbia, MO 65211

INTRODUCTION

The alarming rate of destruction of stratospheric ozone (about 3% in the last decade) can be associated with the anthropogenic release of chlorofluorocarbons and nitrogen oxides (5). Even if release of all such gases is halted today, the predicted increased flux of ultraviolet-B (UV-B, 280 to 320 nm) radiation will continue over the next century. UV-B radiation impinging on terrestrial plants cause reduction in plant growth and yield of a wide range of agronomic species. UV-B radiation has been studied in about 300 different species and varieties of plants. Approximately 50% show some physiological damage or reduction of growth. The response in sensitive species include reduction in photosynthesis, biomass, plant height, leaf area, and seed yield (7).

An extensive study of the effect of enhanced UV-B on the growth of soybean (*Glycine max* (L.) *Merr.*) has shown a definite effect. These long term experiments show that some cultivars of soybean are more sensitive to UV-B than others. This sensitivity to UV-B is observed in growth rate, biomass accumulation and seed yield (8). One study indicated involvement of photosynthesis by a decrease in net carbon exchange in sensitive soybean cultivars under UV-B irradiation (6).

Studies of isolated chloroplasts and to a limited extent whole leaves, show a potential site of action of UV-B in photosystem II (2). There have been several reports of changes in the chlorophyll fluorescence kinetics (Kautsky Effect) of chloroplast or leaves following UV-B irradiation. These data may indicate the extent of the effect of UV-B on PSII (9).

The present study applied enhanced levels of UV-B radiation simulation a 20% loss of stratospheric ozone with previously described sensitive or resistant soybean cultivars. It is clear that plant growth and seed yield are sensitive to this enhanced UV-B, but it is not been shown if PSII may be involved in the UV

---

[2]Abbreviations: CA, cellulose diacetate; M, Mylar type S; chl, chlorophyll; F_0, initial level of chlorophyll fluorescence; F_M, peak or maximum level of fluorescence; F_V, variable fluorescence or F_M-F_0

sensitive soybean cultivars. Chlorophyll fluorescence characteristics of sensitive and resistant cultivars of soybean were recorded in enhanced UV-B and control plants. The data confirm that an effect of UV-B on PSII is evident by changes in fluorescence (both kinetics and spectral forms) in sensitive cultivars of soybean that has less effect on resistant cultivars.

MATERIALS AND METHODS

Field experiments were carried out at the University of Missouri Botany Research Greenhouse, Columbia MO (39 degrees N) from May through September with natural light condition and supplemental irrigation. Soybean (*Glycine max* (L.) *Merr.*) cv *Essex, Williams, York,* and *Forest* were germinated in 4 l pots with soil mixture of ProMix and potting soil. Three or four seedlings were grown per pot with automatic irrigation and liquid nutrient solution provided once per week.

Twenty pots of each culitvar of plants were subjected to one of three treatments throughout the growing season: UV-B and UV-A enhanced treatment (290 to 375 nm) with Westinghouse FS-40 lamps filtered through 0.08 mm cellulose diacetate (CA^2) filters; UV-A enhanced control (320 to 375 nm) obtained from FS-40 lamps and 0.13 mm Mylar (M) Type S filters; or ambient irradiation control. Plants were irradiated about 6 hours each day equally around local solar noon. The intensity was maintained by positioning the lamps as the plants grow over the season. The lamp to canopy distance was from 30 to 90 cm. Spectral irradiance at the canopy height was measured with a double-grating Optronics Laboratories Model 742 Spectroradiometer and recorded with a dedicated IBM 386 computer. The spectroradiometer was calibrated against a National Institute of Standards and Technology traceable 1000 W standard lamp and wavelength accuracy was maintained using the mercury emission lines at 302.2 and 334.1 nm.

Calculation of the biologically effective UV-B was through the used of the generalized plant response action spectrum normalized to 300 nm employing the Green Model (3). Irradiance level was adjust.d biweekly throughout the growing season. All UV-B enhanced doses are compared to 20% depletion of stratospheric ozone and ranged from 5 to 12 kJ m^{-2}.

Plant growth measurements of height, leaf area, leaf weight were made weekly. Chl content was measured with a SPAD (Wescor Inc, Logan UT) meter (4) calibrated by simultaneous chl extractions and absorbance with the Arnon method (1).

Comparison were made with leaves taken at the same node throughout the test period or at several different nodes down the plant axis at one sampling time. Each data point included at least 20 leaves.

Chl fluorescence kinetics were measured with an MF-1 fluorometer with dark adapted leaves. The actinic light was 100 to 300 µmol m^{-2} s^{-1} with a peak at 658 nm. Fluorescence measurements were from 680 to 750 nm. Traces were

recorded with a Tektronix 5103 storage oscilloscope or an Elexor TD-4000 computer. Room temperature Chl fluorescence spectra were recorded with a SPEX FT112 Fluorolog fluorometer. Excised leaves were excited at 470 nm, 100 μmol m^{-2} s^{-1} and emission was recorded at 22.5 degrees from the upper surface of the leaf at room temperature.

RESULTS

Plant Growth

Growth was followed in four cultivars of soybean throughout the growing season on a weekly basis. Measurements were made of plant height, leaf weight, leaf area, chl concentration and chl a/b. under the two UV treatments and controls. Only a limited amount of data is presented here. *York* appeared to be the least effected by UV-B irradiatio. while *Essex* was most effected. The impact of UV-B on *Essex* appeared as a decrease in plant height, decrease in leaf area, decrease in chl concentration on an area basis, and a small increase in Chl a/b as compared to control plants. These data are in agreement with those reported previously (8) though all of these parameters were not previously measured in one experiment.

Chlorophyll Fluorescence Kinetics

To determine if PSII was involved as a site for U -B radiation leading to this decrease in growth, chl fluorescence was followed during the above growth experiment. Chl fluorescence values for F_O, F_M, and F_V were obtained on dark adapted, excised leaves. Fluorescence was compared in treated and control leaves in two different ways. In one approach we examined the third fully expanded trifoliate from the apex every week during UV-B exposure (Fig. 1). In a different approach we examined the values for leaves a various nodes down the plant axis at one point during the growing season (Table I). In general, *Essex* was the most sensitive cultivar to UV-B while *Forest* and *York* were the least sensitive in terms of F_V/F_M values with both experimental approaches. The F_V/F_M values decreased with UV-B irradiation while there was less decrease with UV-A through Mylar filters. At the same time F_O remained near constant. This is the type of response previously observed in other species treated with UV-B doses (9). The results tend to support the suggestion for a site of UV-B in PSII.

Chl Fluorescence Spectra

When complete room temperature leaf fluorescence spectra were obtained for leaves collected from plants in the above experiments, general changes in fluorescence emission forms could be observed. The major change was a loss of the F683-687 peak in the sensitive cultivars under UV-B with little change in F735. This again was most obvious with *Essex* (Fig. 2) and least changed in the *Forest* cultivar (data not shown). Loss of the F683-687 fluorescence was most apparent when leaves were measured throughout the growing season rather than

138
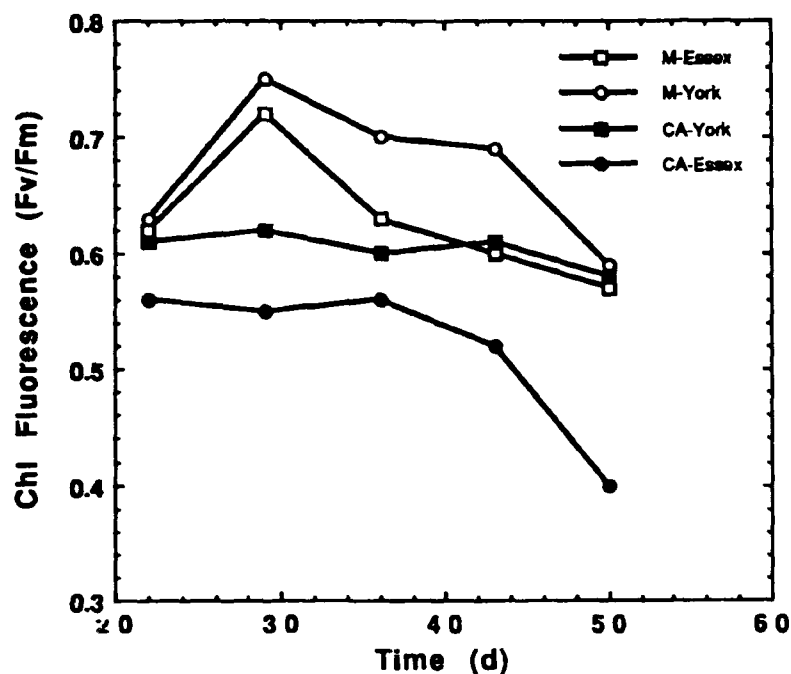
Figure 1. Changes in chl fluorescence of *Essex* and *York* cv with UV-B exposure over 30 d of growth from germination. Values of F_V/F_M are for the trifoliate at the third node from the apex of the plant.

Table I. In vivo *chlorophyll fluorescence characteristics of soybean cultivar leaves along the axis of the plant.*

F_V/F_M was recorded for four cultivars from leaves treated with UV-B and UV-A or controls leaves receiving only UV-A. Fully expanded leaves were analyzed with node one designated at the top of the plant axis nearest the apical meristem.

	Forest		York		Essex		Williams	
Node	CA	M	CA	M	CA	M	CA	M
1	0.65	0.67	0.60	0.59	0.59	0.68	0.73	0.69
2	0.61	0.68	0.64	0.68	0.52	0.69	0.69	0.64
4	0.74	0.71	0.67	0.69	0.48	0.63	0.72	0.66
6	0.72	0.74	0.72	0.80	0.44	0.69	0.67	0.72

CA, Cellulose acetate filters; M, Mylar filters; F_V/F_M, variable chl fluorescence divided by the maximum or peak of fluorescence.
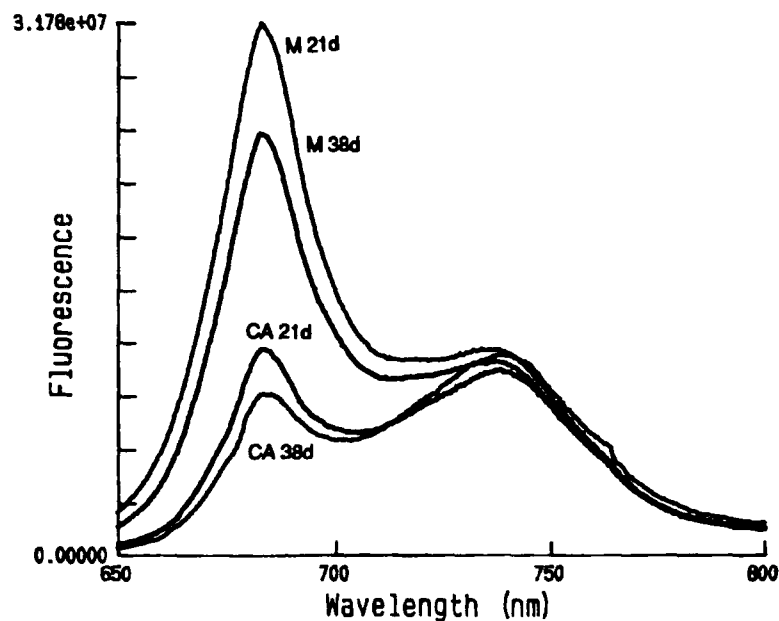
Figure 2. Room temperature leaf fluorescence of *Essex* cv. Lower two curves are treated with UV-B for 21 and 38 d; upper two curves are for Mylar control at 21 and 38 d. Fluorescence units are relative in count/s.

down the axis on a plant at one time. This loss tends to support PSII alterations by UV-B which is not observed in the control plants.

DISCUSSION

The collected data indicates an effect of the radiation from FS-40 lamps with cellulose diacetate filters (UV-B treatment approximating a 20% decrease in stratospheric ozone) relative to the FS-40 lamps with the Mylar filters (control) on the photosynthetic apparatus, especially PSII. This tends to confirm a relationship of the previous observed sensitive and resistant cultivars of soybean and supports the idea that UV-B limitation of PSII could contribute to the overall decrease in photosynthesis in sensitive plants. This is not to suggest that the PSII site for UV-B is the only site limiting photosynthesis, growth and seed yield.

140

LITERATURE CITED

1. **Arnon DI** (1949) Copper enzymes in isolated chloroplasts. Plant Physiol **24**: 115

2. **Bornman JF** (1989) Target sites on UV-B radiation in photosynthesis of higher plants. J Photochem Photobiol B: **4**: 145-158

3. **Green AES, Cross KR, Smith LA** (1980) Improved analytical characterization of ultraviolet skylight. Photochem Photobiol **31**: 59-65

4. **Schaper H, Chacko EK** (1991) Relation between extractable chlorophyll and portable chlorophyll meter readings in leaves of eight tropical and subtropical fruit-tree species. J Plant Physiol **138**: 674-677

5. **Solomon S** (1990) Progress toward a quantitative understanding of Antarcic ozone depletion. Nature **347**: 347-354

6. **Sullivan JH, Teramura AH** (1990) Field study of the interaction between solar ultraviolet-B radiation and drought on photosynthesis and growth in soybean. Plant Physiol **92**: 141-146

7. **Teramura AH** (1987) Ozone depletion and plants. *In* JS Hoffman, ed, Assessing the Risk of Trace Gases that Can Modify the Stratosphere, Vol VIII. United States Environmental Protection Agency, Washington, DC, pp 1-75

8. **Teramura AH, Sullivan JH** (1988) Effects of ultraviolet-B radiation on soybean yield and seed quality: a six-year field study. Environ Pollut **53**: 466-468

9. **Tevini M, Grusemann P, Fieser G** (1988) Assessment of UV-B stress by chlorophyll fluorescence analysis. *In* HK Lichtenthaler, ed, Applications of Chlorophyll Fluorescence, Kluwer Acad Publ, The Netherlands, pp 229-238r cultivars from leaves treated with UV-B and UV-A or controls leaves receiving only UV-A. Fully expanded leaves were analyzed with node

UV-B Driven Degradation of the D1 Reaction-Center Protein of Photosystem II Proceeds via Plastosemiquinone[1]

Marcel A.K. Jansen, Victor Gaba, Bruce Greenberg, Autar K. Mattoo, and Marvin Edelman

Department of Plant Genetics, Weizmann Institute of Science, Rehovot, Israel (MJ,ME); Department of Virology, Volcani Institute, Beit Dagan, Israel (VG); Department of Biology, University of Waterloo, Waterloo, Ontario, Canada (BG); Plant Molecular Biology Laboratory, USDA/ARS, Beltsville Agricultural Research Center, Beltsville, MD, USA (AM).

INTRODUCTION

The core of the photosystem II (PS II) reaction center consists of the D1, D2 and cytochrome b_{559} proteins. Together these proteins form a cluster containing two molecules of pheophytin a, four to five of chlorophyll a, one or two of carotene, two of plastoquinone, and a non-haem iron. This is the minimal unit capable of performing light-driven charge separations (17, 14). D1 and D2 are respectively the apoproteins of the secondary quinone electron acceptor Q_B and the primary electron acceptor Q_A. During photosynthetic electron flow, Q_B goes through three redox states; quinone, semiquinone anion radical, and quinol (4). The D1 protein is thought to mediate electron flow by binding and unbinding Q_B in its various redox states.

The D1 reaction center protein rapidly turns over in the light although it is stable in the dark (6). Degradation is driven by visible [400-700 nm] (15), far red [700-730 nm] (7) and UV [250-400 nm] (10) radiation. Two major steps have been uncovered in the process of radiance-driven D1 degradation. First, a photoreceptor, characterized by its specific action spectrum, is activated by radiation (10). Then, the energized photoreceptor, directly or indirectly, activates a cleavage site resulting in the appearance of a specific breakdown product (11).

Based on analysis of the radiance spectrum for D1 protein degradation, the degradation products, and *in vivo* inhibitor studies, we hypothesized the presence of multiple photoreceptors for degradation (10) and a central role for the Q_B-plastosemiquinone anion in the degradation process (12). The quinone anion radical, a potentially reactive species normally formed during photosynthetic

electron flow, was speculated to be a common, mechanistic intermediate in the cleavage of the D1 protein under all light conditions.

In the past few years, detailed PS II inhibitor studies were performed in visible light. These studies do not support a central role for the Q_B-plastosemiquinone anion in visible-light-driven D1 degradation. Instead, they champion Q_B-niche occupancy as the critical element (21, 9). However, occupancy state alone is insufficient to explain D1 protein degradation in visible light. Some Q_B-displacing PS II inhibitors, such as diuron, stabilize the D1 protein while others, such as bromoxynil, do not (13). Recently, we have found that inhibitors of the latter class become strong stabilizers of D1 in visible light when the dimensions of a specific side chain are increased (Jansen M.A.K., Depka B., Trebst, A., Edelman M. In preparation). Thus, engaging particular sites within the Q_B-niche inhibits D1 protein degradation in visible light.

The arguments for plastosemiquinone anion radical involvement in D1 protein degradation are more relevant for the UV spectral range. Quinones have been hypothesized to be the photoreceptors for UV-driven degradation (10), while UV irradiation *in vitro* leads to breakage of the D1 polypeptide in the Q_B-niche (22). There is a likelihood of increased levels of UV-B radiation reaching the earth as a result of the well known thinning of the stratospheric ozone layer. To assess the impact of such radiation on PS II reaction center stability and photosynthesis, it is important to unravel the mechanism of UV-B driven, D1 protein degradation.

RESULTS AND DISCUSSION

Rates of D1 degradation *in vivo*, driven by UV-B or visible radiation, have been determined in plants grown under intermittent or continuous visible light. Under intermittent light conditions (2 min 50 μE m^{-2} s^{-1} visible light, 2 h darkness), the resulting depletion of bulk chlorophyll does not abolish photosynthesis (1) or D1 protein turnover (10). On the contrary, in intermittent light-grown plants, heightened rates of degradation in the UV-B region, but not in the visible, are observed (Table 1). Thus, the ratio of UV-B driven over visible-light-driven D1 degradation is not constant. Rates of UV-B driven D1 degradation are inversely related to the intensity of photosynthetic light at which the plants were grown (Table 1). However, rates of visible-light-driven D1 degradation are independent of growth radiance conditions. The data in Table 1 support the contention (10) that the UV photoreceptor for D1 degradation is a minor absorbing pigment which is masked when increasing intensities of photosynthetic light induce production of large amounts of other UV absorbing pigments (e.g., chloroplylls, carotenoids, anthocyanins) in the plants.

The action spectrum for D1 degradation in intermittent light grown plants (10) resembles the absorption spectrum of plastosemiquinone (2) (Fig. 1). The suggestion that plastosemiquinone is the UV photoreceptor for D1 protein degradation *in vivo* (10) is in line with the known destructive effects of UV

143

Table I. Rates of UV-B-driven and visible-light-driven D1 protein degradation as a function of radiation conditions during growth. *Spirodela* were grown under the continuous light of cool-white fluorescent bulbs at the intensities indicated, or under intermittent light as described in the legend to Figure 1. Plants were radiolabeled with [^{35}S] methionine at 25 μE m^{-2} s^{-1} of visible radiation and chased either in UV-B radiation (Rayonet 3000Å photoreactor bulb) or visible radiation (cool-white fluorescent bulbs) (10). The chase was stopped by freezing the plants and proteins were separated as detailed in the legend to Figure 2. Values given represent the averages of 9 or more experiments. Standard errors are given.

Plant Growth (visible radiation)	D1 Degradation		
	UV	Visible	
	(6 μ m^{-2} s^{-1})	(6 μE m^{-2} s^{-1})	(25 μE m^{-2} s^{-1})
		(h^{-1})	
Intermittent (2min/2h)	0.38±0.05	0.09±0.01	
Continuous (6 μE m^{-2} s^{-1})	0.14±0.02		0.12±0.01
Continuous (25 μE m^{-2} s^{-1})	0.10±0.01	0.08±0.01	0.13±0.01
Continuous (85 μE m^{-2} s^{-1})	0.08±0.01		0.12±0.01

radiance on plastoquinones (20, 23). It is also in agreement with the recent demonstration that UV-B irradiated thylakoids lose electron flow to artificial electron acceptors, even in the presence of artificial electron donors (16). This loss was paralleled by a decrease in the amplitude of the light-induced absorbance change at 320 nm, representing Q_A semiquinone formation, although primary charge separation and pheophytin reduction were unaffected. Thus, UV-B radiation was suggested to damage the primary quinone acceptor Q_A in addition to the plastoquinone pool (16).

Other studies indicate structural modifications in the D1/D2 reaction center heterodimer due to UV-B radiation. Treatment results in both a reduction of the capacity for water oxidation and atrazine binding to the thylakoids (19). Nedunchezhian and Kulandaivelu (18) have also reported UV-B induced impairment of the PS II water splitting system. The action spectrum for inactivation of PS II (3, 19) (Fig. 1) suggests that while modifications to the reaction center might occur via bound plastoquinones, additional UV photoreceptors, such as tyrosine radicals (e.g., Z^+ and D^+), may be involved. The spectrum for tyrosine radicals (Fig. 1) contains a minor peak around 300 nm and a major one at 250-260 nm (5, 8). The latter peak is clearly absent from the D1 degradation spectrum (Fig. 1). Thus, inactivation of PS II in the UV-C range (<280 nm) does not appear to be linked to differential degradation of the D1
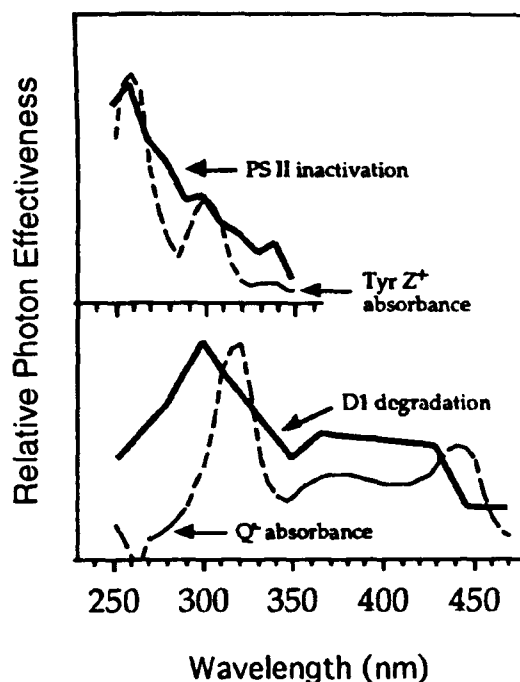
Figure 1. A comparison of PS II related spectra in the UV spectral region. Spectra of degradation of the D1 protein in intermittent light grown plants (adapted from 10); inactivation of photosynthetic activity (adapted from 19); absorbance of the plastosemiquinone anion radical (adapted from 2); and the Z^+Z absorbance difference (adapted from 5), are shown. All data sets are normalized to their maximal values. For the D1 degradation assay, *Spirodela oligorrhiza* plants were cultured under intermittent light/dark cycles of 2 min of 50 µE m^{-2} s^{-1} visible light followed by 2 h of darkness. Plants were transferred to continuous light, and radiolabeled with [^{35}S]methionine. for 2 h in 25 µE m^{-2} s^{-1} visible light and subsequently chased in the UV in the presence of 1mM methionine. The chase reaction was stopped by freezing the plants. Membrane proteins were fractionated by SDS-PAGE and visualized by fluorography. D1 protein degradation was quantified by densitometry. Unit, h^{-1} (10). Inactivation of photosynthetic activity was measured as a decrease in the quantum efficiency of the reduction of DCIP in UV-B-exposed thylakoids. Unit, relative (19). Absorbance spectrum of the plastosemiquinone anion radical was determined in alkaline methanol. Unit, E mM^{-1} cm^{-1} (2). The Z^+Z absorbance difference spectrum was determined in Tris-washed PS II preparations at pH 8.3. Unit, E mM^{-1} cm^{-1} (5).

145
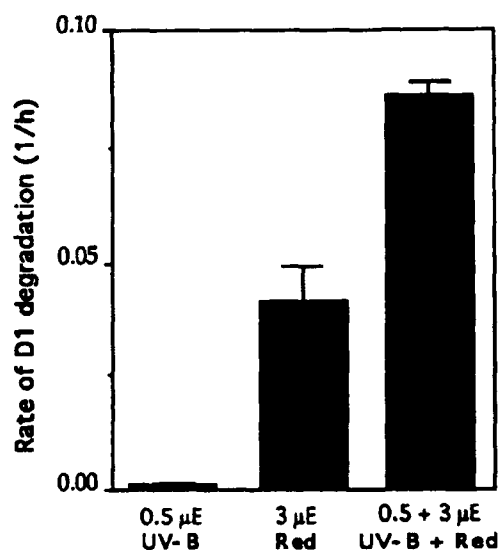
Figure 2. Degradation of the D1 protein in a mixture of UV-B and red light. *Spirodela oligorrhiza* was grown phototrophically under cool-white fluorescent bulbs. Plants were radiolabeled with [^{35}S] methionine for 2 h in 25 µE m^{-2} s^{-1} visible light and subsequently chased in the presence of 1 mM methionine in either red light (3 µE m^{-2} s^{-1}, 660 nm interference filter) or UV-B (0.5 µE m^{-2} s^{-1}, Rayonet 3000Å photoreactor bulb) or in a mixture of both. The chase reaction was stopped by freezing the plants. Membrane proteins were fractionated by SDS-PAGE and visualized by autoradiography. D1 protein degradation was quantified by densitometry. Values represent rates of degradation; n = 6. Standard errors are shown.
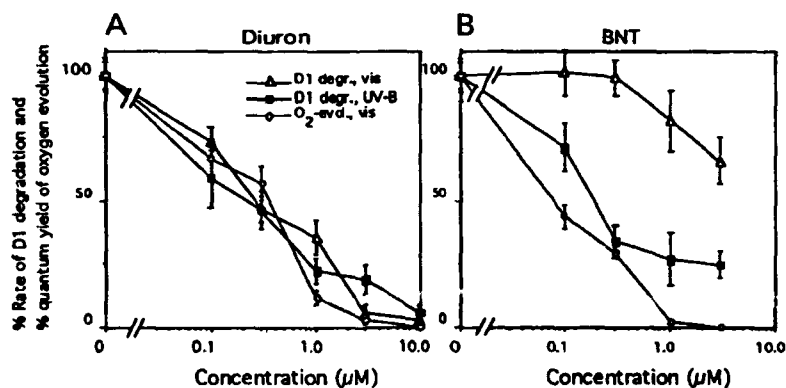
Figure 3. Inhibition of D1 degradation and oxygen evolution by diuron and bromonitrothymol (BNT). Growth and labeling of *Spirodela* were as detailed in the legends to Figure 2. Radiolabeled plants were chased in visible light (6 µE m^{-2}s^{-1}, cool-white fluorescent bulbs), or in UV-B radiation (6 µE m^{-2} s^{-1}, Rayonet 3000Å photoreactor bulb) in the presence of inhibitors. The chase was stopped and samples proteins were separated as detailed in the legend to Figure 2. Oxygen evolution in visible light was measured *in vivo* by photoacoustic spectroscopy as previously described (13). Values were normalized to those obtained in the absence of inhibitor; n = 9-15. Standard errors are shown.

146

(<280 nm) does not appear to be linked to differential degradation of the D1 protein.

All three quinone redox forms absorb in the UV spectral region (2). However, the D1 degradation spectrum resembles specifically that of plastosemiquinone (10). Formation of plastosemiquinones requires photosynthetic electron flow. Yet, UV-B radiation is not effective in driving photosynthesis (10). We therefore hypothesized that providing photosynthetically active radiation to raise the steady state level of plastosemiquinone would stimulate UV-B driven D1 degradation. Indeed, a low flux density of UV-B, which in itself does not drive measurable degradation of the D1 protein, becomes very active in the presence of a continuous background of red light (Fig. 2). Thus, the synergistic effect of a red light background on UV-B driven degradation strengthens the hypothesis of the involvement of plastosemiquinones in this process.

The D1 protein binds a molecule of plastosemiquinone at the Q_B-niche. Diuron, a PS II herbicide which acts by displacing Q_B from its niche, inhibits UV-B driven as well as visible-light-driven degradation of the D1 protein (Fig. 3A). However, bromonitrothymol (BNT), which similarly displaces Q_B, does not impair visible-light-driven degradation of D1 at a concentration almost abolishing photosynthetic oxygen evolution (Fig. 3B). If plastosemiquinone is central to the mechanism of UV-B driven, D1 protein degradation, then we would predict that BNT will inhibit D1-degradation under this radiance. In fact, BNT inhibits UV-B driven degradation with about the same concentration dependence as it does visible-light-driven oxygen evolution (the latter roughly representing binding of the analog to the D1 protein) (Fig 3B).

Thus, we have shown that plastosemiquinone is associated with UV-B-driven D1 degradation by three experimental approaches. The identification of plastosemiquinone as photoreceptor for UV-B-driven D1 degradation is readily accommodated by the proposed primary cleavage site in the loop between helix D and parallel helix de of the Q_B-niche (10, 22).

LITERATURE CITED

1. **Argyroudi-Akoyunoglou J.H., Kondylaki S. and Akoyunoglou G.** (1976) Growth of grana from "primary" thylakoids in Phaseolus vulgaris. Plant Cell Physiol. **17**: 939-954.
2. **Amesz J.** (1977) Plastoquinone. In; Encyclopedia of Plant Physiology, New Series. eds Trebst A., Avron M. (Springer Berlin) Vol. 5, pp. 238-246.
3. **Bornmann J.F., Björn L.O. and Akerlund H.E.** (1984) Action spectrum for inhibition by ultraviolet radiation of photosystem II activity in spinach thylakoids. Photobiochem. Photobiophys. **8**: 305-313.
4. **Crofts A.R. and Wraight C.J.** (1983) The electrochemical domain of photosynthesis. Biochim. Biophys. Acta **726**: 149-185.
5. **Dekker J.P., van Gorkom H.J., Brok M. and Ouwehand L.** (1984) Optical characterization of photosystem II electron donors. Biochim. Biophys. Acta **764**: 301-309.

6. **Edelman M. and Reisfeld A.** (1978) Characterization, translation and control of the 32000 dalton chloroplast memebrane protein in *Spirodela*. In; Chloroplast Development, eds Akoyunoglou G. and Argyroudi-Akoyunoglou J.H. (Elsevier/North-Holland, Amsterdam) pp. 641-652.

7. **Gaba V., Marder J.B., Greenberg B.M., Mattoo A.K. and Edelman M.** (1987) Degradation of the 32 kD herbicide binding protein in far red light. Plant Physiol. **84:** 348-352.

8. **Gerken S., Brettel K., Schlodder E. and Witt H.T.** (1988) Optical characterization of the immediate electron doner to chlorophyll a$^+$II in O_2-evolving photosystem II complexes. FEBS Lett. **237:** 69-75.

9. **Gong H. and Ohad I.** (1991) The PQ/PQH_2 ratio and occupancy of photosystem II-QB site by plastoquinone control the degradation of D_1 protein during photoinhibition *in vivo*. J. Biol. Chem. **266:** 21293-21299.

10. **Greenberg B.M., Gaba V., Canaani O., Malkin S., Mattoo A.K. and Edelman M.** (1989) Seperate photosensitizers mediate degradation of the 32-kDa photosystem II reaction center protein in the visible and UV spectral regions. Proc. Natl. Acad. Sci. USA **86:** 6617-6620.

11. **Greenberg B.M., Gaba V., Mattoo A.K. and Edelman M.** (1987) Identification of a primary *in vivo* degradation product of the rapidly-turning- over 32 kd protein of photosystem II. EMBO J. **6:** 2865-2869.

12. **Greenberg B.M., Sopory S., Gaba V., Mattoo A.K. and Edelman M.** (1990) Photoregulation of protein turnover in the PS II reaction center. In; Current Research in Photosynthesis, ed Baltscheffsky M. (Kluwer Acad. Publ. Dordrecht) Vol. 1, pp. 209-216.

13. **Jansen M.A.K., Malkin S. and Edelman M.** (1990) Differential sensitivity of 32 kDa-D1 protein degradation and photosynthetic electron flow to photosystem II herbicides. Z. Naturforsch. **45C:** 408-411.

14. **Marder J.B., Chapman D.J., Telfer A., Nixon P.J. and Barber J.** (1987) Identification of *psbA* and *psbD* gene products, D1 and D2, as reaction centre proteins of photosystem 2. Plant Molec. Biol. **9:** 325-333.

15. **Mattoo A.K., Hoffman-Falk H., Marder J.B. and Edelman M.** (1984) Regulation of protein metabolism: Coupling of photosynthetic electron transport to *in vivo* degradation of the rapidly metabolized 32-kilodalton protein of the chloroplast membranes. Proc. Natl. Acad. Sci. USA **81:** 1380-1384.

16. **Melis A., Nemson J.A. and Harrison M.A.** (1992) Damage to functional components and partial degradation of photosystem II reaction center proteins upon chloroplast exposure to ultraviolet-B radiation. Biochim. Biophys. Acta **1100:** 312-320.

17. **Nanba O. and Satoh K.** (1987) Isolation of a photosystem II reaction center consisting of D-1 and D-2 polypeptides and cytochrome b-559. Proc. Natl. Acad. Sci. USA **84:** 109-112.

18. **Nedunchezhian N. and Kulandaivelu G.** (1991) Evidence for the ultraviolet-B (280-320 nm) radiation induced structural reorganization and damage of photosystem II polypeptides in isolated chloroplasts. Physiol. Plant. **81:** 558-562.

148

19. **Renger G., Völker M., Eckert H.J., Fromme R., Hohm-Veit S. and Gräber P.** (1989) On the mechanism of photosystem II deterioration by UV-B irradiation. Photochem. Photobiol. **49**: 97-105.

20. **Shavit N. and Avron M.** (1963) The effect of ultraviolet light on photophosphorylation and the Hill reaction. Biochim. Biophys. Acta **66**: 187-195.

21. **Trebst A., Depka B., Kraft B. and Johanningmeier U.** (1988) The Q_B site modulates the conformation of the photosystem II reaction center polypeptides. Photosynth. Res., **18**: 163-177.

22. **Trebst A. and Depka B.** (1990) Degradation of the D-1 protein subunit of photosystem II in isolated thylakoids by UV light. Z. Naturforsch. **45C**: 765-771.

23. **Trebst A. and Pistorius E.** (1965) Photosynthetische reactionen in UV-bestrahlten chloroplasten. Z. Naturforsch. **20b**: 885-889.

Daytime Kinetics of UVA and UVB Inhibition of Photosynthetic Activity in Antarctic Surface Waters[1]

Barbara B. Prézelin, Nicolas P. Boucher, Ray C. Smith

Departments of Biological Sciences (BBP, NPB) and Geography (RCS), University of California, Santa Barbara, CA 93106

INTRODUCTION

During the *Icecolors '90* expedition (5), we directly measured the increase in and penetration of UVB radiation into Antarctic waters and provided the first conclusive evidence of a direct ozone (O_3)-related effect on the productivity of a natural phytoplankton community. Additional *Icecolors* results presented here indicate that 1) the quantum requirement for fractional inhibition of surface primary production by ultraviolet B (UVB) and/or ultraviolet A (UVA) radiation is not constant over the day; 2) phytoplankton photosynthesis is much less susceptible to UVA and UVB photodamage during the middle of the day; and 3) short-term measurements of UVB photoinhibition are higher than those determined for all day incubations, further impacting estimates of the potential carbon loss due to the depletion of stratospheric ozone over Antarctica during the austral spring.

MATERIALS AND METHODS

The 1990 *Icecolors* cruise was carried out in the marginal ice zone of the Bellingshausen Sea aboard the R. V. *Polar Duke*. Sampling strategy and instrumentation have been described elsewhere (2, 5). In the present study, surface samples of natural phytoplankton communities were collected at different times of day and inoculated with $H^{14}CO_3^-$, using described techniques and controls (2-5). Aliquots were dispensed into polyethlyene bags, sealed, and placed in a specially designed deck incubator comprised of 3 optically distinct incubation chambers (DECKWINGS) providing PAR (photosynthetically available radiation, 400-700 nm), UVA + PAR (320-700 nm), or UVB + UVA + PAR (280-700 nm) illumination. Light treatments were obtained with plastic cutoff filters with half-transmittance points of 400 nm (UF3), 323 nm (Mylar)

Light treatment

MYLAR   UF3 Plexiglass   UVT Plexiglass

O.D. 2, 1, 0

250 300 350 400 450 500 Wavelength (nm)
300 350 400 450 Wavelength (nm)
250 300 350 400 450 500 Wavelength (nm)

Production

$P_{QPAR+UVA}$
= production measured
under PAR+UVA radiation

P_{QPAR}
= production measured under
PAR radiation only

P_{QTot}
= production measured under
PAR+UVA+UVB radiation

Fractional inhibition of production

FI_{UVA}
= Fractional inhibition due to
UVA radiation
$= 1 - (P_{QPAR+UVA}/P_{QPAR})$

$FI_{UVA+UVB}$
= Fractional inhibition due
to UVA and UVB radiation
$= 1 - (P_{QTot}/P_{QPAR})$

FI_{UVB}
= Fractional inhibition due to
UVB radiation
$= FI_{UVA+UVB} - FI_{UVB}$

Figure 1. Comparison of the spectral absorption (solid lines) within the 3 light treatments (upper curves) and a flow diagram illustrating how results of the light treatments were combined to determine the fractional inhibition of PAR-rates of photosynthesis by UVA and/or UVB radiation.

or 296 nm (UVT) (Fig. 1). Within each DECKWING, sample chambers (n=14-18) were fitted with different layers of neutral density filters to determine the photosynthesis-irradiance (P-I) relationship for each light treatment. Incubation bags were tested extensively and shown to have no 'toxicity' effect on production measurements (4). Chl concentrations were determined at the beginning and end of each light treatment (2, 5). A Light and UltraViolet Submersible Spectroradiometer (LUVVS) provided above-surface light data every min with a 0.2 nm resolution from 250 to 350 nm and a 0.8 nm resolution from 350 to 700 nm. Light flux within each incubation bag was calculated as the product of the above-surface spectral irradiance and the spectral transmission of each

incubation chamber. Methods for curve fitting and derivation of P-I parameters and *in situ* production (P) rates have been described (2-5). *In situ* primary production was estimated from knowledge of the P-I parameters and the percent light depth (Qparo+) of the sampling depth. The procedures for estimating the percent inhibition of P-I parameters and *in situ* production by UV radiation are described in Figure 1. Each P-I curve was an independent determination and simulated *in situ* estimates of primary production were directly measured under the UVT light treatment.

RESULTS AND DISCUSSION

Figure 2 compares the relative quantum yield (top), photosynthetic potential (middle) and susceptibility to photoinhibition (bottom) for surface samples
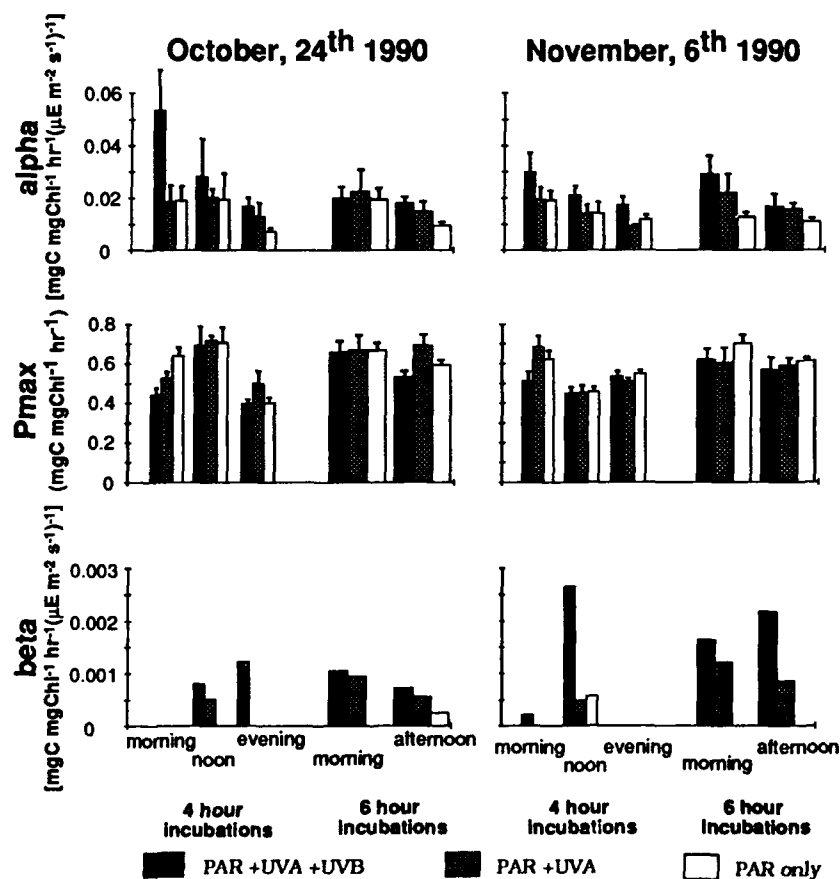
Figure 2. Effects of 3 different light treatments on P-I parameters measured at different times of day. The vertical bars represent the SD. Natural O_3 levels were between 180 and 240 Dobson Units for both days.

collected at different times of day and exposed to natural illumination where UVB and/or UVA radiation had been removed. Note that the P-I relationships are independently derived for each light treatment and the results indicate the different values one would get depending upon the spectral quality of the incubator, the time of sampling and the length of incubation. Of particular interest was the observation that significant photoinhibition of photosynthesis was evident only in light treatments where UVA and/or UVB radiation was present (Fig. 2 bottom). Thus, short term reversible photoinhibition of photosynthesis in the nutrient-replete waters of the Southern Ocean can be induced by UV radiation when Qpar is already at photoinhibitory levels.
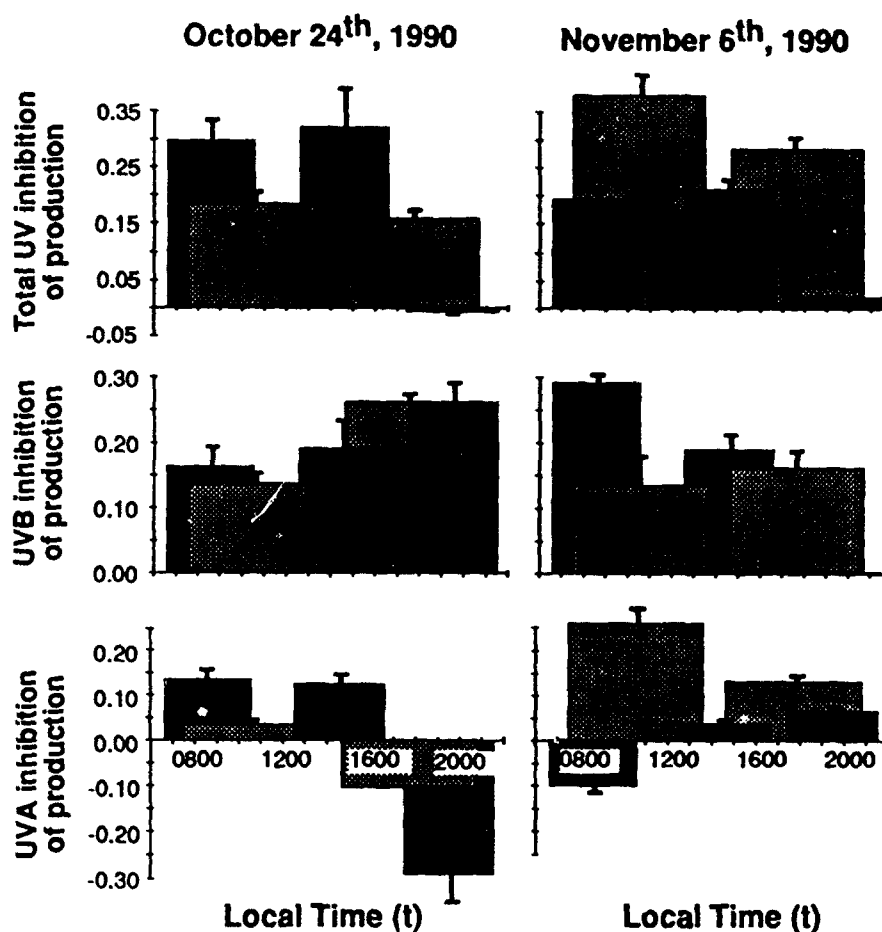
Figure 3. Fractional inhibition and/or enhancement of PAR-based volume-specific *in situ* productivitity (P) by natural levels of UVA + UVB radiation (top), UVB radiation alone (middle) and UVA radiatior, alone (bottom).

Differential photobleaching of Chl pigmentation in the different light treatments (not shown) make it unreasonable to calculate percent UV inhibition of P-I parameters from Chl-specific data presented in Figure 2. To better estimate the actual fractional inhibition of UV radiation on primary production, we analyzed the volume-specific differences in bio-optically modeled *in situ* production (Fig. 3) for replicate samples exposed to the 3 light treatments. These short term estimates indicate up to 30% surface primary production can be photoinhibited by UVB radiation under the ozone hole, a value that is comparable to similar short term incubations on *in situ* moorings (data not shown) and at least 3-fold higher than those reported for *in situ* moorings deployed for 9-12 h under similar field conditions (5). The findings support our view that our previous calculations of carbon loss due to enhanced UVB radiation in Antarctica were conservative and consistent with our view (5) and that of Cullen & Lesser (1990) that apparent UVB inhibition of primary production for any given time period is a reflection of the combined kinetics of UVB photodamage and UVB repair occurring during the same time period.

Unlike UVB, UVA radiation often appeared to have both an inhibitory and an enhancement effect on *in situ* productivity (Fig. 3). It is known (see other articles in this symposium issue) that UVA radiation has multiple effects on plant biology, including i] supplementing PAR radiation in support of photosynthesis, ii] direct photodamage, and iii] induction of UV and PAR photoprotective mechanisms. It is possible that differences in the kinetic balance between these different rate processes will determine the apparent whole cell effect of UVA radiation on rates of production for different time intervals.
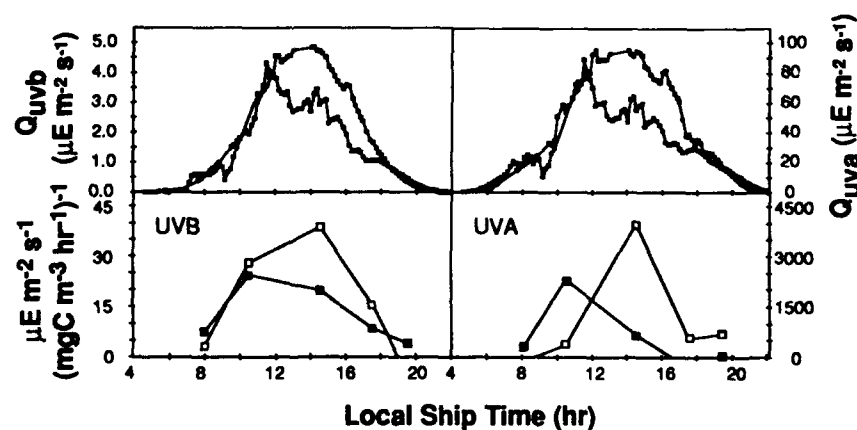
Figure 4. Diurnal variation in the flux of UVA and UVB radiation (top) and the quantum requirement for *in situ* carbon lost due to UVB and UVA radiation. Estimates are based on a ratio of the mean flux of UVB and UVA radiation within the simulated *in situ* incubator for the duration of the incubation to the estimated loss of carbon fixation

154

Figure 4 shows that the UVA and UVB quantum requirement for photosynthetic carbon loss was not constant over the day but rather displayed a pattern of diurnal variability that was similar between replicate experiments and peaked at the time when *in situ* productivity was highest. It is possible that the lower sensitivity to UV inhibition during parts of the day is related to a diurnal increase in photoprotective screening, potential for nonphotochemical energy dissipation or increased synthetic abilities to counteract UV damage to cell constituents. This diurnally varying sensitivity to UVA and UVB inhibition may be an inherent part of the cell cycle biology of these phytoplankton and/or coupled to any number of UV induced photoprotective mechanisms known to occur in terrestrial and aquatic plants.

LITERATURE CITED

1. **Cullen JJ, Lesser MP** (1990) Inhibition of photosynthesis by ultraviolet radiation as a function of dose and dosage rate: Results for a marine diatom. Mar Biol 111: 183-194

2. **Prézelin BB, Boucher NP, Smith RC** (1993) Marine primary production under the Antarctic ozone hole: Icecolors '90. *In* Ultraviolet Radiation and Biological Research in Antarctica, Weiler S, Penhale P, Eds Antarctic Res Series (in press)

3. **Prézelin BB, Glover HE** (1991) Variability in time/space estimates of phytoplankton, biomass and productivity in the Sargasso Sea. J Plankt Res 13S: 45-67

4. **Prézelin BB, Smith, RC** (1992) Reply: UVA and/or UVB treatment of Whirlpak polyethylene bags is not toxic to phytoplankton productivity or growth rate measurements. Science, in press.

5. **Smith RC, Prézelin BB, Baker KS, Bidigare RR, Boucher NP, Coley T, Karentz D, MacIntyre S, Matlick HA, Menzies D, Ondrusek M, Wan Z, Waters KJ** (1992) Ozone depletion: ultraviolet radiation and phytoplankton biology in Antarctic waters. Science 255: 952-959

How Plants Limit the Photodestructive Potential of Chlorophyll[1]

Victor I. Raskin and Jonathan B. Marder

Department of Agricultural Botany, The Hebrew University of Jerusalem, Faculty of Agriculture, P.O. Box 12, Rehovot, 76100, Israel

INTRODUCTION

Chlorophyll is easily the most prevalent pigment in the biosphere owing to its selection as the primary chromophore in many photosynthetic systems. The selection of chlorophyll probably occurred for a number of reasons:

1. Chlorophyll has a high extinction coefficient in the solar spectrum which impinges on the earth's surface.
2. Chlorophyll is biochemically related to numerous other pigments such as haems and bilins, so its synthesis requires only a few special enzymes (1).
3. Chlorophyll has a relatively long-lived excited state allowing the energy to be efficiently "grabbed" by a photochemical process.

Of these reasons, the third requires some explanation which is aided by the diagram in Fig. 1. The reason that the chlorophyll excited state is relatively long-lived is the paucity of *intrinsic* relaxation pathways. In fact, the only significant reactions are fluorescence, or thermal decay *via* the triplet state. Neither does chlorophyll show any great tendency to interact randomly with its surroundings i.e. the "excitation lifetime" (which is the same as the fluorescence lifetime) is similar in a wide range of solvents. However, when chlorophyll is properly packaged, as in photosynthesis, other *extrinsic* processes (marked in Fig. 1 with asterisks) are now possible. Of the three *extrinsic* processes in the figure, exciton transfer and photochemistry are central to photosynthesis, while thermal quenching (non-photochemical quenching) makes no positive contribution to photosynthesis. However, all three *extrinsic* proc_sses compete with the
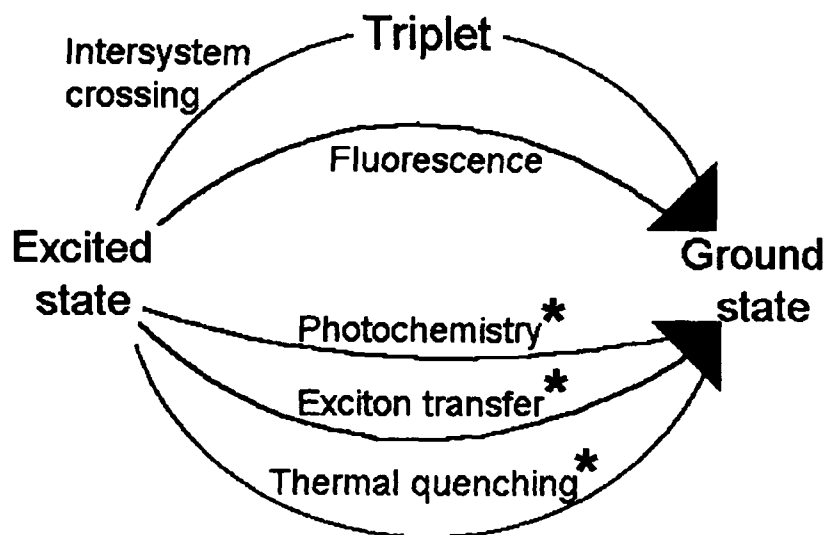
Figure 1. The photodynamics of chlorophyll. When it absorbs a photon, chlorophyll is activated to an "excited state" which can then decay by intrinsic processes, which are available to even a single isolated chlorophyll molecule, or extrinsic processes (marked with asterisks), which require interaction with other molecules. All the processes are in competition and hasten the overall rate of de-excitation.

intrinsic processes which has the effect of shortening the lifetime of the excited state and results in lower yields of fluorescence and triplet formation. In an ideal photosynthetic system, exciton transfer and photochemistry would totally dominate the de-excitation process.

Just as the lack of *intrinsic* relaxation pathways for excited chlorophyll is what makes photosynthesis possible, it also means that when chlorophyll is free, triplet formation inevitably occurs. The mechanism of triplet formation has been described in detail by Clayton (2). For free chlorophyll, the yield of triplet formation is probably close to 70 percent (the remaining 30 percent goes to fluorescence). The problem with this (at least in an aerobic environment) is that *the predominant pathway from triplet to ground state is by interaction with molecular oxygen*. This results in the generation of activated or "singlet" oxygen which is highly destructive to biological molecules (3). Although triplets can also occur (with lower yield) within chlorophyll complexes, an alternative "protective" triplet relaxation pathway exists. This involves interaction with carotenoids which are universally present in chlorophyll-protein complexes. Thus the *free* chlorophyll should be the prime suspect in photosensitizing singlet oxygen. In Fig. 2 we show once chlorophyll becomes free, there could be an amplification effect whereby the initial release of free chlorophyll causes singlet

157
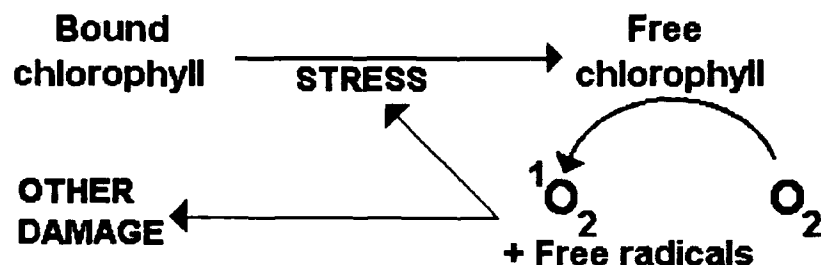
Figure 2. The role of free chlorophyll in causing and amplifying damage. As discussed in the text, free chlorophyll is likely to photosensitize generation of singlet oxygen which then attacks surrounding biomolecules. The result of this could be the release of more free chlorophyll from existing complexes.

Time of illumination (minutes)
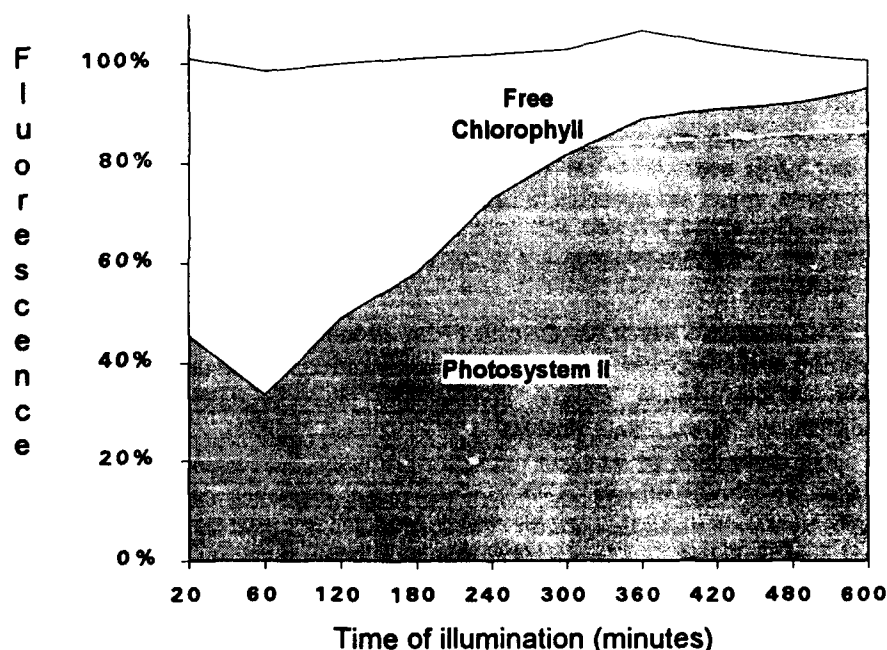
Figure 3. Distribution of fluorescence between components during de-etiolation of barley leaves. Barley seedlings were grown in vermiculite for 5 days in complete darkness and then placed in the light (25 μmol $m^{-2} s^{-1}$) to cause greening. The fluorescence lifetimes were resolved as described elsewhere (4). We have used a "best two component" fit and assumed that the derived 0-0.5 ns component is from PSII and the 4-10 ns component is from free chlorophyll. The "goodness of fit" is indicated by the sum of the two components which in all cases is close to 100 percent.

158

oxygen generation and more free chlorophyll release as well as other damage. It thus seems likely that free chlorophyll plays a role in many forms of plant stress.

THE DETECTION OF FREE CHLOROPHYLL IN LEAVES

For the reasons explained above, free chlorophyll can be distinguished from chlorophyll in complexes by its fluorescence lifetime. We have found that fluorescence lifetimes can be conveniently measured directly in leaves using a phase-modulated fluorometer (4). The fluorescence lifetime is calculated from measurements of the phase displacement and relative modulation of the fluorescence versus the excitation light. We used this system to look at greening barley leaves and found that the fluorescence could generally be fitted to two components of ~6 ns, representing free chlorophyll, and ~0.2 ns from photosystem II (4). This data is summarized in Fig. 3 and shows that the incorporation of chlorophyll into complexes is extemely rapid. By the end of ten hours, fluorescence from free chlorophyll is down to around 6 percent of the total fluorescence. From the difference in lifetime, it can be calculated that the fluorescence yield from free chlorophyll is some 30 times greater than the PSII fluorescence. When taking into account that much chlorop... may have entered totally quenched (i.e. non-fluorescent) complexes such as photosystem I, the conclusion is that the free chlorophyll is no more than a fraction of a percent of the assimilated chlorophyll. We therefore conclude that there is a powerful mechanism to prevent the accumulation of free chlorophyll.

ACKNOWLEDGEMENT

LITERATURE CITED

1. **Castelfranco PA, Beale SI** (1983) Chlorophyll Biosynthesis: Recent Advances and Areas of Current Interest. Annu Rev Plant Physiol **34**, 241-278.
2. **Clayton RK** (1980) Photosynthesis: physical mechanisms and chemical patterns, Cambridge University Press
3. **Halliwell B, Gutteridge JMC** (1985) Free Radicals in Biology and Medicine. Clarendon Press, Oxford
4. **Marder JB, Raskin VI** (1993) The assembly of chlorophyll into pigment-protein complexes. Photosynthetica (in press)

159

Biochemistry of Xanthophyll-Dependent Nonradiative Energy Dissipation[1]

Adam M. Gilmore and Harry Y. Yamamoto

Department of Plant Molecular Physiology, University of Hawaii at Manoa, Honolulu, HI U.S.A. 96822

INTRODUCTION

In the natural environment, light energy available for photosynthesis often exceeds the amount that can be used for carbon fixation. A protective mechanism to avoid the potentially damaging effects from this excess light, ideally, should be able to modulate in response to varying light and sink conditions. Xanthophyll-dependent non-radiative energy dissipation (NRD[2]) from PSII antennae appears be such a mechanism. Xanthophyll-dependent NRD has been related to violaxanthin de-epoxidase (VDE) activity and low lumen pH. In the dark, NRD reverses rapidly with the collapse of the proton gradient while de-epoxidized pigments remain. NRD that appears to be identical to xanthophyll-dependent NRD but independent of xanthophylls has also been reported (4, 7, 9). Both types of NRD presumably 'down- regulate' or reduce the quantum yield of photosystem II (PSII) photochemistry.

Xanthophyll-dependent NRD, measured as non-photochemical fluorescence quenching (NPQ) has been observed in intact leaves (1, 5, 6), chloroplasts (5, 11) and thylakoids (7, 8, 9, 10). Our studies have concentrated on understanding the underlying biochemistry and mechanism using chloroplast and thylakoid systems. Here we summarize our current views on the roles of zeaxanthin, antheraxanthin, and lumen pH on reversible NPQ.

ALL NPQ IS XANTHOPHYLL DEPENDENT AND INCREASES LINEARLY AS THE PRODUCT OF LUMEN ACIDITY AND ZEAXANTHIN *PLUS* ANTHERAXANTHIN

At constant lumen pH, NPQ increases linearly with xanthophyll concentration (9). Conversely, NPQ increases linearly with lumen acidity at any given xanthophyll concentration. These relationships are accurately predicted by the simple multiple linear regression equation,

$$NPQ = X_1(pH)(Zea + Ant) + X_2(pH) + a \quad (1)$$

where NPQ is measured as reversible Stern-Volmer type fluorescence quenching (SV_E) and the major independent variable is the product of xanthophyll and lumen proton concentration (9). pH is relative lumen proton concentration and measured as neutral-red uptake. Zea and Ant are zeaxanthin and antheraxanthin concentrations, respectively. Antheraxanthin is treated as equivalent to zeaxanthin because it contributes significantly to the model. Previously antheraxanthin has been either ignored or assumed to be equivalent to one-half the quenching efficiency of zeaxanthin (4).

Figure 1 shows three-dimensional plots of equation (1) applied to data (n = 25) from peas (*Pisum sativum* L. cv Oregon) and lettuce (*Lactuca sativa* L. cv Romaine). It is evident that NPQ has a pH threshold which decreases with increasing de-epoxidized xanthophyll concentration. In the complete absence of de-epoxidized pigments, little or no quenching develops even at saturating lumen acidity, indicating that all NPQ is xanthophyll-dependent. If the effect of
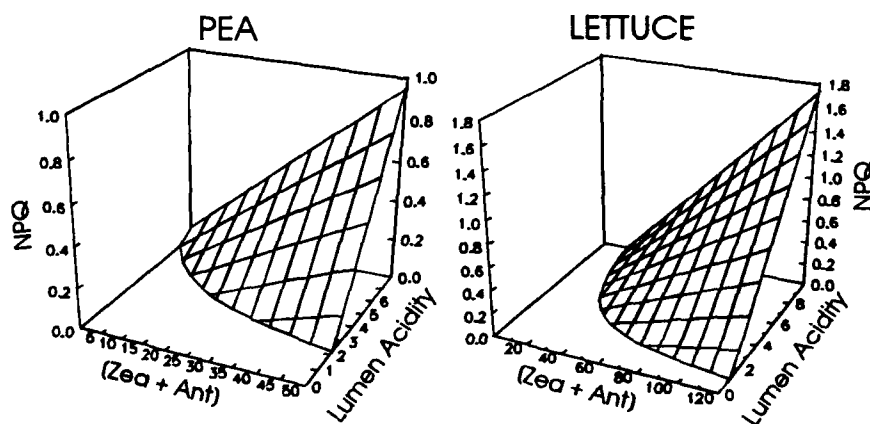
Figure 1. Three dimensional plots of [Zea + Ant], mmol mol^{-1} Chl *a* and lumen acidity, versus predicted NPQ in peas and lettuce. NPQ was measured as SV_N and lumen acidity was measured as neutral-red uptake at A_{520}. The regression coefficients for equation (1) were $r^2 = 0.980$ (n = 25) and 0.982 (n = 25) for peas and lettuce, respectively. Figure adapted from (9).

antheraxanthin is ignored, significant NPQ is present at zero zeaxanthin, giving the impression of the presence of xanthophyll-independent quenching (9). It appears that previously reported zeaxanthin-independent NPQ was due to quenching by antheraxanthin.

The more familiar two-dimensional plot of increasing xanthophyll against NPQ can be visualized as sections in the planes at constant lumen acidity. The effect of increasing lumen acidity can also be visualized in planes at constant [Zea + Ant]. In these views, NPQ increases linearly with either [Zea + Ant] or lumen acidity.

NPQ EFFICIENCY COULD BE FUNDAMENTALLY SIMILAR AMONG SPECIES

Lettuce has up to twice the xanthophyll pool size as peas and so it is interesting that their X_l regression coefficients, which reflect quenching efficiencies, are similar (9). Although coincidence cannot be excluded, this may indicate that quenching efficiency is fundamentally similar among species. According to Thayer and Björkman (12), higher plants adapt to excessive light conditions by increasing the pool size of the xanthophyll-cycle pigments; this increase can be several fold under appropriate conditions. If quenching efficiency is fundamental, it seems reasonable for plants to increase NPQ capacity by increasing the total [Zea + Ant] potential by increasing pool size.

NPQ IS ANTENNAE QUENCHING AND DEPENDENT ON LUMEN ACIDITY, NOT ON ACTINIC LIGHT, REVERSE ELECTRON-FLOW OR REDOX STATE OF ELECTRON TRANSPORT CARRIERS

Xanthophyll-related NPQ can be induced by ATP-hydrolysis driven ΔpH under conditions of little or no reverse electron flow. Thus induced (Fig. 2), the dark energized fluorescence (F_O') can be measured at steady state and related to the energized maximal fluorescence (F_M') by saturating flash in the absence of actinic light. Quenching of F_O' and F_M' was proportional (8) which, according to Butler and Kitajima's (3) bipartite model, is antennae quenching. The presence of MV assured that electron carriers were fully oxidized throughout the course of induction. As for light-induced NPQ, antimycin did not reverse quenching developed by ATP-hydrolysis (8, 10). These results clearly show that the role of light in NPQ is to generate the acidic lumen and not a direct light effect. Also, the redox state of electron-transport carriers is not critical.

While lumen acidity is critical, it is apparent that neither low lumen pH nor de-epoxidized xanthophylls are sufficient for quenching. We propose based on the effects of antimycin A (8, 10) and A23187 (10) that protonation of the NPQ determining site in the inner thylakoid space occurs in proportion to de-epoxidized xanthophyll concentration which then results in static quenching in the pigment bed.

ATP-INDUCED NPQ MAY EXPLAIN FLUORESCENCE QUENCHING
UNDER PHOTOINHIBITORY CONDITIONS

Figure 2 also shows that ATP-induced ΔpH can sustain xanthophyll-dependent quenching of F_M' and F_O' for extended periods of time in the dark. This sustained fluorescence quenching is similar to sustained or slowly reversible fluorescence transients observed after photoinhibitory treatments of leaves (1, 4, 6). The dark-sustained F_M and F_O quenching was thought to be directly related to reversible xanthophyll-dependent quenching but where the quenching conformation was sustained in some unknown way (6). Photoinhibitory treatments of leaves can also increase F_O, which can be interpreted as damage to PSII photochemistry that possibly occurs simultaneously with thermal dissipation (see review by Björkman (2) and Demmig-Adams and Adams (4)). If photoinhibitory treatments lead to accumulation of ATP, the sustained or slowly reversible quenching in leaves could be due to ATP effects similar to those seen *in vitro* (8, 10). If reverse electron flow also occurs, Q_A could become partly reduced giving rise to an increase of fluorescence that would mimic an F_O increase but be unrelated to PSII damage.
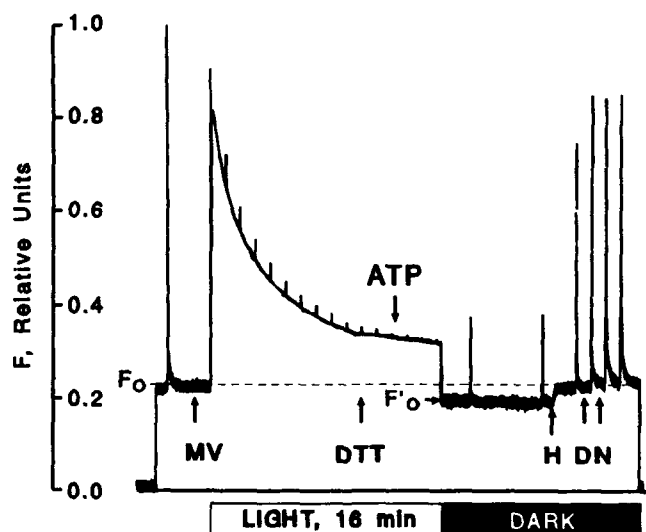
Figure 2. Quenching of F_M' and F_O' in the dark under ATP-hydrolysis driven ΔpH. Methylviologen (MV), dithiothreitol (DTT), hexokinase/glucose (H), dibromothymoquinone (D) and nigericin (N) were added as indicated. Final [Zea + Ant] = 105.4 mmol mol-^{1} Chl a. Figure adapted from (8); see Fig. 1 of this reference for more details.

SUMMARY AND CONCLUSIONS

Figure 3 shows a schematic of the relationships between the xanthophyll-cycle, lumen acidity and NPQ. Coupled light-driven linear, cyclic, or pseudocyclic electron flow can generate the low pH required for NPQ and de-epoxidase activity. Dark ATP-hydrolysis also can generate and sustain the ΔpH needed for these activites. The ability of the Mehler-Peroxidase reaction to support pseudocyclic electron transport that induces VDE activity and NPQ under conditions of reduced CO_2 fixation has been reported (11). Sites of inhibitor actions are also shown. Uncouplers inhibit both de-epoxidation and NPQ. DTT inhibits VDE and thus the level of NPQ but not ΔpH or NPQ directly.
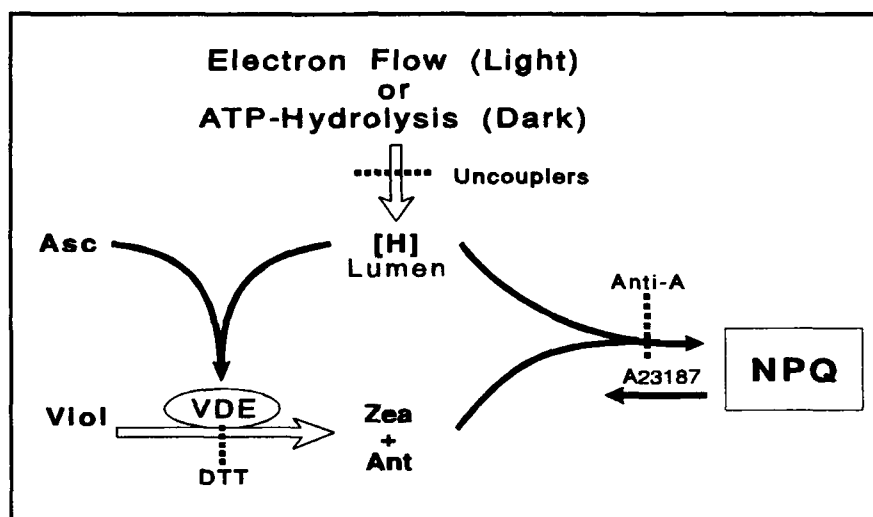
Figure 3. Schematic of the relationships of lumen pH, xanthophyll cycle, NPQ and the sites of inhibitor action.

Antimycin A inhibits NPQ formation but does not reverse it. A23187, in contrast, reverses NPQ and thus also inhibits its development.

The evolutionary significance of the xanthophyll-cycle is implied by its conservation in all higher plants examined so far. According to our view, NPQ represents a complex feedback mechanism where the down regulation of primary PSII photochemistry is dependent minimally on the level of de-epoxidized xanthophylls and lumen acidity. The former is influenced by the level of ascorbate and xanthophyll pool size and the latter by excess ATP and Mehler-ascorbate peroxidase activity. Quenching in the pigment bed requires further changes, possibly conformational, that are directly related to lumen pH and de-epoxidized xanthophyll levels.

164

LITERATURE CITED

1. **Bilger W and Björkman O** (1990) Role of the xanthophyll cycle in photoprotection elucidated by measurements of light-induced absorbance changes, fluorescence, and photosynthesis in leaves of *Hedera canariensis* Willd.. Photosynth Res **25**: 173-185

2. **Björkman O** (1987) Low-temperature chlorophyll fluorescence in leaves and its relationship to photon yield of photosynthesis in photoinhibition. *In:* DJ Kyle, CB Osmond, Arntzen CJ, eds, Photoinhibition, pp 123-144, Dordrecht: Elsevier Science Publishers

3. **Butler WL and Kitajima M** (1975) Fluorescence quenching in photosystem II of chloroplasts. Biochim Biophys Acta **376**: 116-125

4. **Demmig-Adams B and Adams WW III** (1992) Photoprotection and other responses of plants to high light stress. Ann Rev Plant Physiol Plant Mol Biol **43**: 599-626

5. **Demmig-Adams B, Adams WW III, Heber U, Neimanis S, Winter K, Krüger A, Czygan F-C, Bilger W, and Björkman O** (1990) Inhibition of zeaxanthin formation and of rapid changes in radiationless energy dissipation by dithiothreitol in spinach leaves and chloroplasts. Plant Physiol **92**: 293-301

6. **Demmig B, Winter K, Krüger A, and Czygan F-C** (1988) Zeaxanthin and the heat dissipation of excess light energy in *Nerium oleander* exposed to a combination of high light and water stress. Plant Physiol **87**: 17-24

7. **Gilmore AM and Yamamoto HY** (1991) Zeaxanthin formation and energy-dependent fluorescence quenching in pea chloroplasts under artificially mediated linear and cyclic electron transport. Plant Physiol **96**: 635-643

8. **Gilmore AM and Yamamoto HY** (1992) Dark induction of zeaxanthin-dependent non-photochemical fluorescence quenching mediated by ATP. Proc Nat Acad Sci USA **89**: 1899-1903

9. **Gilmore AM and Yamamoto HY** (1993a) Linear models relating xanthophylls and lumen acidity to nonphotochemical fluorescence quenching. Evidence that antheraxanthin explains zeaxanthin- independent quenching. Photosynth Res (in press)

10. **Gilmore AM and Yamamoto HY** (1993b) Zeaxanthin-dependent nonphotochemical quenching of the variable fluorescence arising from ATP-induced reverse electron flow. *In:* N Murata ed, Proceedings of the 9th International Congress of Photosynthesis, Dordrecht: Kluwer Academic Publishers (in press)

11. **Neubauer C and Yamamoto HY** (1992) Mehler-peroxidase reaction mediates zeaxanthin formation and zeaxanthin-related fluorescence quenching in intact chloroplasts. Plant Physiol **99**: 1354-1361

12. **Thayer SS and Björkman O** (1990) Leaf xanthophyll content and composition in sun and shade determined by HPLC. Photosynth Res **23**: 331-343

The Role of Ascorbate in the Related Ascorbate Peroxidase, Violaxanthin De-epoxidase and Non-Photochemical Fluorescence-Quenching Activities[1]

Christian Neubauer and Harry Y. Yamamoto

Julius von Sachs Institut für Biowissenschaften, Universität Würzburg, FRG; and Department of Plant Molecular Physiology, University of Hawaii, U.S.A.

INTRODUCTION

Reversible non-photochemical fluorescence quenching (NPQ[2]), which reflects the protective dissipation of excess energy (7), is highly correlated with the presence of zeaxanthin in leaves (2) and isolated chloroplasts (5). Zeaxanthin is derived from de-epoxidation of violaxanthin by the action of violaxanthin de-epoxidase (VDE) when the lumen is acidic and ascorbate is present (13).

Non-assimilatory iinear electron flow mediated by the Mehler ascorbate-peroxidase (MP) reaction has been shown to induce membrane energization and associated NPQ under limited CO_2-fixation conditions (9). In addition, the MP-reaction generates the ΔpH for de-epoxidation and its associated NPQ (8). In the MP-reaction H_2O_2 formed by the Mehler reaction is reduced to water by ascorbate peroxidase (APO) activity using ascorbate as the electron donor. Ascorbate which is oxidized to monodehydroascorbate is regenerated by reductive photosynthetic electron transport (1). The net result is pseudocyclic photosynthetic electron flow.

We have proposed that the zeaxanthin formation along with the MP-reaction is an *in vivo* system for light protection under conditions of limited electron flow to CO_2 (8). If so, ascorbate plays a pivotal role because it is required for both APO and VDE activities. Here, we report further studies on the possible regulatory role of ascorbate.

MATERIALS AND METHODS

Chloroplasts (intactness: 75-85 %) were isolated from dark-adapted market *Lactuca sativa* L. cv. Romaine (8) and stored on ice until used. Reactions were at 25 ^0C and 30 mg/ml chlorophyll. Iodoacetamide (3 mM) was used to inhibit ribulosebisphosphate carboxylase/oxygenase activity without inhibiting violaxanthin de-epoxidase and ascorbate peroxidase activities. Actinic light was filtered through Corning CS2-38 (red) and CS1-75 (infrared) filter. Fluorescence kinetics were measured with a PAM chlorophyll fluorometer (Walz, Effeltrich, Germany). Non-photochemical and photochemical fluorescence quenching (q_P) were measured by the saturation pulse method. NPQ was calculated as Stern-Volmer type (SV_N). Zeaxanthin formation was recorded at 505-540 nm. For more details on methods, see (8).

RESULTS

Figure 1 shows the effects of ascorbate on fluorescence quenching in intact chloroplasts. In the presence of ascorbate actinic illumination induced substantial NPQ and q_P. Most of the light-induced NPQ (SV_N=0.174) was reversed by the ionophore nigericin (NIG) indicating that it was ΔpH dependent. No significant ΔpH-dependent NPQ (0.07) was observed in the absence of ascorbate. Quantum yield of linear electron flow, $\Delta F/F_M$ (4), decreased from 0.135 to 0.019 (85%) with decreasing ascorbate concentration.
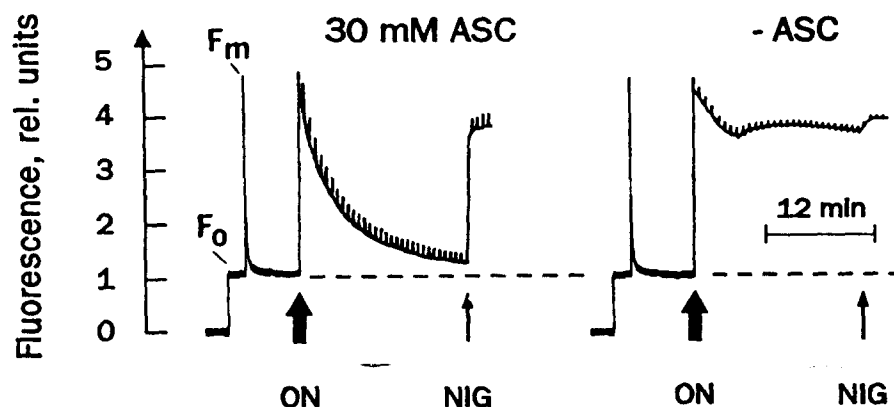
Figure 1. Influence of ascorbate on light-induced fluorescence kinetics. Intact lettuce chloroplasts were illuminated (630 nm; 300 $\mu E\ m^{-2}\ s^{-1}$) in the presence and absence of 30 mM ascorbate. Nigericin (0.3 mM NIG) was added 16 min after onset of light. Saturation pulses (630 nm, 2500 $\mu E\ m^{-2}\ s^{-1}$) were applied every 30 sec to distinguish between q_P and NPQ. Minimal (F_O) and maximal (F_M) fluorescence levels are labelled. For further conditions see materials and methods.

The effect of ascorbate on linear electron flow and NPQ implies involvement of APO and VDE activities. To study the influence of these enzymes on NPQ, chloroplasts were illuminated in the presence of ascorbate (30 mM) and increasing DTT concentrations (Fig. 2). DTT suppressed NPQ formation with an I_{50} of 0.25 mM (Fig. 2A). This inhibition was due to inhibition of zeaxanthin formation as indicated by 505 nm absorbance change and confirmed by HPLC pigment analysis (data not shown). Under low DTT conditions, APO activity and coupled lumen acidification are not inhibited (Neubauer, unpublished). High DTT concentrations inhibit APO and coupled ΔpH formation and thus NPQ (Fig. 2B; I_{50}=3.5 mM), even with zeaxanthin present. Obviously, neither VDE nor APO activity alone is sufficient for NPQ formation.
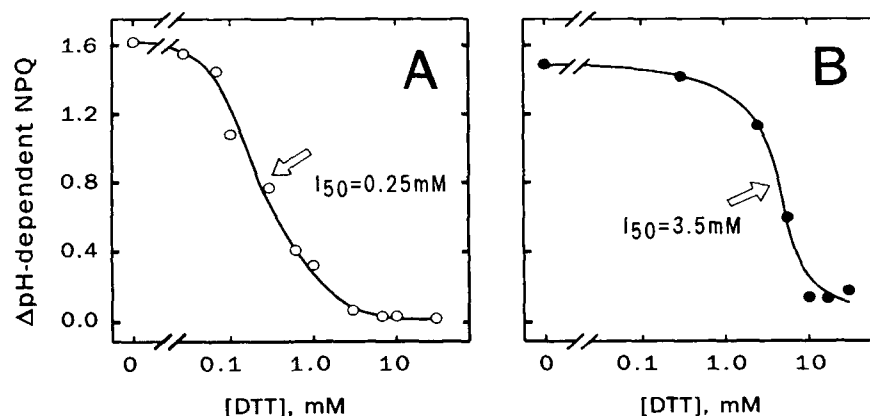
Figure 2. DTT-dependency of NPQ formation. **A.** Intact chloroplasts were illuminated in the presence of ascorbate (30 mM) and increasing concentrations of DTT. **B.** Zeaxanthin (120 mmol/mol Chl a) was preformed in a preceding light period (630 nm; 100 μE m^{-2} s^{-1}). DTT treatment was after 10 min of dark relaxation. For further conditions see Fig. 1.

As is well known, zeaxanthin formation requires ascorbate (Fig. 3). Stimulating APO activity with H_2O_2 totally inhibited zeaxanthin formation (Fig. 3b-d). The effect was transient and zeaxanthin formation recovered during further illumination. The inhibitory effect of H_2O_2 is less at higher (120 mM) ascorbate concentration (data not shown). Siefermann and Yamamoto (11) suggested that the thylakoid membrane forms a diffusion barrier that limits ascorbate availability for VDE activity. The inhibitory effect of H_2O_2 on zeaxanthin formation appears to be a further effect that limits de-epoxidase activity by inducing competitive use of ascorbate by APO. To study this possibility, APO and VDE activities were gradually and selectively inhibited by increasing either KCN or DTT concentrations (Fig. 4A/B). Inhibiting APO with
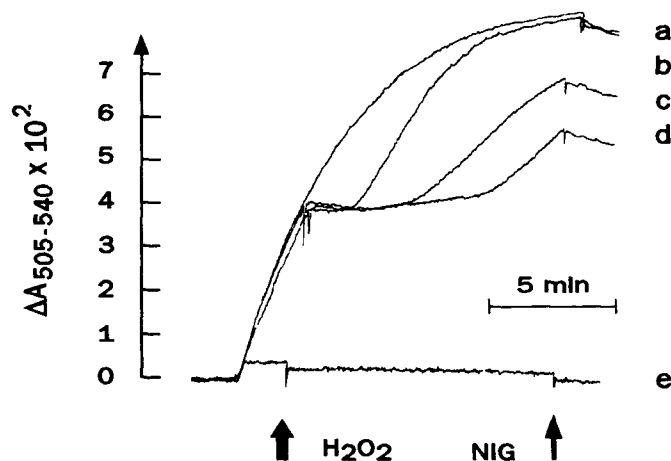
Figure 3. Effect of ascorbate and hydrogen peroxide (H_2O_2) on light-induced 505-540 nm absorbance change. Ascorbate was present (30 mM; a-d) or absent (e) during actinic illumination; b, c, and d, addition of 0.1, 0.5 and 1.0 mM H_2O_2, respectively. For further conditions see Fig. 1 and materials and methods.
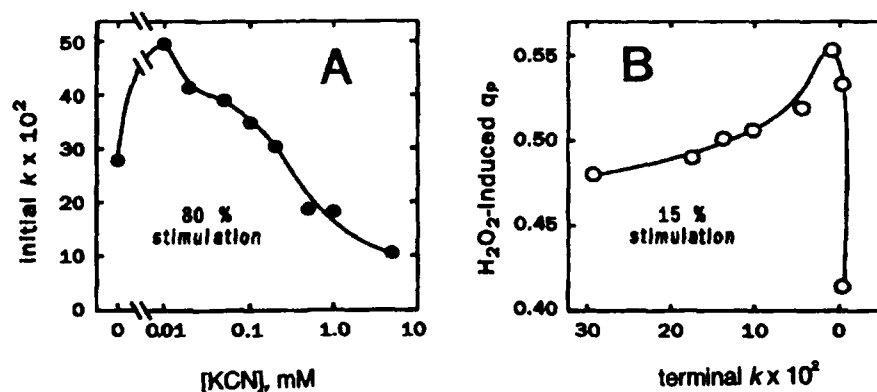
Figure 4. Interaction of violaxanthin de-epoxidase and ascorbate peroxidase activity. Chloroplasts were illuminated in the presence of **A**. increasing KCN and **B**. increasing DTT concentrations to inhibit APO and VDE activity, respectively. VDE activity was calculated as first order rate constant (k, min⁻¹). Initial and terminal rates were determined for the first and the last 4 minutes of illumination, respectively. APO activity was measured as H_2O_2-induced q_p. For further conditions see Fig. 1.

169

KCN increased initial VDE activity 80% (Fig. 4A). This effect was transient due to temporal and KCN-concentration dependent suppression of APO and coupled ΔpH (8). Inhibiting VDE with DTT resulted in 15 % stimulation of APO activity (Fig. 4B). High DTT concentrations suppressed APO activity (compare Fig. 4B and 2).

DISCUSSION

Formation of ΔpH-dependent NPQ in non-CO_2 fixing chloroplasts requires both APO and VDE activities. As previously noted, both activities require ascorbate. The special role of ascorbate is highlighted by the fact that neither of these enzymes operated optimally at 30 mM ascorbate (Fig. 4), which is near the physiological concentration of ascorbate (3). Zeaxanthin formation appears to be more sensitive to ascorbate limitation than APO-mediated ΔpH (Fig. 4A/B). This agrees with the lower affinity of VDE (K_M=3.1 mM) than APO (K_M=0.36 mM) for ascorbate (Neubauer and Yamamoto, unpublished).

When APO activity was inhibited by KCN (10 μM KCN), the transient stimulation of zeaxanthin formation (Fig. 4A) was accompanied by a similar increase of NPQ (not shown). This stimulation was transient because ΔpH is suppressed temporally at this KCN concentration (8). The initial ΔpH is supported by the Mehler-reaction but cannot be maintained without APO activity (8, 10). The stimulation of zeaxanthin formation is attributed to increased ascorbate availability. These findings indicate that zeaxanthin formation is the limiting factor for NPQ formation during induction of photosynthesis and not ΔpH. This conclusion is consistent with Gilmore and Yamamoto (6) that reversible NPQ does not form in the absence of zeaxanthin and antheraxanthin. The variable half times for zeaxanthin formation observed *in vivo* (2) may be due to competition for available ascorbate by APO and VDE which then limits NPQ formation during photosynthesis.

The balance between excitation capture and its use for photochemical reactions by photosystem II requires control by lumen acidification (12). Since APO functions near optimally, the maintenance of ΔpH formation must be important for optimal regulation of photosynthesis. The molecular mechanism of regulation of photosystem-II quantum yield is unknown so far. But it seems reasonable to assume that changes in ascorbate availability are of functional importance for MP-reaction and xanthophyll-dependent NPQ formation and therefore light protection. We suggest that the ascorbate-dependent regulation observed in isolated chloroplasts also operates *in vivo*.

LITERATURE CITED

1. **Asada K and Takahashi M** (1987) Production and scavanging of active oxygen in photosynthesis. *In:* Kyle DJ, Osmond CB and Arntzen CJ ,eds, Photoinhibition, pp 227-287. Elsevier, Amsterdam

2. **Demmig-Adams B** (1990) Carotenoids and photoprotection in plants: A possible role for the xanthophyll zeaxanthin. Biochim Biophys Acta **1020**: 1-24

3. **Foyer C, Rowell J and Walker D** (1983) Measurements of the ascorbate content of spinach leaf protoplasts and chloroplasts during illumination. Planta **157**: 239-244

4. **Genty BG, Briantals JM and Baker NR** (1989) The relationship between the quantum yield of photosynthetic electron transport and quenching of chlorophyll fluorescence. Biochim Biophys Acta **990**: 87-92

5. **Gilmore AM and Yamamoto HY** (1990) Zeaxanthin formation and energy-dependent fluorescence quenching in pea chloroplasts under artificially mediated linear and cyclic electron transport. Plant Physiol **96**: 635-643

6. **Gilmore AM and Yamamoto HY** (1993) Linear models relating xanthophylls and lumen acidity to non-photochemical fluorescence quenching. Evidence that antheraxanthin explains zeaxanthin-independent quenching. Photosynth Res **35**: 67-78

7. **Krause GH and Behrend U** (1986) pH-dependent chlorophyll fluorescence quenching indicating a mechanism of protection against photoinhibition of chloroplasts. FEBS Lett **220**: 298-302

8. **Neubauer C and Yamamoto HY** (1992) Mehler-peroxidase reaction mediates zeaxanthin formation and zeaxanthin-related fluorescence quenching in intact chloroplasts. Plant Physiol **99**: 1354-1361

9. **Schreiber U and Neubauer C** (1990) O_2-dependent electron flow, membrane energization and the mechanism of non-photochemical fluorescence quenching of chlorophyll fluorescence. Photosynth Res **25**: 279-293

10. **Schreiber U, Reising H and Neubauer C** (1991) Contrasting pH-optima of light-driven O_2- and H_2O_2-reduction in spinach chloroplasts as measured via chlorophyll fluorescence. Z Naturforsch **46c**: 635-643

11. **Siefermann D and Yamamoto HY** (1974) Light-induced de-epoxidation of violaxanthin in lettuce chloroplasts. III Reaction kinetics and effect of light intensity on de-epoxidase activity. Biochim Biophys Acta **357**: 144-150

12. **Weis E and Berry J** (1987) Quantum efficiency of photosystem II in relation to energy-dependent quenching of chlorophyll fluorescence. Biochim Biophys Acta **894**: 198-2083

13. **Yamamoto HY** (1979) Biochemistry of the violaxanthin cycle in higher plants. Pure Appl. Chem **51**: 639-648

The Dynamic 531-Nanometer Δ Reflectance Signal: A Survey of Twenty Angiosperm Species[1]

John A. Gamon, Iolanda Filella, and Josep Peñuelas

Department of Biology, California State University, 5151 State University Drive, Los Angeles, CA 90032-8201; and Institut de Recerca i, Tecnologia Agroalimentaries, 08348 Cabrils (Barcelona), Spain

INTRODUCTION

Recent work at the leaf and canopy levels in *Helianthus annuus* L. (sunflower) has shown that indices derived from a dynamic 531 nm reflectance feature correlate both with photosynthetic efficiency and with the epoxidation state of the xanthophyll cycle pigments (1,2). These discoveries present the possibility that reflectance at this wavelength may provide a widely applicable optical index of current photosynthetic function. As a test of the universality of this signal, we examined the spectral dependence of this dynamic reflectance feature in twenty species of widely varying habit, phenology and photosynthetic pathway. If this signal is spectrally consistent across all species, then it might be the basis for a widely applicable optical index of photosynthetic function.

MATERIALS AND METHODS

Because the 531 nm Δ reflectance signal can be readily studied at the leaf level, where complicating effects of canopy structure, sun angle and atmospheric conditions are avoided, we constructed a leaf-level "reflectometer" capable of rapid, non-destructive leaf-level reflectance measurements. This instrument consisted of a 6V, 2900 K halogen lamp, a bifurcated fiber optic bundle, a leaf clamp and a detector. In this case, the detector was a visible-near-IR spectroradiometer (model SE590 with detector CE390 WB-R, Spectron Engineering, Denver, Colorado). The entire instrument was powered by a 12-V

---

[2]Abbreviations: PP, photosynthetic pathway; PPFD, photosynthetic photon flux density; CAM, Crassulacean acid metabolism

battery, allowing either laboratory or field measurements. Leaf radiance was measured after clamping the common end of the fiber optic bundle against the adaxial leaf surface. White light (2000 µmol m^{-2} s^{-1}), delivered by one branch of the fiber optic, served as both the measuring and actinic light.

Leaves had been dark-adapted since the previous evening either by a black paper cover or by storage in a darkened laboratory (0-5 µmol m^{-2} s^{-1}). Within 5 seconds of attaching the reflectometer to a leaf, an initial, "time-zero" spectral scan was taken, followed by periodic scans for 10 minutes. Reflectance was calculated from radiance by normalizing leaf radiance by the radiance of a 99% reflective standard (Spectralon, Labsphere, North Sutton, NH).

Species were chosen to represent a wide range of cultural conditions, phenologies, habits and photosynthetic types (Table I). Container plants, with the exception of *Phaseolus vulgaris* L., were grown in a mix of 2/3 potting soil and 1/3 perlite supplemented with slow-release fertilizer (Osmocote 17-6-10 plus minor nutrients, Sierra Chemical Co., Milpitas, CA) and given regular irrigation. These plants were grown under shadecloth in Los Angeles, CA, with midday PPFD^2 averaging 280 µmol m^{-2} s^{-1}. *Phaseolus vulgaris* was cultivated in full sun in deep flats of a local clay soil. Additional measurements were made on wild and cultivated plants growing in full sun in the ground at Los Angeles and Stanford, CA.

RESULTS AND DISCUSSION

In all species examined, sudden high-light exposure of individual leaves induced a Δ reflectance signal near 531 nm (Table I and Fig 1.). This signal was, on average, 9.4 % of total leaf reflectance in this waveband. The wavelength of this minimum ranged from a low of 517 nm (*Crassula argentea*) to a maximum of 539 nm (*Rhus ovata*), with an average value (± SEM) for all species of 531 (± 0.95) nm. A similar spectral feature has been previously reported for sunflower at both the leaf and canopy levels (1,2). In sunflower, this Δ reflectance signal had two components, one at approximately 525 nm (presumably due to the interconversion of the xanthophyll cycle pigments) and one at approximately 539 nm (presumably due to chloroplast conformational changes associated with the trans-thylakoid pH gradient) (1,3). Thus, the exact spectral position of this signal may vary depending upon the relative contributions of these two components. Spectral shifts of this signal may also be due to varying leaf anatomy, optical errors during measurement or instrument noise. For example, the unusually low waveband of the Δ reflectance signal in *C. argentea* may be partly due to optical effects associated with its succulent leaf anatomy.

The spectral consistency of this Δ reflectance signal suggests that a simple index based on reflectance at two wavebands (531 nm and a reference wavelength) could be applied to most species. This would minimize the need for a spectroradiometer for many routine measurements. The addition of a reference

Table I. *Survey of the Δ reflectance (Δ refl.) signal upon sudden high-light exposure in 20 angiosperm species.* The Δ reflectance has been normalized to reflectance at 570 nm to minimize effects of shifts in background reflectance (e.g. *Zea mays*, Fig. 1), and is also expressed as a percent (%) of the reflectance at time zero. The number of leaves sampled (n) ranged from one to six leaves per species.

Species	common name	P.P.	growth	condition	λ_{min}	Δrefl.	%	n
Ananas comosus (L.) Merrill	pineapple	CAM	shade	container	531	0.0126	7.2	3
Arbutus menziesii Pursh.	madrone	C3	sun	ground	534	0.0141	16.6	3
Arbutus unedo L.	strawberry tree	C3	shade	container	531	0.0040	11.0	1
Citrus limon (L.) Burm.f.	lemon	C3	sun	ground	525	0.0165	11.5	3
Crassula argentea Thunb.	jade plant	CAM	shade	container	517	0.0088	5.6	3
Feijoa sellowiana O. Berg.	pineapple guava	C3	shade	container	531	0.0075	13.0	1
Hedera canariensis Willd.	Algerian ivy	C3	shade	container	534	0.0069	12.4	1
Hedera helix L.	English ivy	C3	sun	ground	536	0.0060	3.5	3
Heteromeles arbutifolia (Ait.) M.J. Roem.	toyon	C3	sun	ground	531	0.0075	8.0	3
Heteromeles arbutifolia (Ait.) M.J. Roem	toyon	C3	shade	container	531	0.0117	10.7	1
Lithocarpus densiflorus (Hook. & Arn.) Rehd.	tanbark oak	C3	shade	container	534	0.0048	4.0	1
Magnolia grandiflora L.	magnolia	C3	shade	container	534	0.0129	12.1	1

Table I. (Continued)

Phaseolus vulgaris L.	green bean	C3	sun	container	531	0.0112	7.7	6
Pittosporum tobira (Thunb.) Alt.	pittosporum	C3	shade	container	531	0.0072	14.2	1
Quercus agrifolia Nee	Calif. live oak	C3	sun	ground	528	0.0081	10.1	3
Quercus agrifolia Nee	Calif. live oak	C3	shade	container	534	0.0041	6.9	1
Rhus laurina Nutt.	laurel sumac	C3	shade	container	528	0.0041	6.3	1
Rhus ovata S. Wats.	sugar bush	C3	shade	container	539	0.0055	5.4	1
Umbellularia californica (Hook. & Arn.) Nutt.	California bay	C3	shade	container	534	0.0029	6.3	1
Vitis girdiana Munson	wild grape	C3	shade	container	534	0.0085	7.5	1
Vitis vinifera L.	wine grape	C3	sun	ground	531	0.0173	14.4	3
Zea mays L.	maize	C4	sun	ground	534	0.0101	11.3	3
mean					531	0.0087	9.4	
(SEM)					0.095	0.0009	0.79	

175
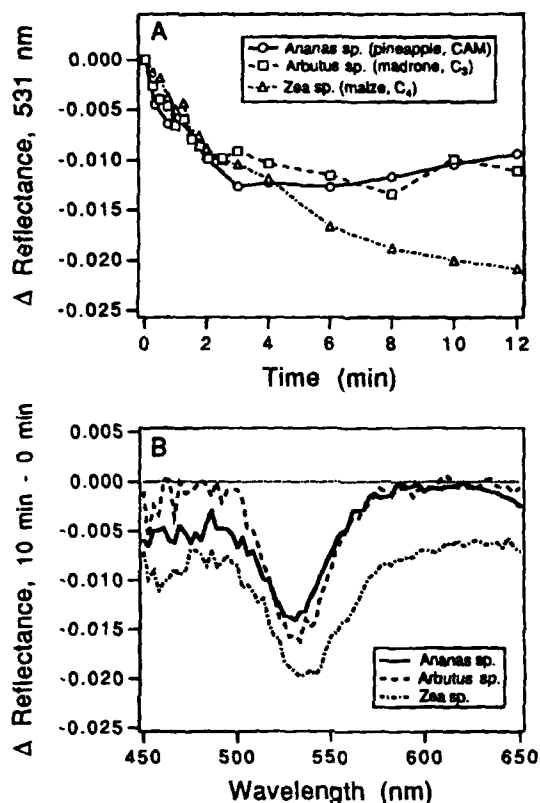
Figure 1. A. Time course of Δ reflectance upon sudden high-light exposure of dark-adapted leaves representing 3 photosynthetic pathways (C₃, C₄ and CAM). Reflectance has been normalized to reflectance at time zero. Each curve represents measurements of a single leaf. **B.** The spectral dependence of the Δ reflectance signal (calculated by subtracting reflectance at time zero from reflectance at 10 minutes). Each spectrum represents the mean of 3 leaves. Note the shift in "background reflectance" in *Zea mays*, possibly due to chloroplast movement.

waveband could help normalize for changes in "background" reflectance (e.g. *Zea mays*, Fig. 1B) caused by a variety of optical effects such as chloroplast movement or sun angle changes). At the leaf-level, 570 nm appears to be a suitable reference wavelength because it is near the right shoulder of the Δ reflectance feature (Fig. 1B).

More work is needed to relate the size and kinetics of the 531 nm Δ reflectance feature to environmental conditions and physiological processes. Simultaneous examination of reflectance, fluorescence, gas exchange and leaf biochemistry, and integration of leaf-level results into canopy radiative transfer models could greatly assist in understanding the physiological significance of this signal at a range of spatial and temporal scales.

CONCLUSION

A 531 nm Δ reflectance signal occurs in a wide range of species representing a wide range of phenologies, habits and photosynthetic pathways. This signal has been correlated with both photosynthetic efficiency and

176

xanthophyll cycle pigment epoxidation state in *H. annuus* (1,2), and may provide a useful optical tool for non-destructive assessments of photosynthetic function. In the near future, applications of this technique may be limited to laboratories and closeup remote sensing from tripods, towers and possibly aircraft. In conjunction with other methods, this reflectance signal may provide a rapid, non-destructive way of assessing photosynthetic function.

ACKNOWLEDGEMENT

LITERATURE CITED

1. **Gamon JA, Field CB, Bilger O, Björkman O, Fredeen A, Peñuelas J** (1990) Remote sensing of the xanthophyll cycle and chlorophyll fluorescence in sunflower leaves and canopies. Oecologia **85**: 1-7
2. **Gamon JA, Peñuelas J, Field CB** (1992) A narrow-waveband spectral index that tracks diurnal changes in photosynthetic efficiency. Remote Sensing of Environment **41**: 35-44
3. **Bilger W, Björkman O, Thayer SS** (1989) Light-induced spectral absorbance changes in relation to photosynthesis and the epoxidation state of xanthophyll cycle components in cotton leaves. Plant Physiology **91**: 542-551

Spectral Regulation of Photosynthetic Quantum Yields in the Marine Dinoflagellate *Heterocapsa pygmaea*.[1]

Bernd Kroon, Barbara B. Prézelin, and Oscar Schofield

Department of Biological Sciences and The Marine Science Institute, University of California, Santa Barbara, CA 93106

INTRODUCTION

Bio-optical models attempting to predict patterns of primary production in the ocean are based upon a mechanistic understanding of photosynthesis and variations in the underwater light field. These carbon-based models all require information on the efficiency with which absorbed light energy is converted into organic carbon (ϕ_C[2], mol C E^{-1}). Sensitivity analyses indicate that the estimate of *in situ* ϕ_C is the most significant source of error present in bio-optical models (1). An alternate approach to estimate rates of primary production is based upon quantifying photosystem II (PSII) activity and to link its activity to rates of carbon fixation (4). Estimates of PSII quantum yield can be derived from measurements of chlorophyll (Chl) fluorescence and oxygen evolution. Recent advances (11) allow simultaneous measurements of the quantum yield of PSII charge separation (ϕ_{IIe}), and oxygen evolution (ϕ_{O2}) to be made for phytoplankton suspensions (7). In this paper we investigate the relationship between ϕ_{IIe}, ϕ_{O2} and ϕ_C for the marine dinoflagellate *Heterocapsa pygmaea*.

---

[2] Abbreviations: ϕ_C, operational quantum yield for carbon fixation; ϕ_{IIe}, operational quantum yield for charge separation at PSII; ϕ_{O2}, operational quantum yield for oxygen evolution; Q_{par}, photosynthetically available radiation; $a_{ph}(\lambda)$, absorption coefficient at λ; $\bar{a}_{ph}$, spectrally-weighted absorption coefficient; AQ_{ph}, rate of absorbed quanta; α, light-limited slope of a photosynthesis-irradiance curve; ϕ_C^*, maximum quantum yield for carbon fixation; ϕ_{O2}^*, maximum quantum yield for oxygen evolution; QR, quantum requirement; P, photosynthetic rate; F_M, maximum fluorescence level; F_O, minimum fluorescence level; F_S, steady state fluorescence; F_M', maximum steady state fluorescence level; F_O', minimum steady state fluorescence level; PCP, peridinin-chlorophyll protein complex; ϕ_{IIe}^*, maximum quantum yield for charge separation at PSII; qNP, nonphotochemical quenching processes; qP photochemical quenching processes; Γ, ratio of O_2 evolved per electrons generated at PSII; f_{II}, fraction of light absorbed by PSII.

[3] The maximum quantum yield is often referred to as ϕ_{max}. Our results showed operational ϕ values, that were higher than the dark-adapted value, which is the so called maximum quantum yield. As this value is determined with the reaction centers in the open state, we denoted the maximum yield by a superscript o.

Based on equations derived by (6), we show what factors lead to a spectral dependency of ϕ_{IIe} with increasing irradiance. The results of our study allow us to assess the linkages between different estimates of photosynthetic quantum yield and to ascertain the nature of chromatic adaptation of PSII activity in a marine dinoflagellate.

MATERIALS AND METHODS

Unialgal batch cultures of *Heterocapsa pygmaea* were grown under constant light, at 18°C in f/2 medium (5). Different light colors were provided by combining Lee photographic filters and/or neutral density filters and the white fluorescent light source (GE F20T12-CW, 20 Watt; 12.8 μE m^{-2} s^{-1} white light, 8.6 μE m^{-2} s^{-1} blue light (Lee 119), 15.3 μE m^{-2} s^{-1} green light (Lee 124), and 19 μE m^{-2} s^{-1} red light (Lee 106)). Methods for quantifying spectral irradiances [Qpar(λ), 400-700 nm] and maintaining log-phase growth have been described elsewhere (9). *In vivo* absorption spectra [$a_{ph}(\lambda)$] were measured using an integrating sphere placed in front of the photomultiplier of an Aminco DW-2 spectrophotometer. To estimate *in situ* quantum yield from photosynthesis-irradiance (P-I) responses, the spectrally-weighted absorption coefficient ($\bar{a}_{ph}$, m^{-1}) was calculated for each culture. The total spectral irradiance absorbed by *H. pygmaea* cells (AQ_{ph}) was calculated as in (10). Methods for measurements of carbon-based P-I relationships and derivation of parameters were as in (10). Oxygen P-I curves were measured polarographically (3) at growth temperature where light intensity was modulated by Wratten neutral density filters. P-I curves were determined for dark adapted replicate samples exposed for 4 min to increasing intensities of white light or the color used for growth. The treatments are coded by first using the first letter of the growth color, then followed by the incubation color. Estimates of the maximum quantum yield for carbon fixation (ϕ_C^*) were calculated by dividing α by $\bar{a}_{ph}$. Estimates of the operational quantum yield (ϕ_{O2} and ϕ_C) and maximum oxygen quantum yields (ϕ_{O2}^*) were calculated by dividing the *in situ* photosynthetic rate by AQ_{ph}. A PAM fluorometer (PAM-101, Heinz Walz, Effeltrich, Germany) was coupled to the oxygen electrode system similar in design to that described by (2) with the exception that a square rather than round temperature-regulated sample chamber was employed. The tungsten light sources within the photosynthetron and the PAM/oxygen electrode system were screened with the same spectral filters used to culture *H. pygmaea* so that spectrally comparable measurements of ϕ_{IIe}, ϕ_{O2} and ϕ_C could be made. The maximum (F_M) and minimum (F_O) fluorescence level in the absence of non-photochemical quenching was measured after 30 min dark adaptation. Maximum fluorescence was induced by a short saturating flash (Schott KL-1200; 900 ms, 2600 μE m^{-2} s^{-1}). Then the sample was exposed to increasing Q_{par}. Steady state fluorescence (F_S) and the maximum fluorescence F_M' were determined at the end of the light incubation. Ten s later the sample

was darkened for 4 s to determine the minimum fluorescence F_O'. Derivation of PSII quantum yields and nomenclature of fluorescence values are as in (7,12).

RESULTS AND DISCUSSION

Maximum Quantum Yields

Figure 1 compares the minimum quantum requirement (QR=$1/\phi^o$) for chromatically adapted cultures of *H. pygmaea* Overall variation in ϕ_{IIe}* was low between the cultures. The blue light cells had the lowest QR for PSII charge separation, with increasing values for the white, green and red adapted cells, respectively (Fig. 1A). As a result of measured values for ϕ_{IIe}*, the QR for oxygen evolution ranged between 14 to 20 (Fig. 1B). When chromatically adapted cultures were studied in a white light field, the QR for O_2 evolution routinely fell by 20-30%. The same was true for $1/\phi_C$*. In general $1/\phi_C$* was
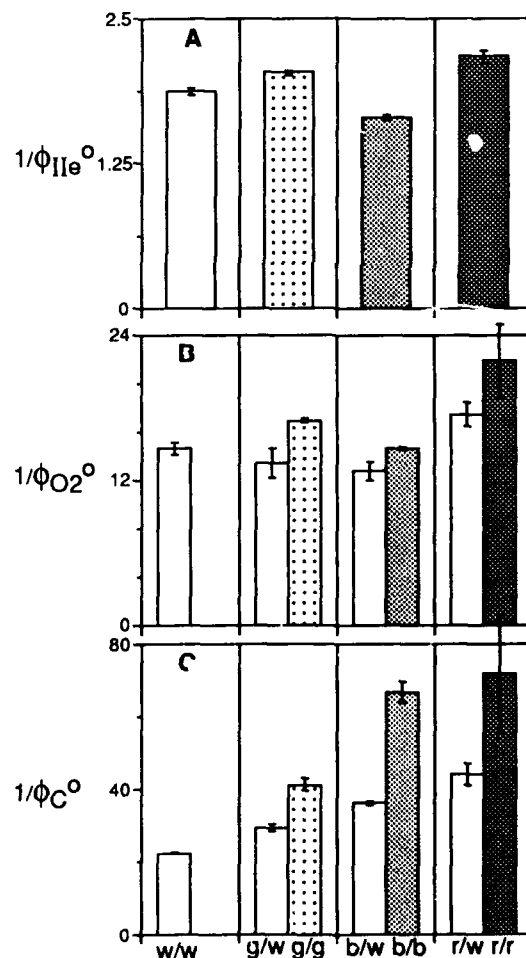
Figure 1. Maximum quantum yield values plotted as quantum requirements (inverse yield, QR) for the four growth conditions. The quantum requirement for charge separation at PSII (A) is given as the average of four measurements plus/minus the standard deviation. The open bars indicate QR for oxygen (B) and carbon dioxide (C) measured under w... t. Shaded bars represent the application of the same color as the growth light. White light measurements were determined in fourfold, growth color measurements in duplicate. Note scale change.

180

5 to 9 fold higher than the theoretical maximum value of 8 (Fig. 1C). The mechanism(s) giving rise to these observations requires that ϕ^{o}_{O2} and $\phi_{C}{}^{\bullet}$ increase under white light, with the relative increase being much greater for $\phi_{C}{}^{\bullet}$ than for $\phi_{O2}{}^{\bullet}$. As shown by (8), the reaction center of PSI in a dinoflagellate lacks its own LHC and, hence, must rely on spillover from PSII to receive excitons. We propose that the rate of cyclic electron transport around PSI is spectrally regulated and is less important to cells exposed to broad-band white light which encompasses all photosynthetically active wavelengths. If true, then under white light more electrons will complete the linear electron transport route, and thus will influence both $\phi_{O2}{}^{\bullet}$ and $\phi_{C}{}^{\bullet}$ equally. The redox poise of ferredoxin is also influenced by cyclic PSI electron transport, and the effect of applying white light to a chromatically adapted culture is greater on $\phi_{C}{}^{\bullet}$ than on $\phi_{O2}{}^{\bullet}$. This hypothesis is in agreement with the relative constancy of $\phi_{IIe}{}^{\bullet}$, which is the result of similar pigment structures under various chromatic adaptations. Chromatic adaptation in *H. pygmaea* is partially based on the optimization of $\phi_{IIe}{}^{\bullet}$, leading to variable cyclic electron transport rates and, hence, to variable ratios of $\phi_{O2}{}^{\bullet}$ and $\phi_{C}{}^{\bullet}$.

Factors Affecting the Operational Quantum Yields

For all conditions measured ϕ_{IIe} decreased with increasing AQ_{ph} (data not shown) In order to evaluate which processes led to the Q_{par}-dependent decrease of ϕ_{IIe}, we applied a theoretical treatment (see (6) for a complete derivation of equations) to assess the relative impact of photochemical (qP) and non-photochemical (qNP) quenching mechanisms on ϕ_{IIe}. A dark normalized measure of $1/F_{M}'$ has been shown to be directly related to qNP quenching which includes spillover from PSII to PSI. Relative changes in the probability for exciton trapping by PSII is directly related to the dark normalized parameter $(1/F_{O}')$-$(1/F_{M}')$. Fig. 2 shows the ratio of $(1/F_{M}'-1)$ and $(1-(1/F_{O}')-(1/F_{M}'))$. A ratio higher than one indicates that qNP processes cause a larger decrease in ϕ_{IIe} than photochemistry, and vice versa. Apparently, qP largely drives ϕ_{IIe} to decrease with increasing Q_{par} for the white and blue light adapted cultures. In contrast, the green and the red light adapted culture, showed that ϕ_{IIe} decreased largely due to qNP processes. Because qP will increase at higher light intensities, any additional increase in qNP will lower the overall efficiency of photochemistry without initiating photochemistry, necessary for carbon assimilation. The data in Fig. 2 also imply, that ϕ_{IIe} must be measured and can not be predicted from $\phi_{IIe}{}^{\bullet}$ and the light field alone.

Oxygen Evolution and Fluorescence

The relationships between ϕ_{O2} and ϕ_{IIe} can be formalized as (7):

$$\phi_{O2} = P_{O2}/AQ_{ph} = \phi_{IIe} \cdot \Gamma \cdot f_{II} \qquad Eq. \ 1$$

181

where Γ is the stoichiometric ratio of oxygen evolved per electron generated at PSII and by definition has a value of 0.25, and f_{II} is the fraction of light directly absorbed by PSII. Eq. 1 indicates that predictions of photosynthetic rates based on ϕ_{IIe} solely will be accurate if f_{II} is relatively constant under various environmental conditions. Table I summarizes the regression results from simultaneously measured ϕ_{O2} and ϕ_{IIe}. While ϕ_{IIe} and ϕ_{O2} correlated for all cultures, there were significant differences for f_{II}. The largest deviations from the mean value of all experimental treatments was found for the red light culture. However, only the W/W, B/B and G/G conditions are relevant to the photoecology of dinoflagellates. For these conditions the average f_{II} was 0.56. If similar f_{II} values are representative of field populations then our results indicate that oxygen production could be predicted within 10% from fluorescence measurements alone.

CONCLUSIONS

Our results indicate that changes in ϕ_{O2} are directly related to changes in ϕ_{IIe} under nutrient replete conditions. Changes we observed in the maximum quantum yield at PSII are consistent with the view that spillover helps maintain balanced electron flow in dinoflagellates where the PCP and Chl a/c complexes appear to donate excitons to PSII exclusively. These changes at PSII did have an upstream effect on processes beyond PSI which appeared to regulate ϕ_C.
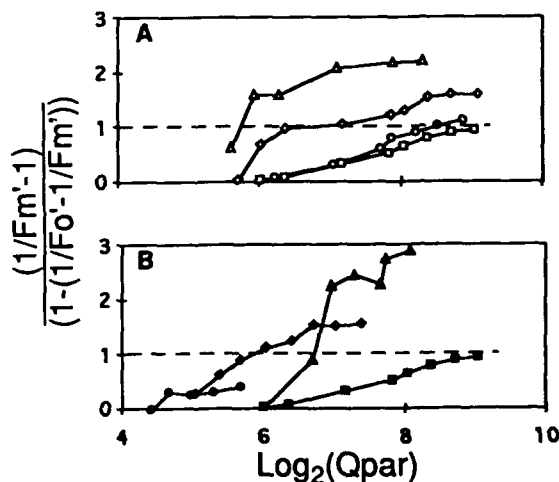
Figure 2. The relative importance of qNP to qP as a function of increasing incident light for white (squares), green (diamonds), blue (circles), and red (triangles) light adapted cultures of *H. pygmaea*. Measurements were with (A) white actinic light and (B) light of the same color as the growth light. Dotted line indicates equal impact of qNP and qP.

Table I. *Influence of color adaptation on the linearity between* ϕ_{O_2} *and* ϕ_{IIe}

Linear regression analyses (y = Ax + B) were performed to check Eq. 1, where x equals absorbed quanta, y equals the rate of oxygen production, A represents the product of Γ and f_{II}. The standard error (SE) for each coefficient is given, as well as the correlation coefficient (R^2). The value of f_{II} is derived by multiplying A with 4 (= 1/Γ).

Growth color	Incubation color	A	SE A	B	SE B	R^2	f_{II}
white	white	0.137	0.0028	-0.0005	0.0021	0.979	0.55
green	green	0.147	0.0031	-0.0022	0.0017	0.991	0.59
green	white	0.157	0.0069	0.0037	0.0038	0.959	0.63
blue	blue	0.138	0.0038	0.0280	0.0040	0.982	0.55
blue	white	0.140	0.0037	0.0107	0.0037	0.990	0.56
red	red	0.165	0.0055	0.0040	0.0014	0.978	0.66
red	white	0.121	0.0056	0.0014	0.0014	0.950	0.48

Further work should focus on the linkages between PSII activity and various processes beyond PSI which regulate the magnitude of the quantum yield of carbon fixation.

LITERATURE CITED

1. **Bidigare RR, Prézelin BB, Smith RC** (1992) Bio-optical models and the problems of scaling. *In* PG Falkowski, AD Woodhead, eds, Primary Productivity and Biogeochemical Cycling in the Sea. Plenum Press, New York, pp 175-212.
2. **Delieu T, Walker DA** (1972) An improved cathode for the measurement of photosynthetic oxygen evolution by isolated chloroplasts. New Phytol 71: 201-223.
3. **Dubinsky Z, Falkowski PG, Post AF, van Hes U** (1987) A system for measuring phytoplankton photosynthesis in a defined light field with an oxygen electrode. J Plankton Res 9: 607-612.
4. **Falkowski PG, Ziemann D, Kolber Z, Bienfang PK** (1991) Role of eddy pumping in enhancing primary production in the ocean. Nature 352: 55-58.
5. **Guillard RR, Ryther JH** (1962) Studies of marine planktonic diatoms. I. *Cyclotella nana* Hustedt and *Detonula confervacea* (Cleve). Gran. Can J Microbiol 18: 229-239.

6. **Havaux M, Strasser RJ, Greppin H** (1991) A theoretical and experimental analysis of the qP and qN coefficients of chlorophyll fluorescence quenching and their relation to photochemical and nonphotochemical events. Photosyn Res **27**: 41-55.

7. **Kroon BMA** (1991) Photosynthesis ii   ass cultures. PhD thesis, University of Amsterdam, The Neth:

8. **Mimuro M, Tamai N, Ishimaru T, Yamazaki I** (1990) Characteristic fluorescence components in photosynthetic pigment of a marine dinoflagellate, Protogonyaulax tamarensis, and excitation energy flow among them. Studies by means of steady state and time resolved fluorescence spectroscopy. Biochim Biophys Acta **1016**: 280-287.

9. **Nelson NB, Prézelin BB** (1990) Chromatic light effects and physiological modeling of absorption properties of Heterocapsa pygmaea (= Glenodinium sp.). Mar Ecol Prog Ser **63**: 37-46.

10. **Schofield O, Prézelin BB, Smith RC, Stegman PM, Nelson NB, Lewis MR, Baker KS** (1991) Variability in spectral and nonspectral measurements of photosynthetic light utilization efficiencies. Mar Ecol Prog Ser **78**: 253-271.

11. **Schreiber U, Schliwa U, Bilger B** (1986) Continuous recording of photochemicalandnon-photochemicalchlorophyllfluorescencequenching with a new type of modulation fluorometer. Photosyn Res **10**: 51-62.

12. **van Kooten O, Snel JFH** (1990) The use of chlorophyll fluorescence nomenclature in plant stress physiology. Photosyn Res **25**: 147-150.

Effect of Elevated CO$_2$ on Photosynthesis, Biomass Production and Chloroplast Thylakoid Structure of Crop Plants

A. Pennanen, V. Kemppi, D. Lawlor and E. Pehu

Dept of Plant Biology (AP) and Dept of Plant Production (VK, EP), University of Helsinki, Viikki SF-00710 Helsinki, Finland, AFRC, Rothamsted Exp. Station, Dept of Biochemistry and Physiology, Harpenden UK (DL)

INTRODUCTION

Enhanced CO$_2$ stimulates the carboxylation reactions catalyzed by Rubisco enzyme. Doubling of CO$_2$ concentration from 330 to 650ppm increases productivity of crop plants markedly (7,12). Enhanced CO$_2$ promotes also net photosynthesis in high temperatures (9,16). In concordance with activated carboxylation light reactions in chloroplast thylakoids are likely to be activated by high CO$_2$. Reactions associated with thylakoid membranes are affected by environmental stresses (17). In particular, PSII appears to be sensitive to high and low temperatures stresses (2,4). Photoinhibition may occur even at moderate light levels if plants suffer simultaneously from other environmental strains. Very little is known about the effects of enhanced CO$_2$ on light reactions and thylakoid proteins, especially when coupled with environmental stresses. The aim of the present study was to monitor the adaptive regulation of photosynthesis and the functions of Rubisco and some thylakoid proteins under enhanced CO$_2$ and high temperatures.

MATERIAL AND METHODS

Plant Material

Experiment on elevated CO$_2$ with wheat (*Triticum astivum*) and barley (*Hordeum vulgare*) was conducted in Saxil-growth chambers (Rothamsted Exp. Station), one having a CO$_2$ concentration of 350ppm and the other 700ppm. Day and night temperatures were maintained at 20 and 15°C, resp. Plant material for the studies on light reactions with barley and turnip rape (*Brassica rapa*) was grown in purpose built greenhouse compartments (Dept. of Plant Production, Helsinki) having the same CO$_2$ concentrations as the Saxil-growth chambers.

185

Daily ambient temperatures ranged from 15 to 23°C. In the temperature stress treatment temperatures ranged from 25 to 30°C.

Photosynthesis Measurements

Rate of photosynthesis was measured from the 7th leaf. Net photosynthesis rates were measured using a 6-chamber open-circuit gas-exchange system with automatic data handling (13). Pn was calculated according to Farquhar and Sarhkey (10).

Rubisco Activity

Leaf samples were stored in liquid nitrogen. Internal activity and total activity were measured as described by Gutteridge et al. (11). Soluble protein was determined by SDS-PAGE and Rubisco protein by Laemmli-method (13).

Ultrastructure and Immunogold Labelling

For ultrastructural studies leaf samples were fixed in 2.9% (v/v) glutaraldehyde in 0.1M Na-phosphate buffer, pH 7.2 for 4 h at room temperature. For immunogold labelling leaf samples were fixed in 1.25% glutaraldehyde. Samples were washed with PB. After dehydration in ascending ethanol concentration series the samples were embedded in L.R.White resin (Bio-Rad) which was later polymerized at 60°C. Thin sections were picked up onto nickel grids. All incubations described below were done at room temperature. Incubations and washes were done in 25 mM Tris-HCl, pH 8.0 containing 500 mM NaCl and 0.3% (v/v) Tween-20 (TBS-T). Grids were incubated for 10 min in TBS-T containing 1% (w/v) BSA (TBS-T-B). Antibodies were against chloroplast thylakoid proteins LHCII, light harvesting protein, and cyt b_{559}. Grids were blotted and incubated for 2 h in primary antibody diluted 1:50 in TBS-T-B followed by blotting and incubating for 10 min in TBS-T-B and four washes in TBS-T-B. After washing the grids were blotted and immersed for 1.5 h in Protein A-gold (10nm particle size; Zymed) solution diluted in TBS-T-B. The grids were then blotted and washed four times in TBS-T-B and two times in TBS-T, and rinsed in distilled water. Ratios of particle densities were calculated for each migrograph (enlarged 30000x) and averaged to determine the distribution of antigen within the chloroplasts.

Fluorescence

Fluorescence measurements were carried out with a Bio Monitor PSM MarkII meter. After 30 min incubation in the dark, fluorescence emission of leaf tissue was measured at a light level of 400 μmol m^{-2} s^{-1} for 10 s.

Cell Number and Size

Cell size was determined according to method described by Lawlor et al. (1989). Leaf samples were submerged into 2% chromic acid and mixed with Ultraturex-mixer for 1 min to separate individual cells. Cells were then counted

186

using a cell counter (ZM, Coulter Instruments). Cell volume was determined by cell size and fresh weight of the sample adjusted by the amount of water in fiber and xylem.

RESULTS AND DISCUSSION

Net Photosynthesis

Observed positive effect of elevated CO_2 on net photosynthesis is in agreement with previous studies (12, 7). Acclimation of net photosynthesis to high CO_2 was evident from the fact that when measured in high CO_2 conditions net photosynthesis of plants grown in high CO_2 was relatively lower than of those grown in low CO_2. This is in agreement with findings of Cure and Acock (7) and Cure *et al*. (8). The observed reduction in the rate of photosynthesis has been contributed to end product inhibition resulting from enhanced supply of carbohydrates which exceeds the capacity of the sink (3). This was also evident from the electronmicrographs of chloroplasts of barley which showed pronounced accumulation of starch indicating deficiencies in translocation.

Rubisco Activity

Internal Rubisco activity increased in both CO_2 treatments as plants matured. In view of the component characteristics there was no clear association of Rubisco activity with net photosynthesis in either barley or wheat. There are reports where the N/C ratio (8, 14), enzyme protein concentration and activity of already synthesized proteins has reduced in plants grown in high CO_2 conditions (5). However, a loss of 40% of Rubisco activity has been shown to have no negative effect on net photosynthesis (14).

Ultrastructure

In both barley and wheat the number and volume of cells in leaf tissue was significantly higher in plants grown in high CO_2 (Fig. 1B, 3B). In both species size of chloroplasts in mesophyll cells was smaller in plants grown in high CO_2. In wheat, the proportion of grana, lipid globules and strach granules of total cell area was higher in plants grown in low CO_2. In barley the proportion of chloroplasts of the total cell area was 4% higher in the high CO_2 treatment.

Ultrastructural changes under enhanced CO_2 referred to similar structure as in chloroplasts of older leaves (Fig. 1B. 3A, 3B), where also LCHII is diminished (15). Proportion of appressed thylakoids was initially low in wheat and barley under high CO_2 conditions, however, the proportion increased gradually (Figs. 1B, 3B). Increase in non-appressed stroma thylakoids was associated with increase in Rubisco activity. Increase in cell number in plants grown in high CO_2 reported by Allen (1) was also observed in this study. The increase in cell number could, in addition to increased leaf area and volume, contribute to increased net photosynthesis.

187
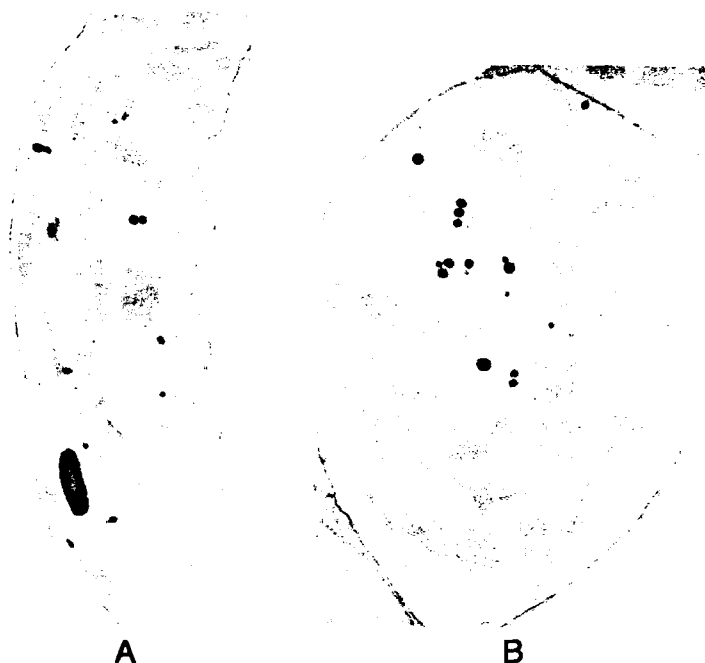
Figure 1. (A) Chloroplast of barley grown under low CO_2 concentration x 25000. (B) Chloroplast of wheat grown under enhanced CO_2 concentration x 15000.

Immunogold Labelling

Goldlabelling of thylakoid proteins indicated significant differences in the organization of these proteins under changing CO_2 concentrations. Amount of light harvesting protein LHCII was doubled in *Hordeum vulgare* and *Brassica rapa* under low CO_2 (Fig. 2A, Table I). Ratio of cyt b559 (part of PSII reaction centre) to LHCII was significantly lower in *Brassica rapa* grown under low CO_2 conditions (Fig. 2B). This further indicated photoinhibition of PSII in *Brassica rapa* under high temperatures. Contrary to the low CO_2 concentration, enhanced CO_2 did not result in significantly low ratio of gold labelled cyt b559 to LHCII. Observed changes under high CO_2 conditions did not result in reduction in the PSII reactions. These results support the postulations that photoinhibition depends directly on the rate of light absorbtion by the PSII light-harvesting antenna.

Immunogold labelling method is not qantitatively as reliable as chlorophyll protein determination by SDS-PAGE. However, chloroplast ultrastructures in *Hordeum* and *Brassica* plants grown under enhanced CO_2 (Figs 3A, 3B) were similar to that of chloroplasts in older leaves where also a reduction of LHCII protein was observed (15).

188
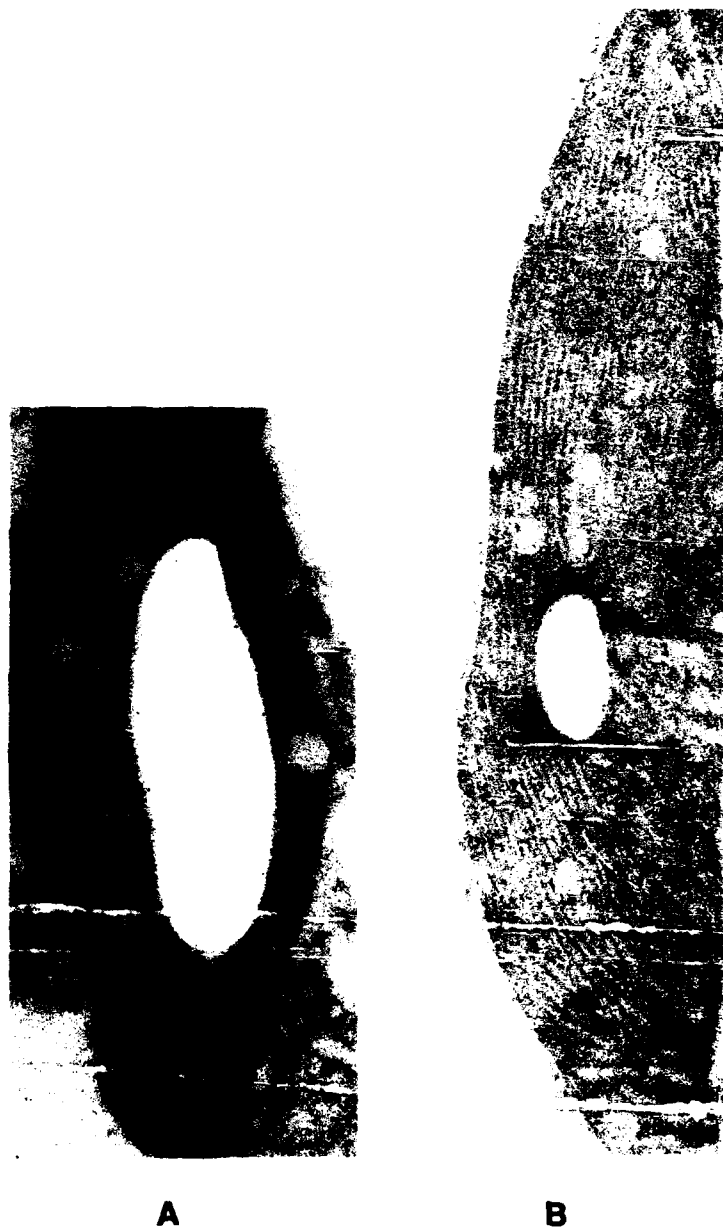
Figure 2. Electron micrograph of *Brassica* labeled with antibody to LHCII,
(A) $-CO_2$ (B) $+CO_2$.

A   **B**
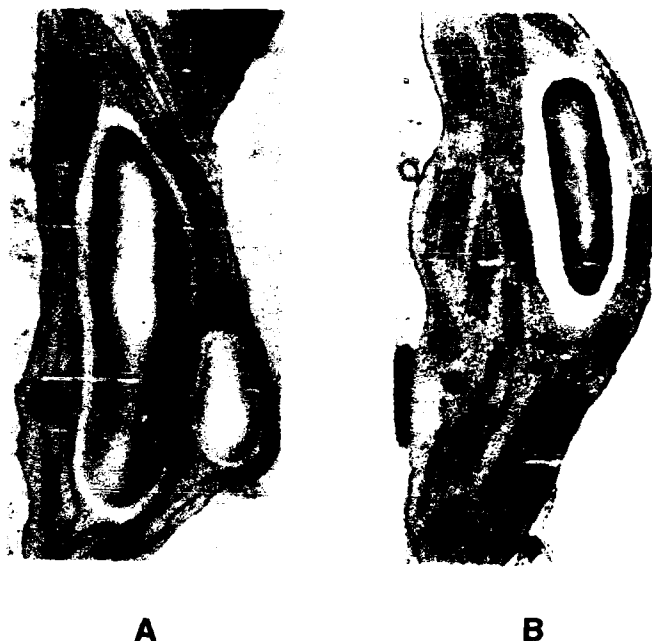
Figure 3. (A) Chloroplast of *Brassica* grown under enhanced CO_2 and high temperature. (B) Chloroplast of *Hordeum* grown under enhanced CO_2 and high temperature x 20000

Fluorescence

There was a significant decrease in the ratio of variable fluorescence to minimum fluorescence (F_V/F_M, Table II) in *Brassica rapa* following high temperature treatment in normal (350ppm) CO_2 concentration. This was not observed in plants grown in high CO_2. This indicated photoinhibition of PSII in low CO_2 conditions (2, 17), whereas a high CO_2 concentration seemed to protect PSII (Table II). On the contrary, in barley only a slight increase was observed in the F_V/F_M ratio in plants grown under enhanced CO_2.

Table I. *Mean density of gold particles in chloroplasts of plants grown in high and low CO_2 concentrations.*

plant	antiserum	- CO_2	+ CO_2
Hordeum	LHCII	203	120
	cyt b559	83	40
Brassica	LHCII	313	147
	cyt b559	49	110

Tab. II. Effect of enhanced CO_2 and high temperature (ca. $30^{\circ}C$) on fluorescence emission in Hordeum vulgare and Brassica rapa leaves.

	Fluorescence parameters			
Hordeum control				
normal T - CO_2	0.77	1.34	1.1	0.31
high T - CO_2	0.73	0.98	0.76	0.27
high T + CO_2	0.72	1.06	0.76	0.31
Brassica control				
normal T -CO_2	0.78	2.29	1.77	0.51
high T - CO_2	0.65	0.91	1.34	0.48
high T + CO_2	0.75	1.71	1.28	0.43

High CO_2 concentration appears to provide protection to the thylakoid reactions in high temperature stress.

LITERATURE CITED

1. **Allen LH Jr** (1989) Global climate change and its impact on plant growth and development. Proceedings of the Plant Growth Regulator Society of America. 16th Ann meeting: August 6-10, 1-13

2. **Aro E-V, Tyystjärvi E, Nurmi A** (1990) Temperature-dependent changes in Photosystem II heterogeneity of attached leaves under high light. Physiol Plant **79**: 585-592

3. **Arp WJ** (1991) Effects of source-sink relations on photosynthetic acclimation to elevated CO_2. Plant, Cell and Environment **14**: 869-975

4. **Berry JA, Björkman O** (1980) Photosynthetic response and adaptation to temperature in higher plants. Ann Rev Plant Physiol **31**: 491-543

5. **Besford RT, Ludwig LJ, Withers AC** (1990) The Greenhouse effect. Acclimation of tomato plants growing in high CO_2, Photosynthesis and Ribulose-1,5-Bisphosphate Carboxylase Protein. J Exp Bot **41**: 229, 925-931

6. **Cleland RE, Melis A** (1987) Probing the events of photoinhibition by altering electron-transport activity and lightharvesting capacity in chloroplast thylakoids. Plant, Cell and Environment **10**: 747-752

7. **Cure JD, Acock B** (1986) Crop responses to CO_2 doubling. A literature survey. Agric and Forest Meterology **38**: 127-145

8. **Cure JD, Rufty TW Jr, Israel DW** (1987) Assimilate utilization in the leaf canopy and whole-plant growth of soybean during acclimation to elevated CO_2. Bot Gaz **148**: 67-72

9. **Drake BG, Leadley PW** (1991) Canopy photosynthesis of crops and native plant communites exposed to long-term elevated CO_2. Plant, Cell and Environment **14**:853-860

191

10. **Farquhar GD, Sharkey TD** (1982) Stomatal conductance and photosynthesis. Ann Rev Plant Physiol **33**: 317-345

11. **Gutteridge S, Schmidt CNG** (1982) The reactions between active and inactive forms of wheat ribulose bisphosphate carboxylase and effectors. European J Biochem. **126**: 597-602

12. **Kimball BA** (1983) CO_2 and Agricultural Yield. An assemblage and analysis of 430 prior observations. Agronomy J **75**: 779-788

13. **Lawlor DW, Kontturi M, Young AT** (1989) Photosynthesis by flag leaves of winter wheat in relation to protein, ribulose-bisphosphate carboxylase activity and nitrogen supply. J Exp Bot **40**: 43-52

14. **Long SP** (1991) *Modification of the response of photosynthetic to rising temperature by atmospheric CO_2 concentrations. Has its importance been underestimated?* Plant, Cell and Environment **14**: 729-739

15. **Nurmi A** (1985) Comparison between thylakoid composition and chloroplast ultrastructure in developing plants of *Brassica, Helianthus, Sisymbrium* and *Tanacetum.* J Ultrastructure Res **92**: 190-200

16. **Stitt M** (1991) Rising CO_2 levels and their potential significance for carbon flow photosynthetic cells. Plant, Cell and Environment **14**: 741-762

17. **Öquist G** (1987) Environmental stress and photosynthesis. In: Progress in Photosynthesis Research, J Biggins ed, Vol 4, Martinus Nijhoff, Dordrecht, pp 1-10

Seasonal Changes in Photochemical Capacity, Quantum Yield, P$_{700}$-Absorbance and Carboxylation Efficiency in Needles From Norway Spruce[1]

Harald Romuald Bolhar-Nordenkampf, Judith Haumann, Elisabeth Gabriele Lechner, Wolfgang Franz Postl, Verena Schreier

Institut für Pflanzenphysiologie der Universität Wien, Althanstraße 14, A-1091 Vienna, Austria

INTRODUCTION

Evergreen coniferous trees are subjected to varying natural stress levels throughout the year. Responses to winter stress affect the photosynthetic apparatus and lead to temporary impairment. If the stress loads exceed the trees' capacity for stress compensation, visible injuries can occur (2). The aim of this study is to correlate variations in the seasonal stress pattern with changes in photosynthetic properties.

MATERIAL AND METHODS

Norway spruce tree clones *(Picea abies (L.) Karst.)* cultivated in the experimental garden (Northern latitude 48°13'35", Eastern longitude 16°22'30") were used to observe seasonal changes in the following photosynthetic parameters (4, 5, 7, 8, 9) :

i.   Photochemical capacity (efficiency), Fv/Fm[2];
ii. Amount of heat deactivating centers (q_{NP}) and active centers (q_P);
iii. Apparent O_2 quantum yield in 50mbar CO_2 at 20°C;
iv. Carboxylation efficiency in saturating light conditions, (800 μmol m^{-2} s^{-1});
v.   Amount of oxidized P$_{700}$ (830nm absorbance changes).

---

[2]Abbreviations: Fv/Fm, ratio of variable to maximal fluorescence; FI, frost index; HLI, high light index; HTI, high temperature index; PCE, photochilling events; PEA, plant efficiency analyzer; PSM, plant stress meter; q_{NP}, non-photochemical quenching; q_P, photochemical quenching.

193

Instrumentation: Plant Stress Meter (PSM, Biomonitor, Sweden); Plant Efficiency Analyzer (PEA), Modulated Fluorescence Measuring System (MFMS, double beam), Leaf Disk Electrode [all from Hansatech, UK]; Portable Infrared Gas Analyzer (LCA-2, ADC, UK) and Parkinson Coniferous Leaf Chamber (PLC-C, ADC, UK); Quantum sensor (SKP 215, Skye Inst., UK); Weather station (Delta-t-Devices, UK); Cold mirror halogen bulb (Philips 6423, 150W, 15V); Graphics program (SIGMAPLOT 4.0).

Ambient photoinhibition was measured as the loss of photochemical capacity, Fv/Fm, (1) after 30 min dark adaptation at 20°C. Measurements were performed with two non-modulated fluorometer (PSM, PEA). Each month, the collected data were compared with those obtained with a modulated system (MFMS). The data from PSM and PEA were comparable. In the case of 'upper side photoinhibition' the Fv/Fm values were higher with the MFMS, because of the use of yellow modulated light which penetrates deeper into the leaves' tissue (3).

To study temporary induced photoinhibitory stress, branches of potted spruce trees were submitted separately to chilling (3°C) and photochilling (3°C, 1200 μmol m^{-2}s^{-1}) for 5 hours. Measurements i. to v. were performed before and after treatment. In general, figures show all experimental data collected; only in Figures 2a and 2b data represent the arithmetic mean of 3 to 5 measurements.

RESULTS AND DISCUSSION

Seasonal changes in photochemical capacity (Fv/Fm) (Fig.1a) correlated perfectly with stress indices for frost (FI <-4°C) and photochilling (PCE, > -4°C < +4°C, >700 μmol m^{-2} s^{-1}) (Fig. 1b). Because of photochilling induced photoinhibition, losses in photochemical capacity were generally more pronounced on the upper, light exposed surface of needles (Fig.1a, open symbols), whereas frost induced changes occurred equally on both surfaces. During March and April these reactions were partly reinforced by new shoot development, which acts as an endogenous stress factor. During summer, high light and high temperature induced photoinhibition occurred predominantly on the upper surface (HLI, >1200 μmol m^{-2} s^{-1}, HTI, >25°C) (Fig.1a).

In general, a good correlation (y=7.25x+0.18, r^2=0.672) was found between quantum yield of oxygen evolution (Fig. 1c. regression 9. order) and photochemical capacity (Fig. 1a, regression 3. order), but only responses of quantum yield to frost and photochilling events were well pronounced. Single branches often show no correlation at all between Fv/Fm and quantum yield (cp 6).

After 36 hours of recovery (12°/18°C, 10 μmol m^{-2} s^{-1}) most of the ambient stress induced changes had disappeared, with the result that the photochemical capacity remained depressed only in February (Fig. 2a). Any additional stress load, especially photochilling, reduced the photochemical capacity by 3-5% irrespective of the season. Reductions in photochemical capacity of almost 10%

194
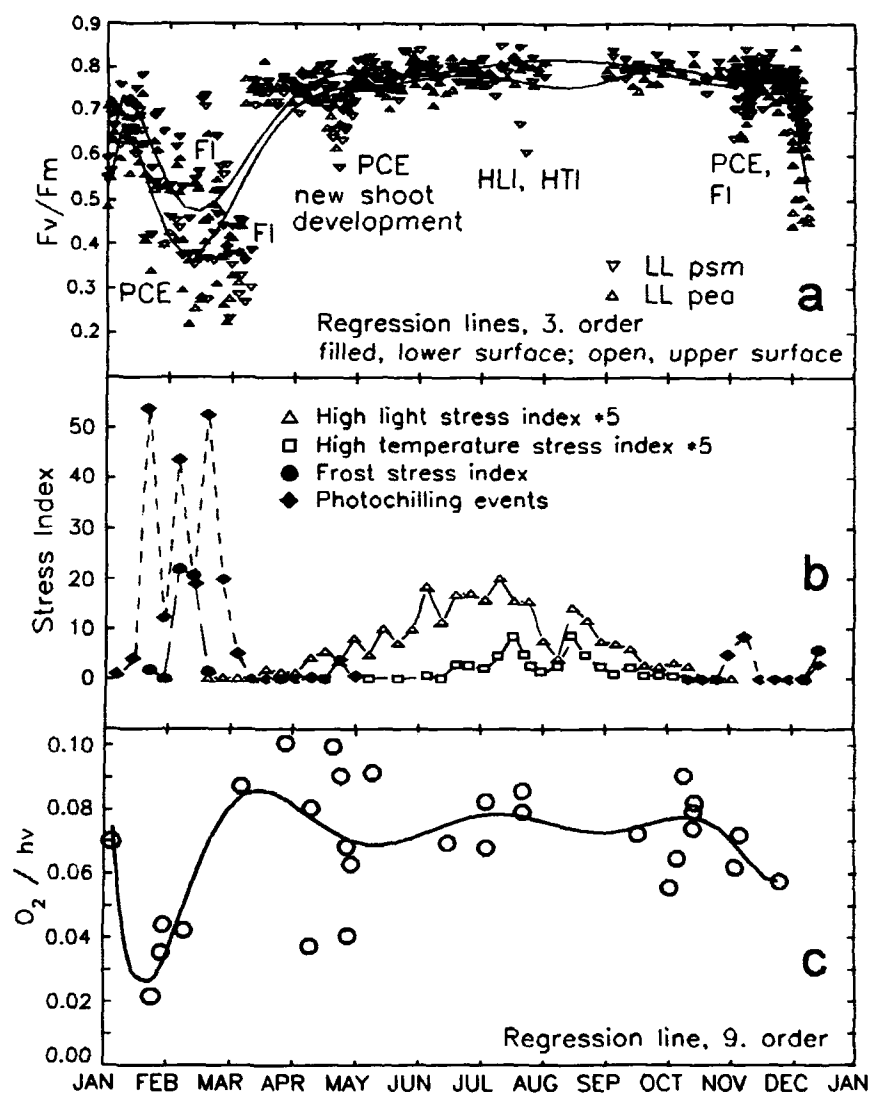
Figure 1. Seasonal variations (1991): (a) Photochemical capacity (Fv/Fm). Regression lines indicate area of maximal differences between upper and lower needle surfaces. LL, low land clone (<800m); psm, plant stress meter; pea, plant efficiency analyzer; FI, elevated frost index; PCE, frequent photochilling events; HLI, elevated high light stress index; HTI, elevated temperature stress index. (b) Pattern of stress factors (see text for explanation). (c) Apparent quantum yield of oxygen evolution (mol O_2/mol photons) in saturating (50 mbar) CO_2 at 20°C.

195
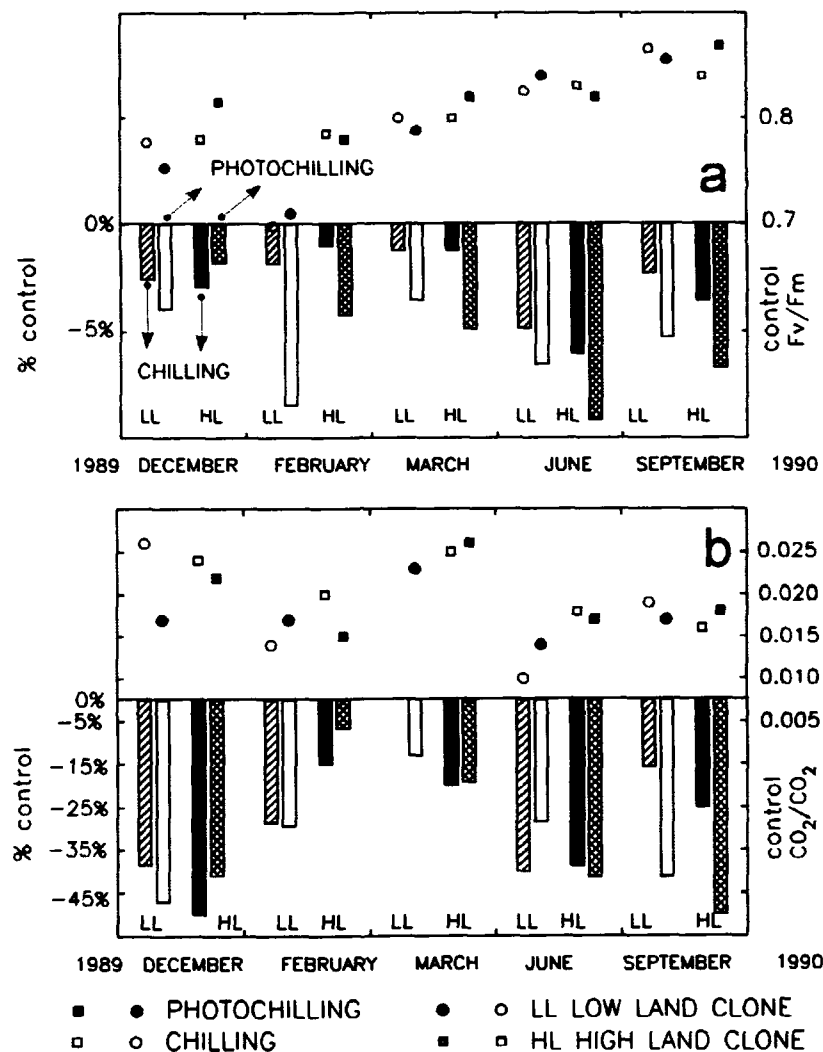
Figure 2. Seasonal variations (1990) after application of chilling or photochilling as additional stress loads. Symbols represent absolute control values; bar charts represent changes after treatment as a percentage of control value. (a) Changes in photochemical capacity (Fv/Fm). (b) Changes in carboxylation efficiency (mol CO_2 carboxylated/mol intracellular CO_2.
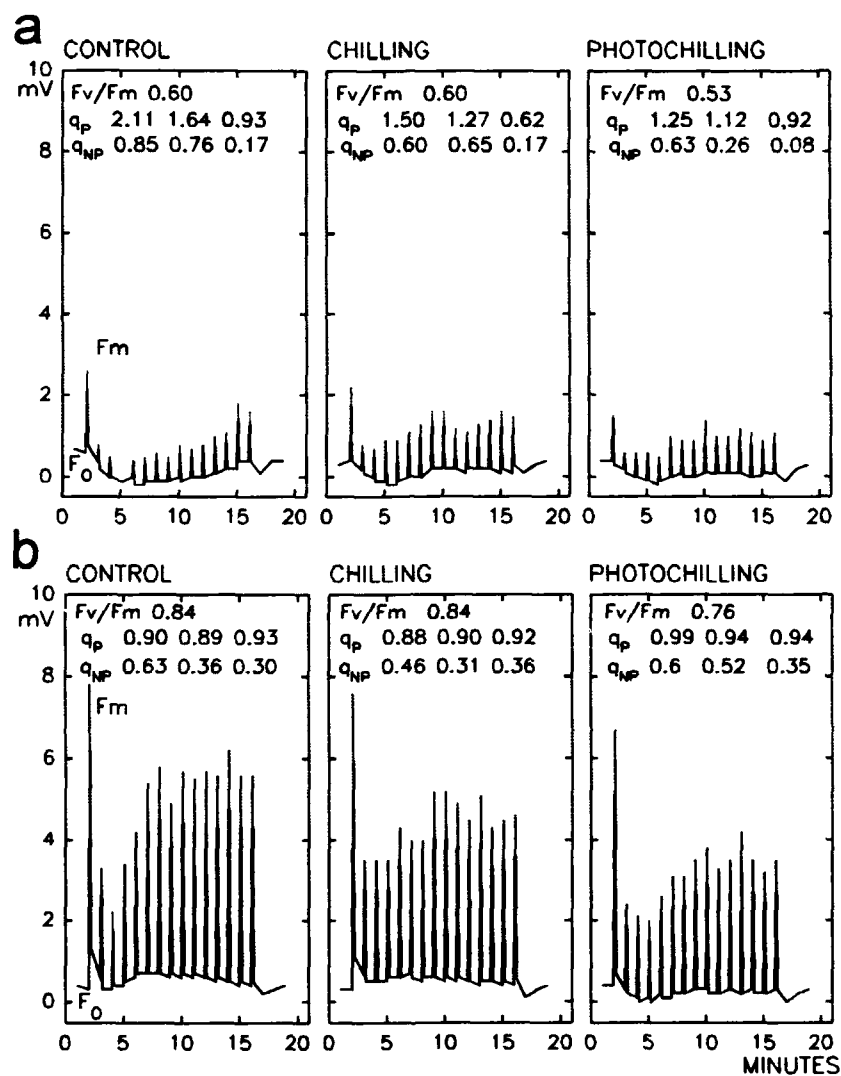
Figure 3. Quenching analyses, upper surface: Fv/Fm, photochemical capacity; F_O, minimal fluorescence; F_m, maximal fluorescence; 3rd, 7th and 15th flash: q_P, photochemical quenching; q_{NP}, non-photochemical quenching. (a) February 1990; (b) April 1990
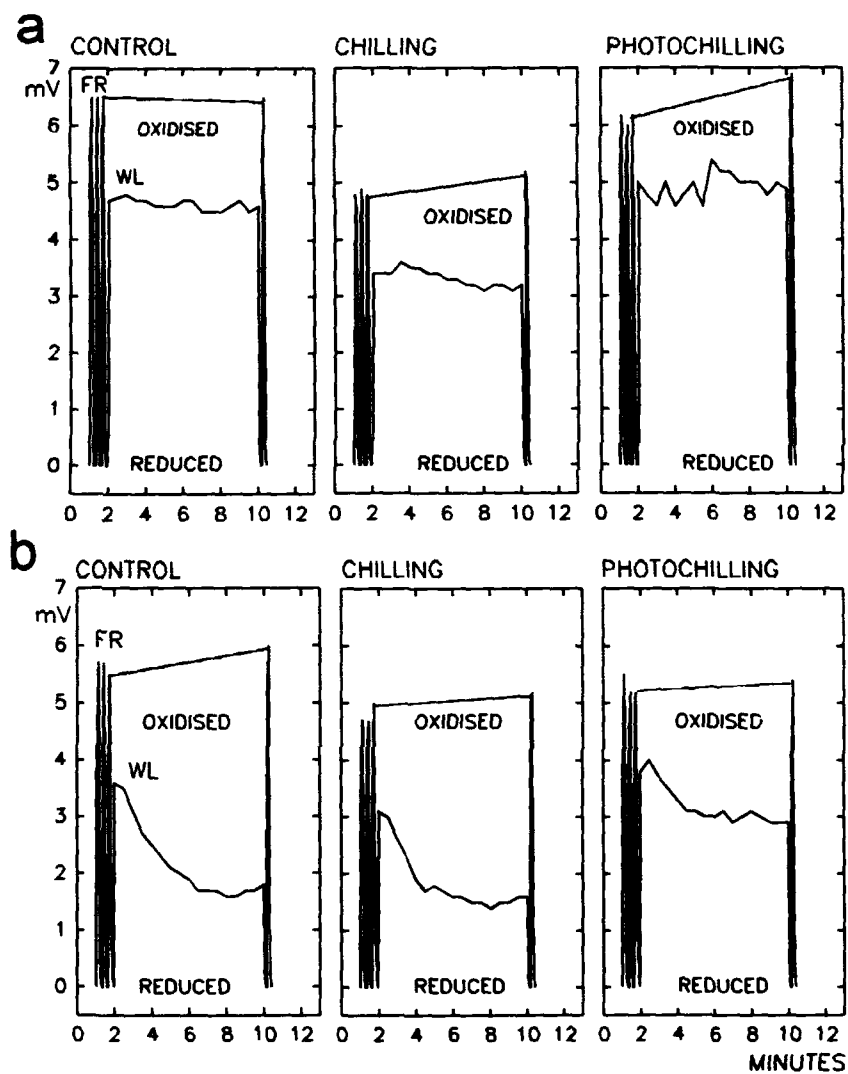
Figure 4. P_{700} absorbance changes at 830nm: FR, far red light pulses (>720nm, 166 μmol m^{-2} s^{-1}); WL, additional, permanent white light (140 μmol m^{-2} s^{-1}). (a) February 1990; (b) April 1990

were observed in the frost sensitive low land clone in February (combination with drought) and the high temperature sensitive high land clone in June.

Much more evident changes in carboxylation efficiency were observed, following the application of an additional stress (Fig. 2b). During periods with more or less uninhibited CO_2 fixation, losses were generally in excess of 30% as a combined effect of reduced photochemical capacity and stomata closure (data not shown). The far less pronounced response to additional stress in February and March can be attributed to a reduction in the amount of active reaction centers.

Using quenching analyses, it was demonstrated that the proportion of photochemically active centers is higher during winter stress (low q_{NP}, high q_P); even after a photochilling induced additional stress load, only marginal changes in q_P and q_{NP} were observed (Fig. 3a-b).

In February, PSII fluorescence signal values were 65% less than in April (Fig. 3a-b). This was interpreted as a substantial loss in reaction centers present. The amount of PSI reaction centers appeared to be unchanged and therefore reduction of P_{700} was 44% of the April value (Fig. 4a-b). After photochilling, the photochemical capacity (Fv/Fm) decreased and the electron flow from PSII correspondingly diminished, which led to more oxidized P_{700} (+40%) (Fig. 4b).

CONCLUSION

The adaptation of the photosynthetic energy conversion process to seasonal changes in stress load is mainly regulated by the amount of reaction centers which are available to undergo the photoinhibitory turn over. The amount of PSI centers is thought to remain unchanged. The redox state of P_{700} is predominantly determined by the electron flow from plastoquinone.

LITERATURE CITED

1. **Bolhar-Nordenkampf HR, Hofer M, Lechner EG** (1991) Analysis of light-induced reduction of the photochemical capacity in field-grown plants. Evidence for photoinhibition? Photosynth Res **27**: 31-39
2. **Bolhar-Nordenkampf HR, Lechner EG** (1989) Synopsis of stress-induced modifications in anatomy and physiology of spruce needles as an early diagnosis in New Forest Decline. Phyton (Austria) **29/3**: 255-301
3. **Bolhar-Nordenkampf HR, Long SP, Baker NR, Öquist G, Schreiber U, Lechner EG** (1989) Chlorophyll fluorescence as a probe of the photosynthetic competence of leaves in the field: a review of current instrumentation. Functional Ecol **3**: 497-514
4. **Bolhar-Nordenkampf HR, Öquist G** (1993) Chlorophyll fluorescence as a tool in photosynthesis research. *In* D Hall et al, eds, Photosynthesis and production in a changing environment, Chapman and Hall, pub, London

5. **Genty B, Briantais J-M, Baker NR** (1989) The relationship between the quantum yield of photosynthetic electron transport and photochemical quenching of chlorophyll fluorescence. Biochim Biophys Acta **990**: 87-92

6. **Giersch CH, Krause GH** (1991) A simple model relating photoinhibitory fluorescence quenching in chloroplasts to a population of altered photosystem II reaction centers. Photosynth Res **30**: 115-121

7. **Long SP, Postl WF, Bolhar-Nordenkampf HR** (1993) Quantum yields for CO_2 uptake in C_3 vascular plants of contrasting habitats and taxonomic groupings. Planta (Berlin) in press

8. **Malkin S, Schreiber U, Jansen M, Canaani O, Shalgi E, Cahen D** (1991) The use of photothermal radiometry in assessing leaf photosynthesis: I.General properties and correlations of energy storage to P_{700} redox state. Photosynth Res **29**: 87-96

9. **Seaton GGR, Walker DA** (1990) Chlorophyll fluorescence as a measure of photosynthetic carbon assimilation. Proc Roy Soc Lond B **242**: 29-35

Photosynthesis, Respiration and Dry Matter Growth of *Lemna gibba*, as Affected by Day/Night [CO₂] Regimes[1]

J. Reuveni, J. Gale and A.M. Mayer

Dept. of Botany, Hebrew University of Jerusalem, Jerusalem, 91904, Israel

INTRODUCTION

We present a study of the direct effect on dark respiration of $[CO_2]$,which has been shown to reduce the rate of CO_2 efflux (1,4,7). This direct effect differs from the indirect effect in which respiration increases in response to the assimilate status of plants grown at high ambient $[CO_2]$ (6). The direct effect should also not be confused with the reduction of respiration found in plants exposed over long periods of time to high $[CO_2]$ (5).

We previously reported an example of the direct effect of $[CO_2]$, on *Medicago sativum*, in which not only was growth not impeded but actually increased, in proportion to the reduced loss of carbon in respiration. A similar effect was found for *Xanthium strumarium* (7). This invites the surprising conclusion that part of the respiration measured under non-stress conditions and "normal" $[CO_2]$ is otiose. This was not the case when respiration was suppressed by high $[CO_2]$ under conditions of temperature stress (3).

Data are presented on the direct effect of CO_2 on the rate of respiration and on growth of *Lemna gibba*. Special attention was paid to the possibility that the apparent reduction in the rate of respiration (as indicated by a lowered rate of CO_2 efflux in the dark) and the associated increase in dry weight, under high $[CO_2]$, is an artefact resulting from dark CO_2 fixation. An indication of this would be a lowering of the RQ (ratio of CO_2 efflux to O_2 taken up).

MATERIALS AND METHODS

Continuous five day photosynthesis and respiration measurements of *Lemna gibba* were carried out using methods and an infra-red CO_2 analysis system (IRGA) similar to those previously described (8). Gas exchange measurements were carried out on ~1.5 g (initial) fresh weight of fronds floating on 250 ml

culture solution, in 800 ml flat cell culture flasks. Eight such flasks were positioned just below the water surface of constant temperature baths, and air samples from their efflux lines were measured sequentially.

Long term batch growth experiments were carried out with fronds floating on 1.5 l culture solution in 5 l erlenmeyer flasks, aerated with filtered air set at the required $[CO_2]$ level.

Respiration quotients at different $[CO_2]$ levels, were determined in a system which was in either a closed or an open flow mode. In the closed mode, O_2 uptake was measured with a Clark type electrode in a 60 ml cuvette. The fronds were in the 20 ml gas phase. Either CO_2 was absorbed by a KOH saturated, fluted filter paper in the air space, or the $[CO_2]$ was allowed to build up in the cuvette (Where the RQ = ~1, a 1% decrease in $[O_2]$ results in a ~1000 Pa build up of $[CO_2]$).

O_2 uptake was calculated from both the water and air phases. After measuring respiration by O_2 uptake, the cuvette was then connected, in open flow mode, with either high (100 Pa) or low (~0) $[CO_2]$, to an IRGA system, for measurement of CO_2 efflux.

The $[CO_2]$ respiration measurement at high $[CO_2]$ was made at concentrations close to 100 Pa, versus the 100 to 1000 Pa range in the oxygen cuvette, in the absence of KOH. This was due to the limitations of the IRGA instrument used. However $[O_2]$ measurements gave no indication of a further reduction of respiration when $[CO_2]$ was allowed to build up in the cuvette to concentrations above 100 Pa.

RESULTS AND DISCUSSION

Five to six day continuous measurements of *L. gibba* photosynthesis and respiration were made under various conditions of day-length and $[CO_2]$. The experiments were repeated with consistent results. Data from two representative runs are depicted below. Fig. 1a shows the gas exchange of plants grown for 5 days, with 8h light periods, at 100 Pa $[CO_2]$, and 16h dark periods with either 0 or 100 Pa $[CO_2]$. Fig 1b shows the gas exchange of plants grown for 5 days and exposed to 16 hour light periods at 100 Pa $[CO_2]$ and 8h dark period with either 0 or 35 Pa $[CO_2]$ at night.

In the experiment depicted in Fig. 1a, days were short and the level of photosynthesis was maintained throughout the 5 day period. In this case high $[CO_2]$ at night (100 Pa) reduced the rate of dark respiration by about 30% (from 105 to 74 nmol g DW^{-1} s^{-1}) as compared to the 0-$[CO_2]$ controls. The percentage reduction appeared to be somewhat less after 5 days.

As seen in Fig. 1b, and previously reported for *L. gibba* (8) exposure to high $[CO_2]$ (100 Pa) during long days results in a rapid drop in the rate of net photosynthesis per unit dry weight. This drop of from ~400 to 200 nmol CO_2 g DW^{-1} s^{-1}, between the first and fourth days is paralleled by a drop in respiration rate of from 60 to 45 nmol between the second and fifth nights in the plants
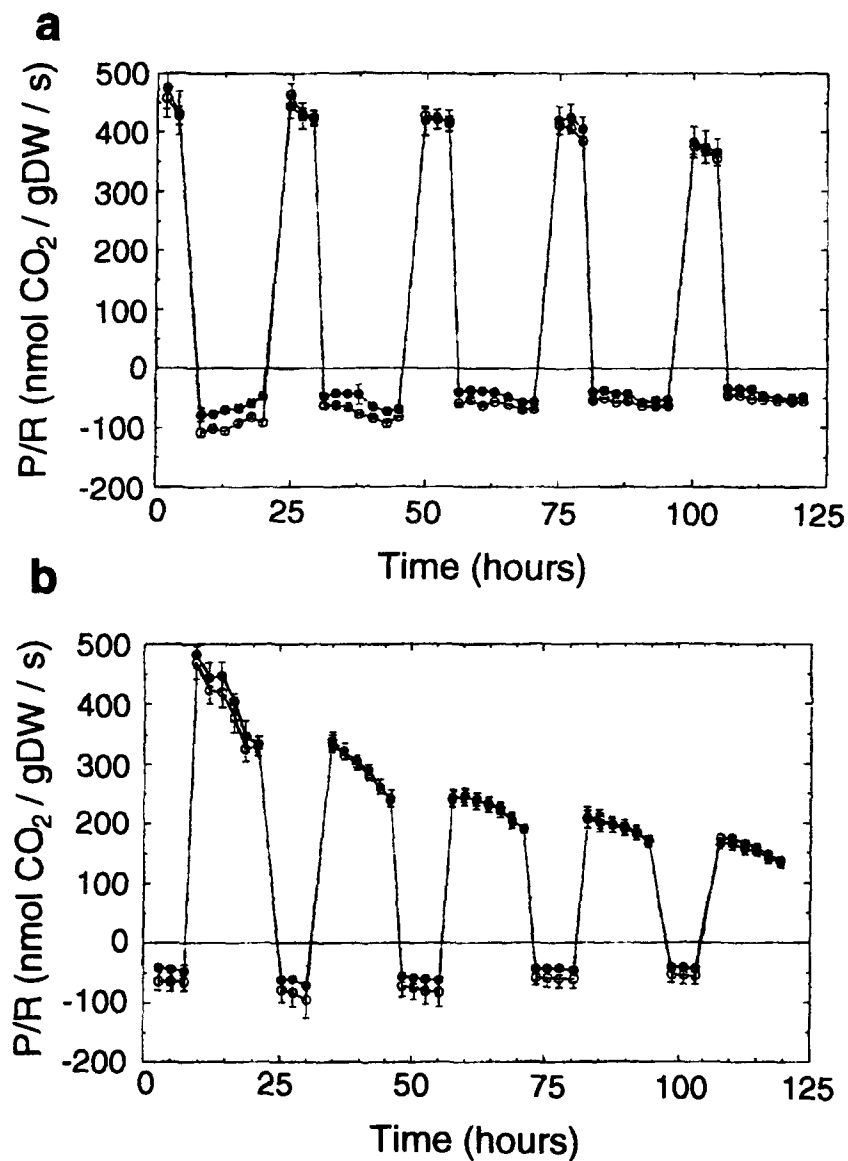
Figure 1. Photosynthesis and respiration of *Lemna gibba* fronds grown under different daytime lengths and night-time ambient $[CO_2]$. All plants received 100 Pa $[CO2]$ and a light intensity of 350 μmol m^{-2} s^{-1} photosynthetic photon flux (PPF) during the day periods. Each point is the average of four flasks, with s.e. bars (frequently smaller than the symbols). a: Short days with 100 Pa $[CO_2]$, and either 0 (O) or 100 Pa (●) $[CO_2]$ at night. b: Long days at 100 Pa $[CO_2]$, and either 0 (O) or 35 Pa (●) $[CO_2]$ at night.

203

exposed at night to 35 Pa $[CO_2]$. A similar drop can be seen in those exposed to 0-$[CO_2]$ of from 85 to 55 nmol CO_2 g DW s^{-1}. Ambient $[CO_2]$ of 35 versus 0 Pa reduced the rate of night-time respiration by about 25%.

Pooling data of many experiments (with different day-lengths) for the ratio of net 24h carbon gain to carbon loss gave an average figure for *L. gibba* of ~7.3 for plants exposed to 0 or to 35 Pa $[CO_2]$ at night versus ~8.0 for those exposed to 100 Pa $[CO_2]$.

In order to learn whether the reduced rate of respiration in response to high night-time $[CO_2]$ was indeed not deleterious, as suggested by the gas exchange experiments, we tested the effect on overall growth. As the expected difference in cumulative dry weight was small and the variability of *L. gibba* cultures large, experiments were carried out at very high day and night $[CO_2]$ (140 +/-5 Pa) with the controls receiving either 0 or 35 Pa $[CO_2]$ at night.

Note that, as seen in Table 1, although the overall batch growth rates were lower in Set 2 than in Set 1, there was no significant difference between the effect of the two low night-time $[CO_2]$ levels (0 and 35 Pa) and the high $[CO_2]$ night-time level (140 Pa).

The experiments summarized in Table 1, were repeated with various day-lengths and night-time $[CO_2]$. Results were variable and trends could not be detected. However, in none of twenty experiments was their any evidence of an injurious effect of high night-time $[CO_2]$. In all experiments there was either no effect on dry weight or growth was increased, sometimes by as much as 20%. The average increase of dry weight, shown in Table 1, was consistent with the decrease of carbon loss in the high night-time $[CO_2]$ treatments (Figs 1a and 1b).

Table I. *Dry weight increment of Lemna gibba as affected by night-time $[CO_2]$.*
Plants were grown for 7 days with 18h day and 6 hour night periods. During the day plants were exposed to 260 µmol m^{-2} s^{-1} PPF and 140 Pa $[CO_2]$. Temperatures were constant at 26°C. Controls (low $[CO_2]$ at night) were raised to 140 Pa one hour before the onset of the light period. Initial dry weights, calculated from parallel FW/DW samples, were -0.015. N = number of averaged experiments (with 4 replications of each treatment in each experiment). RGR - Logarithmic relative growth rate. Results of differences between averaged experiments were analyzed by paired t-test.

	Set 1, N=4				Set 2, N=6			
	Night-time $[CO_2]$		High / low	Sig. of Diff.	Night-time $[CO_2]$		High / low	Sig. of Diff
	0 Pa	140 Pa			35 Pa	140 Pa		
Final DW, g	0.81	0.88	1.11	P<0.01	0.72	0.81	1.13	P<0.01
RGR	0.56	0.574	1.04	-	0.48	0.51	1.04	-

Table II. *Respiration coefficient (RQ) of* Lemna gibba *plants as affected by the ambient* [CO_2]

[CO_2] - Pa	RQ - CO_2/O_2	Significance of Difference
0	1.065 ± 0.016**	n.s. P > 0.1
100 - 1000*	1.008 ± 0.046**	

* See "Materials and Methods"
** Average of 6 pairs of measurements, ± s.e.

As noted above, there was a possibility of an artefact, resulting from dark CO_2 fixation at high [CO_2], simulating a decrease of respiration. If there is a significant dark CO_2 fixation then the RQ value of respiration (ratio of CO_2 given off to O_2 taken up) should be lowered proportionally. This was tested, with the results shown in Table 2. There was only a 5% apparent reduction in RQ at the high [CO_2] level, a difference which was four to six times lower than would be required to explain the lowering of CO_2 efflux. This difference was not satistically significant.

CONCLUSIONS

Night-time respiration rate was lower by about 20 - 30% in *Lemna gibba* at high (~100Pa) than at low (0 or 35 Pa) ambient [CO_2] (Figs 1a and 1b). This was not a result of dark CO_2 fixation (Table 2). There was never any apparent deleterious effect of this suppression of respiration and, in many replicated experiments, dry weight gain increased (Table 1). Under conditions of high-temperature stress, suppression of leaves of *Xanthium strumarium* by [CO_2] damaged the photosynthesis system (3). However, in the present experiments with *Lemna gibba* in the absence of stress, reduction of respiration by high [CO_2] had no apparent deleterious effect. This indicates that part of the respiration was otiose. This small but not insignificant factor should be considered in predicting the effect of increased world atmospheric [CO_2] on global vegetation and in the greenhouse industry, where [CO_2] may be very high at night.

ACKNOWLEDGMENTS

LITERATURE CITED

1. **Amthor JS** (1991) Respiration in a future higher - CO_2 world. Plant Cell and Environment **14:** 13-20.

2. **Amthor JS, Koch GW, AJ Bloom** (1992) CO_2 inhibits respiration in leaves of *Rumex crispus* L. Plant Physiol **98:** 757-760.
3. **Gale J** (1982) Evidence for essential maintenance respiration of leaves of *Xanthium strumarium* at high temperature. J Exp Bot **33:** 471-476.
4. **Kaplan A, Gale J, MA Poljakoff-Mayber** (1977) Effect of O_2 and CO_2 concentration on gross dark CO_2 fixation and dark respiration in *Bryophylum daigremontianum*. Aust J Plant Physiol **4:** 745-752.
5. **Leadley PW, BG Drake** (1993) Open top chambers for exposing a grassland community to elevated ambient CO_2 concentration and for measuring net ecosystem gas exchange. *In* Rozema J, Lambers H, van den Geijin SC, Cambridge ML eds, Kluwer Academic Publ, Dordrecht, pp 3-15.
6. **McCree KJ** (1974) Equation for the rate of dark respiration of white clover and grain sorghum, as functions of dry weight photosynthetic rate and temperature. Crop Sc. **14:** 509-514.
7. **Reuveni J, J Gale** (1985) The effect of high levels of carbon-dioxide on dark respiration and growth of plants. Plant Cell and Environ. **8:** 623-628.
8. **Smernoff DT, Gale J, Macler BA, J Reuveni** (1992) Inhibition of photosynthesis in duckweed by elevated $[CO_2]$ is rapid and is not offset by temperature induced increase in metabolic rate. Photosynthetica **26:** (in press)

Responses of Woody Horticultural Species to High CO$_2$

W. John S. Downton and W. James R. Grant

CSIRO Division of Horticulture, GPO Box 350, Adelaide, South Australia 5001, Australia

INTRODUCTION

The early growth of many horticultural woody plants commonly grown as nursery stock in containers is often slow and should benefit from CO$_2$ enrichment. Similarly, more advanced fruiting plants grown in containers under protected cultivation to produce earlier, blemish-free fruit, e.g. mandarin oranges in Japan, might also benefit from CO$_2$ enrichment. Numerous observations, however, indicate that the expected benefits from high CO$_2$ are often not fully realized due to downward adjustments to the rate of photosynthesis over time. We have examined the effects of CO$_2$ enrichment on the photosynthesis and growth of cropping potted Valencia orange trees, on mangosteen seedlings which have a very slow rate of development which limits orchard establishment, and on variegated cultivars of ornamental species whose growth is retarded compared with their completely green counterparts.

MATERIALS AND METHODS

All plants were grown in controlled environment facilities where they either received ambient CO$_2$ (400 µbar) or supplementary CO$_2$ to approx. 800 µbar. Three-year-old fruiting Valencia orange scions (*Citrus sinensis* (L.) Osbeck) on citrange rootstock were studied over a 12 month period from just prior to flowering until fruit maturity. The trees grew in 9 l pots under conditions of 10h day, day temperature 25°C, night temperature 18°C, relative humidity 60-90% and photon irradiance 600 µmol photons m^{-2} s^{-1} (PAR) (see 4 for further details).

Six-month-old mangosteen seedlings (*Garcinia mangostana* L.) planted into 100mm diameter tubes containing 3.7 l of soil (see 3 for details) were grown for 12 months, under conditions of 12h day, day temperature 30°C, night temperature 22°C, relative humidity 50% and average photon irradiance of 200 µmol photons m^{-2} s^{-1}.

Rooted cuttings of willow myrtle (*Agonis flexuosa* (Willd.) Sweet) were tip grafted with either a variegated cultivar of *Agonis flexuosa* 'Pied Piper' or else its completely green reversion. The plants in 0.8 l pots were moved to growth

cabinets set at 12 h day, day temperature 25°C, night temperature 18°C, relative humidity 50% and photon irradiance of 320 µmol photons m^{-2} s^{-1}. CO_2 enrichment commenced 1 month later for a period of 5 months. Plants were repotted into 2.8 l pots two months after CO_2 enrichment commenced.

Cuttings of green leaved *Nerium oleander* L. were rooted and potted into 1.4 l of soil. Plants of a variegated cultivar of oleander purchased from a nursery were repotted into a similar soil volume. Growth cabinet conditions were the same as for *Agonis flexuosa*. Plants were repotted into 4.3 l of soil one month after CO_2 enrichment commenced. CO_2 enrichment occurred for 3 months before plants were harvested.

All plants were fertilized regularly. Rates of CO_2 exchange at 800 µbar CO_2 were determined using an open gas exchange system with light and temperature conditions the same as those prevailing within the growth cabinets.

RESULTS AND DISCUSSION

The results are consistent with other recent reports that photosynthetic acclimation may be a consequence of sink limitation rather than a high CO_2 effect *per se* (1, 5). Acclimation in citrus in response to high CO_2 was evident during very early fruit set and development and when fruit ripened (Fig. 1, Table I), but not during the linear phase of increase in fruit volume when sink strength would have been high. Overall dry matter accumulation was stimulated by CO_2 enrichment (Table II) and these plants matured 70% more fruit than control plants. Plants were pot-bound and roots fully occupied the soil volume.
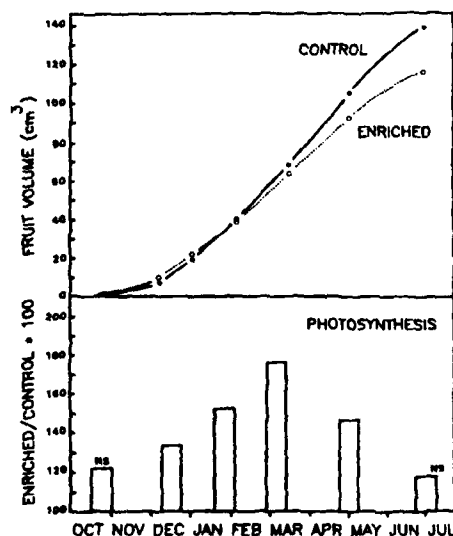
Figure 1. Valencia orange fruit development and the ratio of photosynthetic rates measured at the prevailing partial pressures of CO_2 in the two cabinets (400 µbar and 800 µbar). Final fruit volumes were not significantly different. NS, no significant difference in mean photosynthetic rates at $P<0.05$ (t-test). Adapted with permission from 4.

Table I. *Photosynthetic Rates of Valencia Orange Leaves During Fruit Development as Influenced by CO_2 Enrichment.*

Rates were measured at 800 μbar CO_2 commencing six weeks after CO_2 enrichment began. *Significantly different means at $P<0.05$ (t-test), n=20.

Stage of fruit development	Photosynthesis ($\mu mol\ CO_2\ m^{-2}\ s^{-1}$)		Enriched / Control
	Control	Enriched	
Early fruit set (Oct)	8.9	5.9*	0.67
0.05 final vol. (Dec)	10.7	8.6*	0.80
0.25 final vol. (Jan)	8.7	8.1	0.93
0.50 final vol. (Mar)	8.5	8.2	0.96
0.75 final vol. (Apr)	9.2	7.5	0.81
Coloring (July)	7.9	5.2*	0.66

In Valencia orange maturing fruit greatly suppress further shoot growth and floral initiation until removed thus restricting the development of alternative photosynthetic sinks (4). Mangosteen seedlings, which exhibit growth flushes

Table II. *Dry Matter Accumulation in Valencia Orange, Mangosteen, Willow Myrtle and Oleander as Influenced by CO_2 Enrichment.*

Valencia orange and mangosteen were grown with CO_2 enrichment for 12 months, willow myrtle for five months and oleander for three months. *Significantly different means at $P<0.05$ (t-test), n=3-6.

	Dry Wt. (g)		Enriched / Control
	Control	Enriched	
Valencia orange			
Entire plant	1140.6	1439.0*	1.26
Fruit	377.5	595.9*	1.58
Mangosteen	66.0	116.7*	1.77
Willow myrtle			
Green reversion	89.7	120.8*	1.35
Variegated	12.5	20.4*	1.63
Oleander			
Green plant	80.9	107.0*	1.32
Variegated plant	24.8	38.8*	1.56

Table III. *Photosynthetic Rates of Mangosteen Leaves During Plant Development as Influenced by CO_2 Enrichment.*

Rates were measured at 800 μbar CO_2 commencing six months after CO_2 enrichment began. *Significantly different means at $P<0.05$ (t-test), n=12.

	Photosynthesis $(mol\ CO_2\ m^{-2}\ s^{-1})$		Enriched / Control
	Control	Enriched	
Plant development			
No branches (Jan)	7.0	6.4*	0.91
Early branching (Apr)	7.5	6.6*	0.88
Well branched (July)	7.0	6.9	0.99
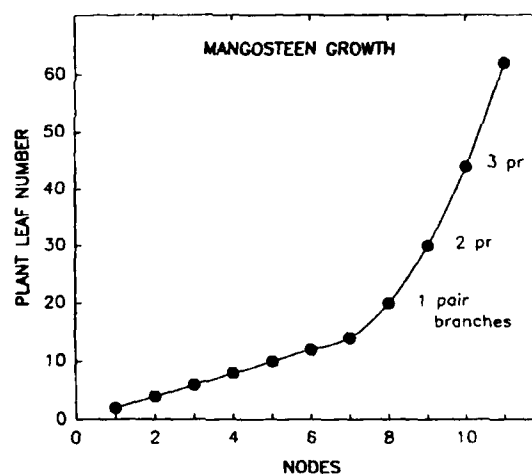
Figure 2. General relationship of leaf production to node position and development of sidebranches in mangosteen.

at intervals of about 45 days (3), showed photosynthetic acclimation during early development even when provided with ample soil volume for root growth (Table III). Once branching became well established, the amount of new leaf and stem tissue generated at each flush (Fig.2) increased considerably and photosynthetic acclimation disappeared. For variegated and green cultivars of oleander and willow myrtle grown in large soil volume to prevent root crowding there was no evidence of photosynthetic acclimation to high CO_2 over a 3-3.5 month period

Table IV. *Photosynthetic Rates of Willow Myrtle and Oleander Leaves as Influenced by CO_2 Enrichment.*

Rates measured at 800 µbar CO_2 following 3.5 months of CO_2 enrichment for willow myrtle and 3 months for oleander. *Significantly different mean at $P<0.05$ (t-test), n=7.

	Photosynthesis ($\mu mol\ CO_2\ m^{-2}\ s^{-1}$)		Enriched / Control
	Control	Enriched	
Willow myrtle			
Green reversion	18.3	17.3	0.95
Variegated leaves			
Green portion	15.8	16.3	1.03
Yellow portion	2.2	2.4	1.09
Oleander			
Green plants	17.1	16.2	0.95
Variegated leaves			
Green portion	15.3	15.2	0.99
Yellow portion	-0.5	-0.6*	1.20

(Table IV). These plants, unlike mangosteen and citrus, exhibit continuous shoot growth. This, combined with unrestricted root development apparently prevented the onset of acclimation, which was observed for oleander grown in full sunlight in an earlier study (2).

It seems likely that the global rise of CO_2 will also result in photosynthetic acclimation for certain species growing in natural habitats due to factors such as growth patterns and competitive plant interactions that operate to prevent unrestricted growth.

LITERATURE CITED

1. **Arp W** (1991) Effects of source-sink relations on photosynthetic acclimation to elevated CO_2. Plant, Cell and Environ. **14**:869-875.
2. **Downton WJS, Björkman O, Pike CS** (1980) Consequences of increased atmospheric concentrations of carbon dioxide for growth and photosynthesis of higher plants. *In* G I Pearman, ed. Carbon Dioxide and Climate: Australian Research. Australian Academy of Science, Canberra, pp. 143-151.
3. **Downton WJS, Grant WJR, Chacko EK** (1990) Effect of elevated carbon dioxide on the photosynthesis and early growth of mangosteen (*Garcinia mangostana* L.). Scientia Hort **44**: 215-225.
4. **Downton WJS, Grant WJR, Loveys BR** (1987) Carbon dioxide enrichment increases yield of Valencia orange. Aust J Plant Physiol **14**: 493-501.

5. **Thomas RB, Strain BR** (1991) Root restriction as a factor in photosynthetic acclimation of cotton seedlings grown in elevated carbon dioxide. Plant Physiol **96**:627-634.

Interactive Effects of Growth Salinity and Irradiance on Thylakoid Stacking in Lettuce Plants[1]

Douglas R. Carter and John M. Cheeseman

Dept. of Bio. Sci., Central Conn. State. Univ., New Britain, CT 06050 (DRC) and Dept. of Plant Biology, Univ. of Illinois, Urbana-Champaign, IL 61801 (JMC)

INTRODUCTION

Based on experiments using relatively high levels of growth irradiance, we previously reported that the degree of thylakoid stacking in lettuce plants was significantly reduced by the presence of 100 mM NaCl in the growth medium (5, 6). For the present study, the experimental design was expanded to also include lettuce plants grown at low and moderate levels of irradiance. The expectation was that the salinity-induced reductions in thylakoid stacking would occur similarly at all growth irradiances; however, this was not the case.

In a set of related experiments, the importance of thylakoid stacking was examined in regards to photoinhibition. It is well established that sun plants, relative to shade plants, have less thylakoid stacking and are less prone to photoinhibition (1,11). If photoinhibition is related to the degree of thylakoid stacking, then 10 and 100 mM NaCl-grown plants should differ in their susceptibility to photoinhibition. This hypothesis is based on the fact that 10 and 100 mM NaCl-grown plants have different degrees of stacking even though both were grown under high irradiance.

MATERIALS AND METHODS

Loose-leaf lettuce plants, *Lactuca sativa* L. c.v. Black-seeded Simpson, were grown by hydroponics inside Conviron growth chambers (model E15). The description of the hydroponic system, the growth solutions, and the maintenance protocols have been presented in detail elsewhere (6). The experimental design consisted of a 2 x 3 comparison of two growth salinity levels (10 and 100 mM NaCl) and three growth irradiance levels (60 to 70, 350 to 400, and 700 to 800 $\mu mol \cdot m^{-2} \cdot s^{-1}$ designated respectively as low, moderate and high). At the time of the experiment, the plants were between 4 and 5 weeks-old.

Thylakoid membranes were isolated from freshly harvested leaves and resuspended in an osmotic solution containing 3 mM $MgCl_2$. Digitonin was used to selectively disrupt thylakoid membranes prior to differential centrifugation which resulted in the separation of stacked and unstacked membrane fractions (2,7). The degree of thylakoid stacking was inferred from the amount of chlorophyll in the granal pellet as a percentage of the total amount of chlorophyll before digitonin treatment: greater chlorophyll percentages indicated greater degrees of stacking. Chlorophyll concentrations were determined according to Arnon (4).

The net O_2 exchange rate and relative fluorescence (F_v/F_m) were measured with the Hansatech Leaf Disk System. Apparent photon yields (based on incident irradiance and net rates of O_2 exchange) were obtained by taking steady-state photosynthesis readings over a series of six irradiance settings which ranged from 0 to 85 $\mu mol\ m^{-2}\ s^{-1}$.

Light-saturated rates of electron transfer from H_2O to FeCN were measured polarographically at 18°C using thylakoid membranes uncoupled with 2 μM nonactin and 3 μM nigericin.

Irradiance treatment was given in three different manners: 1) plants were grown under long-term, steady-state irradiances in growth chambers, 2) leaf disks from the afore-mentioned plants were floated in a temperature-controlled bath while being irradiated by a heat-filtered PAR lamp, or 3) plants were removed from growth chambers and an attached leaf was illuminated with a heat-filtered PAR lamp.

RESULTS

Our results suggested that growth salinity and irradiance produce interactive effects on thylakoid stacking in lettuce plants. The presence of 100 mM NaCl in the nutrient solution was associated with less-than-normal amounts of stacking at high irradiances but greater-than-normal amounts of stacking at low irradiances (Fig. 1). These differences in thylakoid stacking corresponded to differences in apparent photon yield; in general, there was a positive correlation between the two variables (Fig. 2).
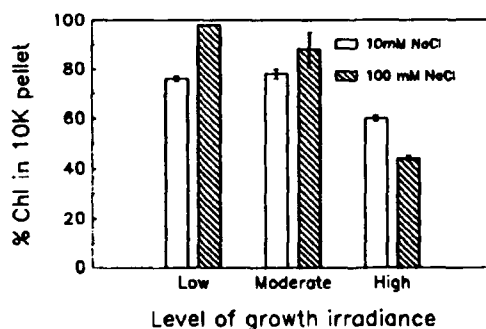
Fig. 1. The percentage of the total chlorophyll in the 10K pellet prepared from lettuce plants grown with different combinations of salinity and irradiance. All of the expanded leaves on each plant were included in the assay. Mean ± s.e., n = 8 for high irradiance, n = 4 for low and moderate irradiance.

214
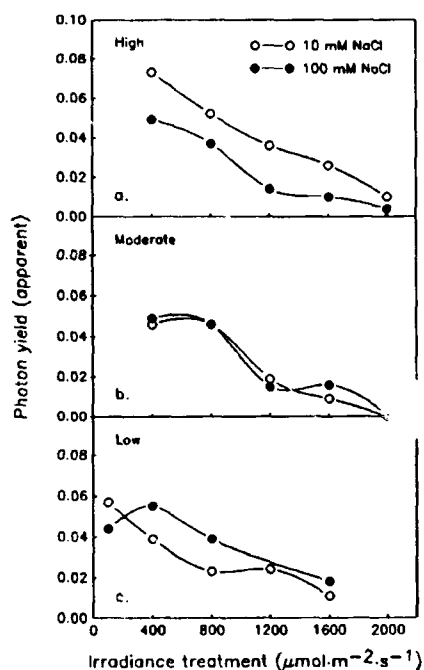
Fig. 2. Apparent photon yields of O_2 evolution measured at 5% CO_2 following two hours of exposure to various levels of irradiance treatment. Each oint represents a plant which was grown at either a) high, b) moderate, or c) low irradiance. Open and closed symbols depict 10 and 100 mM NaCl-grown plants, respectively.

Irradiance treatment ($\mu mol \cdot m^{-2} \cdot s^{-1}$)

Table I. *Photosynthetic characteristics of lettuce plants grown at low, moderate, or high irradiance in combination with either 10 or 100 mM NaCl .*

Maximum rates of net photosynthesis were achieved at saturating light and 5% CO_2. Rates of uncoupled electron transport were determined with saturating red light. Fluorescence measurements were made following 8 hrs of growth chamber darkness.

	LOW	MED	HIGH
	10 mM NaCl		
Max. net photosyn. ($\mu mol\ O_2\ m^{-2}\ s^{-1}$) mean ± s.e., n=5	5.9 ± 0.6	17.0 ± 1.1	8.2 ± 0.6
Thylakoid activity ($\mu mol\ O_2$ mg $chl^{-1}\ hr^{-1}$) mean ± s.e., n=4	210 ± 10	440 ± 10	310 ± 30
F_v/F_m	0.81	0.80	0.73
	100 mM NaCl		
Max. net photosyn. ($\mu mol\ O_2\ m^{-2}\ s^{-1}$) mean ± s.e., n=5	5.4 ± 0.9	17.0 ± 1.6	14.9 ± 1.0
Thylakoid activity ($\mu mol\ O_2$ mg $chl^{-1}\ hr^{-1}$) mean ± s.e., n=4	190 ± 10	380 ± 20	440 ± 20
F_v/F_m	0.84	0.81	0.84

215
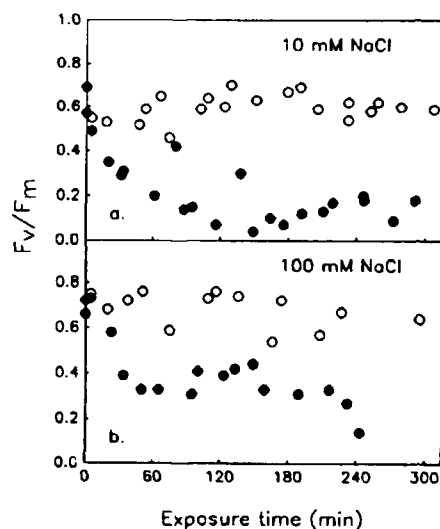
Fig. 3. Values of F_v/F_m after various exposure times of leaf disks to 150 (control) or 2000 $\mu mol\ m^{-2}\ s^{-1}$ irradiance treatment. Four leaf disks were taken from the fifth oldest leaf on each of several plants which had been grown at high irradiance with either a) 10 mM NaCl or b) 100 mM NaCl. The number of leaf disks was equally divided and then floated in two temperature-controlled baths; one was irradiated at the control level and the other received high irradiance. Prior to fluorescence measurements, the leaf disks were kept in a darkened chamber for 5 min. Open symbols are controls.
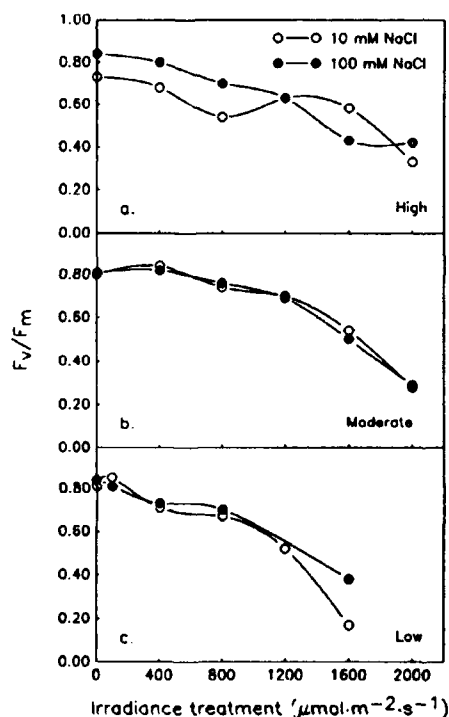
Fig. 4. Values of F_v/F_m after two hours of exposure to various levels of irradiance treatment for lettuce plants grown at either a) high, b) moderate, or c) low irradiance. Prior to fluorescence measurements, the leaf disks were kept in a darkened chamber for 5 min. Open and closed symbols depict 10 and 100 mM NaCl-grown plants, respectively. $F_v = F_m - F_o$.

216

Under steady-state conditions of irradiance and salinity, the symptoms of photoinhibition were detected only in plants grown with a combination of high irradiance and 10 mM NaCl (Table I). Plants grown at high irradiance in combination with 100 mM NaCl showed little or no signs of photoinhibition. Photoinhibition was easily induced in leaf disks taken from both types of plants by subjecting them to 2000 µmol m^{-2} s^{-1} for a 2-hour period (Fig. 3); nonetheless, the residual amounts of relative fluorescence were greater for 100 mM NaCl-grown plants. In experiments using attached leaves, 10 and 100 mM NaCl-grown plants differed in their response to irradiance treatment when plants were grown at high irradiance but not at low or moderate growth irradiance (Fig.4).

DISCUSSION

The effects of growth salinity on thylakoid stacking have been noted elsewhere (5,6,10), but, to the best of our knowledge, there has been no report on the interactive effects of salinity and irradiance on thylakoid stacking. There are, however, publications which describe the interactive effects of salinity and photoinhibition (9,12). Contrary to our findings, those publications concluded that salinity enhances photoinhibition. This discrepancy probably exists because the light-saturated rates of net photosynthesis were much reduced by the given level of salinity in those studies (9,12) but were not reduced in lettuce plants grown with 100 mM NaCl for this study. Without a reduction in photosynthetic capacity, the susceptibility to photoinhibition is not increased by salinity. Under moderate conditions, a salinity-induced decrease in thylakoid stacking may actually reduce the susceptibility to photoinhibition. This possibility is supported by the observations of Mäenpää et al. (8) who found that PS II centers in non-appressed regions appear to be less sensitive to photoinhibition than PS II centers in appressed regions.

CONCLUSIONS

Depending upon the level of growth irradiance, the presence of 100 mM NaCl in the growth solution can either increase or decrease the degree of thylakoid stacking in lettuce plants.

As previously thought (e.g., 3), there appears to be some correlation between photon yield and the degree of thylakoid stacking.

Overall, lettuce plants grown at high irradiance showed fewer signs of photoinhibition when grown in combination with 100 mM NaCl as compared to 10 mM NaCl. The salinity-induced difference in thylakoid stacking may be a factor.

217

ACKNOWLEDGMENTS

LITERATURE CITED

1. **Anderson JM, Osmond CB** (1987) Shade-sun responses: compromises between acclimation and photoinhibition. *In* DJ Kyle, CB Osmond, CJ Arntzen, eds, Photoinhibition, Elsevier Science Publishers, pp 1-38.
2. **Argyroudi-Akoyunoglou JH** (1976) Effect of cation on the reconstitution of heavy subchloroplast fractions (grana) in disorganized low-salt agranal chloroplasts. Arch Biochem Biophys 176:267-274.
3. **Armond PA, Arntzen CJ, Briantais J-M, Vernotte C** (1976) Differentiation of chloroplast lamellae: light harvesting efficiency and grana development. Arch Biochem Biophys 175:54-63.
4. **Arnon DI** (1949) Copper enzymes in isolated chloroplasts. Polyphenoloxidase in *Beta vulgaris*. Plant Physiol 24:1-15.
5. **Carter DR** (1990) The effects of growth salinity and irradiance on thylakoid stacking in lettuce plants. PhD thesis. University of Illinois, Urbana-Champaign.
6. **Carter DR, Cheeseman JM** The effects of external NaCl on thylakoid stacking in lettuce plants. Plant, Cell and Environment (in press).
7. **Goodchild DJ, Park RB** (1971) Further evidence for stroma lamellae as a source of photosystem I fractions from spinach chloroplasts. Biochim Biophys Acta 226:393-399.
8. **Mäenpää P, Andersson B, Sundby C** (1987) Difference in sensitivity to photoinhibition between photosystem II in the appressed and non-appressed thylakoid regions. FEB 215:31-36.
9. **Neale PJ, Melis A** (1989) Salinity-stress enhances photoinhibition of photosynthesis in *Chlamydomonas reinhardtii*. J Plant Physiol 134:619-622.
10. **Pfeifhofer AO, Belton JC** (1975) Ultrastructural changes in chloroplasts resulting from fluctuations in NaCl concentration: freeze-fracture of thylakoid membranes in *Dunaliella salina*. J Cell Sci 18:287-299.
11. **Powles SB** (1984) Photoinhibition of photosynthesis induced by visible light. Ann Rev Plant Physiol 35:15-44.
12. **Sharma PK, Hall DO** (1991) Interaction of salt stress and photoinhibition on photosynthesis in barley and sorghum. J Plant Physiol 138:614-619.

The Short-term Effect of Seawater Dilution on the Photosynthetic Activity of Seaweeds Growing in Shallow Tide Pools[1]

Nobuyasu Katayama, Kumi Takakura and Yautsugu Yokohama

Department of Biology, Tokyo Gakugei University, Koganei-shi, Tokyo 184, Japan (NK, KT); Shimoda Marine Research Center, The University of Tsukuba, Shimoda-shi, Shizuoka 415, Japan (YY)

INTRODUCTION

Seaweeds growing in the intertidal zone experience drastic environmental changes during tidal change. In tide pools, although the environmental changes are not so severe as on a rock, seaweeds occurring there are exposed not only to changes in temperature but also to changes in salinity, pH and DIC[2] concentration.

The photosynthetic characteristics of seaweeds are considered to be closely related to the temperature regimes of their habitats (4, 5, 8). In addition, there seem to be some correlations between the vertical distribution of seaweeds in the intertidal zone and the photosynthetic abilities to tolerate the changes in salinity, pH and DIC concentration (1, 2, 7, 9, 10, 12, 15, 16, 18).

The results of studies focused on the immediate responses of photosynthesis to changes in seawater concentration (6, 13, 17, 20) showed that there are some differences between the immediate, or short term, and long term responses of photosynthesis. In these studies, however, seaweed samples were transferred directly into different concentration media. So, their experimental conditions were somewhat different from natural conditions. The immediate response of photosynthesis to changes in seawater concentration of seaweeds occurring in tide pools, therefore, are still obscure.

In the present work, we have observed the photosynthetic responses of seaweeds occurring in shallow tide pools at different positions in the intertidal zone to a progressive seawater concentration fall which should resemble their *in situ* conditions.

---

[1]Contribution from the Shimoda Marine Research Center, No. 544

[2]Abbreviations: DIC, dissolved inorganic carbon; DW, distilled water; Tris, Tris(hydroxymethyl)aminomethane.

MATERIALS AND METHODS

Plant Materials

The algal fronds of *Enteromorpha crinita*, *Ulva pertusa* and *Grateloupia filicina* were collected from tide pools of Nabeta Bay, Izu Peninsula, Shizuoka, Japan, during a period from October in 1990 to March in 1991. In Nabeta Bay, growth habitats of these seaweeds used are as follows. *Enteromorpha crinita* occurs in tide pools at the uppermost position in the intertidal zone. *Ulva pertusa* is distributed widely, not only in tide pools, but also on rocks in the mid- to lower intertidal zone. Most of the *G. filicina* also occurs in tide pools at the same positions as *U. pertusa* is found. These fronds were brought back to the laboratory immediately and were kept in running seawater until use.

Measurement of Photosynthetic Rate

Fresh weights (0.1 g) of *E. crinita*, 3.4 cm^2 disks from a frond of *U. pertusa*, or an appropriate size of *G. filicina* the area of which was measured after the experiment, were used to measure photosynthetic rates. The improved 'Productmeter' (19) was used to determine the changes in the rate of apparent photosynthetic oxygen production at 20°C under the light intensity of 30 klux (ca. 550 µE m^{-2} s^{-1}) during a stepwise decrease in seawater concentration. In the reaction vessel of the Productmeter, one of the plant materials was placed with 10 ml of various concentrations of seawater. DW or buffered saline (0.05 M Tris buffer, pH 8.2, containing 0.53 M NaCl) was used to dilute seawater. The concentrations of seawater prepared were 100% (normal seawater), 80%, 60%, 40%, 20% and 0% (DW or buffered saline).

As the photosynthetic activity in some seaweeds shows diurnal rhythm (3, 14), the photosynthetic rate of a seaweed in normal seawater was measured in parallel with every measurement of the rate in the series of seawater dilutions. Four or more replicate samples of each species were used.

Determination of the Retained Photosynthetic Activity in DW

After the final measurement of its photosynthetic rate in a series of stepwise dilutions of seawater, a frond was left in the DW for a further 2 hours. As it took one hour to measure the rate in DW, the frond had been immersed in the DW for 3 hours. The photosynthetic rate in normal seawater was measured immediately after reimmersing it in normal seawater.

Determination DIC Concentration in Diluted Seawater

The concentration of DIC in each dilution of seawater was determined as the volume of CO$_2$ evolved from 1 ml of seawater by adding 1. 5 ml of 0. 2 N HCl.

RESULTS

Not only salinity, but also pH and DIC concentration fell when seawater had been diluted by DW (Table I and II). On the other hand, as buffered saline was isotonic to seawater and its pH was the same value as that of seawater, only the DIC concentration fell when seawater had been diluted by the buffered saline (Table II).

The apparent photosynthetic rates of each seaweed in different concentrations of seawater diluted by DW or buffered saline are shown as the relative values to the rate in normal seawater in Fig. 1.

In *E. crinita*, the rate of photosynthesis measured in seawater diluted with DW decreased gradually until 40% seawater and thereafter decreased steeply as the seawater concentration fell. The photosynthetic oxygen evolution in DW, however, was observed at a rate about 20% of the rate obtained in normal seawater. In seawater diluted with buffered saline, the rate of photosynthesis was higher than that in the normal seawater until 40% seawater. The photosynthetic rate in buffered saline was as high as 60% of that in normal seawater.

Table I. *The change in pH as a stepwise decease in seawater concentration.*

	Seawater concentration*					
	100	80	60	40	20	0
pH	8.2	8.1	7.7	7.2	6.6	6.4

*Seawater concentration is shown as percent of normal seawater.

Table II. *The concentration of DIC* in various concentrations of seawater diluted with DW or buffered saline.*

	Seawater concentration**					
	100	80	60	40	20	0
DW	1.0	0.65	0.48	0.36	0.16	0.03
Buffered saline	1.0	0.80	0.58	0.53	0.29	0.23

*Relative ratio to seawater.
**Seawater concentration is shown as percent of normal seawater.
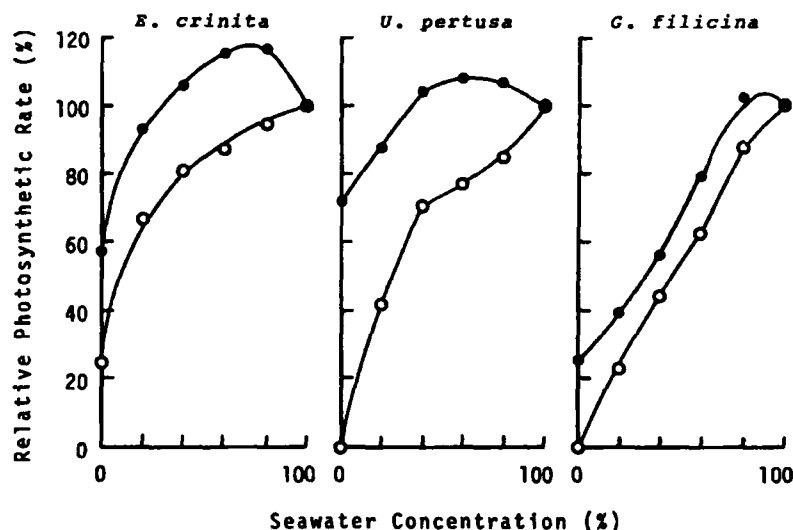
Figure 1. The effect of a stepwise seawater dilution on the rate of apparent photosynthetic oxygen evolution of *Enteromorpha cinita*, *Ulva pertusa* and *Grateloupia filicina*. The rate was measured at 20°C under the light intensity of 30 klux. Seawater was diluted stepwise with DW or buffered saline and the concentration is shown as percent of normal seawater. The rate at each concentration is shown relative to the rate measured in normal seawater. Seawater diluted with DW (O); seawater diluted with buffered saline (●).

In *U. pertusa*, the changing profile of the photosynthetic rate obtained as the seawater concentration fell, was similar to that in *E. crinita* though the decrease in the rate was steeper than that in *E. crinita*. In this species, however, photosynthetic oxygen evolution could not be detected in DW. On the other hand, the photosynthetic rate in buffered saline was as high as 70% of the rate in normal seawater.

In *G. filicina*, the rate of photosynthesis decreased gradually as the seawater concentration fell until completely stopping in DW. The rate also decreased gradually at concentrations lower than 80% of seawater diluted with buffered saline. The photosynthetic oxygen evolution could be detected in buffered saline. The rate was about 20% of that in normal seawater.

After being kept in DW for 3 hours, the frond of each seaweed was reimmersed in normal seawater, then the photosynthetic rate was measured. The photosynthetic activities of *E. crinita*, *U. pertusa*, and *G. filicina* were recovered by 105%, 91% and 80% of the control level, respectively (Table III). The photosynthetic ability of these seaweeds is retained even in freshwater for at least 3 hours.

222

Table III. *The recovery of the rate of photosynthetic oxygen evolution in three seaweeds by reimmersion of their fronds into normal seawater after keeping them in DW for 3 hours.*

	E. crinita	U. pertusa	G. filicina
Recovery(%)	105	91	80

Fronds of each species had been kept in DW for a further 2 hours after measuring the photosynthetic rates in seawater diluted stepwise and in DW. These fronds were transferred into normal seawater, then the photosynthetic rates were mesured. The recovery represents the percent of its initial photosynthetic rate.

DISCUSSION

Photosynthetic responses of seaweeds to salinity changes reported so far are not always comparable with each other. These differences in the responses might be dependent on the differences in experimental conditions and/or on the genetic differences among individual populations of the species examined (15).

Addition of $NaHCO_3$ to diluted seawater, which causes enrichment of CO_2 or HCO_3^-, partially reduced the decrease in the photosynthetic rate of seaweeds (9, 10, 12). From their results, Ogata and Matsui (9, 10) suggested that *salinity* may indirectly affect photosynthetic activity because of differences in CO_2 supply. On the other hand, Zovodnik (20) suggested that subtidal algae can not live in the midlittoral zone as the result of irreversible damage in their cell membranes caused by lower salinity. Thomas *et al.* (17) emphasized that the ability to maintain ionic equilibrium is a major factor governing salt tolerances.

In the present study, these two suggestions were examined. When seawater had been diluted with buffered saline, the concentration of DIC in every dilution step was higher than that of the same step diluted with DW. At 0%, it was about 8 times higher in buffered saline than in DW (Table II). It might be the reason why the photosynthetic rates of these seaweeds measured in a series of seawater dilutions with buffered saline did not decrease so much as those measured in a series of seawater dilution with DW. In cases where the rate of photosynthesis measured in seawater diluted by DW decreases in parallel with the rate measured in seawater diluted by buffered saline, the photosynthetic activity of the seaweed is considered to be affected mainly by the decrease in DIC concentration. The photosynthetic activity of *G. filicina*, therefore, seems to be more sensitive to the decrease in DIC concentration than the other two species.

The photosynthetic saturation in *Ulva* sp. had been obtained at the DIC concentration of about half of that in normal seawater (1). The present results

obtained with *U. pertusa* and *E. crinita* coincide with it. In *U. pertusa* the activity was rather affected by both pH and salinity.

Ogata and Takada (11) have pointed out a tendency that fine filamentous or thin leafy algae are easily affected by the salinity change. Our results, however, are not comparable with them: a fine filamentous alga, *E. crinita*, showed a considerable extent of tolerance to a progressively decreasing salinity. Compared to the other two species, the photosynthetic activity of *E. crinita* seems to be less sensitive to seawater dilution.

The present results indicate that toleration of the dilution of seawater by rainfall must be one of the important properties of seaweeds growing in tide pools although their photosynthetic activities are immediately affected to some extent. Since the extent of changes in the environmental factors depends on the position and size of the tide pool in the intertidal zone, it is reasonable to consider that there are some differences in the abilities to tolerate these changes among seaweeds growing in tide pools at different positions in the intertidal zone. The difference in photosynthetic characteristics among these seaweeds observed in the present study might represent such differences in their growth habitats.

LITERATURE CITED

1. **Beer S, Eshel A** (1983) Photosynthesis of *Ulva* sp. II. Utilization of CO_2 and HCO_3^- when submerged. J Exp Mar Biol Ecol **70**: 99-106.
2. **Bird CJ, McLachlan J** (1986) The effect of salinity on distribution of species of *Gracilaria* Grev. (Rhodophyta, Gigartinales): an experimental assessment. Bot Mar **29**: 231-238.
3. **Kageyama A, Yokohama Y, Nisizawa K** (1979) Diurnal rhythm of apparent photosynthesis of a brown alga, *Spatoglossum pacificum*. Bot Mar **22**: 199-201.
4. **Katayama N, Tokunaga Y, Yokohama Y** (1985) Effect of growth temperature on photosynthesis-temperature relationships of a tide pool alga *Cladophora rudolphiana* (Chlorophyceae). Jap J Phycol **33**: 314-318.
5. **Katayama N, Saitoh M** (1989) The influence of temperature shift on the photosynthesis of two marine macrobenthic algae, *Cladophora densa* and *C. opaca*. Korean J Phycol **4**: 143-147.
6. **Koch EW, Lawrence J** (1987) Photosynthetic and respiratory responses to salinity changes in the red alga *Gracilaria verrucosa*. Bot Mar **30**: 327-329.
7. **Lignell A, Pedersen M** (1989) Effects of pH and inorganic carbon concentration on growth of *Gracilaria secundata*. Br Phycol J **24**: 83-89.
8. **Mizusawa M, Kageyama A, Yokohama Y** (1978) Physiology of benthic algae in tide pools. I. Photosynthesis-temperature relationships in summer. Jap J Phycol **26**: 109-114.
9. **Ogata E, Matsui T** (1965a) Photosynthesis in several marine plants of Japan in relation to carbon dioxide supply, light and inhibitors. Jap Journ Bot **19**(4): 83-98.

10. **Ogata E, Matsui T** (1965b) Photosynthesis in several marine plants of Japan as affected by salinity, drying and pH, with attention to their growth habitats. Bot Mar **8**: 199-217.

11. **Ogata E, Takada H** (1968) Studies on the relationship between the respiration and the changes in salinity in some marine plants in Japan. J Simonoseki Univ Fish **16**: 117-138.

12. **Ohno M** (1976) Some observations on the influence of salinity on photosynthetic activity and chloride ion loss in several seaweeds. Int Revue ges Hydrobiol **61**: 665-672.

13. **Penniman CA, Mathieson AC** (1985) Photosynthesis of *Gracilaria tikvahiae* McLachlan (Gigartinales, Rhodophyta) from the Great Bay Estuary, New Hampshire. Bot Mar **28**: 427-435.

14. **Ramus J, Rosenberg G** (1980) Diurnal photosynthetic performance of seaweeds measured under natural conditions. Mar Biol **56**: 21-28.

15. **Reed RH, Russell G** (1979) Adaptation of salinity stress in, populations of *Enteromorpha intestinalis* (L.)Link. Estuarine Costal Mar Sci **8**: 251-258.

16. **Reed RH, Barron JA** (1983) Physiological adaptation to salinity change in *Pilayella littoralis* from marine and estuarine sites. Bot Mar **26**: 409-416.

17. **Thomas DN, Collins JC, Russell G** (1989) Physiological responses to salt stress of two ecologically different *Cladophora* species. Bot Mar **32**: 259-265.

18. **Yarish C, Edwards P, Casey S** (1979) Acclimation responses to salinity of three estuarine red algae from New Jersey. Mar Biol **51**: 289-294.

19. **Yokohama Y, Katayama N, Furuya K** (1986) An improved type of 'Productmeter', a differential gasvolumeter, and its application to measuring photosynthesis of seaweeds. Jap J Phycol **34**: 37-42 (in Japanese).

20. **Zovodnik N** (1975) Effects of temperature and salinity variations on photosynthesis of some littoral seaweeds of the North Adriatic Sea. Bot. Mar. **18**: 245-250.

Plant Isoprene Emission Responses to the Environment

Francesco Loreto and Thomas D. Sharkey

*Department of Botany, University of Wisconsin, Madison, WI 53706
USA*

INTRODUCTION

Isoprene (2-methyl 1,3-butadiene) is the simplest member of the isoprenoid or terpenoid family. It has five carbons, two double bonds, and is branched. Both plants and animals emit isoprene. Isoprene in the atmosphere is almost all from plants, primarily trees. People lose about 1 mg per day for an estimated total of 2×10^9 grams per year, 5 orders of magnitude less than plants. Isoprene synthesis in plants occurs in chloroplasts (8) and is a major biochemical pathway. Often about 1% of the carbon fixed in photosynthesis is rapidly emitted as isoprene. In certain species or under specific environmental conditions the percentage of carbon emitted as isoprene can be up to 8%.

Isoprene accounts for 55 to 95% of the total nonmethane hydrocarbon flux from the biosphere to the atmosphere, depending upon location (Consensus reached at the Southern Oxidants Research Program on Emissions and their Effects meeting at Raleigh, NC, Oct. 1991). The total flux of isoprene to the atmosphere is similar to that of methane, about 300×10^{12} grams per year. The residence time of methane in the atmosphere is about 10 years and the concentration is over 1.5 ppm. The residence time of isoprene in the atmosphere is less than one day and the concentration of isoprene in the atmosphere is typically 2 to 5 ppb, and often much less, for example at night.

The breakdown of isoprene in the atmosphere can lead to the formation of particles which scatter light causing a blue haze which can be seen above forested mountains (9). When NO_x is in low concentration, isoprene oxidation removes ozone and hydroxyl radicals from the lower atmosphere. However, when the concentration of NO_x is high, isoprene oxidation can cause ozone formation in the lower atmosphere (1). Each isoprene molecule can produce many ozone molecules. Lower atmosphere ozone is a significant pollutant in the eastern United States. We have studied isoprene biosynthesis because it is a relatively large flux of carbon in the biosphere whose function is unknown. We are also interested in making better estimates of the role of biogenic isoprene in ozone pollution episodes. We report some of our work on the interaction between isoprene emission and the environment which may improve estimates of the magnitude of isoprene flux from the biosphere to the atmosphere.

226

RESULTS AND DISCUSSION

Isoprene Emission by Plant Leaves and Environmental Parameters

Light. The response of isoprene emission to light paralleled the response of photosynthesis (Fig. 1). No isoprene was produced in the dark. Isoprene emission was greatest from leaves grown in full sunlight. It was lower in leaves grown in the shade, even when corrected for the effect of growth in the shade on the rate of photosynthesis (Table 1). This indicates that in groves and forests, isoprene is produced primarily by the upper part of the canopy. Leaves lower in the canopy are expected to produce less isoprene both because of the direct effect of lower light (Fig. 1) and because of the effect of shade during leaf development (Table 1). Although isoprene emission is clearly a light-dependent process, we found no evidence for a relationship between isoprene emission and photorespiration or reduction status of the photosynthetic electron transport chain (4, 2). Light may be required for the enzymatic synthesis of isoprene (7).

Carbon dioxide. Carbon dioxide, which strongly influences the rate of photosynthesis, also affects the rate of isoprene emission, though the responses were not parallel (Fig. 2). We found that isoprene is derived directly from carbon being assimilated by photosynthesis (6). We also have evidence from gas-exchange results, inhibitor studies (2) and direct metabolite measurement (Loreto and Sharkey, unpublished) that ATP status is the most important photosynthetic metabolite affecting isoprene emission.
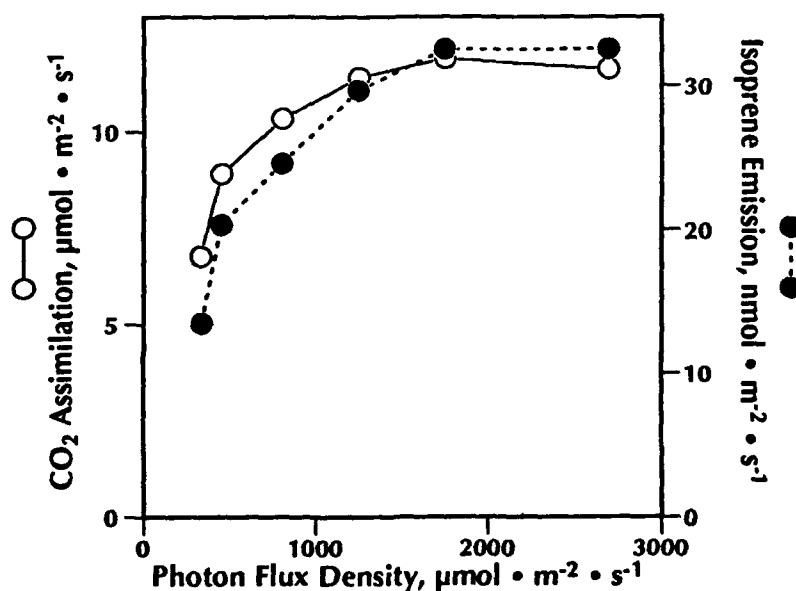
Figure 1. Response of isoprene emission and CO_2 assimilation to light intensity. Redrawn from Loreto and Sharkey (1990).

227

Table I. Isoprene emission, CO_2 assimilation, and chlorophyll a/b ratio, from leaves of oak exposed to sun or shade and assayed at 25°C. under a light intensity of 400 μmol $m^{-2}s^{-1}$. **, ***, indicate that differences are statistically significant at 5 and 1% level, respectively (ANOVA, n=5). Data from Sharkey et al. (1991).

	Isoprene (nmol $m^{-2} s^{-1}$)	CO_2 Assimilation (μmol $m^{-2} s^{-1}$)	Isoprene/CO_2 (%)	chl a/b ratio
Sun	22.0 ± 4.3	10.0 ± 1.7	1.1 ± 0.1	3.29 ± 0.12
Shade	5.5 ± 2.1	7.2 ± 0.6	0.53 ± 0.07	2.86 ± 0.11
ANOVA	***	***	***	**
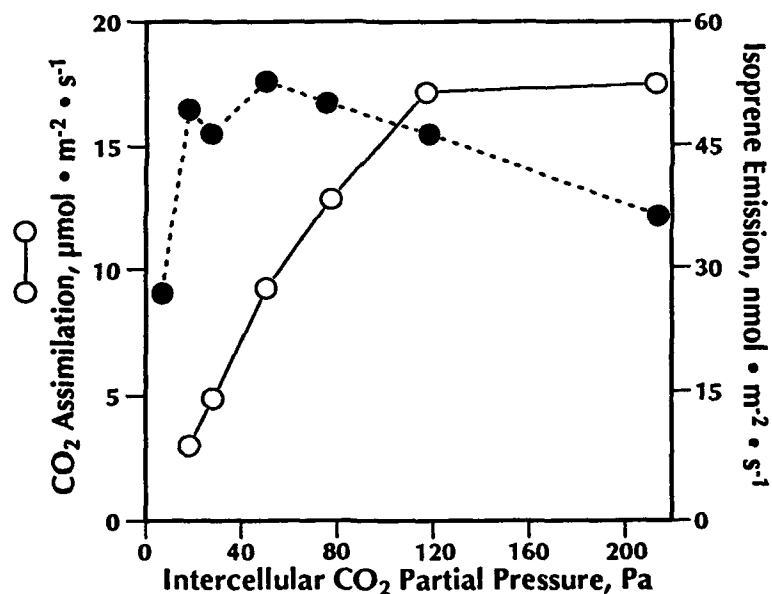
Figure 2. Response of isoprene emission and CO_2 assimilation to intercellular CO_2 partial pressure. Redrawn from Loreto and Sharkey (1990).

Temperature. Isoprene emission is dramatically affected by temperature (Fig. 3). We have generally found a Q_{10} around 3; however, the Q_{10} may exceed 5, particularly above 25°C. The response of isoprene emission to temperature is different from that of photosynthesis and likely reflects the temperature sensitivity of the isoprene synthase (3).

228

Isoprene Emission By Plant Leaves and Environmental Stresses

Mechanical stresses. We imposed a series of mechanical stresses whose occurrence is common in nature and we found that mechanical stresses generally reduce isoprene emission by leaves (Fig. 4). The rate of photosynthesis, as well as stomatal conductance, were often unaffected by the stress. When they were affected, they responded more slowly than isoprene emission, indicating that the isoprene response was not a consequence of changes in photosynthesis. The reduction of isoprene emission depended on: a) the **severity** of the stress; mild stress (e.g. a 25 km h^{-1} wind) caused less reduction. b) the **duration** of the stress; reduction of isoprene emission persisted for as long as the stress was under way.
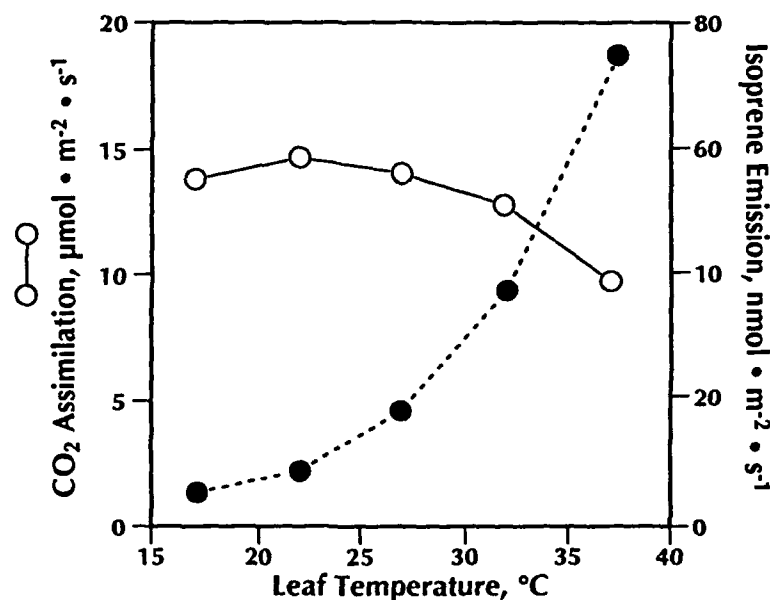
Figure 3. Response of isoprene emission and CO_2 assimilation to temperature. Redrawn from Loreto and Sharkey (1990).

c) the **distance** of the stress; isoprene emission responded to mechanical stresses affecting leaves of other nodes in the same stem or even in different stems of the same plant. The signal affecting isoprene emission traveled upstream or downstream for at least 52 cm and with a constant velocity of 1.7 mm s^{-1} (Fig. 5). This speed is comparable to the speed of propagation of electrical signals (5). The response of isoprene to mechanical stresses is very consistent and this makes isoprene emission an excellent stress indicator in plants.

Water stress. Isoprene emission is generally stimulated by mild water stress (Fig. 6). When the water stress was severe, however, the rate of photosynthesis dropped and isoprene emission was reduced, probably because of carbon
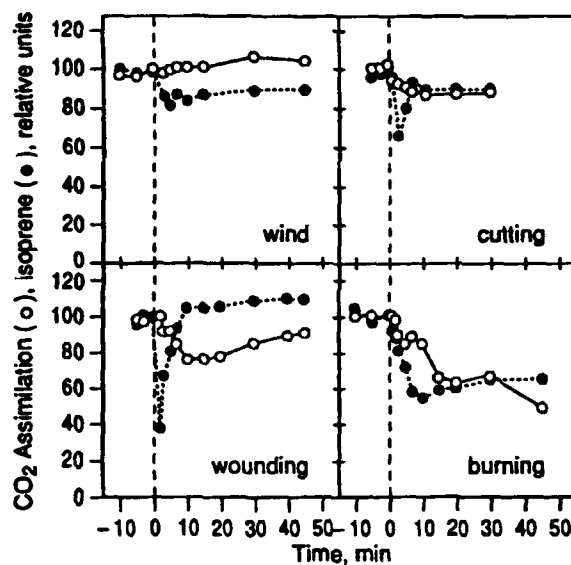
Figure 4. Effects of mechanical stresses on isoprene emission and photosynthesis. From Loreto and Sharkey (unplublished).
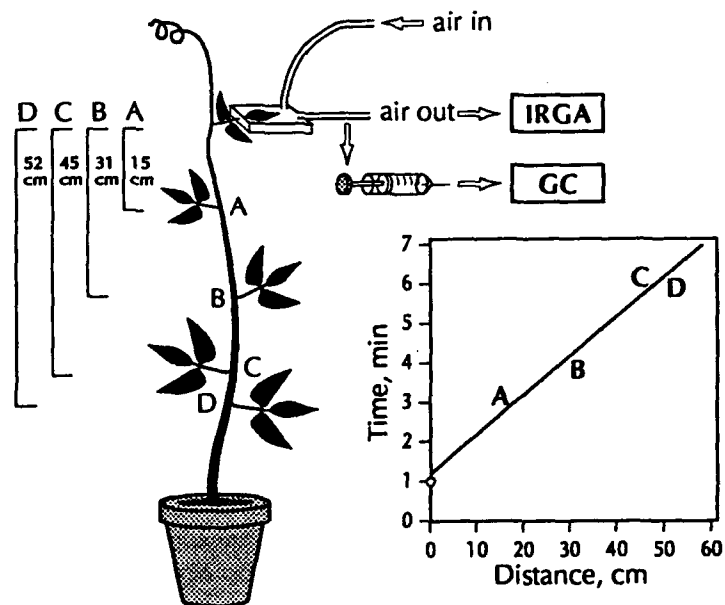
Figure 5. Sketch of the apparatus for isoprene detection. In the inset, effect of distance on the time-course of isoprene response to burning. (Loreto and Sharkey, unpublished).
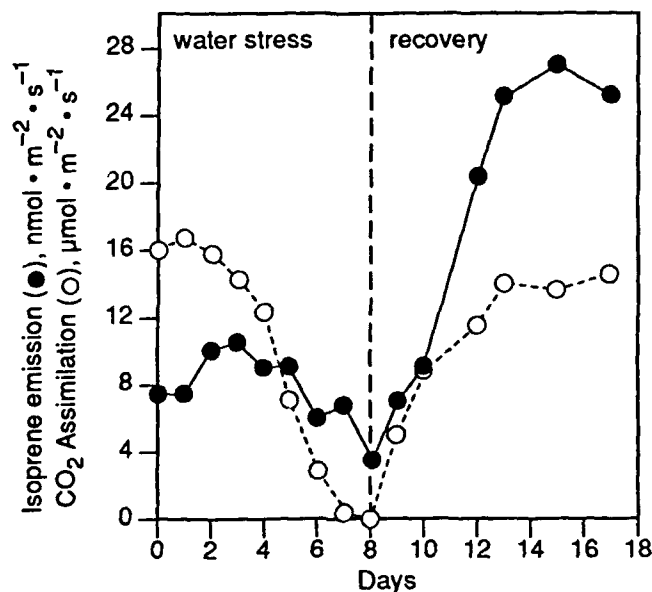
Figure 6. Response of isoprene emission and photosynthesis to water stress affecting the whole plant and to the following water stress recovery.

starvation. Water stress recovery surprisingly stimulated isoprene emission. This stimulation persisted until leaf senescence began. Water stress may cause favorable changes in the activation of enzymes responsible for isoprene synthesis. A relationship could also exist between isoprene stimulation and increased sugar availability during a recovery from water stress (J. Passioura, person... communication).

CONCLUSIONS

Isoprene emission by vegetation responds strongly to changes in the environment. The response to environmental stresses, in particular, adds new variables to algorithms for estimating isoprene emission in plant communities. Many procedures for measuring isoprene emission rates mechanically perturb the leaves or change the surrounding environment. We have shown that manipulation of any part of the plant may reduce the rate of isoprene emission. Particularly when the wind is calm and temperature high the difference can be relevant and the underestimation of isoprene emission may result in an underestimation of tropospheric ozone production from biogenic precursors.

231

LITERATURE CITED

1. **Chameides WL, Lindsay RW, Richardson J, Kiang CS** (1988) The role of biogenic hydrocarbons in urban photochemical smog: Atlanta as a case study. Science **241**: 1473-1475.
2. **Loreto F, Sharkey TD** (1990) A gas-exchange study of photosynthesis and isoprene emission in *Quercus rubra* L. Planta **182**: 523-531.
3. **Monson RK, Jaeger CH, Adams WWIII, Driggers EM, Silver GM, Fall R** (1992) Plant Physiol **98**: 1175-1180.
4. **Monson RK, Fall R** (1989) Isoprene emission from Aspen leaves. The influence of environment and relation to photosynthesis and photorespiration. Plant Physiol. **90**: 267-274.
5. **Pickard BG** (1983) Action potentials in higher plants. Bot. Rew. **39**: 172-201.
6. **Sharkey TD, Loreto F, Delwiche CF** (1991) High carbon dioxide and sun/shade effects on isoprene emission from oak and aspen tree leaves. Plant Cell & Environ. **14**: 333-338.
7. **Silver GM, Fall R** (1991) Enzymatic synthesis of isoprene from dimethylallyl diphosphate in aspen leaf extracts. Plant Physiol. **97**: 1588-1591.
8. **Sanadze GA** (1990) The principle scheme of photosynthetic carbon conversion in cells of isoprene releasing plants. Cur. Res. Photosyn. IV: 231-237.
9. **Went FW** (1960) Blue hazes in the atmosphere. Nature **187**: 641-643.

PHOTOINHIBITION AS A TOOL FOR PROBING THE SITES OF ELECTRON DONOR PHOTOOXIDATIONS: ^{125}I-PHOTOOXIDATION AND IODINATION OF D_L

Danny J. Blubaugh and George M. Cheniae

Dept. of Chemistry and Biochemistry, Utah State University, Logan, UT 84322 (DJB) and University of Kentucky, Lexington, KY 40546 (GMC)

Exogenous electron donors to PSII have been shown to be oxidized via two independent sites, both of which are incapacitated during weak-light (40 μE m^{-2} s^{-1}) photoinhibition when O_2 evolution is impaired. Site 1, or Y_{Z+}, is incapacitated relatively rapidly ($t_{1/2}$ ~2 min), whereas Site 2 is lost slowly ($t_{1/2}$ > 1 h). The identity of Site 2 has not been definitively established, though it has been attributed to Y_{D+}. In this experiment, the capacity of NH$_2$OH-extracted wheat PSII membranes to be iodinated via photooxidation of ^{125}I- was examined. Samples were subjected to SDS-PAGE, and gel slices were analyzed by γ-scintillation counting. Two bands contained the ^{125}I label; both reacted with antibody raised against the D_1 but not D_2 protein. Both bands also carried a ^{14}C label if the membranes had been photoaffinity labeled with ^{14}C-azido-atrazine. Thus, the two bands are conformers of D_1. No ^{125}I labeling of D_2 was observed, although I$^-$ is shown to be nearly as efficient an electron donor at Site 2 as at Y_{Z+}. The capacity for iodination of the D_1 protein was lost biphasically during photoinhibition ($t_{1/2}$ ~ 3 min and 35 min). The fast phase, corresponding to >80% of the loss, paralleled the loss of electron donor photooxidations by Y_{Z+} and loss of the Y_{Z+} EPR Signal II$_f$. The ~20% slow phase may be due to ^{125}I-photooxidation at Site 2, followed by reaction of ^{125}I- with Y_Z or another Tyr residue of D_1. Thus, Site 2 is probably located within or extremely close to D_1. The data are not supportive of, but do not necessarily rule out, assignment of Y_{D+} to Site 2.

ROLE OF PHOTOSYNTHESIS IN AMELIORATION OF UV-B DAMAGE

Steven J. Britz and Paulien Adamse

Climate Stress Laboratory, USDA, ARS, NRI,
Beltsville, Maryland 20705

Sensitivity of plants to UV-B radiation (280-315 nm) is generally reduced at high background illumination. The relative contribution of photosynthesis to this effect was investigated by treating 10 d old cucumbers for 4 d with supplemental UV-B (18 k. m^{-2} daily "biologically-effective" radiation) at high photosynthetically-active radiation (1000 µmol m^{-2} s^{-1}) and either 450 or 750 ppm atmospheric CO_2. Both UV-sensitive and insensitive cultivars were examined with similar results for each. Brief UV-B treatment inhibited leaf growth, as indicated by reduced area and dry matter in the expanding third leaf, but photosynthetic gas exchange on a chlorophyll or dry matter basis was not affected. Elevated CO_2 enhanced plant dry matter accumulation and reversed the inhibition of growth of the third leaf by UV-B. The accumulation of UV-absorbing flavonoid compounds was enhanced by UV-B exposure, but was not affected by CO_2 enrichment.

A MECHANISM OF UV-B DAMAGE IN MARINE CHROMOPHYTES

S.K. Clendennen, R.S. Alberte, and D.A. Powers

Hopkins Marine Station of Stanford University, Pacific Grove, CA 93950 (SKC, DAP) and University of California, Los Angeles, Los Angeles, CA 90007 (RSA)

Anthropogenic ozone depletion is expected to result in drastic regional and seasonal increases in solar ultraviolet light reaching the earth's surface and penetrating the water column. Marine chromophytes, because of their unique light harvesting system, are at increased risk for ultraviolet light damage. In this study, UV-B irradiation (280-320nm) is shown to affect photosynthesis in the chromophyte *Macrosystis pyrifera* (the giant kelp). Changes in the absorptive characteristics and energy transfer capabilities of light harvesting pigments are implicated in the reduction of photosynthesis.

MEASUREMENTS OF PHOTOSYNTHETIC EFFICIENCY AND PHOTOINHIBITION OF MARINE PHYTOPLANKTON BY MEANS OF CHLOROPHYLL FLUORESCENCE

C. Geel, J.F.H. Snel, J.W. Hofstraat and J.C.H. Peeters

Department of Plant Physiological Research, Wageningen Agricultural University, Gen. Foulkesweg 72, The Netherlands (CG, JFHS, JWH) and Tidal Waters Division, Public Works Department, P.O. Box 20907, NL-2500 EX The Hague, The Netherlands (JCHP)

The saturating pulse method can be used to obtain information on the photosynthetic characteristics of marine phytoplankton using chlorophyll fluorescence. This is illustrated with the chlorophyte *Dunaliella tertiolecta* grown in batch cultures at 8 different light regimes. F_O, F_M, F and F_M' and the number of cells were determined every day using a PAM-fluorimeter and a custom-built flow-cytometer respectively. During exponential growth the efficiency of photosystem II electron transport ($F_M'-F/F_M'$) and ($F_M-F_O)/F_M$ which is related to photoinhibition were constantly high. As nutrients become limiting exponential growth stops. At this moment the efficiency of photosystem II starts to decrease. So the photosynthetic efficiency seems to be a useful parameter to monitor the growth state of *Dunaliella tertiolecta*. As the exponential growth stops also F_V/F_M starts to decrease indicating a kind of photoinhibition related to the availability of nutrients as it wasn't visible during the exponential growth phase. The saturating pulse method is a non-invasive method to measure photosynthetic parameters in phytoplankton and could be made suitable for application *in situ*.

CAROTENOID CONTENT OF THE OLIGOMERIC FORM OF THE MAJOR LIGHT-HARVESTING PROTEIN COMPLEX, LHC IIb, AT VARYING LIGHT CONDITIONS

Angela I. Lee and J. Philip Thornber

Dept. of Biology, University of California, Los Angeles, CA, 90024.

We are interested in the structure and function of the multiple pigment-protein complexes involved in photosynthesis. These complexes bind carotenoids as well as chlorophylls *a* & *b*. I am characterizing the carotenoid content of the major light-harvesting protein complex, LHC IIb, in barley plants exposed to high light. The oligomeric form of LHC IIb from plants exposed to dim light binds the carotenoids neoxanthin, violaxanthin and lutein. Under high light, violaxanthin is converted to zeaxanthin via the xanthophyll cycle. This conversion may have a photo-protective role for the plant, since the appearance of zeaxanthin has been

correlated with increased non-radiative energy dissipation. To date, this xanthophyll cycle has only been studied in the whole leaf. I am attempting to localize the site of the xanthophyll cycle within the chloroplast. My studies so far indicate that the zeaxanthin produced during photoconversion of violaxanthin is not associated with the LHC IIb complex. Analysis of the carotenoid content of the other pigment-protein complexes from plants exposed to differing environmental conditions will further elucidate the role of these pigments in photoprotection.

PHOTOINHIBITION IN *ULVA*: PHOTOPROTECTION AND PHOTOINHIBITORY DAMAGE

Barry Osmond, Joe Ramus, Linda Franklin, Guy Levavasseur and Bill Henley

Duke University Marine Laboratory, Beaufort NC 28516, USA (JR, LF), Research School of Biological Sciences, ANU, Canberra 2601, Australia (BO), Station Biologique, CNRS F-29680 Roscoff, France (GL), and Marine Science Inst, University Texas at Austin, Port Aransas TX73373-1267 USA (BH)

The PFD response profiles of photosynthetic O_2 evolution, photochemical (qP) and nonphotochemical (qN) chlorophyll fluorescence quenching, and assessment of the cumulative PFD dependence of changes in 5 minute dark adapted F_O and F_V/F_M were made using a PAM 101 fluorescence detector (Walz, Effeltrich, FRG) synchronised with a computer operated LED light source and O_2 electrode system (Hansatech, Kings Lynn, Norfolk UK). Effects of growth light environment, dissolved inorganic carbon (DIC) and inhibitors (CMP chloramphenicol and DTT, dithiothreitol) on photoprotective processes ($F_O\downarrow$ $F_V/F_M\downarrow$) and photoinhibitory damage ($F_O\uparrow$ $F_V/F_M\downarrow$) were examined. Shade-grown *Ulva*, with only about half the rate of photosynthetic O_2 evolution in seawater at light saturation (50 - 200 µmol photons $m^{-2}s^{-1}$) of sun grown tissue, showed greater photoinhibitory damage ($F_O\uparrow$), more rapid and extensive qP$\downarrow$, and smaller, slower qN$\uparrow$. Greatest photoinhibitory damage was observed in shade-grown *Ulva* exposed above light saturation in -DIC +DTT +CMP treatment. This treatment which also led to severe photoinhibitory damage in sun-grown *Ulva*. Removal of DIC alone was sufficient to accelerate qP$\downarrow$ and photoinhibit ($F_O\uparrow$) in both shade and sun-grown tissue, in spite of accelerated qN$\uparrow$. Only part of the qN$\uparrow$ in -DIC treatments was inhibited by DTT, but DTT treatment accelerated $F_O\uparrow$ showing that this part of qN$\uparrow$ was photoprotective. Treatment with CMP did not alter qN$\uparrow$ response in -DIC treated sun-grown tissue but it did accelerate $F_O\uparrow$, showing that inhibition of chloroplast protein synthesis accelerated photoinhibitory damage.

PURIFICATION OF VIOLAXANTHIN DE-EPOXIDASE BY LIPID AFFINITY PRECIPITATION

David C. Rockholm and Harry Y. Yamamoto

Dept. of Plant Molecular Physiology, University of Hawaii at Manoa, Honolulu, HI 96822

Violaxanthin de-epoxidase (VDE) catalyzes the conversion of violaxanthin to zeaxanthin in chloroplast thylakoids. In higher plants, whenever light exceeds a plant's capacity for carbon-fixation, zeaxanthin apparently plays a role in photoprotection by mediating non-radiative dissipation (i.e. heat) of light energy. In view of VDE's central role in this process, its structure and properties are of considerable interest. Previously, VDE was partially purified from *Lactuca sativa* var. Romaine by extracting broken chloroplasts at different pH's and chromatographing by size exclusion. VDE has now been further purified through anion-exchange (Pharmacia Mono Q column) followed by a unique lipid affinity precipitation step to yield one major polypeptide as detected in 2-D SDS-PAGE. VDE associates with a mixture of monogalactosyl diacylglycerol (MGDG), the principal thylakoid lipid, and violaxanthin in pH 5.2 buffer. Replacing violaxanthin with zeaxanthin reduces the association to levels below that with MGDG alone. Very little VDE precipitated when lecithin, digalactosyl diacyglycerol, phosphatidylcholine, or phosphatidylethanolamine replaced MGDG. Active VDE was resolubilized using n-octyl β-D-glucopyranoside. The purified protein has a pI of 5.4 and determined to have K_M's for ascorbate and violaxanthin of 4.5 mM and 0.35 μM respectively.

THE ISOLATION OF FLAVONOL MUTANTS IN *ARABIDOPSIS THALIANA*

John J. Sheahan and Garry A. Rechnitz

Department of Chemistry, University of Hawaii at Manoa. 2545 The Mall, Honolulu HI 96822.

Depletion of the ozone layer is increasing the amount of UV-B radiation reaching the earths surface. The enhanced aging and mutation associated with UV-B damage suggests that crop yields may be threatened. However, plants are protected by flavonols which absorb UV-B. Although a great deal of research has been done on the flavonols, progress has been hampered by their lack of color. To overcome this problem, a staining procedure that provided sensitive

237

and specific fluorescence identification of flavonols in *Arabidopsis thaliana* was developed. Three T-DNA insertional mutants, which lacked flavonols were identified, and the heritability of each has been confirmed by its multiple occurrence in the parental line. The mutants are being outcrossed, and analysis of the F2 will test if any of the mutations are tagged by a T-DNA insert. If so, the tagged gene will then be cloned.

INACTIVE PHOTOSYSTEM II CENTERS IN SPINACH LEAVES: OCCURRENCE AND PROPERTIES

Jan F.H. Snel, Hans Boumans and Wim J. Vredenberg

Department of Plant Physiological Research, Wageningen Agricultural University, Gen. Foulkesweg 72, NL 6703 BW Wageningen, The Netherlands

The fraction inactive, or non-Q_B-reducing, PSII centers was studied in spinach leaves in relation to light adaptation. The fraction inactive PSII centers was determined 1) by means of flash-induced absorbance changes at 520 nm using isolated chloroplasts and 2) by new procedure using combined photoacoustic and fluorescence measurements on leaf discs. The fraction inactive PSII centers was very small in leaves kept in the dark for more than 7 hrs. After 7 hours of adaptation to daylight this fraction has been observed to be as high as 0.45. The lifetime of inactive centers in the closed state is estimated to be about 300 ms. The fraction inactive centers did not appear to be correlated with either the magnitude of the initial fluorescence rise 0-I in the presence of FeCy nor a lower F_V/F_M. Properties, occurrence and role of inactive PSII centers will be discussed.

REDOX STATE OF A ONE ELECTRON COMPONENT CONTROLS THE RATE OF PHOTOINHIBITION OF PHOTOSYSTEM II

John Whitmarsh, Guy Samson and Ladislav Nedbal

Photosynthesis Research Unit, USDA/Agricultural Research Service (JW, GS) Departments of Plant Biology (JW, LN) and of Physiology and Biophysics (JW), University of Illinois 197 PABL, 1201 W.Gregory Dr., Urbana, IL61801

We discovered a one electron redox component that, when chemically reduced prior to light exposure, increased more than 15-fold the initial rate of photoinhibition (Nedbal et al. 1990, Proc.Natl.Acad.Sci. USA, *in press*). By

performing polarographic redox titrations of photoinhibition in isolated thylakoid membranes in anaerobic medium, it was found that the midpoint potential of the component was +27mV at pH 7.5 and exhibited a slight pH dependence of -9 mV/pH unit. Our preliminary data show that these redox characteristics correspond well with those of the low potential cytochrome $b559$. We propose that the low potential cytochrome $b559$ is able to protect PSII against photoinhibition by accepting electrons from reduced pheophytin. At low redox potential, accelerated photoinhibition is observed because the cytochrome $b559$ is reduced and the protective electron transfer cannot occur.

LASER INDUCED FLUORESCENCE OF INTACT PLANTS

Emmett W. Chappelle, J.E. McMurtrey, M.S. Kim, and L. Corp

*NASA/GSFC, Code 693, Greenbelt, MD 20771 (EWC),
ARS, USDA, Beltsville, MD (JEM) Univ, of MD, College Park, MD
(MSK, LC)*

Green plants contain a number of compounds which fluoresce when excited by light of the proper wavelength. The irradiation of plants with a high intensity laser beam induces a measurable fluorescence in intact plants. The use of laser induced fluorescence (LIF) in the assessment of certain plant parameters are being investigated. A pulsed nitrogen laser was used in these studies. It has been found that differences in the biochemical composition of different plant types allow the identification of plant types on the basis of their fluorescence spectra fingerprints. The plant types included herbaceous dicots, monocots, hardwoods, and conifers. The dicots and monocots had fluorescent maxima at 440, 685, and 740 nm. The monocots could be distinguished from the dicots by virtue of having a much higher 440 nm/685 nm ratio. Hardwoods and conifers had an additional fluorescence band at 525 nm, but healthy conifers did not have a band at 685 nm. Algorithms have been developed relating fluorescence changes to a number of stress factors at a previsual stage. These stress factors include environmental (atmospheric pollutants such as ozone, "acid rain", and heavy metals), drought, nutrient deficiencies, and disease. Most recently, an algorithm has been developed by which the fluorescence band at 440 nm can be used to estimate the rate of photosynthesis.

THE PHOTOSYNTHETIC CHARACTERISTICS OF *SAINTPAULIA*

J. Harbinson and P. van Vliet

ATO-DLO, P.O. Box 17, 6700 AA Wageningen, Netherlands

Saintpaulia is a genus of tropical African herbs of which the best known is *S. ionantha*, the African Violet of commerce. These plants are shade demanding, slow growing and with low rates of photosynthesis. They are, in many respects, the photosynthetic antithesis of crop plants. The relationships between the quantum yield for electron transport by photosystems I and II, and CO_2 fixation have been determined for these plants. They show that though the photosynthetic characteristics of wild type *Saintpaulia* are broadly comparable to those of crop plants, though with a lower throughput, the responses of the horticultural types is unusual in many respects. These unusual responses will be considered in the context of the control of electron transport and whole plant physiology of the plants.

THE EFFECT OF A PHOTOINHIBITORY TREATMENT ON CARBON FIXATION WITHIN LEAVES OF PLANTS GROWN UNDER "SUN" AND "SHADE" CONDITIONS

Jindong Sun and John N. Nishio

Department of Botany, University of Wyoming,
Laramie, WY 82071-3165

We are interested in leaf anatomical features that may be involved in a plant's ability to withstand a high photon flux density. We have successfully investigated the effects of photoinhibition on carbon fixation within spinach *(Spinacea oleracea)* leaves by $[^{14}C]$-CO_2 labeling. The relative distribution of carbon reduction across a leaf is different in growth chamber grown "sun" and "shade" (decreased R:FR ratio) plants. Changes in the relative distribution of CO_2 fixation across a leaf after a photoinhibitory treatment also changed. Additionally chlorophyll content and Chl *a/b* ratios across the leaf have been measured. The extent of the photoinhibition was illustrated at the whole leaf level by pulse amplitude modulated fluorescence of the adaxial surface. The data may impact directly current models of photosynthesis across leaves. Work in progress is investigating changes in protein composition and synthesis within leaves.

THE EFFECTS OF ANAEROBIOSIS ON CHLOROPHYLL FLUORESCENCE

Gary C. Harris[1] and Ulrich Heber[2]

[1]Biol. Dept., Wellesley College, Wellesley MA 02181 [2]Inst. Botanik, Dallenbergweg 64, 8700 Wuerzburg, Germany

When spinach leaf discs were incubated in a dark anaerobic environment (N_2), the chlorophyll fluorescence yield, as measured by a pulsed modulated exciting beam of extremely low intensity, increased dramatically. Following prolonged periods of anaerobiosis the fluorescence yield was sometimes seen to approach 80% of the fluorescence maximum (F_M). The increased fluorescence yield could be relaxed by O_2 or by light which preferentially excites photosystem I. Whereas the weak red light source (7.4 mW m^{-2}), normally used to measure chlorophyll fluorescence yield, elicited no chlorophyll fluorescence induction phenomena in the presence of O_2, it did so under N_2. This induction involved both a rapid and slow rise in fluorescence yield that was often followed by a slow quenching. Induction was observed by light levels as low as 400 µW/m^2. The data suggests that an algal type chlororespiration exists in higher plants and that O_2 can directly interact with the quinone pool regulating its redox status.

EFFECTS OF VARIOUS ENVIRONMENTAL STRESSES ON ELECTRON FLOW THROUGH PHOTOSYSTEM I OF *SYNECHOCOCCUS*

Stephen K. Herbert and David C. Fork

Department of Biological Science, University of Idaho, Moscow, ID 83843 (SKH) and Department of Plant Biology, Carnegie Institution of Washington, Stanford, CA 93405 (DCF)

The photoacoustic method was used to quantify Photosystem 1-driven electron flow in intact cells of the cyanobacterium *Synechococcus* following various stress treatments. Measurements were made in the presence of 25 µm DCMU and the activity observed was taken to represent primarily cyclic electron flow around Photosystem I. Photosystem I activity was found to be much more resistant to photoinhibition by both visible and ultraviolet (254 nm) light than was whole-chain, oxygen-evolving electron flow. In cells starved for nitrogen, phosphorus, or sulfur, Photosystem I activity also decreased much less than did oxygen evolving electron flow. Oxidative stress, induced by methyl viologen and weak light, was strongly inhibitory of electron flow through Photosystem I, however. Time-resolved spectroscopic measurements at 705 nm indicated that the primary

241

site of this oxidative damage was at a secondary electron acceptor of Photosystem 1, possibly ferredoxin in the cytosol.

QUENCHING OF CHLOROPHYLL FLUORESCENCE IN FE-DEFICIENT SUGAR BEET (*BETA VULGARIS* L.) LEAVES

Fermín Morales, Anunciación Abadía, and Javier Abadía

Dept. of Plant Nutrition, Aula Dei Experimental Station, CSIC, Apdo. 202, 50080 Zaragoza, Spain

The effects of iron deficiency on the efficiency of excitation energy capture by open photosystem II reaction centers, the quantum yield of linear electron transport and the fluorescence quenching mechanisms at steady-state photosynthesis have been investigated by measuring modulated chlorophyll fluorescence in intact, attached leaves from Fe-deficient sugar beet (*Beta vulgaris* L.). Iron deficiency decreases the quantum yield of linear electron transport and modifies the relative extent of several fluorescence quenching mechanisms at steady-state photosynthesis. Even moderate Fe deficiency apparently induces a decreased quantum yield of photosystem II electron transport and a decreased photochemical quenching, most likely through a closure of photosystem II centers, in the conditions prevailing in the growth chamber. When Fe deficiency became more intense there was an increase in non-photochemical quenching (mostly energy dependent quenching). In leaves affected by severe Fe deficiency the values of initial fluorescence quenching approached those of non-photochemical quenching. Additionally, these severely Fe-deficient leaves exhibited quite large photochemical quenching values, suggesting they are capable of maintaining the acceptor side of photosystem II in an oxidized state.

CO$_2$ DEPENDENT GROWTH AND NITROGEN ASSIMILATION IN PHYTOPLANKTON

David H. Turpin

Department of Botany, University of British Columbia, Vancouver, B.C. Canada. V6T 1Z4

CO$_2$ is a resource capable of limiting photosynthesis and growth in phytoplankton. Phytoplankton can adapt to lowered CO$_2$ concentrations by inducing a CO$_2$ concentrating mechanism which is capable of lowering the half-saturation constant of photosynthesis for dissolved inorganic carbon by up to 2 orders of magnitude. This adaptation permits near maximal growth rates to be

maintained as CO_2 concentration decline dramatically. Consequently the rate of phytoplankton CO_2 availability only under extreme conditions usually where pH is well below neutrality. In those systems where CO_2 limits phytoplankton growth rates, competition for inorganic carbon can play a role in shaping community structure. Carbon availability also has striking effects on the ability of algal cells to assimilate inorganic nitrogen into protein. These effects are dependent upon the nitrogen status of the cells and are mediated by both photosynthetic (Rubisco) and non-photosynthetic (PEPC) CO_2 fixing reactions. Some of the regulatory mechanisms which integrate carbon and nitrogen metabolism will be discussed.

REAL-TIME DETECTION OF PHYTOPLANKTON PHOTOSYNTHETIC RESPONSES TO THE ENVIRONMENT

Zbigniew Kolber and Richard Greene

Department of Applied Science, Brookhaven National Laboratory, Upton, New York 11973.

Photosynthetic properties of phytoplankton, such as the efficiency of light harvesting, the efficiency of energy conversion, and kinetic parameters of photosynthetic processes change significantly in response to light and temperature, as well as the availability of macronutrients and trace metals. Understanding how these parameters vary in natural phytoplankton communities requires real-time measurements of photosynthetic properties. We have developed new methodology called fast repetition rate (FRR) fluorescence to facilitate this task. Using data collected from the eastern Equatorial Pacific in March/April 1992, we will demonstrate the feasibility of the FRR methodology for detecting the effects of nitrate and iron limitation, light, and UV radiation on phytoplankton physiology.

PHYTOPLANKTON PHOTOSYNTHESIS IN A TURBID RIVER IMPACTED COASTAL ENVIRONMENT

Donald G. Redalie, Steven E. Lohrenz and Gary L. Fahnenstie

Center for Marine Science, University of Southern Mississippi, Stennis Space Center, Mississippi 39529 (DGR, SEL) and NOAA Great Lakes Environmental Research Laboratory, Ann Arbor, Michigan 48105 (GLF)

As part of the NOAA Nutrient Enhanced Coastal Ocean Productivity program we have examined temporal and spatial variability in the relationship between

phytoplankton photosynthesis and environmental characteristics for the Mississippi River Plume and adjacent Gulf of Mexico shelf waters. Four process study cruises have been conducted (July/August, 1990; March, 1991; September, 1991; May, 1992). Seasonal differences in river discharge results in variability in ambient nutrient concentrations, salinity, turbidity which impact phytoplankton community rate processes and composition. Rates of phytoplankton growth and photosynthesis were greater (by a factor of 2 or more) in the river plume than in the shelf waters during each cruise. However, horizontal variations in P^B_{max} (gC gchl^{-1} h^{-1} at optimal irradiance) and α (gC gchl^{-1} [E M^{-2}]$^{-1}$) were small relative to the large differences in phytoplankton community composition, growth rates and ambient nutrient concentrations. In addition, phytoplankton populations living in the shallow and turbid photic zone often exhibited low C/chl ratios (12-25 g g^{-1}) indicative of adaptation to low light while maintaining growth rates in excess of 2 d^{-1} and rates of photosynthesis of 4-10 gC M^{-2} d^{-1}.

CHARACTERIZATION OF *IN VIVO* ABSORPTION FEATURES OF CHLOROPHYTE, PHAEOPHYTE AND RHODOPHYTE ALGAL SPECIES

Celia M. Smith and Randall. S. Alberte

Dept. of Botany, Univ. of Hawaii, Honolulu HI 96822 (CMS) and Dept. of Biology, Univ. of California, Los Angeles CA 90024 (RSA)

Despite their plentiful diversity and abundance in coastal environments, few studies have examined the *in vivo* absorption features of marine macrophytes. Here, common intertidal and subtidal algae representing three algal divisions were examined. Computer assisted analyses were used to obtain 4th derivative spectra of room temperature spectra to provide two things: 1) spectral diagnostics for each algal division and 2) a means of testing whether spectral features could be used to identify stress responses among these plants. Spectral features associated with each algal division were identified via this approach. For plants in stress environments, this approach provided a rapid, non-invasive means to characterize subtle responses by macrophytes in ways not possible previously.

PHOTOSYNTHETIC GAS EXCHANGE AND CARBON ISOTOPE DISCRIMINATION IN SUGARCANE GROWN UNDER SALINITY

Zvi Plaut, Frederick C. Meinzer, and Nicanor Z. Saliendra

Hawaiian Sugar Planters' Assoc. P. O. Box 1057, Aiea, HI 96701

Physiological features associated with differential resistance to salinity were evaluated in two sugarcane cultivars over an 8-week period during which greenhouse-grown plants were drip-irrigated with water, or with NaCl solutions of 0.2, 0.4, 0.8 and 1.2 S m^{-1} electrical conductivity (EC). The CO_2 assimilation rate (A), stomatal conductance (g) and shoot growth rate (SGR) began to decline as EC of the irrigation solution increased above 0.2 S m^{-1}. A, g and SGR of a salinity-resistant cultivar (H69-8235) were consistently higher than those of a salinity-susceptible cultivar (H65-7052) at all levels of salinity and declined less sharply with increasing salinity. Carbon isotope discrimination (Δ) in tissue obtained from the uppermost fully expanded leaf increased with salinity and with time elapsed from the beginning of the experiment, but Δ values of cv H69-8235 were consistently lower than those of cv H65-7052 at all levels of salinity. Gas exchange measurements suggested that variation in Δ was attributable largely to variation in bundle sheath leakiness to CO_2 (Φ). The strong correlation between Δ and A, g, Φ and SGR permitted these to be predicted from Δ regardless of the genotype and salinity level. Δ thus provided an integrated measure of several components of physiological performance and response. These results suggest that in *L. gibba*, neither anabolic nor true maintenance components of respiration are inhibited by high $[CO_2]$. Under conditions of high ambient $[CO_2]$, a part of respiration which is evidently otiose, is suppressed at night.

HEAT-STABILITY OF CYANOBACTERIAL THYLAKOID CORRELATES WITH INCREASED MEMBRANE MICROVISCOSITY ATTAINED DURING THERMAL ACCLIMATION

László Vigh, Zsolt Török, Zoltán Gombos,
Eszter Kovács and Ibolya Horváth

Dept. Biochemistry (LV, ZT, EK, IH) and Plant Biolology (ZG), Biol. Res. Centr. Hungarian Acad. Sci., H-6701 Szeged, POB 521, Hungary

Parallel with reduction of fatty acid unsaturation and increase of the protein-to-lipid ratio within thylakoids, long-term acclimation of *Synechocystis* sp PCC6803 cells to elevated growth temperatures resulted in a higher neat stability of their photosynthetic membranes. Short-term sublethal heat-treatment induced additional thylakoid thermotolerance that could be ascribed to a further increase

of protein-to-lipid ratio of thylakoids and presumably also to membrane-association of a GroEL-related molecular chaperonin, HSP64 purified first in this laboratory. Both long- and short-term phases of acclimation resulted in enhancement of membrane molecular order which suggests that the ability for maintenance of optimal level of membrane physical state (fluidity and lipid-protein interactions) is part of a mechanism ensuring increased thermostability of the photosynthetic apparatus.

USING MODELS AND SATELLITE DATA TO CALCULATE THE FLUXES OF ENERGY, HEAT, WATER AND CARBON ON THE LARGE SCALE

Piers J. Sellers

923, NASA/GSFC, Greenbelt, MD 20771

The photosynthesis-stomatal function model developed by the Carnegie Institute group was integrated to provide a description of canopy photosynthesis and transpiration. One of the constants of integration is closely related to the fraction of photosynthetically active radiation absorbed by the green canopy (FPAR) and hence to remotely sensed vegetation indices (SVI) provided by analysis of satellite data. The model has been implemented into a general circulation model of the atmosphere (GCM) and uses time-series of SVI to specify the global fields of photosynthetic capacity. Preliminary results from a simulation run will be discussed with particular emphasis on the calculated fields of energy, water, heat and carbon fluxes over the continents.

PHYTOPLANKTON RESPONSES AND FEEDBACK TO GREENHOUSE FORCING

Paul G. Falkowski

Oceanographic and Atmospheric Sciences Division, Brookhaven Nation Laboratory, Upton, New York 19973

Phytoplankton can potentially modify the radiative balance of the Earth by drawing down atmospheric CO_2 and by increasing the albedo of low altitude clouds. The efficiency and effects of phytoplankton productivity appears to be critically dependent on nutrients, which are primarily supplied from below the upper mixed layer. For decades oceanographers have understood that the circulation of ocean is coupled to that of the atmosphere, and, simultaneously is

the major driver of phytoplankton production. Coupled ocean-atmosphere circulation models of the projected transient changes in atmospheric CO_2 suggest stronger thermal contrasts between land and ocean margins. Over the past 100 years this effect appears to have stimulated productivity along the ocean margin of the Pacific, but decreased productivity in the central ocean gyre. The net effect of primary production in the central ocean basins on atmospheric CO_2 levels has been undetectable in time scales of a tens of decades, negative feedback on time scales appears to have been significant only on time scales of millennia. However, short-term changes in the species composition of phytoplankton communities, especially at higher latitudes, could have profound consequences on cloud albedo, which strongly influence radiative balance, The sign of this feedback would depend on the species selected, which we cannot predict at present.

REMOTE SENSING OF OCEANIC PRIMARY PRODUCTION

Charles S. Yentsch

Bigelow Laboratory for Ocean Sciences, West Boothbay Harbor, ME 04575

Most recognize the influence that terrestrial productivity has on the social/economic development of modern societies. Less obvious is the influence of oceanic productivity which is largely because of an inability to visualize the processes of growth. Satellite remote sensing is changing this perspective for we can now observe the growth of primary producers (microalgae) over wide areas of the worlds oceans. These observations support the concept that the energy associated with large scale features of the oceans circulation is responsible for the time and space changes in the rate of photosynthetic production.

INDEX

efficiency 235
membrane 132, 245
oxygen evolution 222
potential 152
photosystem I 3, 113, 159, 241
photosystem II 3, 14, 20, 23, 30,
40, 113, 136, 142, 159, 160,
178, 233, 238, 242
phytoplankton 45, 61, 126, 150,
235, 242, 243, 246
Picea abies 193
Pisum sativum 161
Pittosporum tobira 176
plant emission 226
plastoquinone 142
plastosemiquinone 147
Pmax 1
polyunsaturated fatty acids 81
primary production 46, 126
in situ 46, 152
marine 46
productivity 37
prokaryotic 78
protective acclimation 14
protoplast 93
Q_A 16
quantum yield 3, 152, 160, 167,
178, 179, 193, 242
Quercus agrifolia 176
quinone 142
electron acceptor 142
radiative balance 246, 247
reductive pentose phosphate
pathway 132
reductive nitrate 132
reflectance measurement 172
relaxation pathway 157
remote sensing 247
respiration 201
respiratory quotients 202
Rhodendrum 21
Rhodophyta 102, 244
Rhus laurina 176
Rhus ovata 173, 176

ribosomes 132
river plume 244
RNA 127
Rubisco 3, 9, 105, 113, 127, 187
RUBP 105
Rumex patientia 49
Saintpaulia 240
salinity 213, 219
satellite
data 246
remote sensing 247
seasonal changes 193
senescence 1, 2
sensed vegetation indices 246
shade 2
plant 14, 21
shelf waters 244
singlet oxygen 16, 157
sodium azide 93
soybean 39, 41
species composition 247
spectral irradiance 48, 179
spectrum 47, 244
Spinacia oleracea 4, 30, 240
Spirodela oligorrhiza 146
state 1-2 14
Stern Volmer 161, 167
stress 193, 229
distance 229
duration 229
environmental 185
fluorescence algorithm 239
irradiance 70
light 62
mechanical 229
oxidative 241
plant 157
responses 230
salinity 245
severity 229
temperature 245
water 229
sun plant 14, 21
superoxide dismutase 88, 93